UNIVERSITA' DEGLI STUDI DI PADOVA

Sede Amministrativa: Università degli Studi di Padova

Dipartimento di GEOSCIENZE

DOTTORATO DI RICERCA IN : SCIENZE DELLA TERRA
CICLO XX

TITOLO TESI

STRATIGRAPHIC AND COMPOSITIONAL STUDY OF MIXED SHALLOW-WATER CARBONATE-SILICICLASTIC UNITS OF CARNIAN AGE (LATE TRIASSIC) IN DOLOMITES AND JULIAN ALPS (ITALY)

STUDIO STRATIGRAFICO E COMPOSIZIONALE DELLE UNITÀ MISTE TERRIGENO-CARBONATICHE, DI BASSA PROFONDITÀ, DEL CARNICO (TRIASSICO SUPERIORE) DI DOLOMITI E ALPI GIULIE

Coordinatore : Ch.mo Prof. Gilberto Artioli
Supervisore :Ch.mo Prof. Nereo Preto

Dottorando : Renata Meneguolo

DATA CONSEGNA TESI
31 luglio 2008

AKNOWLEDGEMENTS

Dr. Guido Roghi, CNR, Università di Padova, is gratefully appreciated for performing the palynological analyses

All my family; and Tom and his family: no need to say why

Piero, without you this wouldn't have been possible!!!

Betty and Valentina, the best friend one could desire.

Chiara ("fashion stylist") for her invaluable aesthetic advice
KARSTEN for intermediation with Northern Norway (I kept my promise, here you are in capital letters!)
Anna because she's Anna
Manuel because he's Manuel (and for intermediation with Italy)
Matteo ("software wizard") for IT support; Lisa, Marco, Jacopo and the other PhD students from Padua for general support and friendship
Stefano, Lorenzo, Nicola, Maui and the lab
Stefano Furin, Rachele and other people from Ferrara

SH INT GEX ENA LIB people (translated: my colleagues in Stavanger!) for support (and patience!)

Donatella (and Adolfo) for precious advise and friendship
Alessia for "amatriciana" and "frittatona di cipolle" (and for friendship!)

Il Dr. Guido Roghi, CNR, Università di Padova, è sentitamente ringraziato per le analisi polliniche

Tutta la mia famiglia; Tom e la sua famiglia: niente da aggiungere

Piero, senza di te questo non sarebbe stato possibile!!!

Betty e Valentina, le migliori amiche che si possano desiderare

Chiara ("fashion stylist") per i suoi inestimabili consigli estetici
KARSTEN per l'intermediazione con la Norvegia settentrionale (promessa mantenuta: eccoti in maiuscolo)
Anna perchè è Anna
Manuel perchè è Manuel (e per intermediazione con l'Italia)
Matteo ("mago del computer") per supporto informatico; Lisa, Marco, Jacopo e gli altri dottorandi di Padova per il sostegno e l'amicizia
Stefano, Lorenzo, Nicola, Maui e il laboratorio
Stefano Furin, Rachele e gli altri da Ferrara

Le persone in SH INT GEX ENA LIB (tradotto: i miei colleghi a Stavanger!) per il sostegno (e la pazienza!)

Donatella (e Adolfo) per i preziosi consigli e l'amicizia
Alessia per l'amatriciana e la "frittatona di cipolle" (e per l'amicizia!)

INDEX

Acknowledgements **i**
Index **ii**
Abstract **v**
Riassunto ***vi***

INTRODUCTION **1**

Scopes of work 1

Geological setting **2**
Late Triassic global paleogeography 2
Late Triassic paleoclimate 2
Geology of the Southern Alps 3

Formation nomenclature and description **3**
Heiligkreuz Formation 3
Travenanzes Formation 5
Rio del Lago Formation 7
"Dogna" formation 7

CHAPTER I LOWER CARNIAN MIXED RAMP OF THE JULIAN ALPS **9**

1.1 Introduction **9**
1.1.1 Geological setting 10

1.2 Methods **12**
1.2.1 Sample Collection and Preparation 12
1.2.2 Counting Technique and Tabulation 12
1.2.3 Statistical analyses 13
1.2.3.1 Cluster analysis specifications 14

1.3 Sedimentology **15**
1.3.1 Facies Association 1: lower Rio di Terrarossa Dolomite 16
1.3.2 Facies Association 2: upper Rio di Terrarossa Dolomite 16
1.3.3 Facies Associations 3 and 4: Rio Pontuz oolite 17
1.3.4 Facies Associations 5, 6, 7 and 8: Rio del Lago and Tor Formations 19

1.4 Petrology **27**
1.4.1 Components 27
1.4.1.1 Major skeletal grains 27
1.4.1.2 Calcareous green algae 28
1.4.1.3 Other grains 29
1.4.2 Bioerosion and microbialite encrustations 29
1.4.3 Carbonate mud 32

1.5 Cluster analysis **34**
1.5.1 Lower Carnian subtidal ramp (88 samples) 34
1.5.2 Whole dataset (155 samples) 35

1.6 Discussion **37**
1.6.1 Environmental significance of petrofacies (clusters) 37
1.6.2 Distinction between ramp subenvironments 37
1.6.3 Cool water versus tropical carbonate factories 38
1.6.4 Terrigenous input 40

1.7 Conclusions **41**

CHAPTER II UPPER CARNIAN TERRIGENOUS DEPOSITS OF THE DOLOMITES AND JULIAN ALPS **43**

2.1 Introduction **43**

2.2 Methods **44**

2.3 Logs description and interpretation **48**
2.3.1 Heiligkreuz Formation 48
2.3.2 Travenanzes Formation 65
2.3.3 Rio del Lago Formation 68
2.3.4 "Dogna" formation 68
2.3.5 Correlation between the Dogna area and the Dolomites 75

2.4 Results **82**
2.4.1 Components 82
2.4.1.1 NCE 82
2.4.1.2 CI 84
2.4.1.3 NCI 84
2.4.1.4 Interstitial material-considerations on diagenesis 86
2.4.2 Framework composition 88
2.4.3 Petrofacies description 92
2.4.3.1 Dolomites -Heiligkreuz Formation 92
2.4.3.2 Dolomites -Travenanzes Formation 96
2.4.3.3 Julian Alps –“Dogna” formation 97

2.5 Discussion **99**
2.5.1 Interpretation of volcanic grains 99
2.5.2 Interpretation of carbonate grains 100
2.5.3 Compositional factors: premises 101
2.5.4 Negligible factors (tectonic activity, diagenesis, recycling) 102
2.5.5 Influencing factors 103

2.6 Carnian Pluvial Event correlation 105
2.6.1 Consideration on paleosols 105
2.6.2 Anatomy of the Carnian Pluvial Event 106

2.7 Model for short-term to long-term compositional changes **107**

2.8 Conclusions **109**

GENERAL CONCLUSIONS **111**
REFERENCES **113**

APPENDIXES

Appendix I	Petrographical results, subtidal ramp of Dogna
Appendix II	Petrographical results, Heiligkreuz Fm.
Appendix III	Petrographical results, Rio del Lago and “Dogna” Fms.
Appendix IV	Petrographical results, Travenanzes Fm.
Appendix V	Correlation panel of petrographic results

ABSTRACT

The Julian to Tuvalian (Carnian, Late Triassic) units of the Dolomites and Julian Alps (Eastern Southern Alps, Northern Italy) have been studied under a sedimentological and petrographical point of view. This stratigraphic interval records an important turnover in the sedimentary system with at least two phases of coarse terrigenous input interfingered with carbonate deposits. This episode seems coeval with a wet climatic event named “Carnian Pluvial Event (CPE)”. The arenite petrography of the Carnian coarse siliciclastics has been studied in order to provide insights on the structure and climatic nature of the CPE, and the underlying carbonates of Dogna were examined, in order to provide an understanding of the “benchmark” sedimentation before the CPE in a region where the depositional profile did not change significantly throughout the Carnian.

The Julian (Early Carnian) succession of the Dogna area (Julian Alps, Eastern Northern Italy) shows the geometrical character of a carbonate ramp (associable to a “cool-water factory”) with terrigenous influx, in contrast with the rimmed platforms of the adjacent Dolomites area (recognized as “tropical-water factory”). The contradictory carbonate succession of Dogna has thus been investigated under a sedimentological and petrographical profile in order to refine the sedimentological model of the ramp, identifying the depositional sub-environments and to test the fit of the cool-water carbonate factory model. Lithofacies recognized are micrite-supported (indicator for “tropical-water”), while petrographical associations of bioclasts are mainly heterotrophic (“cool-water” indicator) but with dominance of halimedacean algae in the inner ramp facies. Fragmented halimedaceans represent also the origin of micrite, unraveled by SEM analyses. Overall, five sedimentary sub-environments for the subtidal ramp have been recognized from integration of field observations and petrographical analyses. A new insight for carbonate production in the Upper Triassic is given: the coexistence of tropical- and cool-water features can be explained by the terrigenous influx, hampering the growth of autotrophic organisms (as presently occurring in stressed tropical platforms), and halimedacean algae appear to be already major carbonate producers.

Arenites of the Heiligkreuz and Travenanzes Formations (Dolomites) and of the “Dogna” formation (Julian Alps) were analyzed with standard sedimentary petrology techniques in order to detect the influence of the climatic change in the sedimentary systems.

Arenites composition displays a repetitive alternation between lithic and quartzose lithologies, with an overall increase in quartz content.

Within each terrigenous phase, arenites composition displays repetitive alternations of lithic and quartzose arenites, with an overall quartz increase.
Compositional variations have been related to climate with the detection of the modifications of known mechanisms affecting arenite composition. Short-term variations can be caused by the different weathering extent in the pedogenetic environment, while long-term variations from the change of the general depositional setting.
The CPE can thus be described as a parossistic event with extreme seasonality, represented by the repeated alternation of humid (lithic arenites) and arid (quartzose arenites) periods, in strong contrast with the current understanding of climate influence on arenite compositions.

RIASSUNTO

Le unità tardo-triassiche juliche e tuvaliche (Carnico) delle Dolomiti e Alpi Giulie (Sudalpino orientale, Italia settentrionale) sono state studiate dal punto di vista sedimentologico e petrografico.
Questo intervallo stratigrafico registra un importante cambiamento nei sistemi sedimentari, con almeno due fasi di apporti terrigeni grossolani intercalati ai depositi carbonatici. Tale episodio sembra essere contemporaneo ad un evento climatico umido chiamato “Carnian Pluvial Event (CPE)”. La petrografia delle areniti dei depositi silicoclastici grossolani del Carnico è stata studiata allo scopo di fornire dettagli nella struttura e nella natura climatica del CPE, e i sottostanti depositi carbonatici di Dogna sono stati esaminati per ottenere il confronto con la sedimentazione antecedente il CPE, in una regione di relativa omogeneità deposizionale durante l’intero Carnico.
La successione julica (Carnico inferiore) dell’area di Dogna (Alpi Julie, Italia settentrionale orientale) presenta le geometrie di una rampa carbonatica (associabile ad una “cool-water factory”) con influsso terrigeno, in contrasto con le piattaforme orlate delle vicine Dolomite (riconosciute come “tropical-water factory”). La contrastante successione carbonatica di Dogna è quindi stata investigata sotto il profilo sedimentologico e petrografico allo scopo di migliorare il modello sedimentologico della rampa, di identificare i sub-ambienti de posizionali e di verificare il modello di “cool-water factory”. Le litofacies riconosciute sono fango-sostenute (indice di “tropical-water factory”), mentre le associazioni di bioclasti riconosciute attraverso la petrografia sono principalmente eterotrofiche (indice di “cool-water factory”), ma con predominio delle alghe halimedacee nella rampa interna. Frammenti di halimedacee rappresentano anche l’origine della micrite, determinata con analisi al SEM.

In tutto, cinque sub-ambienti sedimentari sono stati riconosciuti nella rampa sub-tidale tramite l'integrazione di osservazioni di campagna e analisi petrografiche.

Viene perciò introdotta una nuova prospettiva per la produzione di carbonato nel Triassico Superiore: la coesistenza di caratteri tropicali e temperati può essere spiegata dall'influsso terrigeno, che arresta lo sviluppo degli organismi autotrofi (come accade attualmente nelle piattaforme tropicali stressate), e le alghe halimedacee appaiono per la prima volta come maggiori produttori di carbonato.

Le areniti delle Formazioni di Heiligkreuz e Travenanzes (Dolomiti) e della formazione di "Dogna" (Alpi Giulie) sono state analizzate con tecniche standard di petrografia del sedimentario allo scopo di verificare l'influenza del cambiamento climatico nei sistemi sedimentari.

Entro ciascuna fase terrigena, la composizione delle areniti presenta alternanze ripetitive di areniti litiche e quarzose, con un generale aumento del quarzo.

Le variazioni compositive sono state messe in relazione con il clima tramite l'individuazione delle modificazioni nei meccanismi noti che influenzano la composizione delle areniti. I cambiamenti a breve termine sarebbero causati dal diverso grado di alterazione in ambiente pedogenetico, e quelli a lungo termine dal cambiamento generale di ambiente deposizionale.

Il "Carnian Pluvial Event" può quindi essere descritto come un evento parossistico ad estrema stagionalità, rappresentato dalla ripetuta alternanza di fasi umide (areniti litiche) ed aride (areniti quarzose), in forte contrasto con la presente concezione dell'influenza climatica sulla composizione delle areniti.

INTRODUCTION

SCOPE OF WORK

The main issue undertaken in this work is the analysis of mixed carbonate and siliciclastic units of late Triassic age (Carnian) in the Eastern Southern Alps, Italy.

The main reason of interest about the Carnian stage is the recording of a climatic change, named the Carnian Pluvial Event (CPE, Simms et al., 1997; Simms and Ruffell, 1991).

The general climatic conditions for the Late Triassic were recognized as monsoonal (Mutti and Weissert, 1995; Kutzbach e Gallimore, 1994) with arid regime (Price, 1999), but an abrupt change in the overall conditions happened nearly at the Julian/Tuvalian (lower/upper Carnian) boundary, recognized as a humid shift (Simms and Ruffell, 1989). This event was testified by a significant biological turnover (Simms and Ruffell, 1989 and 1990; Hochuli e Frank, 2000; Stanley jr., 2001), and marked by a sudden coarse terrigenous input (Schlager and Schöllnberge, 1974; Weissert, 1990).

The present work is aimed at depicting the possible effects of the climatic change on the siliciclastic sedimentary systems with the integration of stratigraphy and sedimentary petrology. The selected study areas are the Dolomites and the Julian Alps (easternmost Southern Alps), where the upper Carnian successions represent diverse depositional settings, in order to discriminate those effects of the CPE which are not facies controlled.

In the Dolomites area, the physiographic configuration of deep basins and rimmed carbonate platforms inherited from the lower Carnian (De Zanche et al., 1993) provides proximal to distal depositional trends, but also results in a slightly more complicated interpretation of the petrological data from the upper Carnian arenites.

The Julian (lower Carnian) sedimentary successions in the Julian Alps were instead considered of overall stable shallow-marine carbonate-ramp environment (Preto et al., 2005), in a strong contrast with the coeval sedimentation style of the Dolomites (Keim and Schlager, 2001; Russo et al., 1997; Bosellini, 1984). This dissimilarity is presently not totally understood.

The confirmation of a more homogeneous carbonate ramp environment for the lower Carnian of the Julian Alps would then provide both an insight of the lower Carnian carbonate systems and a valid constrain for the understanding of compositional trends of the upper Carnian terrigenous deposits, tentatively linked to the climatic event.

In this framework, the present work is subdivided into a first part dealing with the sedimentology and petrology of the lower Carnian carbonate succession of the Julian Alps, and a second part undertaking the sedimentology and petrology of upper Carnian terrigenous-

carbonate succession in Dolomites and Julian Alps, with main focus on the effects of climate on the sedimentation.

GEOLOGICAL SETTING

Late Triassic global paleogeography

During the whole Triassic the global configuration was of a single supercontinent called Pangaea, surrounded by a single superocean called Panthalassa.

The western margin of Pangea was characterized by a deep engulfment stretched in longitudinal direction around the equator, called Tethys.

The current Southern Alps belonged to the African plate and were positioned in the southern tethyan edge at around 15°N latitude (Muttoni et al., 1996).

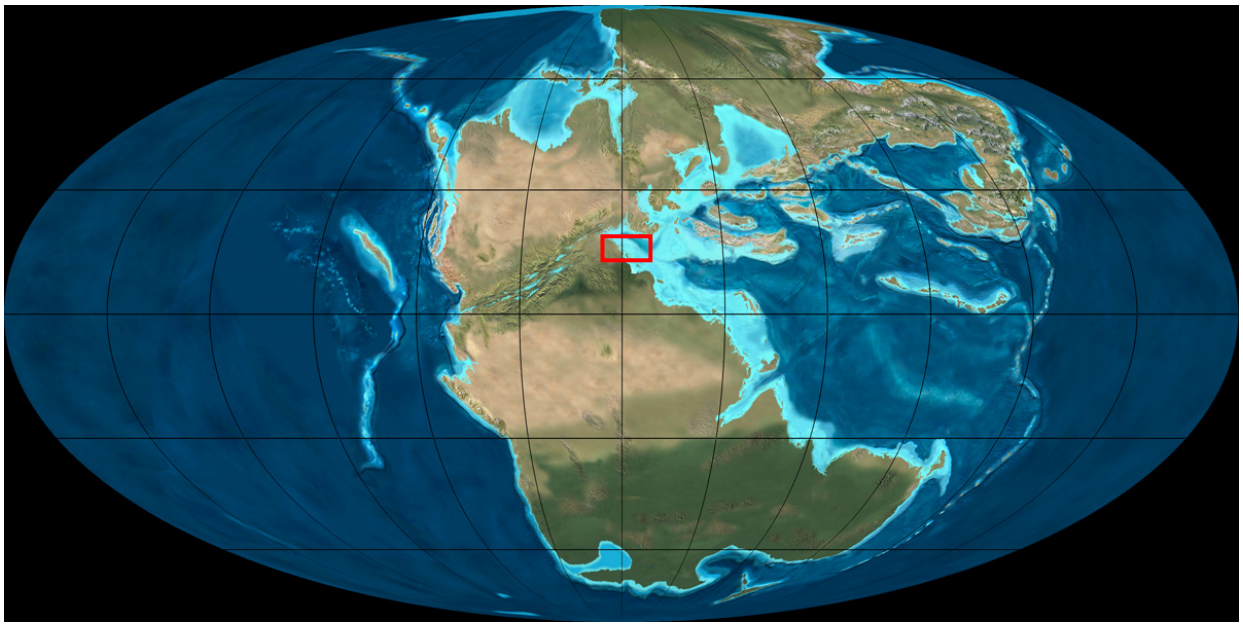

FIGURE 1 - Global configuration in the Triassic time from 220 My. The whole continental crust was grouped in the Pangaea supercontinent while the whole oceanic basin was represented by the Panthalassa, with the longitudinal Tethys Ocean engulfment. Red rectangle: approximate position of Southern Alps. From: www.earthscienceworld.org

Late Triassic paleoclimate

Triassic climate within the tropics is reconstructed as warm and arid. As a consequence of the land/ocean distribution, atmospheric circulation in the Triassic was most likely strongly monsoonal (Kutzbach and Gallimore, 1994), and therefore climate was mostly arid, with enhanced seasonal variability.

These conditions were though altered during the Carnian (Late Triassic). A sudden climate change was recorded, named Carnian Pluvial Event (CPE, Simms et al., 1997), defined as a humid shift of the conditions.

Geology of the Southern Alps

The Southern Alps are a east-west trending mountain chain derived by the south-vergent folding and thrusting of the passive margin of the Africa (Adria) plate (Bosellini, 1996). Main tectonomagmatic events took place between the Permian and the Jurassic.

The easternmost edge of the Southern Alps (Dolomites and Julian Alps) had a uniform stratigraphic evolution until the Ladinian (Late Triassic), when a complex physiography given by rimmed carbonate platforms (Schlern Dolomite) and deep basins developed.

At the beginning of the Carnian (Julian) a differentiation occurred between the Dolomites and the Julian Alps. In the Dolomites the topographic variations between rimmed platforms and basins were still enhanced (Cassian Dolomites 1 and 2 vs. San Cassiano Formation), while in the Julian Alps a homogeneous carbonate shelf was predominating, without topographical differentiations, represented by the Rio di Terrarossa Dolomite and the Rio del Lago Formation (with the Rio Pontuz oolite member).

At the end of the Julian (lower Carnian), decrease of subsidence in the Southern Alps led to a general progradation of the coastline (Picotti and Prosser, 1987; Gianolla et al., 1998).

In the Dolomites, the inherited paleotopography was filled up and eventually flattened by the Heiligkreuz Formation (Neri et al., 2007). In the Julian Alps, the homogeneous sedimentation continued with a complex carbonate-terrigenous unit informally called “Dogna” formation (Preto et al., 2005).

FORMATION NOMENCLATURE AND DESCRIPTION

Heiligkreuz Formation

The name Heiligkreuz was first used by Wissmann in Wissmann and Münster (1841) to indicate an interval distinguished by the presence of the bivalve *Unionites*, but with uncertain stratigraphic position. The correct stratigraphic assignment to the late Carnian was performed by Koken (1913), but the term was then abandoned.

Successively, Pia (1937) defined as *Dürresteindolomit* the interval comprised between the inner and slope facies of Cassian Platform buildups, of basinal San Cassiano Fm., and the Travenanzes (Raibl) Fm.

The high lateral variability and the lack of a stratigraphic criterion caused different Authors to extend its definition. The term Dürrestein Formation was introduced by Pisa (1980) accounting for the terrigenous intervals, but the unclear nomenclature led eventually to the retrieval of the prior term Heiligkreuz (Breda et al., 2008).

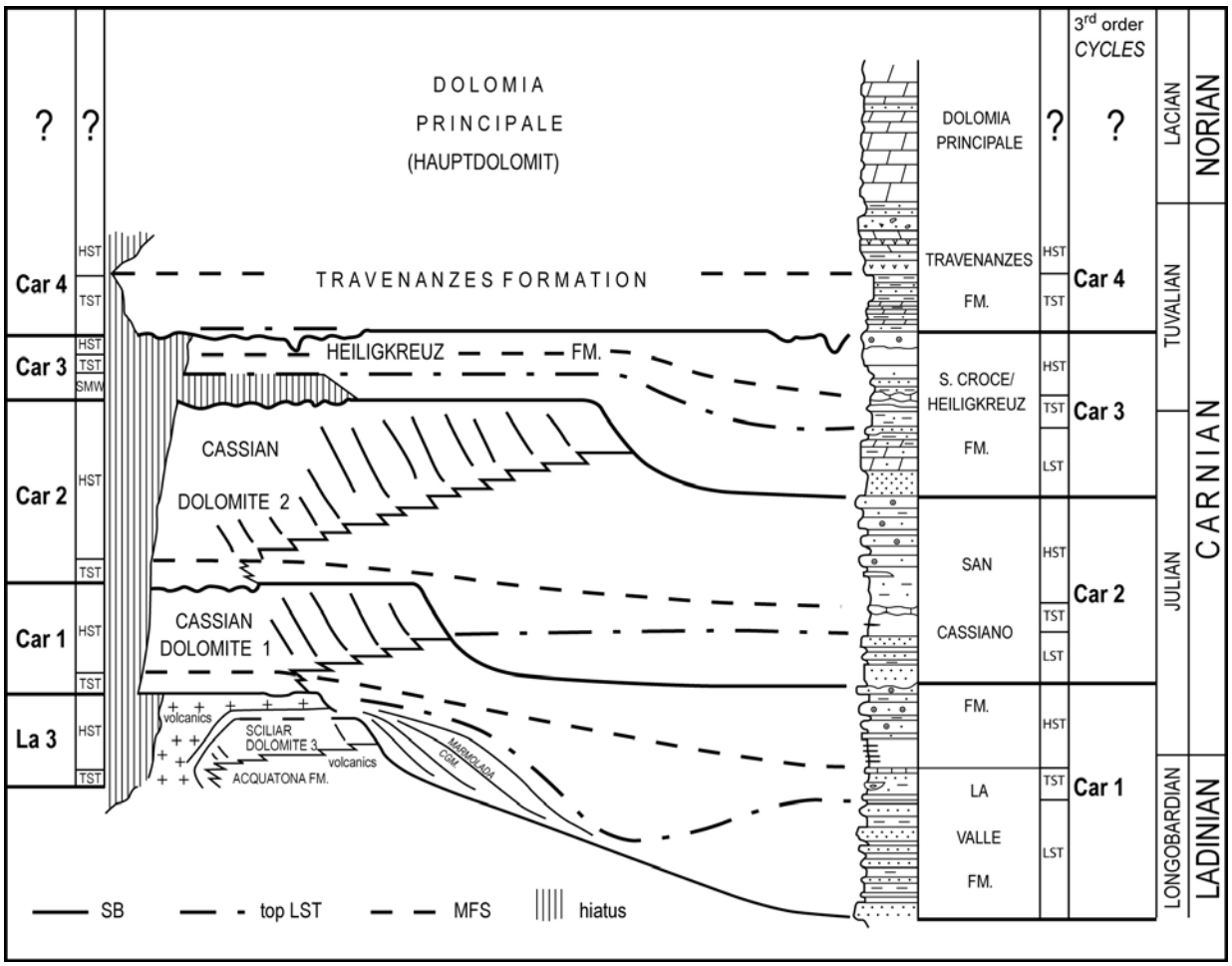

FIGURE 2 - Late Triassic sequence stratigraphy of the Dolomites area (mod. from De Zanche et al. 1993). A strong physiographic differentiation is present until the Upper Carnian. Palaeotopography is flattened after deposition of the Heiligkreuz Fm.

Currently, the Heiligkreuz Fm. *sensu* Keim et al. (2001) and Stefani et al. (2004) corresponds entirely to the Dürrestein Formation of Pisa et al. (1980), De Zanche et al. (1993), Gianolla et al. (1998a,b), Preto and Hinnov (2003). It includes some previously defined informal units like “Areniti del Dibona” and “Areniti del Falzarego” (Bosellini et al., 1982), “Member A” (Russo et al., 1991).

The Heiligkreuz Formation overlies conformably the San Cassiano Formation, it onlaps the slope of Cassian platforms and can overlay unconformably (with karst surfaces) the Cassian platform tops. The upper boundary with the Travenanes Fm. is unconformable. The unit represents a complete depositional sequence (e.g., Zanche et al. 1993; Neri and Stefani 1998; Gianolla et al. 1998a; Gianolla et al. 1998b, De Preto and Hinnov, 2003) and is constituted by a mixed terrigenous-carbonate succession that records a complex series of events, possibly climate-driven (Preto and Hinnov, 2003). The deposits of the Heiligkreuz Fm. complete the

filling of the pre-existing physiographic depressions and determine the general flattening of paleotopography in the Dolomites area (Preto and Hinnov, 2003; Neri et al., 2007).

The overall succession is not visible in one single outcrop. Following Neri et al. (2007), the Heiligkreuz Fm. can be divided, in the Cortina area, into three members: Borca Member, Areniti del Dibona Member, Lagazuoi Member.

The Borca Member corresponds to Lithozones A to D of Preto and Hinnov (2003) and is made up of pelite deposits with freshwater influence (Neri et al., 2007), dolomitized mudstone-grainstones, arenitic dolostones and hybrid arenites with pelitic intercalations. Boundstones and patch reefs are also present. The clinoforms of the "membro tiltato" (tilted member) of Bosellini et al. (1982) belong to lithozone C. Note that Bosellini et al. (1982) interpreted this unit as a tectonically tilted peritidal succession, while Preto and Hinnov (2003) suggested instead it constitutes a clinostratified, strongly dolomitized body of granular carbonates. Lithozone D repeatedly shows karst features associated with aggrading histic paleosols (organic-rich terrestrial black shales).

The Areniti del Dibona Member corresponds to the "Areniti del Di Bona" of Bosellini et al. (1982) and to the Lithozones E and F of Preto and Hinnov (2003). It is represented by polygenic conglomerates, alternated cross-bedded arenites and hybrid arenites, dark clay intervals, and packstone-grainstones commonly with sedimentary structures, sometimes rich in amber grains (Gianolla et al., 1998b; Roghi, 2004).

The Lagazuoi Member corresponds to the Lithozones G and H of Preto and Hinnov (2003). It is mainly constituted by arenaceous dolostones and oolitic-bioclastic grainstones. Locally, hybrid arenites with bimodal cross-bedding are present ("Arenarie del Falzarego" of Bosellini et al., 1982). The thick peritidal deposits of the Lithozone H are of regional significance, and correspond to the Portella Dolomite Formation in the Julian Alps area.

Travenanzes Formation

The succession comprised between the Heiligkreuz Fm. and the Dolomia Principale was defined as *Raibler Schichten* by Hauer (1855) and Richtofen (1860) from the Raibl locality in the easternmost Southern Alps (Julian Alps, Tarvisio, Italy).

The term "Raibl Group" was then introduced for the Tarvisio area by Assereto et al. (1968), and extended to the Dolomites by Pisa et al. (1980), including also most of the Cassian succession.

For this reason, and for the absence in the Dolomites area of the typical deposits of the Julian Alps, the term is considered inappropriate.

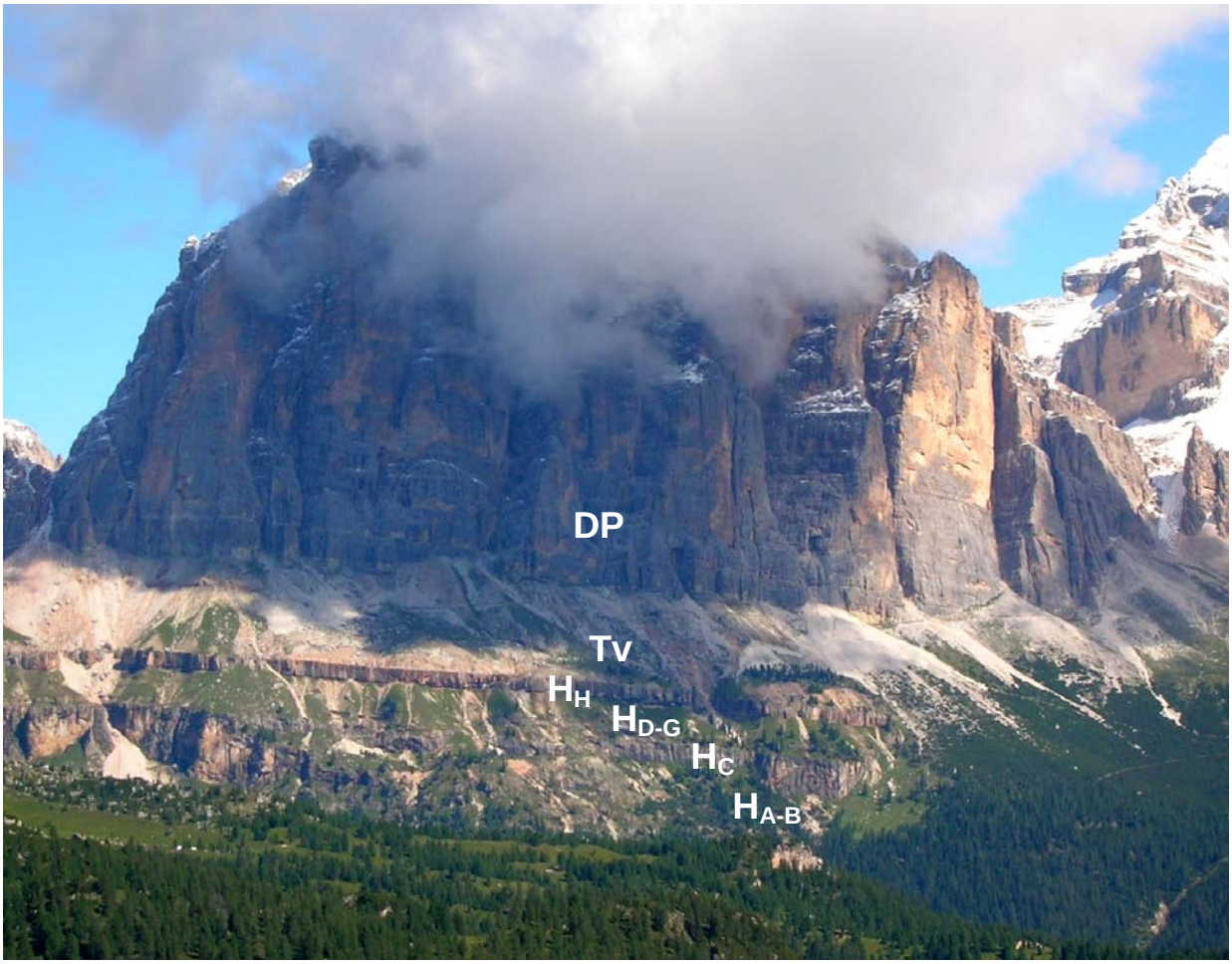

FIGURE 3 - Carnian/Norian stratigraphy in the Tofane/Cortina d'Ampezzo area. H_{A-B}: Heiligkreuz Fm., lithozones A/B; H_C: Heiligkreuz Fm., lithozone C; H_{D-G}: Heiligkreuz Fm., lithozones D to G; H_H: Heiligkreuz Fm., lithozone H; Tv: Travenanzes Fm.; DP: Dolomia Principale (*Hauptdolomit*). The thick dolostone bank of lithozone H corresponds to the Portella Dolomite in the Julian Alps (De Zanche et al., 2000).

The expression Travenanzes Formation is used instead, after the usage of the term "Argilliti di Travenanzes" (Travenanzes claystones) by Bosellini et al. (1996), to indicate the same interval (cf. Neri et al., 2007).

The Travenanzes Formation consists of about 200m of multicolored clays and marls alternated to cm- to dm-thick aphanitic dolomites, rare arenite layers and evaporitic intervals. It represents a continental to shallow-marine succession, with interfingering alluvial plain, flood basin, and lagoonal deposits. Three transgressive-regressive sequences can be recognized (Breda et al., 2006).

Rio del Lago Formation

The Rio del Lago Formation is a lithostratigraphic unit of the Julian Alps, established in 1968 by Assereto et alii.

The succession is more than 200m thick (Preto et al. 2005, De Zanche et al. 2000). It starts with 20m of oo-bioclastic grainstones (Rio Pontuz oolite member) followed by subtidal dark marly shales with bioturbated to nodular wackestone-packstone intercalations. Fossil content is mainly bivalves, foraminifers, algae fragments and gastropods.

“Dogna” formation

The unit interposed between the Rio del Lago Fm. and the Portella Dolomite is still informally defined as “Dogna” formation from the most representative locality, the village of Dogna, close to Tarvisio, in the Julian Alps.

Previous work describing this unit is Preto et al. (2005).

The “Dogna” fm. is a mixed carbonate-siliciclastic succession with two main coarse siliciclastic intervals separated by vuggy dolomites. Arenites are dm-to m-thick, massive to cross-bedded, with bivalves and intraclasts.

CHAPTER I LOWER CARNIAN MIXED RAMP OF THE JULIAN ALPS

1.1 INTRODUCTION

Carbonate platforms where, as in modern tropical shallow waters, carbonate is produced mostly by autotrophic organisms, were repeatedly established during geologic time, and can be grouped in a model of "tropical carbonate factories" or "T factories" (Schlager, 2003; 2005).

Tropical factories are usually associated to rimmed carbonate platform geometries.

At higher latitudes, carbonate production is instead dominated by heterotrophic biological associations (e.g., Carannante et al., 1988; Schlager, 2005). Presently, major carbonate producers of the "cool-water factory" or "C factory" are molluscs, bryozoans, foraminifers and red algae, and the associated geometries are those of carbonate ramps.

Finally, the "mud-mound factory" or "M factory" is characterized mostly by microbiologically induced carbonates (automicrite-dominated facies), and is associated to high relief buildup geometries.

The shallow water carbonate factory developing in a particular time and region is determined, beyond latitude, by geochemical, climatic and environmental factors (e.g., Schlager, 2003; 2005; Brennan et al., 2004; Mutti and Hallock, 2003; Stanley and Hardie, 1998; Read, 1998). Consequently, carbonate production styles result rather uniform at any given time, at least at the regional scale. The Upper Triassic, and particularly the Carnian, was in the Southern Alps a time of mud-mounds (Russo et al., 1997; Keim and Schlager, 2001; Schlager, 2005), as inferred from the carbonate buildups of the Dolomites (northern Italy). The lower Carnian carbonate platform of Dogna, represented by the Rio di Terrarossa Dolomite and by the Rio del Lago Formation, represents instead a mixed carbonate-siliciclastic ramp, which shows coexistence of heterotrophic assemblages and abundant carbonate mud. It appears thus significantly different in geometry from the well-known high-relief carbonate buildups of the classical Dolomites area, only ca. 100km apart.

Different carbonate factories seem to exist contemporaneously in the shallow water of early Carnian western Tethys. This suggests a unexpected variability of the environmental conditions which is, at present, totally unexplored.

On the other hand, carbonate mud is rather typical of tropical and mud-mound factories: in particular, a large part of the carbonate produced by recent tropical carbonate platforms is micrite derived from the breakdown of aragonitic halimedacean algae (e.g. Neumann and Land, 1975; Rees et al., 2007; Ries 2005; 2006), while cool-water carbonates are almost free of carbonate mud. However, halimedaceans are not known to be major carbonate producers in the early Mesozoic (Bassoullet et al., 1983). The carbonate ramp of Dogna is thus apparently

difficult to reconcile both with present-time and with known coeval (Carnian) carbonate platforms.

In order to clarify these issues, we undertook a detailed study of the lower Carnian carbonates of Dogna, aimed at:

1) refine the sedimentological model of the carbonate ramp, identifying the depositional sub-environments and their spatial relationships;
2) determine the origin of carbonate mud;
3) test how well the carbonates of Dogna fit into the model of the cool-water carbonate factory.

1.1.1 Geological Setting

The Carnian of Dogna, in the western Julian Alps (Fig. 4), lies unconformably on a strongly dolomitized Middle Triassic carbonate platform (Schlern Dolomite). Following Preto et al. (2005), six lithostratigraphic units constitute the Carnian of the lower Dogna valley below the Dolomia Principale: the Rio di Terrarossa Dolomite (Jadoul et al., 2002), a succession of well layered dolostones with thin marl interlayers; the Rio del Lago Formation (Assereto et al., 1968), bioclastic packstones and wackestones intercalated to fine siliciclastics, including the Rio Pontuz oolite in its lower part. An abrupt stratigraphic turnover is represented by the "Dogna formation", mainly constituted by coarse siliciclastic deposits; the recovery of the mixed carbonate-siliciclastc system is represented by the Tor Formation, (Assereto et al., 1968) a succession of marls, siltstones and bioturbated marly limestones; the Portella Dolomite (De Zanche et al., 2000), a single, massive, shallow-water carbonate bank; and the Monticello Formation, constituted at Dogna by alternated peritidal aphanitic dolostones, granular limestones and dark shales (Fig. 5). Altogether, they are interpreted as being deposited in a carbonate-siliciclastic ramp (see § 1.3, sedimentology).

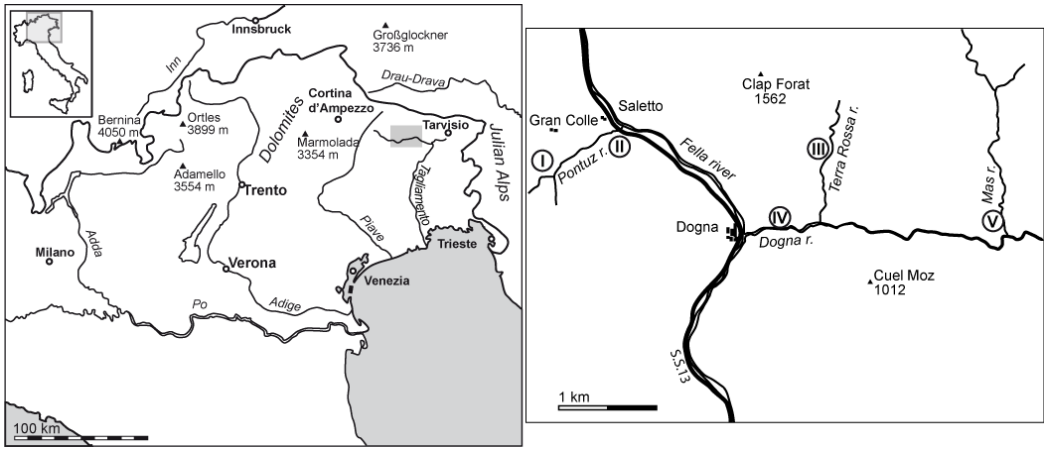

FIGURE 4 - Map of the study area. Stratigraphic sections analyzed: I =Gran Colle; II = Rio Pontuz; III = Rio di Terrarossa; IV = Dogna river; V = Rio Mas.

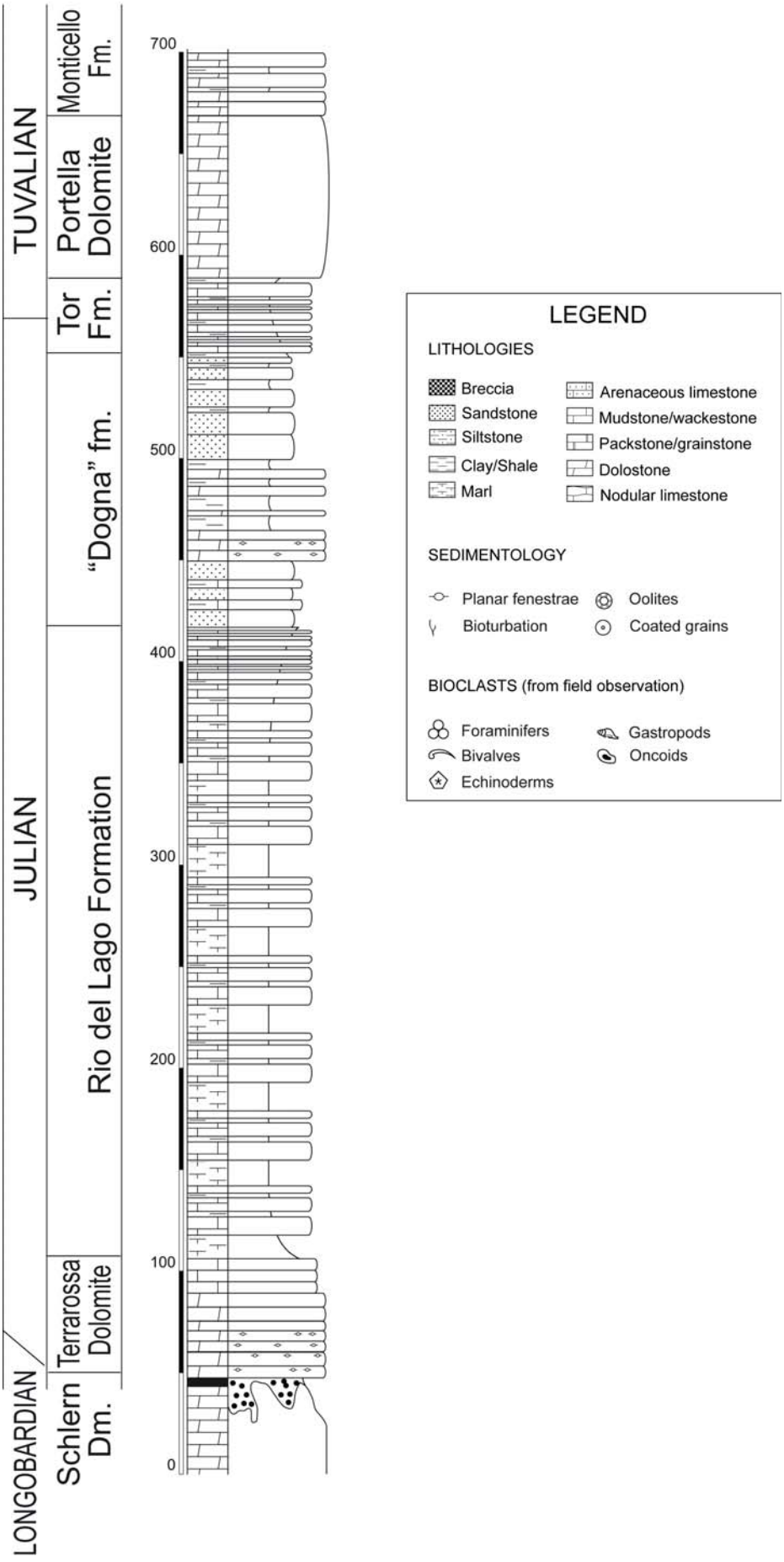

FIGURE 5 - Carnian stratigraphy of the Dogna area (modified from Preto et al., 2005).

1.2 METHODS

1.2.1 Sample collection and preparation

The Carnian succession of the Dogna area has been studied and sampled in five different localities: Gran Colle, Rio Pontuz, Rio di Terrarossa, Dogna river, Rio Mas. (Fig. 4)

Three hundred and forty meters of stratigraphic sections have been logged, and a total of 155 samples for thin section have been collected. Sterile or excessively diagenized samples have been excluded from petrographical analysis.

A total of 106 stained thin sections from the lower Carnian units of the Dogna area have been effectively analyzed with a polarizing microscope. Samples from the Rio di Terrarossa Dm. have been collected in the Rio Pontuz section (11 samples). The Rio del Lago Fm. has been studied in the Rio Pontuz section (7 samples), in the Rio di Terrarossa section (34 samples) and in the Gran Colle section (44 samples). The overlying "Dogna fm." (3 samples) and Tor Fm. (7 samples) have been analyzed in the Pontuz and Dogna river sections, respectively, for comparison purposes and to discriminate changes in the sedimentary environment.

The abundant matrix component was investigated separately. Average micrite content was estimated from visual comparison charts from Baccelle and Bosellini (1965).

SEM (scanning electron microscopy) analyses were performed on eighteen well-preserved samples from the Rio del Lago Fm., selected as representative of the various facies associations, in order to investigate the origin of carbonate mud (see Table 4 for list). Blocks of the samples were mounted on glasses, polished and etched with 0.1 N hydrochloric acid for 20-40 seconds.

1.2.2 Counting technique and tabulation

The variable, but mostly high matrix (micrite or pseudosparite) content of the studied samples required a slightly modified counting technique.

A pure traditional point count (Dunham, 1962; Purdy, 1963) with a fixed grid could have missed completely some small bioclast categories, unless thousands of points per section were counted. Conversely, a conventional, predetermined area-count (Flügel, 1996 and references therein) could have provided an insufficient number of grains for significant statistical analyses in certain matrix-dominated lithologies.

The method applied to the present study (a "weighted" area counting) consists in the counting of all bioclasts in a set of adjacent square mm, until 500 determinations are reached. Interstitial component is excluded from counting.

Estimations made on this number of points have a maximum standard deviation on rough counting of 4.5%, with a 95% reliability (Van der Plas and Tobi, 1965). The counting has been

performed with a transparent millimeter grid superimposed on the thin section, thus avoiding multiple evaluations of grains.

Since most grains have average constant dimensions, this counting approach preserves the relative abundances of each category between samples, thus allowing cluster analysis. On the other hand, relative volumes of categories and the grain/matrix ratio are lost with this counting technique.

Nine broad categories of bioclasts have been recognized: foraminifers, bivalves, gastropods, ostracods, echinoderms, calcareous green algae, bryozoans, sponges, and others (undetermined). Foraminifers have been subdivided into four sub-classes on the base of their test (hyaline, porcelanous, agglutinated, aragonitic) and bivalves have been subdivided into two sub-categories depending on the mineralogy of shell (calcitic or aragonitic).

Within some categories, separate evaluation of large (> 1mm) and small (< 1mm) individuals, and of fragments vs. entire individuals has been carried out in order to account for strong dimensional variability and to weight where possible the relative contributions of the component.

Foraminifers and gastropods have always been counted as entire exemplars because of their low susceptibility to fragmentation.

Single fragments/parts of echinoderms, calcareous green algae and sponge spicules have been considered as unit determinations for the impracticality of determining the relative contribution of each fragment to a whole individual. These grains show narrow dimension variability.

Single valves of small aragonitic bivalves and ostracods were straightforwardly considered half an individual.

Calcite bivalves were evaluated by counting the number of single prisms within each piece/valve/individual.

Finally, extension of macroscopic aragonitic bivalves was measured with the transparent millimeter paper, and this value was added to the number of small individuals, whose area is stated as unitary. This was necessary because aragonitic bivalves are present in a large range of dimensions.

1.2.3 Statistical analyses

Data from quantitative petrographic analyses have been analyzed with multivariate statistics in order to objectively assess petrofacies. Hierarchical Q-mode cluster analysis has been applied in order to extract distinct, statistically-significant groups from the continuous data set.

The selected dataset is formed by 106 samples (i.e. thin sections), each composed of 13 variables (percent abundances of bioclast types).

Calculations have been performed with “Euclidean” distance between samples. Firstly, “Single” clustering technique was used in order to detect outliers. Then, “Ward’s” clustering method was ultimately used in order to obtain small-size, easily-readable clusters without dispersed samples (see next § for specifications).

This process has been applied to the entire data set as well as to the Rio del Lago Fm. only, in order to 1) confirm and improve sedimentary environment reconstruction and detect its possible variations in time, and 2) distinguish sub-environment divisions of the lower Carnian subtidal carbonate ramp (mostly represented in the Rio del Lago Fm.) on the base of petrofacies.

1.2.3.1 Cluster analysis specifications

This ordination technique operates in two steps: 1) detecting distance between observations and similarity between samples (Q-mode), or categories (R-mode); and 2) collecting them in clusters so that distance (dissimilarity) between groups results maximized.

In the present study, a Q-mode analysis was operated (similarity between samples = composition) so that the clusters indicated genetically-related groups (petrofacies).

The approach was as follows:

1) the distance calculation was performed with the “Euclidean” formula (sum of coordinates’ squares in a N-dimension space, with N = number of categories). For the present study, N = 13.

2) two different cluster creation algorithms were used at different stages. First, a *Single* linkage was performed in order to detect outliers. *Single linkage*, also called *nearest neighbor*, uses the smallest distance between objects in the two groups. Hence, those samples with the larger distance and isolated can be considered as outliers.

Final clustering was then performed with the *Ward*’s method, also known as *Minimum Variance*. Clusters are formed in order to minimize the increase in the within-cluster sums of squares. The within-cluster sum of squares is defined as the sum of the squares of the distance between all objects in the cluster and the centroid of the cluster. In other words, the distance between two clusters is the increase in these sums of squares if the two clusters were merged.

The Ward's method has a strong tendency to split data in groups of roughly equal size. This means that when the "natural" clusters differ much in size, the big ones will be split in smaller parts roughly equal in size to the smaller "natural" clusters.

The advantage of Ward's Method is that it doesn't leave any "loose ends": no clusters with only one or a few elements. All data is grouped in smaller portions, which are easier to evaluate.

1.3 SEDIMENTOLOGY

Lower Carnian Rio di Terrarossa Dm. and Rio del Lago Fm. (including the Rio Pontuz oolite in its lower part) have been investigated under a sedimentological and petrographical profile. Petrofacies analysis (§ 1.4) was not incorporated in the recognition of lithofacies associations, but have been integrated in a later stage in order to improve sub-environment discrimination.

On the whole, 8 lithofacies associations and 17 lithofacies have been recognized from fieldwork data, and are summarized in Tables 1 and 2. The overlying "Dogna" and Tor formations (upper Carnian) differ from the lower Carnian units for a greater terrigenous component, but all formed in a shallow-marine setting (see also Preto et al., 2005).

Fm.	Code	Lithology	Layers	Sedimentary structures	Fossils
RTR Dm.	A	Bioclastic dolostone	Sharp to slightly undulose. cm-thick.	Structureless or plane-parallel laminated.	Algal nodules (oncoids), rare bivalves and gastropods.
	B	Laminated dolostone	Sharp. cm-to dm- thick.	Algal lamination (stromatolites); tepee/sheet cracks, planar fenestrae.	Rare ostracods.
	C	Flat pebble breccia	Sharp to erosive cm-thick.	Structureless.	None.
	D	Mudstone/ wackestone	Sharp to slightly nodular. dm-thick.	Structureless to bioturbated.	Scattered bivalves, secondary echinoderms and foraminifers.
	E	Packstones	Sharp to slightly nodular. dm-thick.	Structureless to bioturbated.	Foraminifers, molluscs, and echinoderms.
RP oolite	F	Oolite/bioclastic grainstone	Mainly sharp. dm-thick.	From structureless to large scale cross-bedded.	Bivalves, gastropods, foraminifers, algae, echinoderms, plant debris.
	G	Oolite/bioclastic wackestone/ packstone	Mainly sharp. dm-thick.	From structureless to large scale cross-bedded.	Bivalves, foraminifers, calcareous algae including dasycladaceans.
	H	Algal bindstone	Mainly sharp. dm-thick.	Algal lamination.	Algae fragments, ostracods.
RdL/ Dogna /Tor Fms.	I	Marls/silty marls	Sharp. cm- to m-thick	Plane-parallel lamination.	Bivalves, plant debris, occasional cephalopods.
	J	Thin mudstones/ wackestones	Sharp to undulose. cm-thick.	Structureless to bioturbated.	Foraminifers, algae, secondarily bivalves.
	K	Thin wackestones/ packstones	Sharp to erosive. cm-thick.	Plane-parallel lamination, normal grading, shell carpets, occasionally preferential orientation of valves.	Bivalves, foraminifers, echinoderms, occasionally cephalopods and plant remains.
	L	Marly wackestone/ packstone	Sharp. dm-thick.	Slightly bioturbated.	Foraminifers, bivalves, echinoderms.
	M	Wackestone/ packstone	Sharp. dm-thick.	Structureless to plane-parallel laminated. Slightly bioturbated.	Foraminifers, algae, secondarily echinoderms and bivalves.
	N	Nodular wackestone/ packstone	Undulose to strongly nodular. dm-thick.	Structureless to plane-parallel laminated. Bioturbated.	Bivalves, calcareous algae, foraminifers, sponge spicules.
	O	Silty arenites	Sharp to undulose. cm- to dm-thick.	Mainly structureless; small-scale cross lamination occur. Bioturbated.	Bivalves, echinoderms, plant debris.
	P	Mudstone	Sharp. cm- to dm-thick.	Structureless.	None.

TABLE 1 - Main features of studied Carnian units: lithology, bedding, sedimentary structures and fossil content. RTR Dm.= Rio di Terrarossa Dolomite; RP oolite= Rio Pontuz oolite; RdL Fm.= Rio del Lago Formation.

Formation	Facies association	Main lithologies	Sedimentary environment - interpretation
RTR Dm.	1 (A, B, C)	Dolostone	Carbonate internal lagoon/tidal flat
	2 (D, E)	(Marly) wackestone/packstones	Shallow subtidal lagoon
RP oolite	3 (F, G)	Oolite/bioclastic grainstone/packstones	Near-surface, high-energy ooid shoal barrier (inner ramp)
	4 (G, H)	Algal wackestone/bindstones	Shallow subtidal inner ramp – algal meadow
RdL Fm. "Dogna" fm. Tor Fm.	5 (I, M, N, O)	Wackestone/packstones, minor arenites	Upper shoreface (inner ramp)
	6 (I, J, K, L)	Alternated wackestone/packstones and siltstone/marls	Median ramp (with storm influence)
	7 (K, P)	Mudstone and siltstone/marls	Outer ramp

TABLE 2 - Facies associations and depositional setting of the studied units. Abbreviations as in Table 1.

1.3.1 Facies association 1: lower Rio di Terrarossa Dolomite

Lower Rio di Terrarossa Dolomite is a 10m thickening-upward dolomitic succession of dm-thick sedimentary cycles. It lies above a deeply karstified surface with pockets of flat/black-pebble breccia infilling karst cavities up to 3 m-deep at the Rio Pontuz section (Fig. 10A), or above a pedogenetic horizon (bauxite) at the Rio di Terrarossa section (Jadoul et al., 2002) (Figure 6).

Sedimentary cycles start with slightly nodular, faint-laminated dolostones with molluscs, lithoclasts and intraclasts (facies A). Coquina beds and erosive-based bivalve concentrations also occur.

Dolostones with both stromatolite laminae and planar fenestrae, mud/sheet cracks and small tepees (facies B) are present in the upper part of cycles. Breccias (facies C), in some cases with flat pebbles, may be also present as separate layers or as breccia horizons on top of rocks of the facies A. The entire succession is thickening upwards due to the increase in occurrence of the nodular limestones (facies A).

Interpretation: Peritidal succession formed in a carbonate internal lagoon/tidal flat environment with a deepening trend, suggested by the thickening-upwards trend. Coquinas with erosive base may represent storms.

1.3.2 Facies association 2: upper Rio di Terrarossa Dolomite

Upper Rio di Terrarossa Dolomite succession is about 20m thick. It is represented by alternated intervals of bioclastic wackestones and packstones in cm- to dm- thick structureless layers, commonly bioturbated, with marl interlayers. Carbonate micrite content increases upwards (Fig. 6).

Wackestones (facies D) are arranged both in dm-thick stacks of cm-thick beds, and in distinct dm-thick layers, in some cases nodular. They mainly contain bivalves, echinoderms and foraminifers; calcareous sponge spicules are found as well.

Packstones (facies E) are organized in dm- to m-thick packages of cm- to dm-thick layers, and are generally slightly more bioturbated than wackestones. Fossils are mainly foraminifers, bivalves and echinoderms. Scattered reworked oolite are present.

In the upper part of the upper Rio di Terrarossa Dolomite the terrigenous component increases. Few, dm-thick silt intervals can be found. Slightly nodular, dm-thick mudstone to wackestone layers with increasing silty interlayers dominate.

Interpretation: low-energy, shallow subtidal lagoon. Reworked ooids, possibly transported landwards in washover fans by storms, testify the presence of an oolitic bar in the seaward margin.

1.3.3 Facies associations 3 and 4: Rio Pontuz oolite

Rio Pontuz oolite is a 20 m-thick sequence of oolitic grainstones/packstones with intraclasts, bivalves, echinoderms and algal remains. Bioturbation is common. It crops out in the Rio Pontuz and Rio Mas sections. The boundary with the underlying Rio di Terrarossa Dolomite is gradational, by alternation (Figure 6).

Lowermost grainstones (facies F, facies association 3) show alternated thickening/thinning-upwards, meter-thick stacks of sharp-based, in cm- to dm-thick structureless layers. They are capped by thickening-upwards nodular grainstone layers, with large-scale cross bedding and marl intercalations. A 2-m thick interval of intercalated, dm-thick marly mudstones and wackestones follows, with low fossil content (rare molluscs) (facies D of facies association 2).

The upper part of the Rio Pontuz oolite (facies association 4) is represented by alternated thickening/thinning-upwards, dm- to m-thick successions of oolite-bioclastic grainstones and packstones (facies G) in dm-thick, structureless layers with some bioturbation, or large-scale cross bedding in some cases.

At the top of the Rio Pontuz oolite a 75 cm-thick layer of algal wackestone/bindstone is present (facies H of facies association 4), featuring algal lamination and containing fragments and stems of calcareous algae, both scattered or concentrated in levels, and some connected ostracods.

Interpretation: high-energy, backstepping oolite bar, at the edge of the Rio di Terrarossa Dolomite lagoon. In the seaward margin a calcareous algal meadow is present. One episode of progradation of the lagoon over the bar is recorded at Rio Pontuz by a thin interval of intercalated marly mudstones and wackestones.

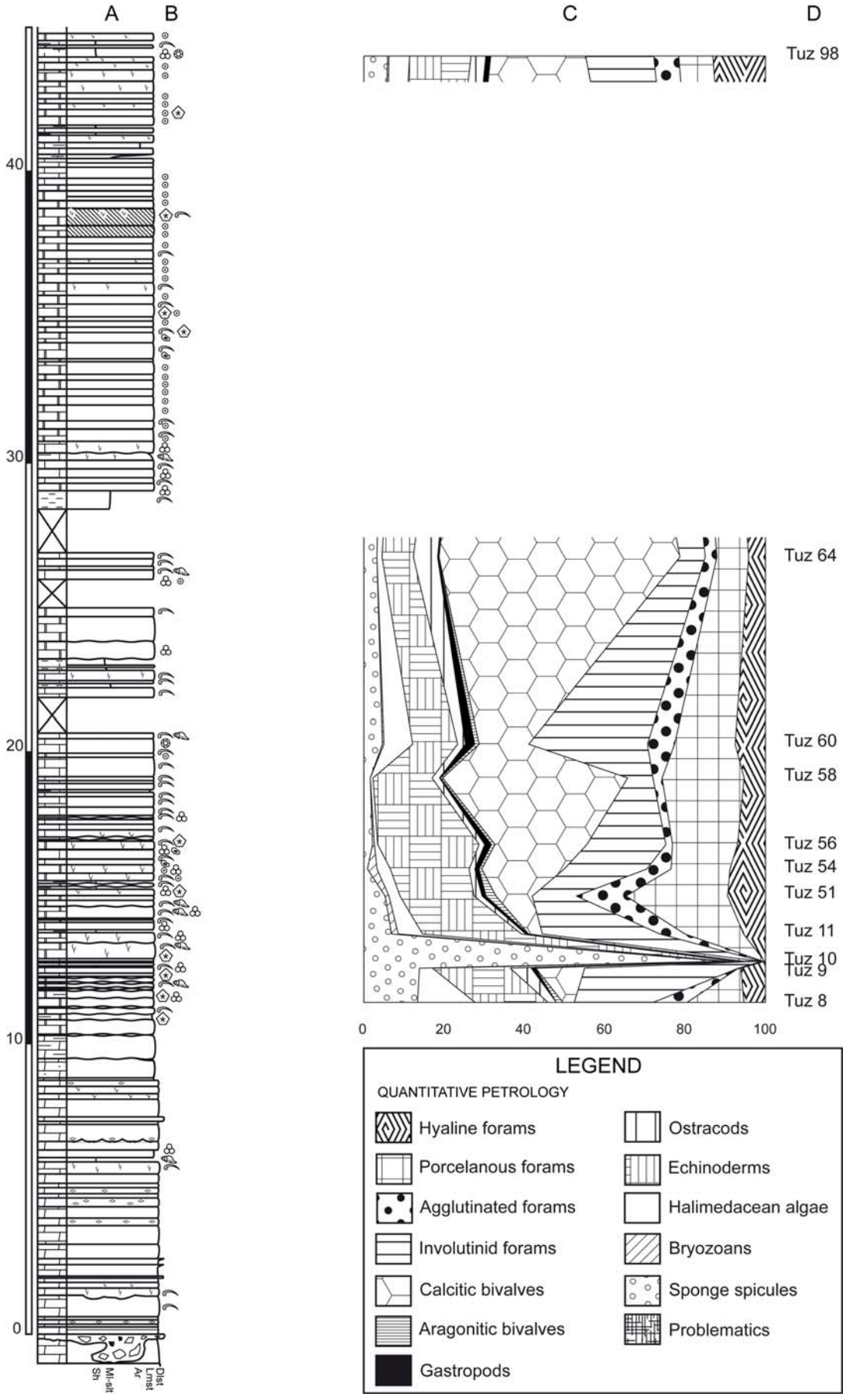

FIGURE 6 - Lithologic logs and petrography results, Rio di Terrarossa Dolomite and Rio Pontuz oolite, Rio Pontuz section. A) Lithological log (same legend as Figure 5). Sh: shales; Ml/Slt: marl/siltstones; Ar: arenites; Lmst: limestones; Dlst: dolostones. B) Bioclasts (from field observation). Same legend as Figure 5. C) Quantitative petrology. D) Sample labels.

1.3.4 Facies Associations 5, 6, 7 and 8: Rio del Lago and Tor Formations

The sudden increase in micrite and siliciclastics and the absence of oolites mark the onset of the Rio del Lago Formation, which lower boundary is exposed at the Rio Pontuz and Rio Mas sections (Figure 7).

The lower Rio del Lago Formation crops out in the Rio Pontuz, Rio Mas and Rio di Terrarossa sections. Rio di Terrarossa exhibits the longer succession, which is ca.150 m thick (Preto et al., 2005), (Figures 5 and 6).

It mainly consists of cm- to dm-thick layers of bioclastic wackestone/packstones, organized in dm-to m-thick banks (facies association 5) or intercalated to silty marls (facies association 6) (Fig. 10B).

Thick wackestone/packstone banks (facies association 5) are up to 1 m-thick, intensively bioturbated, structureless, and contain bivalves, calcareous green algae, foraminifers and secondarily sponge spicules and echinoderm fragments.

Thin (cm- to dm-thick) alternations of bioclastic wackestone/packstone and marls/silty marls can be found in intervals up to 3 m-thick (facies association 6). Within each interval, both structureless, slightly nodular and/or flow-laminated wackestones and packstones can occur. Erosive base, normal grading, shell concentration and iso-orientation of valves are other transportation features. Fossil content is represented by foraminifers, algae, bivalves and echinoderms.

For some intervals the mudstone/wackestone intercalations within marls/silty marls result thinner (cm- to dm-thick) and scattered (facies association 6), are in some cases lens-shaped and have a lower, smaller-size fossil content. Those intervals, up to 2 m-thick, occur throughout the succession.

Fine terrigenous intervals, up to 3m-thick, also occur in the upper part of the succession (facies I).

Minor occurrences are marly wackestone/packstone (facies L, facies association 5), arenite layers (facies O, facies association 5) and thin intercalations of mudstone and siltstone/marl (facies association 7).

Upper Rio del Lago Formation succession is only visible at the 80 m-thick Gran Colle section. It is characterized by higher abundance of facies associations 5, 6 and 8 (Figure 11).

Interpretation: On the whole, the lower Rio del Lago Formation represents a carbonate ramp environment with strong siliciclastic input. Inner and median ramp prevail over deeper facies. Inner ramp facies are represented by thick bioclastic wackestone/packstone banks, often bioturbated (facies association 5). Median ramp facies are represented by arrangements of thin

wackestone/packstone and fine siliciclastics (facies association 6). Storm layers are common, and imply landward and seaward transportation of bioclasts and carbonate mud. In the upper Rio del Lago Formation, lower-energy median and outer ramp facies (facies association 6 and 7) slightly prevail over inner and median ramp facies, testifying a continuous, minor deepening trend.

The carbonates of overlying units ("Dogna" fm. and Tor Fm.) are described by the same facies associations. The onset of the "Dogna" fm. is characterized by thick layers of massive arenites (Fig. 10C). The following Tor Fm. testifies the recovery of the carbonate platform (Figure 12, Fig. 10D).

All facies associations may be arranged in a complex, storm-influenced carbonate ramp system with terrigenous influx, which inner part comprises a lagoon, a tidal flat and an oolite shoal margin with an algal meadow on the front, as shown in Figure 16. The facies associations described in § 3.1 to 3.4 are now found in vertical superposition (Rio Pontuz and Rio Mas sections), testifying a long-term transgression that lasted, in the Dogna area, during most of the early Carnian.

Peculiarity of this arrangement is the coexistence of contrasting features such as a sparite-cemented oolite bar associated with an algal meadow (Rio Pontuz oolite, facies associations 3-4), typical of tropical carbonates, and facies dominated by heterotrophic organisms (Rio del Lago Fm., facies associations 5-7), which would better fit into a cool-water factory, although unusually rich in micrite.

Major parts of the ramp can be identified already from sedimentological and stratigraphical field observation. In the next chapters, quantitative petrographic studies and multivariate statistical techniques will be used to endeavor a more detailed ramp characterization and to complete sedimentological and paleontological data.

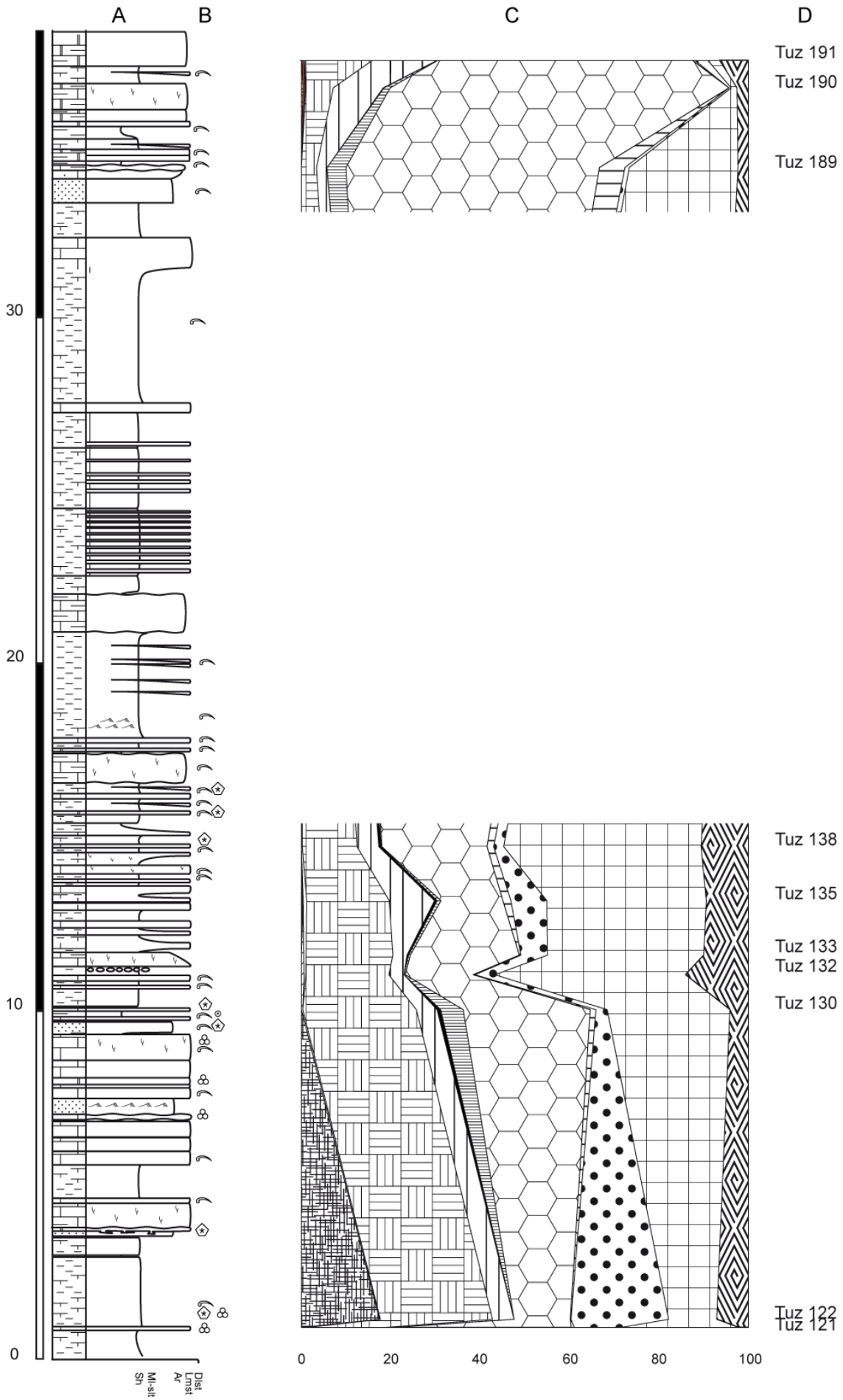

FIGURE 7 - Lithologic logs and petrography results, Rio del Lago Fm., Rio Pontuz section. Legend as in Figg. 2 and 3.

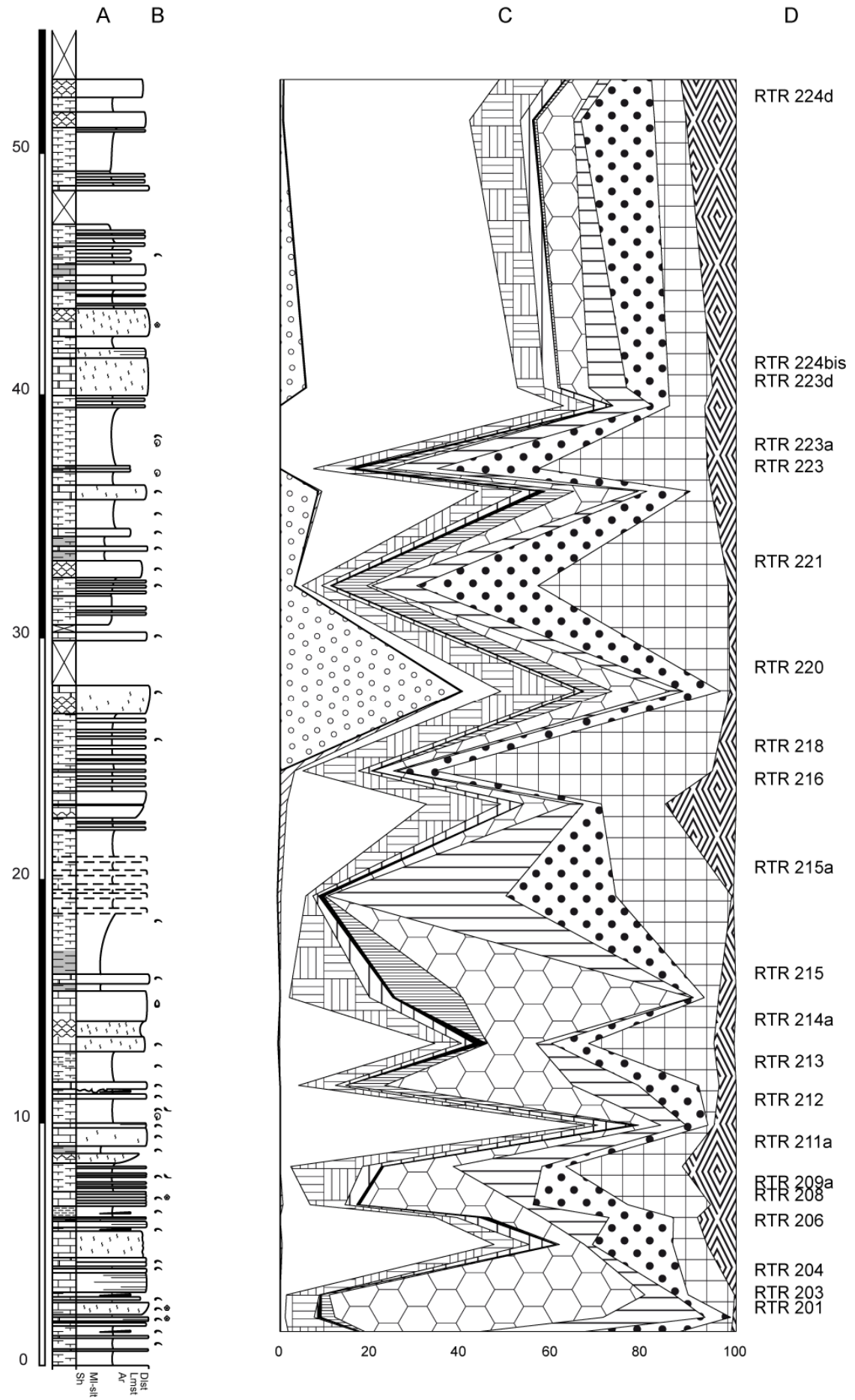

FIGURE 8 - Lithologic logs and petrography results, Rio del Lago Fm., lower part, Rio di Terrarossa section. Legend as in Figg. 2 and 3.

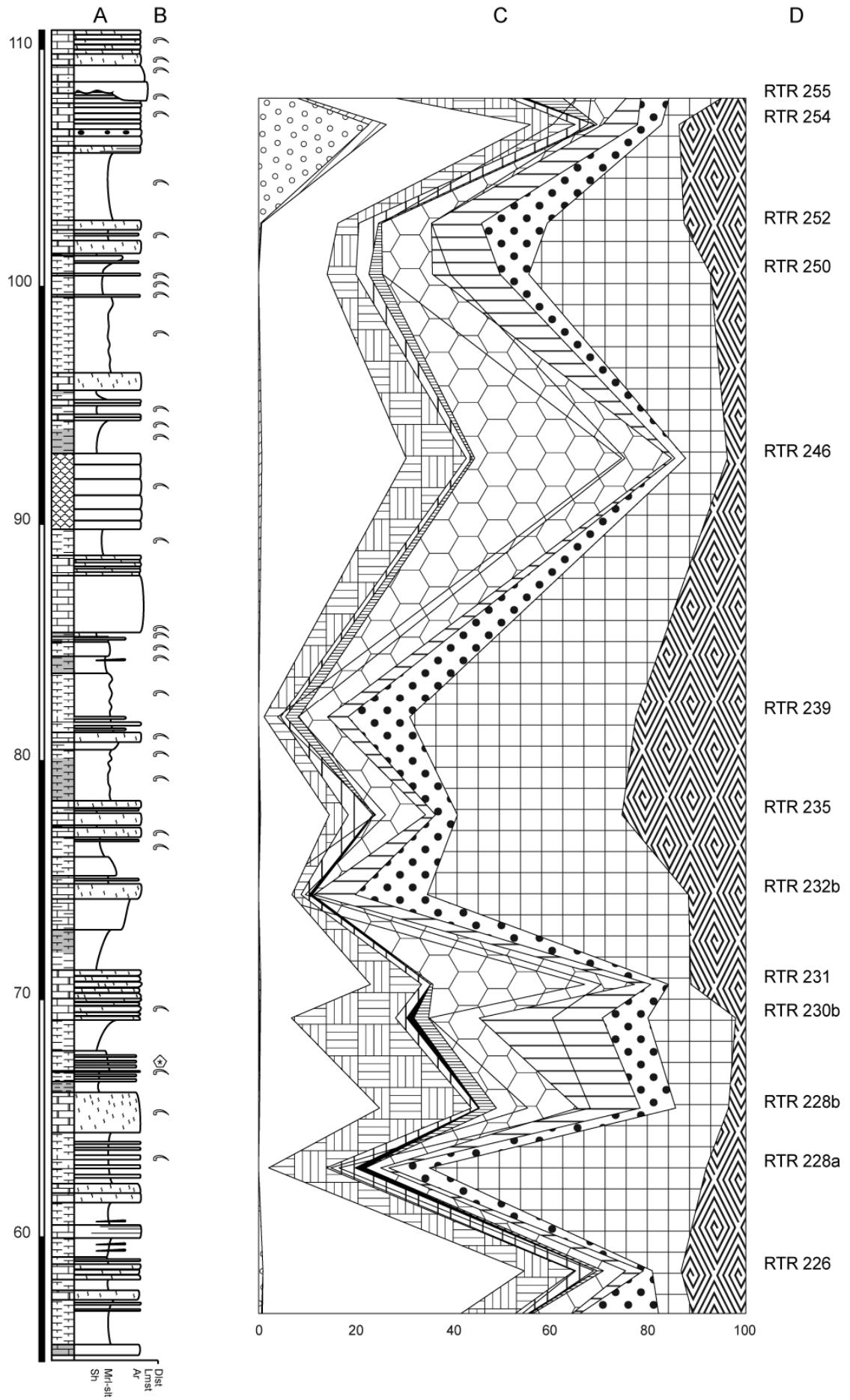

FIGURE 9 - Lithologic logs and petrography results, Rio del Lago Fm., upper part, Rio di Terrarossa section. Legend as in Figg. 2 and 3.

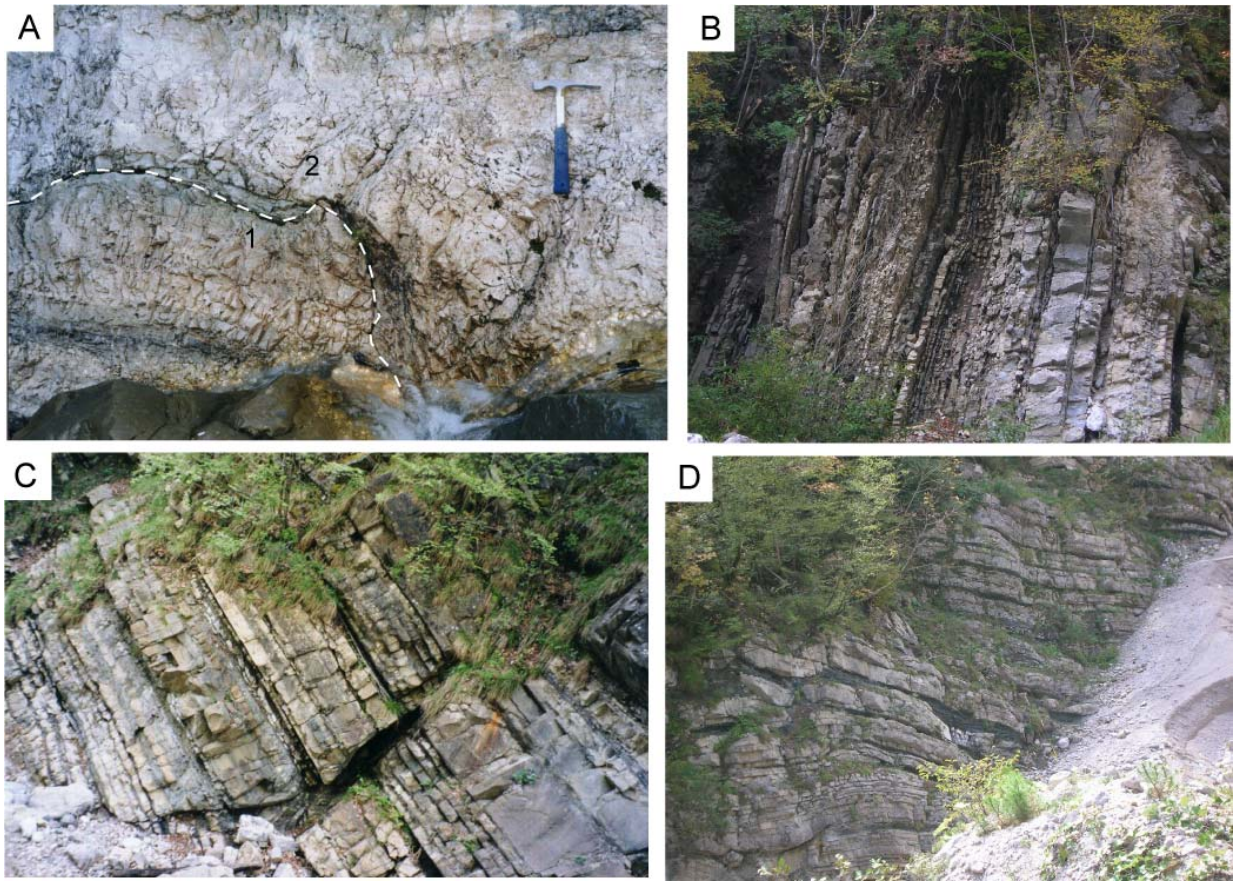

FIGURE 10 - Lithofacies of the Dogna carbonate ramp. A) Karstified erosional top of the Schlern carbonate platform (1), and base of Rio di Terrarossa Dolomite (2), Rio Pontuz section. Dashed line: erosional surface. B) Rio del Lago Fm., Rio di Terrarossa section. From the left side: tight intercalation of marls and dm-thick wackestone layers (facies ass. 6, median ramp), followed by a package of thin, nodular wackestone-packstone (facies ass. 5, inner ramp). In the centre: tight intercalation of cm- to dm-thick layers of wackestone and clay-marls (facies ass. 6, median ramp), followed by a package of nodular wackestone-packstones (facies ass. 5, inner ramp). To the right: dm-thick layer of slightly nodular packstones (f. ass. 5, inner ramp), followed by a package of cm-to dm-thick wackestone-packstones (f. ass. 5, inner ramp). C) Arenites of the "Dogna" fm., Rio Pontuz section. D) Tor Fm., Rio Mas section. From bottom to top: m-thick package of cm-thick packstone layers (f. ass. 5, inner ramp), followed by a m-thick package of dm-thick wackestone/packstone intercalated to marl/silt (f. ass. 6, median ramp) culminating with 50 cm thick dark shales (f. ass. 8, outer ramp). Shallower deposits then follow (dm-thick wackestone-packstones intercalated to marl/silt, and slightly nodular dm-thick packstones: f. ass. 6, median ramp and 5, inner ramp).

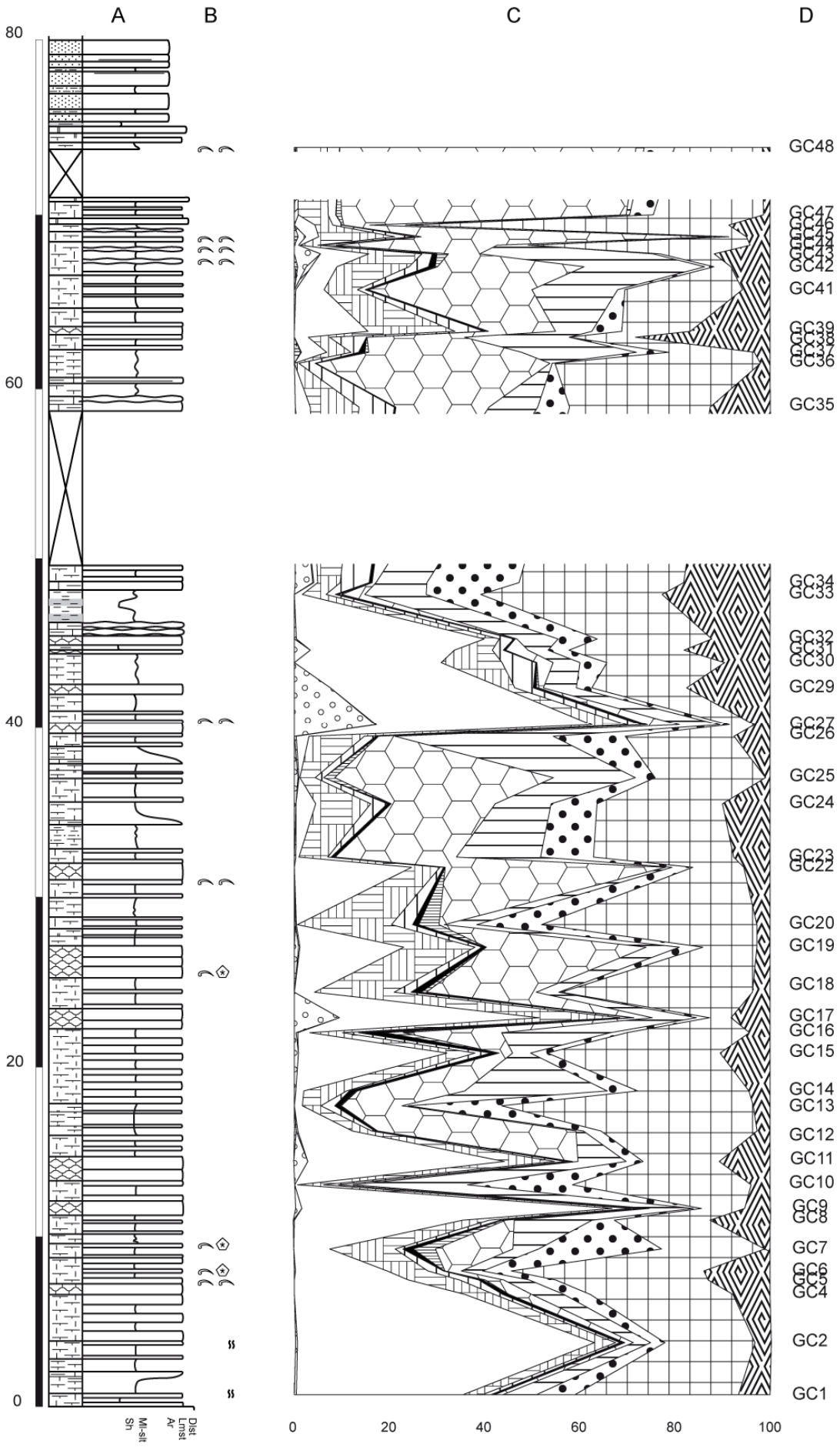

FIGURE 11 - Lithological logs and petrography results, uppermost Rio del Lago Fm., Gran Colle section. Legend as in Figg. 2 and 3.

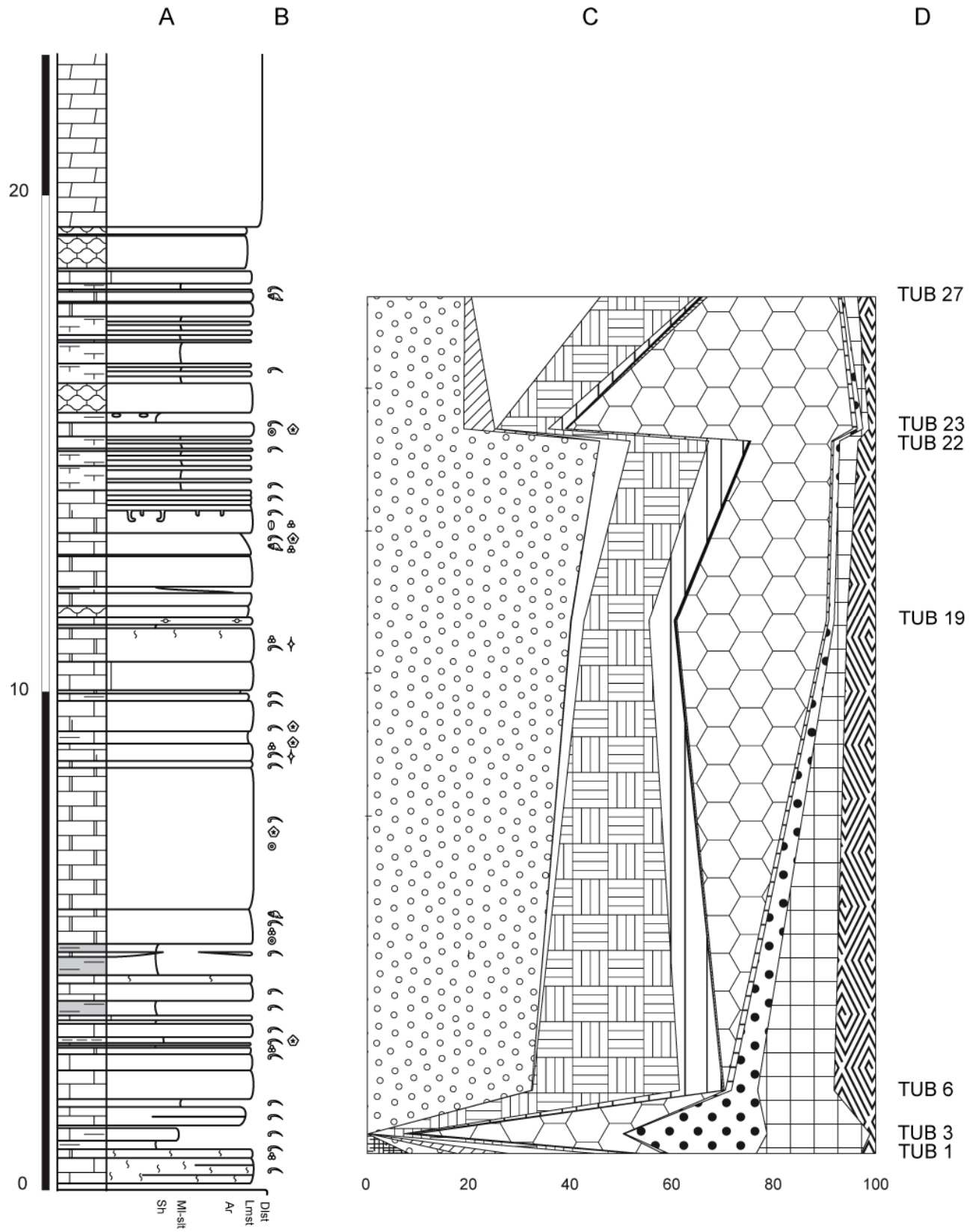

FIGURE 12 - Lithological logs and petrography results, Tor Fm., Rio Mas section. Legend as in Figg. 2 and 3.

1.4 PETROLOGY

1.4.1 Components

1.4.1.1 Major skeletal grains

Thirteen categories of bioclasts have been recognized. Microfacies composition and distribution are summarized in Table 3. The main skeletal components are: bivalves (calcitic and aragonitic), foraminifers (4 classes), algae and echinoderms.

Bivalves are one of the most important components of the studied succession. They represent 21% of the components on average, reaching a maximum of 77%.

They have been found both as articulated shells, disarticulated valves and small fragments (Fig. 14A). Valves are typically fragmented and disarticulated in inner ramp facies (facies ass. 5), whereas complete individuals are mainly found in median ramp facies (facies ass. 6).

Shell structure of calcitic bivalves is prismatic, recrystallized aragonite shells occur as well.

Benthic foraminifers are widespread in all the thin sections examined, ranging from 1% (facies C, Rio di Terrarossa Dolomite) to 89% (facies K, median ramp). Four groups of foraminifers were identified: hyalines, agglutinated, porcelanous and aragonitic.

Hyalines are found both entire and, secondarily, in single-chamber fragments (Fig. 14B). They constitute the 7% of the components on average and they are particularly abundant in inner and median ramp environments, where they reach a maximum abundance of 28%

They belong mainly to the family *Nodosariidae* Ehrenberg, 1838.

Entire, thin- and thick-walled, small (< 0.2mm) and large (> 0.2mm) forms of agglutinated foraminifers are found (Fig. 14A).

They appear to be inversely proportional to hyaline varieties, and range from less than 1% to 28% (facies K, with pervasive encrusting foraminifers).

They are tentatively attributed mainly to the family *"Trochamminidae"* Schwager, 1877 and partly to the family *Ammodiscidae* Reuss, 1862.

Small, thin-walled porcelanous foraminifers are always found as complete tests (Fig. 14E).

They result very common in Rio di Terrarossa Dolomite and Rio Pontuz oolite, becoming abundant in the Rio del Lago Fm (facies K).

Average content is 21%, with a maximum amount of 67%.

They have been recognized as belonging to the family *Ophtalmidiidae* Wiesner, 1920, and to the family *Meandrospiridae* Saidova, 1981.

Lens-shaped, thick-layered aragonitic foraminifers are found almost exclusively as entire specimens substituted by sparite (Fig. 14E and 10A). Remnants of the original aragonitic mineralogy were observed at the SEM (Figure 15F).

Aragonitic foraminifers range from very low relative abundances to 39%.

They primarily belong to the family *Aulotortidae* Zaninetti, 1984, and secondarily to the family *Triadodiscidae* Zaninetti, 1984.

Category	Average abundance (max)	Main facies	Stratigraphic units	Notes
Bivalves	21 (77)%	M, K	Rio del Lago Fm.	Absent only in some foraminifer- and algae-dominated inner and median ramp samples (facies N and K).
Foraminifers	45 (89)%	J, K, G	Rio Pontuz oolite, Rio del Lago Fm.	Dominant in facies J and K (median ramp) of the Rio del Lago Fm.
Calcareous green algae	14 (67)%	N, K	Rio del Lago Fm.	The association green algae/hyaline foraminifers is typical of inner ramp facies (M and N).
Echinoderms	10 (29)%	K	Rio di Terrarossa Dm., Rio Pontuz oolite, Rio del Lago Fm.	Lower amounts are found in the lower Rio del Lago Fm., increasing again in the upper part of the Fm.
Gastropods	<1 (5)%	K	Rio del Lago Fm.	
Ostracods	<1 (14)%	M	"Dogna" fm.	
Sponge spicules	4 (89)%	M, N	Rio del Lago Fm.	Unusually high concentration of sponge spicules found in subtidal lagoon (facies C, Rio di Terrarossa Dm.). Association of spicules and foraminifers characteristic of the Tor Fm. (facies M and N).
Bryozoans	<1 (10) %	N	Tor Fm.	
Problematics	<1 (14) %	J, K	Rio del Lago Fm.	

TABLE 3 - Summary of bioclasts distribution. Overview of relative amount of bioclasts in relation to facies and formation. Facies code as in Table 2.

1.4.1.2 Calcareous green algae

These components occur in most cases as strongly elongated or irregular fragments of branches with elliptical or circular section, replaced by sparite (Fig. 14D and 10A). The original mineralogy of these algae was aragonite, as determined by SEM microscopy (Figure 15C, D). In some instances, and especially in large fragments, a central cavity is visible. These fragments have been determined as belonging to genus *Collarecodium* (Brandner and Resch, 1980, Senowbari-Daryan and Zamparelli, 2005), family Halimedaceae (Link, 1832). They are thus fragments of calcified green algae.

Uncertainties on taxonomy of calcareous green algae lead to classification of the Halimedaceae family as synonymous of Udoteaceae (Endlicher, 1834) (e.g., Senowbari-Daryan and Zamparelli, 2005, after Hillis-Colinvaux, 1984). However, recent works by Dragastan et al. (1997) and Lam and Zechman (2006) keep the two families separated. According to this last interpretation, the late Triassic algal fragments of Dogna belong to the same family of some of the most important modern carbonate producers (MacIntyre and Reid, 1992 and 1995; Milliman, 1993). Halimedacean algae content ranges from very low to about 67% (facies N and K), with average values of 14%.

1.4.1.3 Other grains

Echinoderms are 10% on average, with a range from 1% to 29%. They occur mainly as porous, single plates of echinoids (Fig. 13F), and secondarily as rounded or star-shaped crinoid fragments, and as echinoid spines. Crenulated rectangular sections of holothurian sclerite fragments are rare.

Gastropods are mainly found in thin-walled complete individuals (Fig. 14E). They are generally rare (less than 1% on average); only in one sample (facies K, median ramp, Rio del Lago Fm.) they reach 5%.

Ostracods are always present. They range from a minimum of less than 1% to a maximum value of 14% (facies M, "Dogna fm."). They occur both as small, isolated valves and as articulated specimens (Fig. 13F).

Calcareous sponge spicules are occasionally found in noticeable amounts in some inner ramp samples of the Rio del Lago Fm. (facies M and N), but usually account for only 4% of the grains on average. Exceptionally, one sample of the Rio di Terrarossa Dolomite (facies C, subtidal lagoon) displays a concentration of complete, needle-like sponge spicules (89%) together with few foraminifers (Fig. 14C).

Bryozoans appear as calcite-walled colonies. They are only an occasional component of the analyzed succession.

Problematic, tubular grains with thin micritic walls sparsely occur in some samples of facies J and K. Diameter is around 0,2mm. The longest fragment found is around 2.5mm. These elements reach a maximum abundance of 17% in the lowermost Rio del Lago Fm. (facies J, median ramp).

1.4.2 Bioerosion and microbialite encrustations

Bioerosion and microbialitic carbonate encrustations or coatings appear at several levels in the Carnian succession of the Dogna area, although microbialitic micrites are a largely minor component of fine carbonates.

First occurrences of microbial coatings are in the Rio di Terrarossa Dm., in some subtidal lagoon samples (facies C), then scattered presence is detected in the upper Rio del Lago Fm., inner ramp environment (facies M and N). Encrustations become developed and abundant only at the boundary

between Rio del Lago and "Dogna" formations, and remain frequent in the lowermost part of the latter.

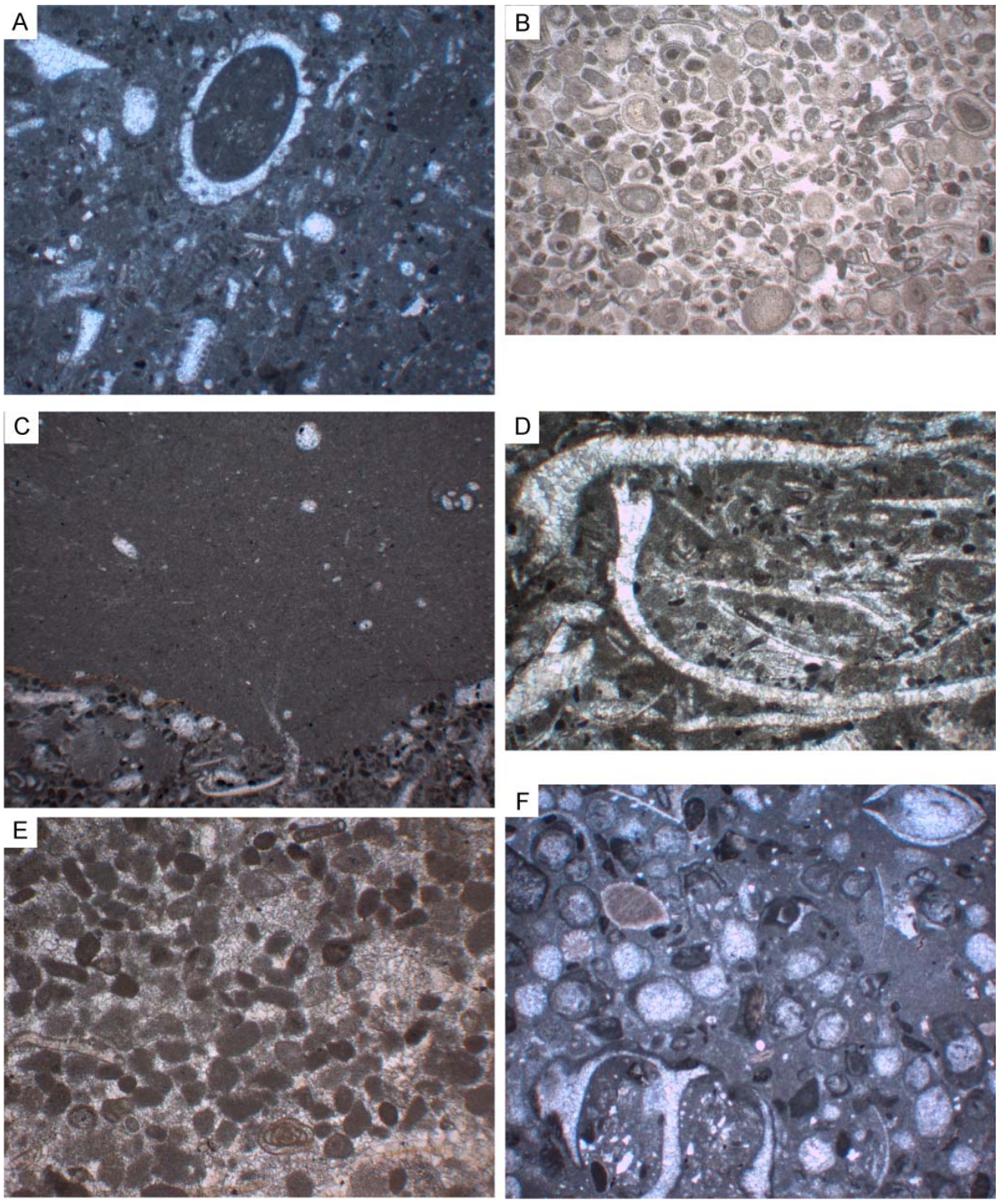

FIGURE 13 - Microfacies of the Dogna carbonate ramp. A) Packstone with codiacean algae, involutinid foraminifers and agglutinated foraminifers, Rio del Lago Fm., sample RTR 215a. B) Oolitic grainstone, Rio Pontuz oolite, sample Tuz 92. C) Erosional contact between mudstone and packstone (base of a tempestite), Rio del Lago Fm., sample Tuz 121. D) Tempestite layer with large bivalves, disarticulated, and foraminifers, Rio del Lago Fm., sample GC 25bis. Deposition by storm event is suggested by iso-orientation of elongated bioclasts, disarticulation of bivalves and wide size range of bioclasts. E) Packstone with aragonitic foraminifers, gastropods, echinoderms and ostracods, Tor Fm., sample Tub 1.

Microbialites occur as thin, lobate, clotted coatings of fine-grained micrite, mainly on bivalves and echinoderm fragments; and/or as more developed, layered coatings (up to 1mm thick).

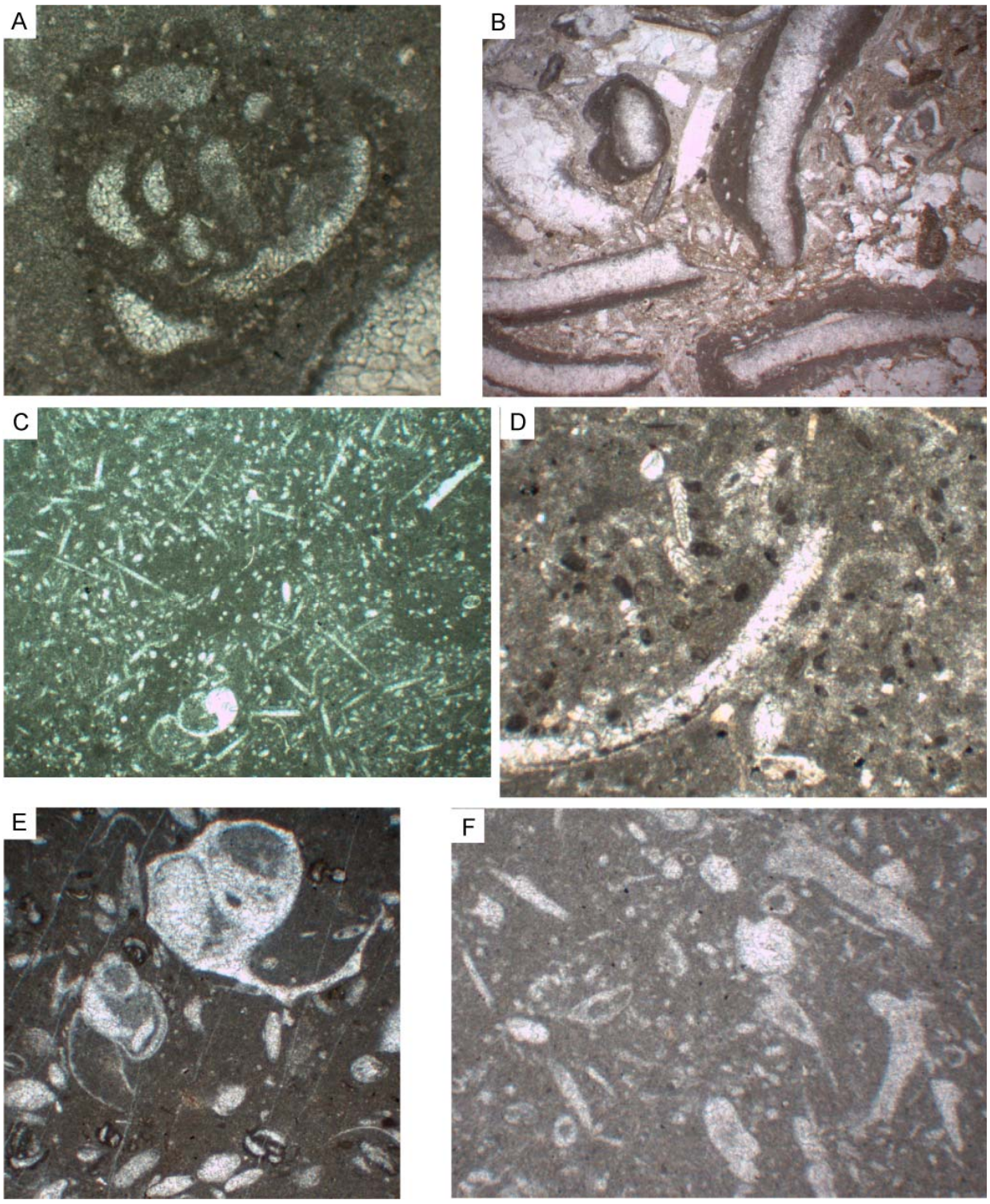

FIGURE 14 - Microphotographs of bioclasts from the Dogna carbonate ramp. A) Agglutinated foraminifer, sample RTR 213, Rio del Lago Fm. B) Bivalves with microbialite encrustations, sample GC 47, uppermost Rio del Lago Fm. C) Calcareous sponge spicules, sample Tuz 10, Rio di Terrarossa Dolomite D) Halimedacean algae (*Collarecodium* sp.), fragments of branches, sample RTR 226III, Rio del Lago Fm. E) Gastropods and porcelanous foraminifers, sample RTR 215a, Rio del Lago Fm. F) Hyaline foraminifers (arrows) associated with other foraminifers and molluscs, sample GC 44, Rio del Lago Fm.

Most of the encrusted shells have irregular, unevenly jagged outlines and variable, irregular shapes indicating micritization and bioerosion. Internal structure of the coatings often shows microscopic elongate filaments (Fig. 14F).

1.4.3 Carbonate mud

Fine carbonate matrix is present in almost all studied thin sections as interstitial material (e.g., Fig. 13A, C, D, F). Identified lithologies comprise packstones and wackestones from the subtidal lagoon (Rio di Terrarossa Dm.) to the distal ramp (Rio del Lago Fm.). This interstitial component is homogeneous and microcrystalline (between 5 and 10 μm) carbonate, i.e., microsparite sensu Folk (1959). Its volume abundance ranges from 20% (Tuz 11) to 90% (Tuz 132), with average around 45% Microsparite is always associated to bioturbation, terrigenous material and flow sedimentary structures, and is thus interpreted as the finer allochemical component, i.e., it is not automicrite.

Matrix-free, granular facies are present only in the Rio Pontuz oolite (Fig. 13B), and a layer of peloidal grainstone is present in the uppermost Rio del Lago Fm. (Fig. 13E).

SEM analyses indicate that interstitial material is mainly composed of calcite crystals slightly larger than 5 μm, with evident pits and irregular outline. Fine-grained argillaceous material is widespread (Figure 15A, B). The mineralogy of precursor carbonate mud was mostly aragonitic, as determined by the dimension and shape of calcite crystals, and by abundant pits, interpreted as vugs left by dissolved aragonite needles (e.g., Munnecke et al., 1997; Chatalov, 2007). This interpretation is confirmed by observations on bioclasts with known original mineralogy (Figure 15C, D, E, F).

Facies association 5	Facies association 6	Facies association 7
GC 8 (wks/pks)	GC 6 (wks)	TUZ 145 (mds)
GC 11 (wks/pks)	GC 8 (wks/pks)	GC 3 (mds)
GC 22 (wks/pks)	GC 10 (pks)	RTR 215b (mds)
GC 45 (wks)	GC 20 (fls)	
	GC 34 (wks/pks)	
	GC 37 (wks/pks/fls)	
	GC 42 (pks)	
	GC 44 (pks)	
	GC 46 (wks)	
	RTR 209a (wks/pks)	
	TUZ 121 (pks)	

TABLE 4 - Selected samples for SEM observations, grouped for facies associations (see § 1.3). Lithology in brackets: mds: mudstone; wks: wackestone; pks: packstone; fls: floatstone.

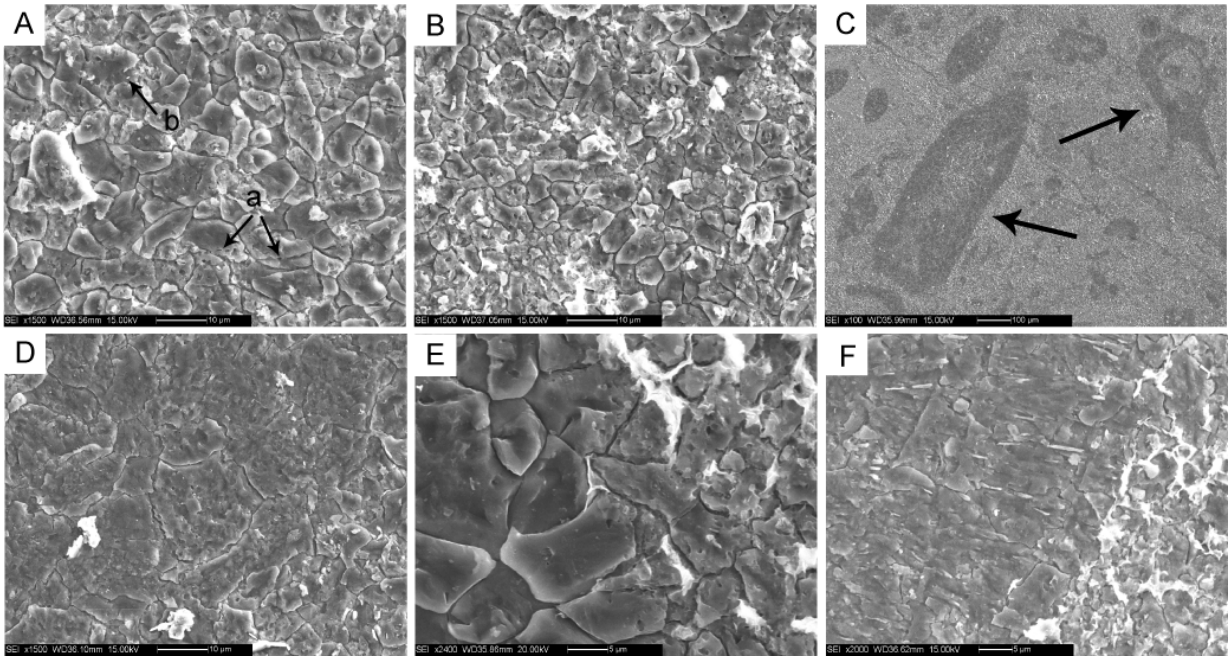

FIGURE 15 - SEM microphotographs. A) Interstitial matrix made of large microsparite crystals with pits (a) and some aragonite crystals (b). Sample GC 37. B) Pitted microsparite crystals with irregular boundaries, highlighting mainly aragonite mineralogy of the precursor, sample GC 37. C) Fragments of halimedacean algae (*Collarecodium* sp.), sample RTR 209a. D) Detail of the larger algal fragment in C. Calcite crystals within the algae show pits, and thus engulfed aragonite needles of the original algal structure, now dissolved (compare with A and F). Sample RTR 209a. E) Enlargement at the border of a calcareous sponge spicule. Microsparite calcite crystals that substituted both the spicule and carbonate mud of the matrix show pits only in correspondence of matrix. This proves pitting is not an effect of preparation (etching). Sample GC 44. F) Involutinid foraminifer with some preserved aragonite crystals. Sample RTR 209a.

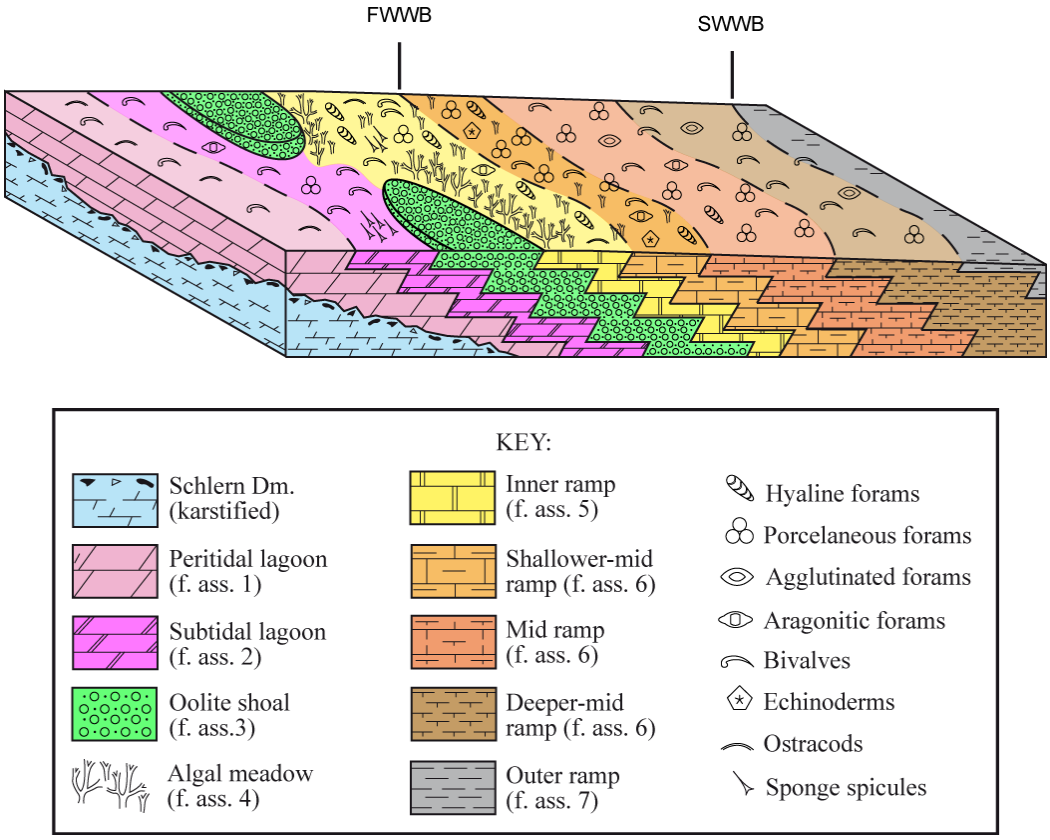

FIGURE 16 - Reconstruction of the carbonate ramp of Dogna in early Carnian times, with fine subenvironment divisions, as reconstructed by sedimentology and petrography.

1.5 CLUSTER ANALYSIS

1.5.1 Lower Carnian subtidal ramp (88 samples)

Based on fieldwork observation, the subtidal portion of the lower Carnian carbonate ramp of Dogna is represented in the Rio del Lago Fm. and lowermost "Dogna" fm.

Cluster analysis has been applied to this dataset for its capability of distinguishing statistically meaningful groups within a complex database. This approach hopefully allows detecting statistically significant petrofacies, which may then be interpreted to represent sub-environments. A two-step approach, with different methods has been used in order to 1) detect outliers and 2) obtain a subdivision of the dataset in homogeneous groups. Such groups (clusters) are then interpreted as fossilized biological associations, mirroring subenvironments of the carbonate ramp (e.g., Purdy, 1963; Smosna and Warshauer, 1978).

After the first "single" linkage, 8 samples have been excluded from the overall ramp dataset because they stand nearly isolated in the dendrogram, and they display the highest degree of dissimilarity (Fig. 17). This is due to uncharacteristic fossil contents: most of the excluded samples are in fact readily recognized as peculiar because of their unusual high content of, e.g., problematics (Tuz 122), spicules (RTR 220 and 254), ostracods (GC 7). A list of the excluded samples is available in Table 5.

Three main clusters can be subsequently identified by the "Ward's" method, each roughly subdivided into two sub-clusters (Fig. 17).

Cluster 1 groups samples dominated by halimedacean algae (31 samples).

This first cluster mainly comprises M and N facies (facies association 5, inner ramp), with only few belonging to facies J and K (facies association 6, median ramp). Samples of sub-cluster 1a (15 samples) are characterized, along with halimendacean algae, by a high foraminifer content, mainly porcelanous. Sub-group 1b (16 elements) links samples with more differentiated bioclasts. It comprises the exclusive association hyaline foraminifers/halimedacean algae (see § 4.1.2.1), and the association of these categories with echinoderms and calcareous sponges.

Cluster 2 groups samples with abundant foraminifers (37 samples). It encompasses almost exclusively median ramp (facies associations 6, facies J, K and secondarily L).

Sub-cluster 2a (12 samples) contains porcelanous-dominated foraminifer assemblages. Within sub-cluster 2a, samples belonging to facies J dominate over samples of facies K (facies ass. 6, median ramp).

Sub-group 2b (assemblages dominated by aragonitic foraminifers) (25 samples) results equally shared between samples from facies J and K (median ramp, facies ass. 6).

Cluster 3 groups bivalve-rich samples (12 samples).

The small sub-cluster 3a (4 samples) is made up only by samples belonging to the inner ramp (lithofacies M, facies ass. 5). They mainly contain bivalves and echinoderms.

Sub-cluster 3b (13 samples) reflects a prominent difference from the previous ones. It includes all three samples from the "Dogna" fm.. They mainly belong to an inner-ramp environment (facies M and N, facies ass. 5). The main characteristic of this sub-group is the presence of pervasive bioerosion and microbialite encrustations on bioclasts. This suggests that intense microbial activity and bioerosion is associated to a distinctive association of skeletal grains.

Sample label	Facies	Formation	Notes
Subtidal ramp (Rio di Terrarossa Dolomite, Rio del Lago Fm.)			
Tuz 122	J	Rio di Terrarossa Dm.	high problematics-content
RTR 203	N	Rio del Lago Fm.	high bivalves-content
RTR 213	M	Rio del Lago Fm.	foraminifers and bivalves-dominated
RTR 220 and 254	N	Rio del Lago Fm.	high sponge spicules-content
GC 7	J	Rio del Lago Fm.	ostracods-rich
GC 38	J	Rio del Lago Fm.	bivalves- and foraminifers-dominated
GC 43	N	Rio del Lago Fm.	algae and foraminifers-dominated.
Whole dataset			
Tuz 9 and 10	E	Rio di Terrarossa Dm.	calcareous-sponge spicules-dominated
TUB 1	N	Tor Fm.	high problematics-content
TUB 6, 19, 23, 27	M	Tor Fm.	spicules-rich
TUB 22	K	Tor Fm.	spicules-rich
All the outliers from the subtidal ramp dataset (except GC 43).			

TABLE 5 – Samples excluded from cluster analysis (outliers) after the first screening of the dataset with "single" linkage method. Facies code as in Table 1.

1.5.2 Whole dataset (155 samples)

Cluster analysis has been extended to the whole dataset in order to compare the facies of the Rio di Terrarossa Dm. and Tor Fm. with the subtidal ramp facies of the Rio del Lago and "Dogna" formations. Statistic procedures have been maintained as for the subtidal ramp dataset. The three-fold subdivision of samples remains recognizable, and 4 out of 6 sub-clusters identified from analysis of the only subtidal ramp are noticeably unvaried; elements characterizing clusters and sub-clusters remain the same.

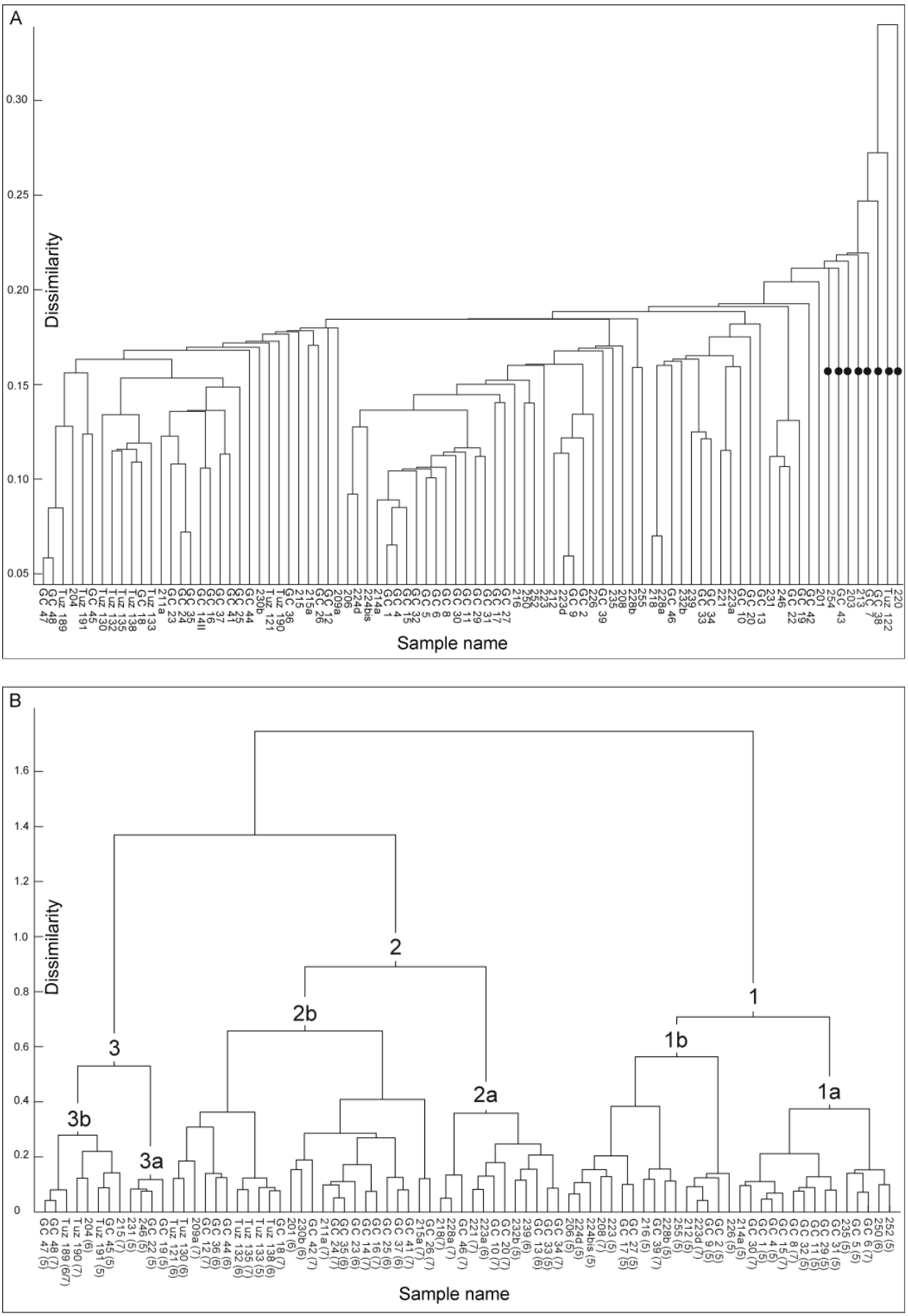

FIGURE 17 - Dendrograms for the lower Carnian subtidal ramp (Rio del Lago and "Dogna" Fms.). A) "Single" linkage; outliers are indicated with a solid circle (see Appendix I for details). B) "Ward's" linkage, after exclusion of outliers. Facies association indicated in brackets.

1.6 DISCUSSION

1.6.1 Environmental significance of petrofacies (clusters)

The use of paleontological associations characterizing petrofacies as a tool for paleoenvironmental interpretations requires fossil content to be of autochtonous or parautochtonous origin. In the studied succession the origin of paleontological associations is most likely parautochtonous, and interpretation of biotic associations as subenvironment markers is justified. Three of the nine broad bioclast categories explain most of the variability as highlighted by cluster analysis, and can be associated to bathymetric or ecological positions within a carbonate ramp. These bioclasts are bivalves, foraminifers and halimedacean algae.

A rough bathymetric subdivision from foraminifer presence/content is shown in § 4.1.1, with lagoonal facies indicated by common aragonitic foraminifers, inner ramp characterized by hyaline species, and median ramp indicated by dominant porcelanous and secondarily by agglutinated types. Bivalves are most abundant in median ramp lithofacies. The bathymetric distribution observed in the Dogna carbonate ramp is thus in agreement with observations by Schäfer and Senowbari-Daryan (1981) and Rettori et al., (1998).

Generally, comparison between petrofacies identified by cluster analysis and field sedimentological observations highlighted a good correspondence between cluster grouping and sedimentological characteristics (i.e., samples within each cluster belong to the same facies association). This allowed a refined environmental interpretation.

1.6.2 Distinction between ramp subenvironments

On the whole, three subenvironments can be distinguished in the subtidal carbonate ramp of Dogna on the base of sedimentology: inner, middle and outer ramp. Petrographical/statistical analyses confirm this identification, and improves the detail with the possible distinction of two more subenvironments.

Inner ramp sequences (above fair-weather wave base) are the most easily identifiable in the field on the base of higher energy features, pervasive bioturbation and maximum biological richness including abundant green algae. These deposits are represented by petrofacies of sub-cluster 1b (bioclastic-rich lithofacies with high algal and foraminifer content, mainly hyalines) and cluster 3 (bivalves- and echinoderms-rich) (§ 6.1). The abundance of algae testifies photic conditions, while the high biological richness and variability are usual for high energy, shallow-water environments.

The splitting of inner ramp between three different sub-clusters (1b, 3a and 3b) can possibly be explained by internal differences in environmental conditions (1b and 3a). The peculiar nature

of sub-cluster 3b, grouping samples affected by bioerosion/microbialite encrustation, can be interpreted as forced by temporarily modified ecological conditions.

For sub-cluster 1a, the combination of shallower and deeper facies (Fig. 17), in association of a fewer amount of bioturbation and of a higher content in porcelanous foraminifers indicate a deeper setting (Flügel, 1996). This subenvironment, identified from cluster analysis, may represent the transition between inner and median ramp and is thus defined "shallow-median".

Median ramp environment (between fair-weather and storm wave base) is characterized by the correspondence of maximum lithofacies unevenness, related to the alternation of high and low energy levels, and richest biological assemblages (al types of foraminifers, bivalves). Sub-cluster 2b encompasses all those features (Fig. 17). The highest variability of biological assemblages probably testifies mixing processes with possible sediment supply from the inner sector and landwards transportation by storms.

Subcluster 2a is characterized by abundant porcelanous and agglutinated foraminifers, and testifies

for an overall decrease in biological richness and variability. From the sedimentological side, samples belonging to subcluster 2a show evidence of distal storm deposition (thin mudstone/wackestone layers, higher amount of fine-grained sediments).

The combination of these two elements can define a deeper-median sub-environment.

Outer ramp subenvironment (below storm wave-base) could only be detected by sedimentological features, being characterized by fine-grained, low-energy sterile mudstones and siltstones/marls.

1.6.3 Cool water versus tropical carbonate factories

The carbonate bodies of Dogna represent a ramp, a typical geometry of cool-water carbonates. A generally flat or gently dipping geometry can be inferred from sedimentological features, such as absence of skeletal reefs/mounds and slope facies. In addiction, no hints of a shelf/slope break could be detected from fieldwork observations.

The carbonate ramp of Dogna, however, displays features of both cool water and tropical carbonates (Schlager, 2003; 2005). While abundance of light-independent, heterotrophic biologic assemblages (bivalves and foraminifers) and the absence of corals hint at a cool-water factory, the presence of an oolitic shoal and of an algal meadow, overall high micrite content and abundance of calcareous halimedacean algae fragments in the inner ramp are more typical of tropical carbonate platforms. More specifically, the internal ramp facies are dominated by the

halimedacean algae *Collarecodium* sp., that constitute a chloralgal association (e.g., Carannante et al., 1988).

The key to the understanding of the Dogna carbonate factory lies in the interpretation of microsparite, which often constitutes the bulk of the sediment. Microsparite is common in inner ramp facies (around 40 %), but becomes less abundant in more distal portions of the ramp, dominated instead by fine terrigenous sediment. Observations with SEM indicate an aragonite precursor for microsparite.

Presently, carbonate mud is forming as aragonite, and secondarily as hi-Mg calcite because of the high Mg/Ca ratio of seawater (e.g., Morse et al., 2006, Stanley and Hardie, 1998). All recent halimedaceans, including those yielding recognizable sand-sized or coarser fragments as *Halimeda*, calcify mostly in the form of micrite-sized aragonite needles (e.g., Neumann and Land, 1975). The mineralogy of the halimedacean precipitates is only slightly affected by seawater chemistry (Ries 2005; 2006). We suggest that micrite in the carbonate ramp of Dogna was also mostly produced by fragmented halimedacean algae. This implies that late Triassic halimedacean *Collarecodium* sp. was a major carbonate producer in some carbonate platforms, as that of Dogna.. Recent halimedaceans supply aragonite sediment in quantities largely exceeding accommodation space in the locus of production (e.g., Neumann and Land, 1975; Rees et al., 2007). Similarly, in the lower Carnian ramp of Dogna microsparite was produced in the internal ramp by halimedaceans, and overproduction was exported into the middle and outer ramp. Processes as abiotic precipitation on nuclei of resuspended aragonite (Morse et al., 2003) might have contributed to the net carbonate budget of the platform.

In summary, the greater part of the carbonate in the lower Carnian ramp of Dogna was deposited as microsparite with an aragonite precursor, and fragments of halimedacean algae. The carbonate production at Dogna was thus not different from that of modern tropical lagoons, where micrite derives from the breakdown of halimedacean algae (e.g., Neumann and Land, 1975; Rees et al., 2007). The carbonate ramp of Dogna thus fits well in the model of tropical factories (Schlager, 2003; 2005), and is characterized by a typical chloralgal association.

The outer part of the ramp without doubt contains a higher proportion of elements typical of cool-water factories (foraminifers and molluscs especially). This is, however, not surprising. Firstly, modern carbonate platforms normally host cool-water biological communities in deep parts of the open shelf (e.g., Carannante et al., 1988; Schlager, 2003). Secondly, terrigenous input may have resulted in average turbid waters in deeper portions of the ramp, thus hampering the growth of algae and favoring heterotrophic carbonate producers (see § 1.6.4 for further discussion).

1.6.4 Terrigenous input

Fine-grained terrigenous material is conspicuous trough the whole carbonate ramp succession of Dogna, but it is mainly recorded in the lower-energy mid-outer ramp deposits, while lagoon and inner ramp are mostly carbonate. It is represented by siltstones, marly siltstones and silty shales, tightly interbedded to carbonate layers or in isolated packages, up to 4m thick; only one arenite layer is recorded.

Terrigenous beds sometimes contain marine fossils (bivalves) and scattered plants remains, and in some cases are bioturbated.

Along dip transportation by rivers (as detected, e.g., by Dunbar and Dickens, 2003) can be excluded for the absence of structured siliciclastic bodies (e.g., river/delta deposits) in the studied area. Such coarse-grained sedimentary bodies may be present only in the "Dogna formation", i.e., in the upper part of the study interval, and cannot account for the general style of sedimentation in the lower Carnian ramp. Terrigenous material is thus supposed to derive from a source lateral to the sedimentary system, possibly through alongshore currents transportation, as reported for example by Brachert et al. (2003).

Accumulation of fine siliciclastics in proximal facies is possibly prevented by high energy processes (winnowing/washing by wave and storm currents). Consequences of such a high terrigenous flux on carbonate sedimentation can be recognized throughout the whole ramp. In the distal parts of the ramp, fine terrigenous material inhibited the development of a chloralgal association through increased turbidity (Mutti and Hallock, 2003), thus allowing an heterotrophic foraminiferal association to grow.

In the inner sector, the raise in nutrients necessarily associated with high terrigenous input (Mutti and Hallock, 2003) could have favored the growth of calcareous green algae in place of corals. As recognized also by Carannante et al. (1988), tropical platforms with terrigenous pollution become ramps dominated by green algae. More specifically, Wilson and Vecsei (2005) indicate how present-day tropical carbonate platforms affected by terrigenous input can mimic the geometry of cool-water carbonates, with contributions from halimedacean algae (*Halimeda*).

Under this profile, the Upper Triassic carbonate ramp of Dogna results noticeably similar to some modern, stressed tropical carbonate systems.

1.7 CONCLUSIONS

The lower Carnian succession in the Dogna area represents a mixed carbonate-siliciclastic ramp. The overall configuration of the lower Carnian ramp of the Dogna area results quite peculiar for the co-existing features of tropical and cool-water carbonate factories.

Quantitative sedimentary petrology and multivariate statistical analyses confirmed the ramp subdivision drawn from sedimentological observation and allowed the identification of the following five sedimentary sub-environments: inner, shallow median, median, deeper median and outer ramp.

The inner ramp is dominated by fragments of the halimedacean algae *Collarecodium* sp., while bioclasts of the mid and outer ramp form a heterotrophic assemblage.

The larger part of the carbonate is given by fine carbonate matrix (microsparite).

Microsparite has a prevailing aragonitic precursor, and is considered to derive mostly from calcifying green algae: the carbonate ramp of Dogna thus represents a tropical carbonate factory, with a significant contribution of heterotrophic producers in its outer part. Differences with the high-relief tropical or mud-mound platforms of the Dolomites can be attributed to the fine terrigenous supply delivered by alongshore currents, hampering the growth of autotrophic organisms. This can explain both the heterotrophic association of the mid-outer ramp, where the terrigenous component is more conspicuous, and the absence of reef-building communities in the shallower part of the ramp.

This case also demonstrates that, in some carbonate platforms, halimedacean algae were principal carbonate producers already from the Late Triassic. The Dogna carbonate ramp thus reveals features typical of modern tropical carbonate factories under environmental stressed conditions, where halimedacean green algae replace corals and high relief buildups do not develop.

CHAPTER II UPPER CARNIAN TERRIGENOUS DEPOSITS OF THE DOLOMITES AND JULIAN ALPS

2.1 INTRODUCTION

Climate is considered one of the major driving factors for the development of sedimentary systems.

Climatic influence was recognized at the regional scale in the creation of sequence stratigraphic series (Vail et al., 1991; Van Wagoner et al., 1988); as a major factor in determining lithologies (Lottes and Ziegler, 1994; Cecil, 1990) and the composition of terrigenous deposits (Jones and Manning, 1994; Suttner and Dutta, 1986; Basu, 1985; Suttner et al., 1981).

Climate-driven alteration and physical disgregation/removal of pre-existing rocks are the ultimate origin of arenite-size grains, yet presently knowledge about the interplay between weathering and erosion is lacking (Lebedeva et al., 2007; West et al., 2005).

Nevertheless, traditional sedimentary petrology of arenites can be a powerful tool to qualitatively investigate climatic influence in terrigenous units (Zuffa, 1987).

In this framework, a petrographical investigation of some late Carnian (late Triassic) units of the eastern Southern Alps (northern Italy) is undertaken, with special focus on the possible effect of climate changes in the deposits development.

In the time frame of deposition of the Heiligkreuz and Travenanzes Formations in the Dolomites area, and of the informal “Dogna” formation in the Julian Alps, a sudden climatic change is recorded (Gianolla et.al., 1998b; Preto and Hinnov, 2003; Preto et al., 2005), corresponding to the Carnian Pluvial Event of Simms et al. (1997).

The studied successions display a complex sedimentation pattern with alternation of carbonate and siliciclastic deposits.

The aims of this part of the work are

1) to investigate the origin of the late Carnian units trough the interpretation of detrital modes of the terrigenous sand-size deposits;
2) to determine the provenance of constituents; and
3) to discriminate between the main driving factor(s) in the composition, paying special attention to the climatic signal.

2.2 METHODS

Modal analysis has been carried out with a polarising optical microscope. The standard Gazzi-Dickinson's technique (Gazzi, 1966; Dickinson, 1970) has been applied in order to minimize grain size influence on clasts classification; at least 500 points for each thin section have been identified. The counting has been performed on a square grid with point distance larger than the largest grain, in order to prevent multiple identification of the same element.

Evaluation enclosed the whole framework composition and interstitial material. Grains were considered as particles with diameter > 63μm (Pettijohn, 1957). Optical distinction between calcite and dolomite was allowed by staining of thin sections with alizarine red.

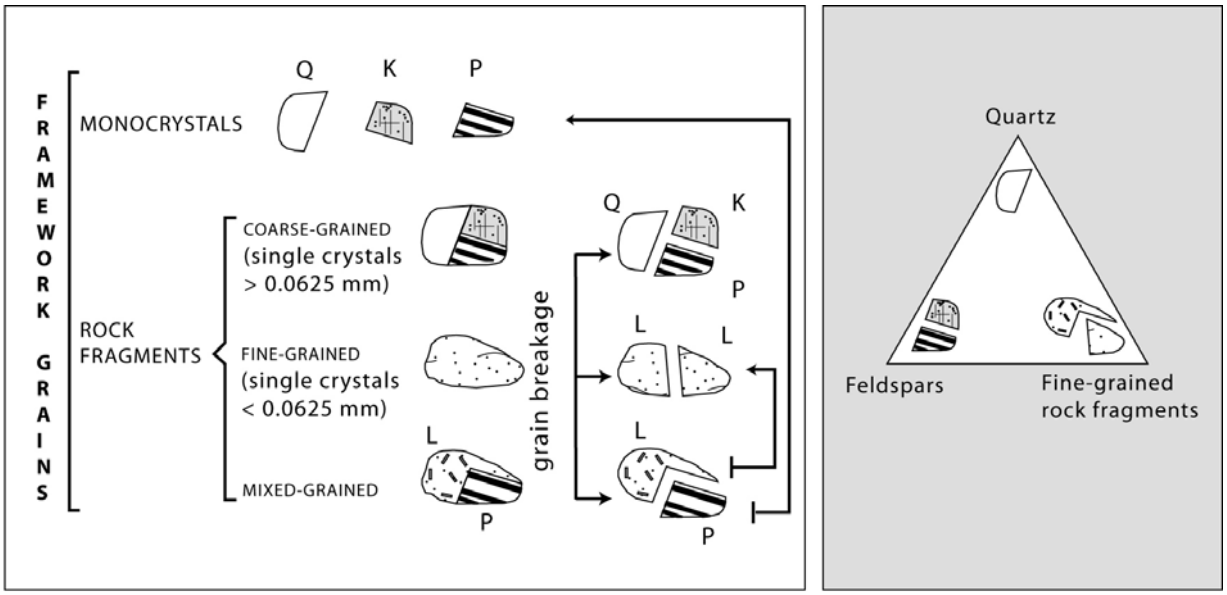

FIGURE 18 - The Gazzi-Dickinson counting technique. Detrital monocrystals and single-crystal minerals deriving from breakage of coarse-grained rocks or from composite-grained rock fragments are grouped together in the Quartz or Feldspars categories. In the Lithic category either fine-grained rock fragments or matrix from composite-grained rock fragments are listed. Modified after Zuffa (1980).

A first broad classification indicates sediments compositional and textural maturity, providing information on arenites controlling factors such as tectonic setting, climate, transportation, and recycling (i.e.: Dickinson 1970; Cavazza et al., 1993; Nesbitt and Young, 1989; Zuffa, 1987). The intergranular component records the post-depositional history (McBride, 1985; Fontana et al., 1989).

Following Zuffa (1980) (Fig.19), grain types have been subdivided into:

(1) Non-carbonate, Extrabasinal (NCE). This category makes up the framework composition of a terrigenous arenite, and provides direct information on the source-area constituents.

The major classes *Quartz* (Q), *K-feldspar* (K) and *Plagioclase* (P) are further subdivided into subclasses indicating whether the grains are constituted by single crystals or belong to a rock fragment, in order to preserve information on the rock type. Other specifications for quartz are

based on the extinction (undulose and right) and crystal dimensions in polycrystalline aggregates. The class *Calcite on*, where present, indicates clasts partially replaced by calcite but still recognizable; in this way even the presence of replacement is recorded, which is important for detection of the post-depositional history of the sample.

Other detrital and heavy minerals, found in single crystals, are enclosed in NCE.

In *Fine-grained Lithics* (L) siliceous rock fragments like volcanics (of either acidic or intermediate composition), metamorphics, chert and siltstones are included, subdivided on genetical and/or textural base. *Other minerals* groups heavy minerals, either transparent or opaque. They can be found also within rock fragments. They provide direct information on source-area lithologies.

(2) Carbonate, Extrabasinal (CE). Categories within this class are marked by the carbonate rock type of the fragment (limestone or dolostone). Just like NCE, they generally are non-coeval to sedimentation, and they give direct information on history and configuration of the source-area.

(3) Non-carbonate, Intrabasinal (NCI). This class may provide information on physical and chemical conditions of the basin. It's made up only by phosphate and green particles of the glauconite family.

(4) Carbonate, Intrabasinal (CI). These coeval clasts are represented mainly by bioclasts, oolites and peloids. Two further sub-classes (nodules and arenaceous intraclasts) have been recognized in the Travenanzes Fm.

A further estimation focused on lithic fragments only, distinguished on genetic base (volcanic, plutonic/gneissic, fine-grained metamorphic, sedimentary). Where necessary, extra points were counted in order to reach statistically reliable 200 determinations (with maximum standard deviation = 7%) (Van der Plas and Tobi, 1965). Those values directly mirror the parent rock assemblages and source areas configuration. Table 6 shows the petrographical classes used in this work for the modal composition calculation.

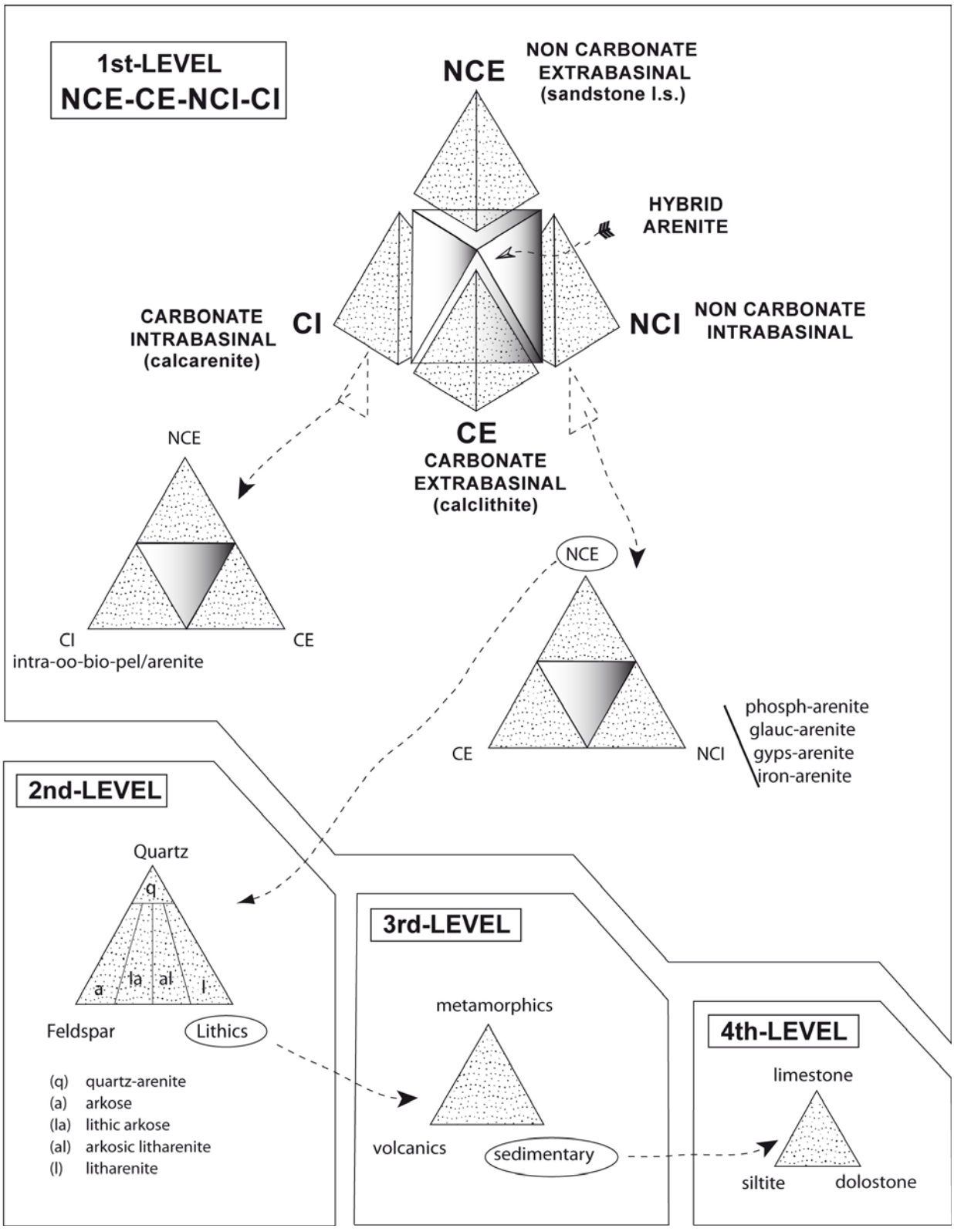

FIGURE 19 - Arenites classification from compositional petrographical analyses. Modified after Zuffa (1980).

I level	Abbreviation	Grain type	Framework	Lithics
NCE	QmP	Monocrystalline quartz, plutonic	Q	
	QmV	Monocrystalline quartz, volcanic		
	QmU	Monocrystalline quartz, undulose extinction		
	Qpxc	Polycrystalline quartz		
	Qva	Quartz within volcanic rock		V
	Qpl/gn	Quartz within plutonic/gneissic rock		Pl/gn
	Qmet	Quartz within metamorphic rock		M
	Cqm	Calcite on quartz		
	Cqva	Calcite on quartz in volcanic rock		V
	Cqpl/gn	Calcite on quartz in plutonic/gneissic rock		Pl/gn
	Cqpx	Calcite on polycrystalline quartz		
	Calced.	Chalcedony (fibrous quartz)		
	Pl	Plagioclase	F	
	Pl alter	Altered plagioclase		
	Ppl/gn	Plagioclase within plutonic/gneissic rock		Pl/gn
	Plv	Plagioclase within volcanic rock		V
	Cpl	Calcite on plagioclase		
	Kfs	K-feldspar		
	Kfs alter	Altered K-feldspar		
	Kpl/gn	K-feldspar within plutonic/gneissic rock		Pl/gn
	Kv	K-feldspar within volcanic rock		V
	Ckfs	Calcite on k-feldspar		
	Va	Acidic volcanic rock	L+CE	V
	Vi	Intermediate volcanic rock		V
	Va silicif	Silicified volcanic rock		V
	Vi alter	Altered volcanic rock		V
	Glass	Volcanic glass		V
	Dvtr	Devetrified glass		V
	Pl/gn	Plutonic/gneissic rock		Pl/gn
	Mmic	Phyllite		M
	Mq	Quartzite		M
	Ch	Chert		S
	Silt	Siltstone		S
	Bt	Biotite	Micas/ Phyllosilicates	
	Chl	Chlorite		
	Ep	Epidote	Other minerals	
	Op	Opaque minerals		
	Zr	Zircon		
	Btv	Biotite within volcanic rock	L+CE	V
CE	Cmc	Microcrystalline limestone	L+CE	CE
	Cms	Microsparitic limestone		CE
	Dsp	Spatic dolostone		CE
	Dpx	Polycrystalline dolostone		CE
CI	Bio	Bioclasts		
	Carb. intr.	Carbonate intrabasinal clasts		
	CI aren.	Arenaceous carbonate intrabasinal clasts		
	Nod.	Nodules		
NCI	Ph	Phosphate grains		
	Gr	Green grains		

TABLE 6 - Grain types and categories employed for arenites classification from petrographical analyses.

2.3 LOGS DESCRIPTION AND INTERPRETATION

The Upper Carnian succession of Dolomites and Eastern Southern Alps has been studied in 6 and 7 different localities respectively, for an overall 100m logged thickness.

Localities for the Heiligkreuz and Travenanzes Fms. were Borca di Cadore (lithozones A-B), Rifugio Dibona (lithozones A-B and D-E-F, and first interval of Travenanzes Fm.), Rifugio S. Marco (lithozones D-E and first interval of Travenanzes Fm.), Lagazuoi (lithozone F), Passo Falzarego (lithozone H) and Forcella Falzarego (first interval of Travenanzes Fm.) (Figure 20).

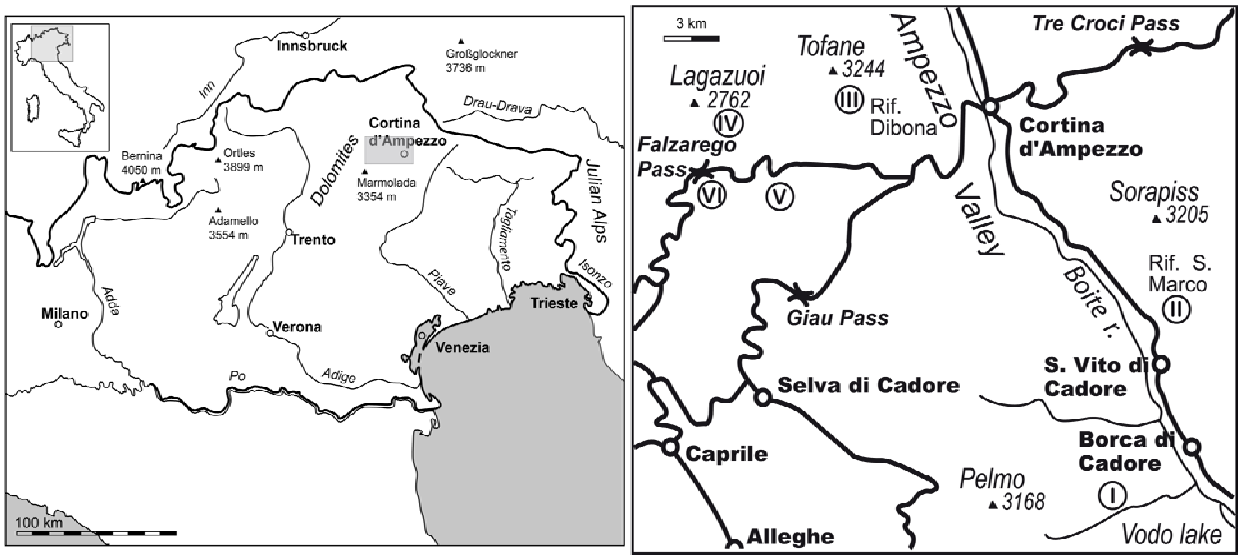

FIGURE 20 – Map of the study area. Stratigraphic sections analyzed: I) Borca di Cadore, lithozones A/B, Heiligkreuz Fm.; II) Rifugio S. Marco, lithozones D to H, Heiligkreuz Fm., and Travenanzes Fm.; III) Rifugio Dibona , lithozones A to H, Heiligkreuz Fm., and Travenanzes Fm.; IV) Lagazuoi, Travenanzes Fm.; V) Rio Falzarego, lithozones A/B, Heiligkreuz Fm.; VI) Passo Falzarego, lithozone H, Heiligkreuz Fm.

Localities for the Rio del Lago Fm. and for the "Dogna" fm. were Rio Pontuz, Rio Mas, Gran Colle 1 and 2 and Rio di Terrarossa (see Figure 4, Chapter I).

An overview of the studied Formations was presented in the § Formation nomenclature and description in the Introduction.

The following is a description of the logged sections and an interpretation of the main lithofacies associations and sedimentary environments.

2.3.1 Heiligkreuz Fm.

The Heiligkreuz Fm. is stratigraphically interposed between the Cassian Dolomite/San Cassiano Fm. and the Travenanzes Fm. The upper boundary is erosional while the lower boundary is erosional in the proximal sections overlying the Cassian Dolomite, and conformable in the distal sections overlying the S. Cassiano Fm. (De Zanche et al., 1993; Preto and Hinnov, 2003) (see Formation nomenclature and description in the Introduction).

In the studied sections of the Dolomites area, the Heilgkreuz Fm. overlies the basinal deposits of the S. Cassiano Fm. at the Rifugio Dibona section, and the carbonate platform deposits at the Rifugio S. Marco section.

The base of the Heiligkreuz Formation is visible in small creeks below the Rifugio Dibona (Preto and Hinnov, 2003) and in the Rio Falzarego river.

It is mainly represented by dark shales, interbedded with oolite-bioclastic grainstones and coarse-grained-conglomeratic sandstones (Rifugio Dibona), or followed by a m-thick conglomerate (Rio Falzarego) (see below).

Due to the high erodibility of shales, the contact between the Heiligkreuz Fm. and the underlying units is barely outcropping, and of limited lateral extension.

Rio Falzarego section – lithozones A/B

Along Rio Falzarego (Cortina d'Ampezzo), the basal Heiligkreuz Fm. overlies the S. Cassiano Fm.

It is represented by dark shales with gastropods, ostracods and bivalves (*Unionites sp*.) (Neri et al., 2007) and by a m-thick conglomerate with plants remains, rip-up clasts and cm-sized quartz and lithic clasts (Fig. 21 and Fig. 22 a, b, c). Bed top is erosive and overlain by mudstones. The base of the conglomerate is erosive, marked by flute casts, bioturbation, and plant debris (Fig. 22 d, e). Plant fragments are elongated, up to 30cm long, with bimodal orientation of 30° span.

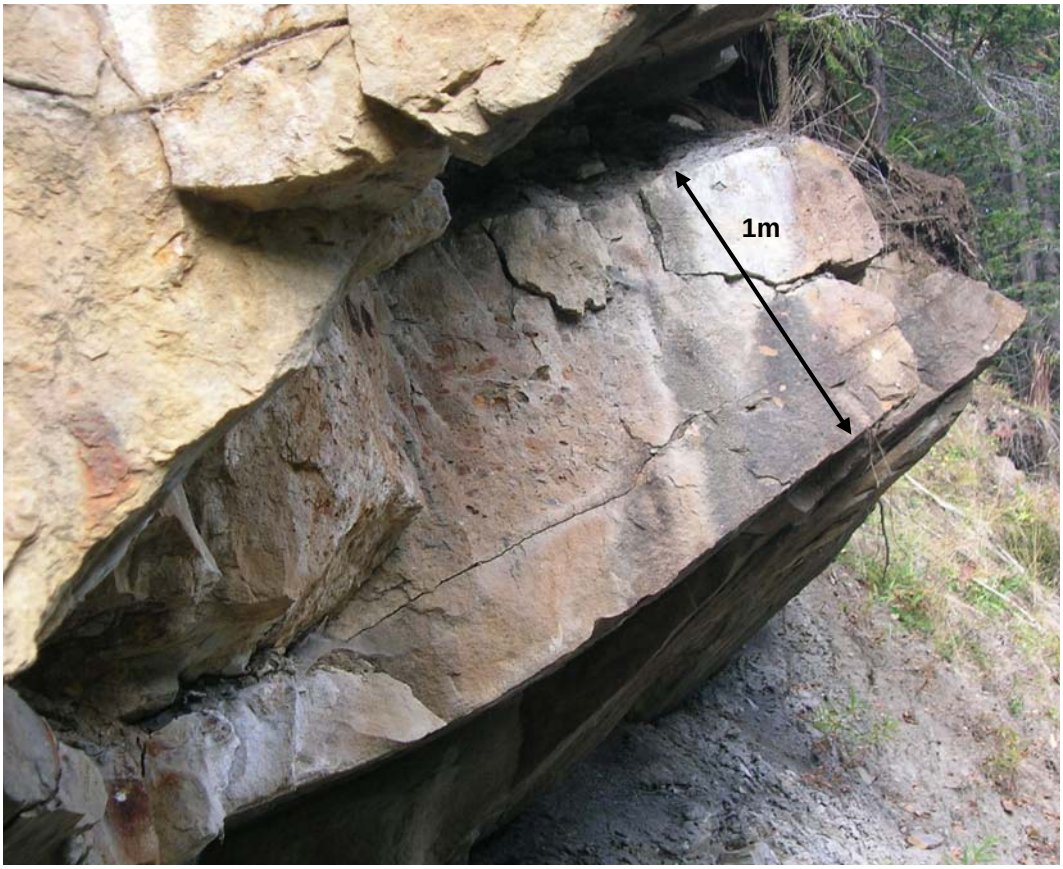

FIGURE 21 – Conglomerate at the base of the Heiligkreuz Fm., Rio Falzarego section. It represents a complex high-density turbidite flow.

The bedset is formed by a lower laminated sandstone, by an inverse- to normal-graded conglomerate and by an upper massive sandstone.
The lower bed, 20cm thick, displays vague plane-parallel lamination and scour-and-fill structures. The central bed is the coarsest, with pebble-size clasts, poorly sorted, distributed in inverse- to normal grading. Clasts are either sub-angular (mainly of volcanic origin) or sub-rounded (intraformational micritic clasts). The volcanic grains look like chert probably because of silicification of glass ground-mass (Fig. 22c) (see § 2.4.1.1).
The uppermost bed is 20cm thick, massive to faintly planar laminated, with scattered rip-up clasts.

Interpretation:
The unit can be interpreted as a highly concentrated, turbulent, waxing flow followed by a waning flow. The faint-laminated basal bed may suggest sustained flow, probably of hyperpicnal origin. The conglomerate bed may represent waxing- to waning flow, while the uppermost bed can testify a S_3 subdivision of Lowe (1982).
The overall body may represent a channel because of the erosive base and scarce lateral continuity. The uniqueness of the unit suggests a slope setting fed by a (shelf-edge?) delta system (Mellere et al, 2002). The character and the energy of the deposit suggest a sudden increase in sediment supply possibly due to a change in the basin physiography or climate.
Continental control is also testified by the high content of plants.

Borca di Cadore section – lithozone B
In Borca di Cadore, the displayed succession records lithozone B. The terrigenous portion is at the base and is represented by 1m of dark shales, massive, followed by 2m of arenites of medium grain-size. In the uppermost part of the interval, inverse grading can be observed. The contact between shales and sandstone is slightly erosive, undulose. The first 60cm are massive, followed by large trough cross-bedding with plant remains. At 110cm above the base an interval with tight stratification is found, capped by massive arenites with clay chips draping faint cross-bedding. Upper beds are amalgamated.
The siliciclastics are overlain by 50cm of thin intercalations of clay and dolomitized mudstone-wackestone, with yellow coatings. More than 3m of dolomitize mudstone/wackestones and marly wackestones follow, in dm-thick layers, with terrigenous input decreasing upwards, without bioturbation.

FIGURE 22 – Details of the basal conglomerate, Heiligkreuz Fm., Rio Falzarego section. A) Inverse grading of pebble-sized grains and rip-up clasts. Grains include quartz and volcanics. B) dm-size plant stems, with bimodal orientation. C) Close-up view of altered volcanic clasts, with glassy/chert-like appearance. D) *Planolites* bioturbation. E) Escape (?) trace.

Interpretation:

The succession result similar to the one in Rio Falzarego because of richness in plant debris and overall trend, though with smaller energy and grain size of the deposits. It is thus tentatively suggested that the overall sedimentary environment and depositional processes are also equivalent to those of Rio Falzarego.

The lower massive to through-laminated bed could represent to the Ta and Tc Bouma intervals while the plane-parallel laminated interval could correspond to the Tb Bouma interval. The faint lamination in the uppermost bed could represent a scour-and fill structure.

The overlying structureless, marly granular carbonates could represent distal ramp deposits.

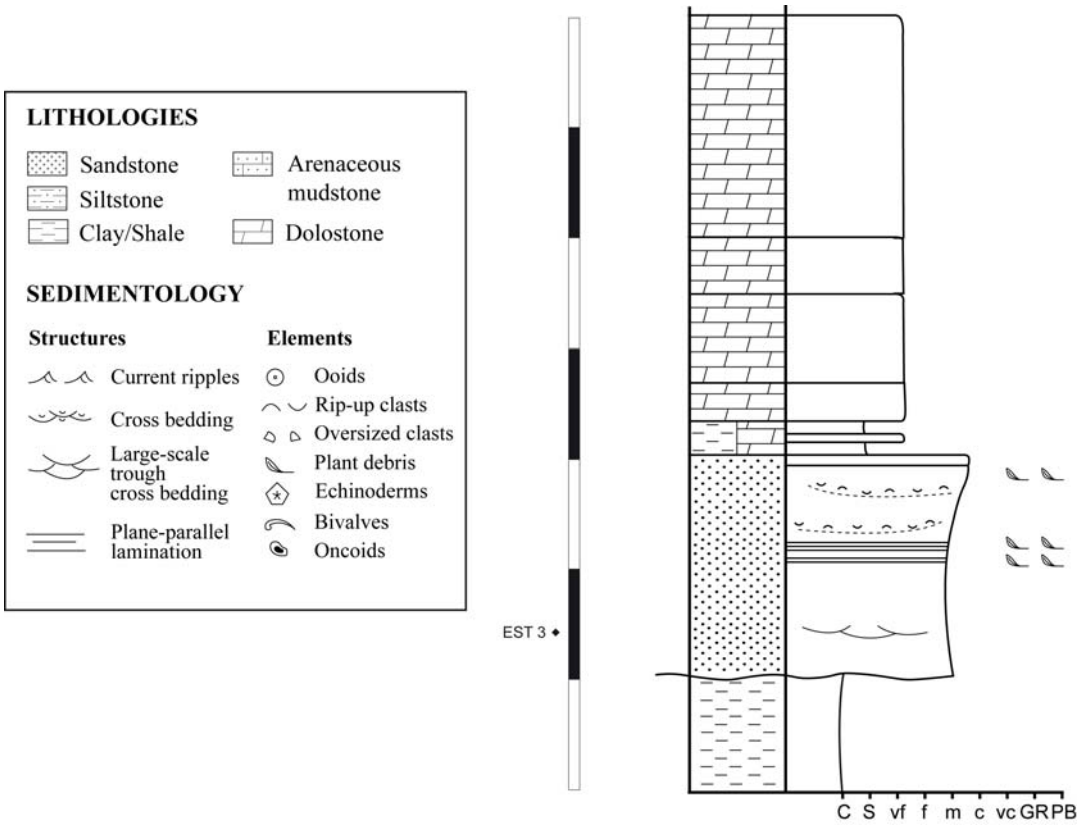

FIGURE 23 – Log of the basal Heiligkreuz Fm., Borca di Cadore section. Legend is also valid for the following logs. Scale bar = 1m.

Rif. Dibona section – lithozones A and B

At Rifugio Dibona, the series opens with a six m-thick carbonate succession consisting of bioclastic grainstone-rudstones, grainstones and bindstones, followed by five meters of mixed terrigenous-carbonate coarse deposits. The main recognized facies are listed in Table 7.

Two intervals of bioclastic grainstone-rudstones can be found, each around 2m thick. Single layers are dm-thick and result slightly nodular. They contain echinoderms, bivalves, gastropods and algal nodules (facies 1).

The two intervals are separated by a wedge unit of bioclastic grainstones, with highly erosive base (facies 2). Minimum thickness is 1.5m, erosional relief >1m. Main structures are large-scale cross-bedding and sigmoidal bedding, up to 1.3m of amplitude, with weak normal grading. Fossil content is plant stems, bivalves, gastropods and echinoderms.

The second grainstone-rudstones interval embeds a confined oval body 1m thick and 2m large, made up by a framework of corals and sponges in life position (facies 3a). A thin (20cm) rudstone layer wedges out the bindstone unit, containing coral debris (facies 3b).

Code	Grain size/ lithology	Features	Fossils – bioturbation	Layer thickness	Interpretation
SUBTIDAL MEDIAN RAMP					
1	Grs-Rds	Slightly nodular	Echinoderms, gastropods, algal nodules	dm-thick	Subtidal median ramp
2	Grs	Highly erosive base (>1m relief), downlapping large-scale cross- and sigmoidal-bed	Plant debris, molluscs, corals	1.5m min	Inlet (?)
3a	Bns	Oval shaped body	Corals, sponges (life position)	1x2 m max	Patch reef (subtidal median ramp)
3b	Pks	Wedge-shaped, slightly erosive base	Coral fragments	20cm max	Talus breccia from patch reef
4	Flt-rds and Cglm in sandy matrix	Massive, erosive to planar base, scattered pebbles.	Plant debris, molluscs	> 1.5m	Cohesionless debris flow and sheet flow deposits, subtidal median ramp. The latter are formed by flashflood events.

TABLE 7 – Main facies of the lithozones A and B, Rifugio Dibona section. Grain size key: VF: very fine; F: fine; M: Medium; C: coarse; VC: very coarse; P: pebbles. Lithology key: Cglm: conglomerates; Ar: arenites; Slt: siltstones; Cl: clays; Ml: marls; Lms: limestones; Wks: wackestones; Pks: packstones; Bns: boundstones; Flt: floatstone; Rds: rudstone; Ds: dolostones.

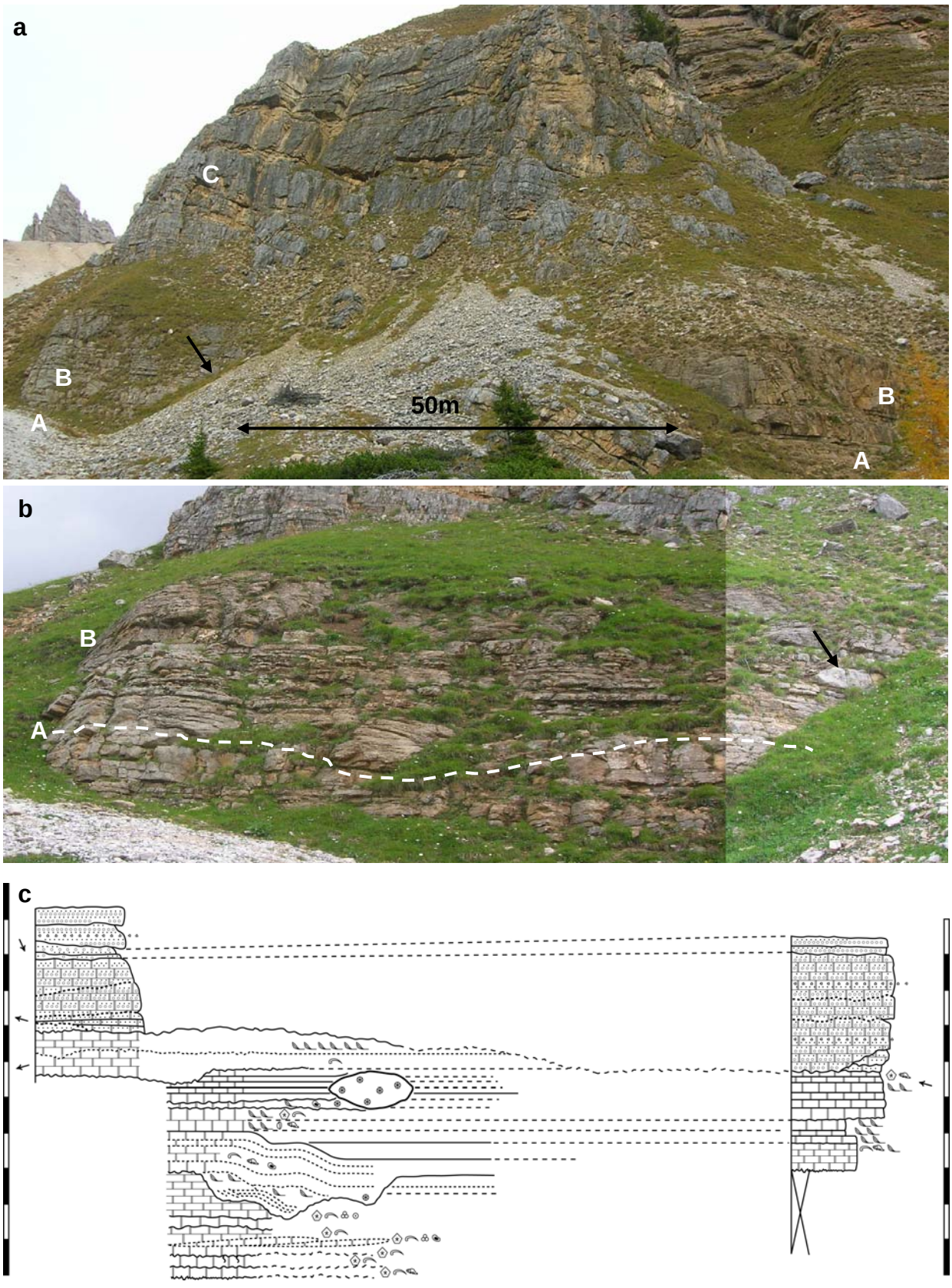

FIGURE 24 – Lower Heiligkreuz Fm., Rifugio Dibona section. a) Stacked lithozones A, B and C. b) Close-up view of left outcrop, lithozones A and B. The lower part of the succession is represented by lithozone A, with median ramp facies and channels (dashed line). Patch reef indicated by arrow. c) Schematic log of lithozones A and B. Scale bars = 1m, distances between sections not to scale. Small arrows: paleocurrent directions from cross-bedding. Lithology and symbols as in Fig. 23.

Interpretation: The two bioclastic grainstone-rudstone interval could testify a subtidal median ramp environment because of the fossil association (see § 1.3.4), in particular for the presence of a patch reef.
The interposed grainstones is interpreted as a channel fill for the erosional base and the tractive structuration, fed by the collapse of the prograding shoal barrier at its back. Continental influence is testified by plant debris.

The overlying succession represents an abrupt change in the sedimentation pattern. It's a 5m sequence of floatstone-rudstones and breccia-conglomerates (facies 4), massive, with highly erosive to planar base, rich in plant debris and molluscs. The siliciclastic fraction increases upwards. Beds are > 1.5m thick, with inverse grading. Terrigenous grains are mm- to cm-sized, sub-angular, scattered altered and non-altered volcanic rock fragments and quartz clasts.

Interpretation: The mixed conglomerates can derive from semiplastic flows (sheet flows) of continental origin. Terrestrial input increases upwards. The overall setting can still be considered a subtidal median ramp because of the richness in molluscs and because of the catastrophic style of the deposits.
Transit of river flood fluxes trough the inner ramp could account for the mixing of terrigenous and carbonate material ("punctual mixing" of Mount, 1984).

The succession continues with the overall carbonate lithozone C, representing progradation from the carbonate shoreline. See § Formation nomenclature and description, Introduction. The topset of lithozone C are overlain by the marginal-marine lithozone D.

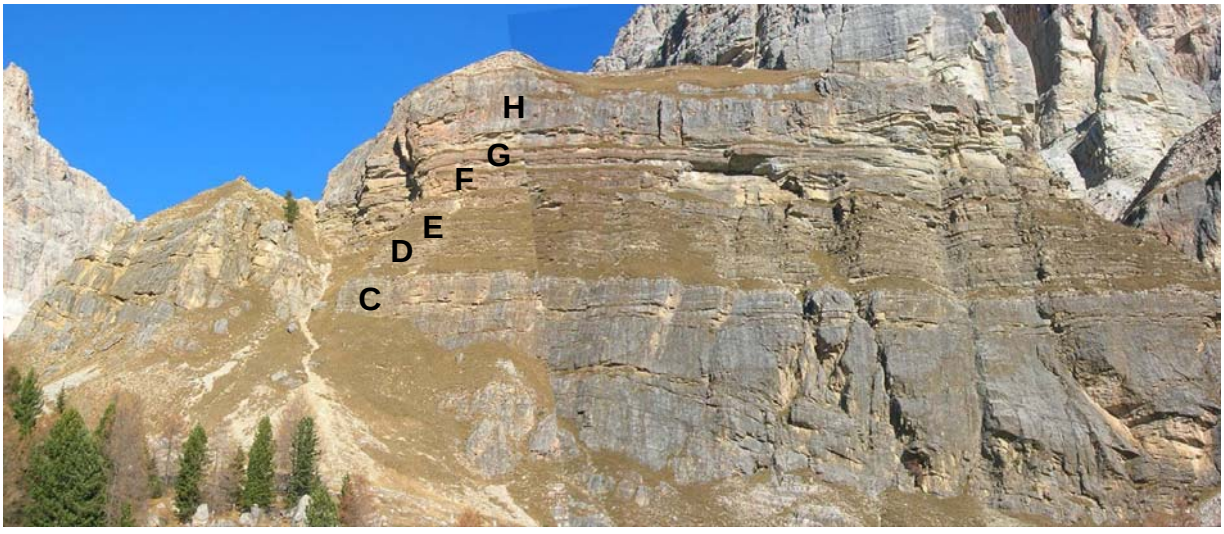

FIGURE 25 – Overview of lithozones C to H, Rifugio Dibona section.

Rif. Dibona section –lithozones D and E

The measured portion of the succession including the lithozones D and E at Rifugio DIbona is 16m thick overall, and is made by a basal fine-grained carbonate unit, followed by a mixed carbonate-terrigenous coarsening-upwards sequence with trough cross-bedding and by a succession of arenites with basal conglomerate lag and oblique lamination. Terrigenous input increases upwards. An overview of the recognized facies is shown in Table 8.

The fine-grained carbonate unit is represented by 7m of bioclastic dolostones in dm-thick layers, with planar fenestrae, desiccation cracks, peloids and rare molluscs (facies 5). At the base, a package of fine grained hybrid arenites is present, with dm-thick lens-shaped layers, massive. It contains plant debris, bivalves and oolites (facies 6).

Towards the top, some thin silty-clay layers, dark, with colored coatings are present, containing sometimes rootlets (facies 7).

Interpretation: The isolated arenite layer can be interpreted as a channel because of erosive base and lateral wedging. Planar fenestrae and desiccation cracks alternated to peloids and molluscs in the carbonate interval testify repeated emersion and flooding in a peritidal succession of inner carbonate ramp to tidal flat.

A major flooding is represented by the pelite interval with coatings and rootlets (paleosol).

The mixed carbonate-terrigenous coarsening-upwards sequence is represented by oolitic-bioclastic grainstones in dm-thick layers, with sharp to erosive base. Trough-cross bedding, as well as planar lamination are present. Fossil content is bivalves, echinoderms, plant debris, oncoids, with terrigenous input (facies 8).

Interpretation: Fossiliferous grainstones with erosive base and tractive lamination can be interpreted as a bar or channel fill in a subtidal carbonate ramp, due to the openly marine fossil association.

The upper lithozone E is mainly terrigenous. It is constituted by fine arenites with coarser bioclastic lenses and low-angle cross stratification, in m-thick layers (facies 9) and by three sequences of medium arenites with basal conglomerate lag, rip-up clasts, plane- or trough-cross bedding. Bioclasts are common and include plant debris, bivalves and echinoderms (facies 10).

Throughout lithozones D and E amber findings are widespread (Roghi et al., 2006; Gianolla et al., 1998b).

Interpretation: Bimodal granulometric variations and tractive structures suggest a tide-controlled deposition. The subtidal ramp (shoreface?) environment is indicated by the marine bioclasts. Continuous continental influence is testified by amber and plant debris.

Code	Grain size/ lithology	Features	Fossils - bioturbation	Layer thickness	Interpretation
PERITIDAL CARBONATE RAMP					
5	Ds.	Planar fenestrae, sheet cracks.	Peloids, rare bivalves.	dm	Peritidal carbonate ramp.
6	F Ar.	Massive, erosive base, wedge-shaped.	Plant debris, bivalves, oolites.	dm	Bedload channel deposits. Subtidal inner ramp?
7	Slt.-Cl.	Dark, mottling with yellow and red coatings.	Scattered rootlets.	cm	Paleosols
SUBTIDAL INNER RAMP					
8	Grs.	Sharp to erosive base, trough cross bedding. Rapid lateral thickness variations.	Bivalves, echinoderms, plant debris, oncoids, oolites.	dm	Bedload channel deposits in subtidal inner ramp
SUBTIDAL INNER RAMP - SHOREFACE					
9	F Ar.	Bimodal granulometric variations, low-angle cross-stratification, lenses of coarser bioclasts.	Bivalves, echinoderms	m	Inner ramp (shoreface?)
10	M Ar.	Basal conglomerate lag, rip-up clasts, plane- or trough-cross bedding	plant debris, bivalves, echinoderms	dm	Inner ramp (shoreface?)

TABLE 8 – Main facies of the lithozones D and E, Heiligkreuz Fm., Rifugio Dibona section. Grain size/lithology key as Table 7.

FIGURE 26 – Overview of lithozones C, D and E, Heiligkreuz Fm., Rifugio Dibona section. From bottom to top: topset of prograding clinoforms (lit. C), peritidal lit. D, coastal-subtidal lit.E.

FIGURE 27 – Lithozone E, Heiligkreuz Fm., Rifugio Dibona section. Tidal-influenced coastal sediments.

FIGURE 28– Lithozone E, Heiligkreuz Fm., Rifugio Dibona section. Large-scale cross bedding in a prograding bar.

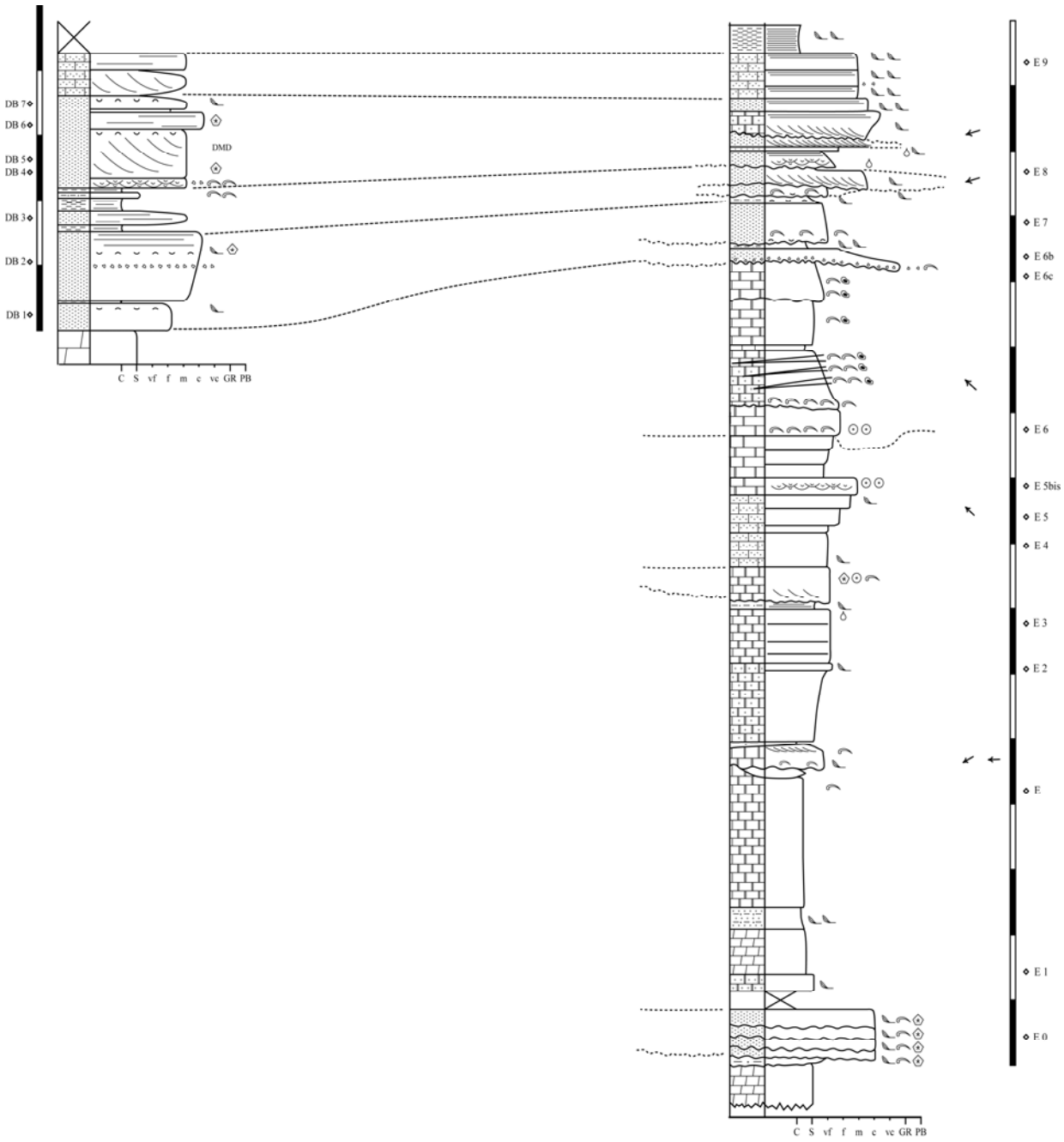

FIGURE 29 – Log of lithozone E, Heiligkreuz Fm., Rifugio Dibona section. Legend as in Fig. 23. Distance between logs ca. 100m.

Rifugio Dibona section – lithozone F

The lithozone F represents an overall inner carbonate ramp/beach succession (Preto and Hinnov, 2003) with some arenite intercalations. At the Rifugio Dibona section, arenites of lithozone F are represented by two lenticular layers separated by a 4m-thick level which is a marker layer of regional importance.

The lower arenite layer is 55 cm-thick, with erosional base and inverse grading from medium-to coarse-grained, massive. cm-sized rip-up carbonate clasts are present. The upper arenite layer is 50 cm-thick, inverse graded from fine- to medium- grained, massive, with a gravel lag at 15cm from the base. Scattered oolites are present.

Interpretation: The general sedimentary environment is known to be shallow-marine from the adjacent carbonate succession. In this setting, both layers can tentatively be interpreted as channelized (tempestite?) deposits for the lateral wedging, the inverse grading, and the reworking of oolites from shoal bars.

Passo Falzarego section–lithozone H

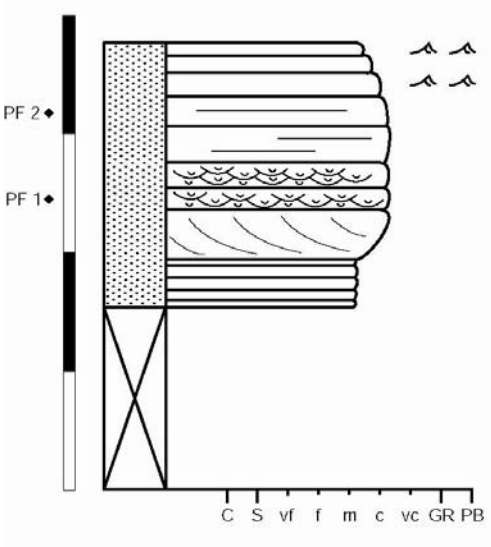

The uppermost arenite levels of the Heiligkreuz Fm. crop out at the Falzarego Pass, and correspond to the "Arenarie di Passo Falzarego" of Bosellini et al. (1982). Main occurring facies are trough cross-bedding and herringbone cross stratification. Layers are dm-thick, grain size medium to coarse; sorting is good.

FIGURE 30 – Log of lithozone H, Heiligkreuz Fm., Passo Falzarego section. Legend as in Fig. 23.

Interpretation: the bimodal bedding and the general high energy of the deposits (grain size, sorting) point towards a tidal environment.

Rif. S. Marco section–lithozones D and E

The Rifugio S. Marco section displays an almost continuous succession from lithozone D, Heiligkreuz Fm., to the Travenanzes Fm.

A 1m portion of lithozone D was included at the base of the measured succession, constituted by limestones with planar fenestrae, intraclasts and oncoids. The boundary between lithozone D

and E is characterized by a surface with karst cavities infilled by the overlying black siltstones/clays. Laterally, cavities are infilled by the overlying arenites (Fig. 31A).

Lithozone E is represented by a 30m succession of siliciclastics, only rarely interbedded to carbonates. Plant remains are very common throughout the whole succession.
Two cycles can be recognized, each starting with m-thick conglomerates overlain by plane-parallel laminated arenites intercalated to clay/silt. The two cycles are separated by an interval of medium-to coarse arenites with scour-and-fill features.
The conglomerates show erosive base, load casts and rip-up clasts. The first cycle is made of three conglomerate intervals, from 1 to 3m thick, fining-upwards. The last interval display large-scale cross-bedding and plane-parallel lamination at the top. It is capped by thin alternation of plane-parallel arenites and clay-silt, 3m thick.
A 4m interval of arenites follows, characterized by large-scale scour-and-fills. Direction of the scours are divergent. Coatings and plant remnants are present.
The second cycle results thinner, with only 1 conglomerate interval, 3m thick, overlaid by 3m of arenites, mainly plane-parallel laminated, and secondarily massive. The conglomerate display evident load casts, concentration of pebbles and bimodal cross-bedding at the top.
The succession continues with 4m of coarse arenites, with erosive base and rip-up clasts. Bivalves are present, and some times bimodal cross-bedding can be found.
In the whole succession, carbonate sediments are present only at the base and at the top of the second conglomeratic cycle. The first occurrence is made by alternation of dolomites and dark clay/silt. The second is represented by dolomites with rootlets.

Interpretation: The coarse conglomerate events can be interpreted as river channel fills in a braided river system. A catastrophic flood regime can be inferred by the upper-regime plane-parallel lamination and by the thickness of each event. Overlying plane-parallel laminated arenites and heterolitics can be interpreted as waning phases of overbank or levee deposition.
Large-scale cross-bedded intervals between the channels can be interpreted as migrating bars.
The isolated marly limestone layers can testify abandonment events in the flood-plain for the lack of bioclasts and of structures.
A general deepening trend is visible in the overlying deposits.
The last thick conglomerate event can be interpreted as a channel in a lagoonal environment for the presence of bidirectional bedding (tidal reworking?). The following arenites also show tidal influence because of cross-bedding (sometimes bimodal), pelite intercalations and high plant fragments content testify a continental provenance.

Uppermost arenites with bivalves and tractive lamination can be interpreted as lagoonal deposits, and testify a deepening trend towards the subtidal ramp carbonates, slightly nodular, with bivalves, gastropods and echinoderms.

Code	Grain size/ lithology	Features	Fossils - bioturbation	Layer thickness	Interpretation
RIVER CHANNELS					
1	F-M Ar.	Sharp contact, plane-parallel lamination	-	cm to dm	Overbank deposits
2	C Ar./Cglm	Erosive base, cross-bedding, basal lag, elongated rip-up clasts, load casts	Plant stems, coal clasts	m, 60dm-thick sets	Coarse-grained bedload river deposits
3	C-P Ar.	Structureless to normal graded	Plant stems	dm	Cohesionless debris flow and sheet flow deposits. The latter formed by flashflood events.
BARS					
4	M Ar.	Large-scale trough cross-bedding, reactivation surfaces	-	60cm, dm-thick sets	Lateral bar migration
5	M Ar.	Scour-and fill	-	dm	Lateral bar
ALLUVIAL PLAIN					
6	Cl.-Slt.	Plane-parallel lamination	Rootlets, coal clasts	cm to dm	Paleosols
7	Alternating Ml and Lms.	Massive, wedge-shaped layers	-	cm to dm	Desiccation of pod or ephemeral lake. Abandonment event.
LAGOON-SHOREFACE					
8	F-M Ar.	Low-angle sigmoidal beds, rip-up clasts, mud drapes, bimodal grain size	Coal debris	cm	Subtidal bar - lagoon
9	F-M Ar.	Planar to faint cross-bedded, thin mud drapes	Bivalves	m, dm-thick sets	Subtidal bar - lagoon
10	Pks	Cross-bedding. Presence of oolites	Bivalves, oolites, gastropods, echinoderms	dm	Subtidal carbonate ramp

TABLE 9 – Main facies of lithozones D and E, Heiligkreuz Fm., Rifugio S. Marco section. Grain size/lithology key as Table 7.

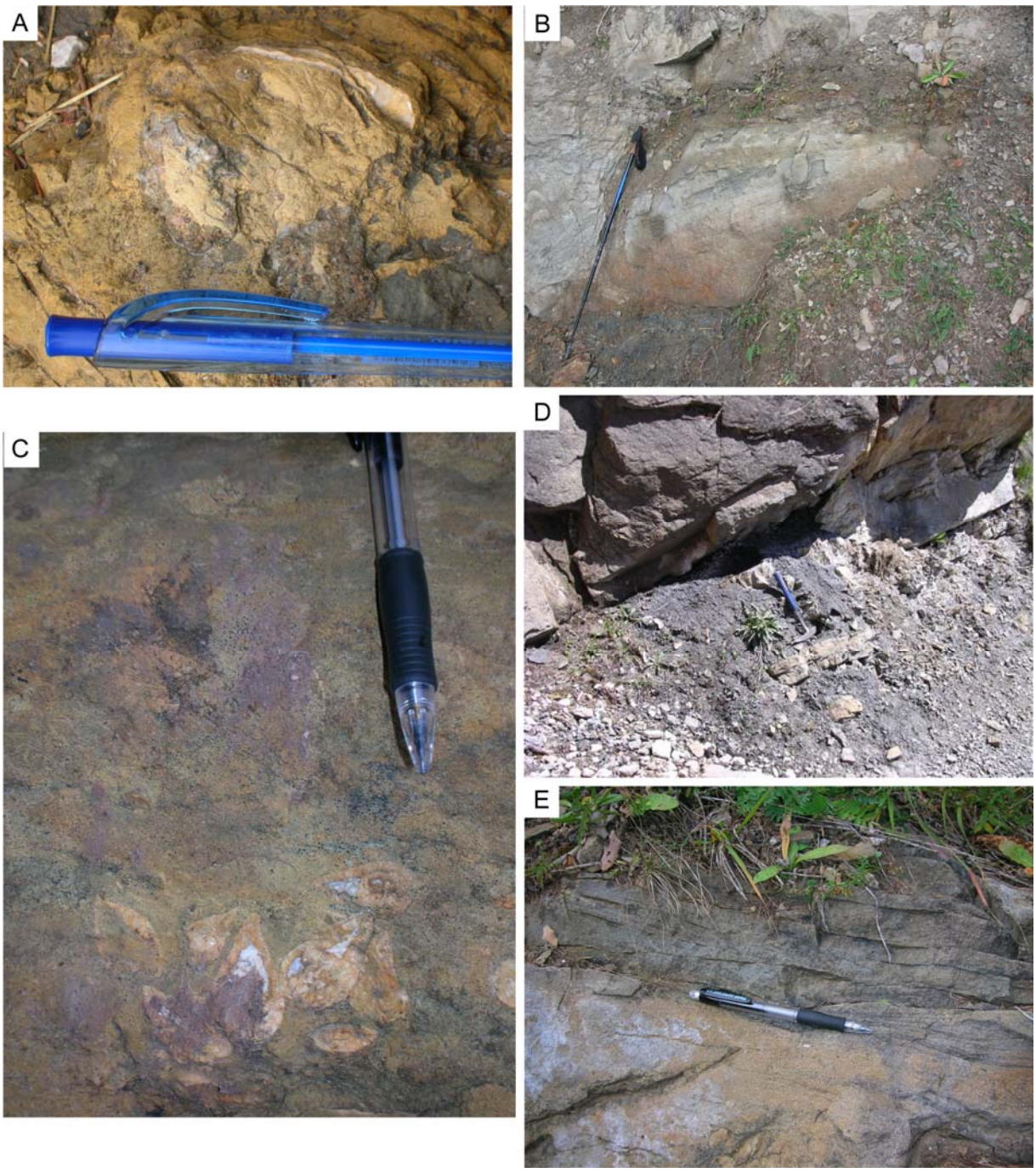

FIGURE 31 – Main facies of lithozones D and E, Heiligkreuz Fm., Rifugio San Marco section. A) Contact between the lithozones D and E: cm-scale karst cavities infilled by arenites. B) Cross-bedding in fluvial bar (facies 4 and 5). C) Megalodontidae bivalves in life position (facies 9). D) Conglomerate with load casts (facies 2) overlaying massive marls and carbonates of a desiccation pod (hammer) (facies 7). E) Sigmoidal stratification and mud drapes in tidally-influenced arenites (facies 8).

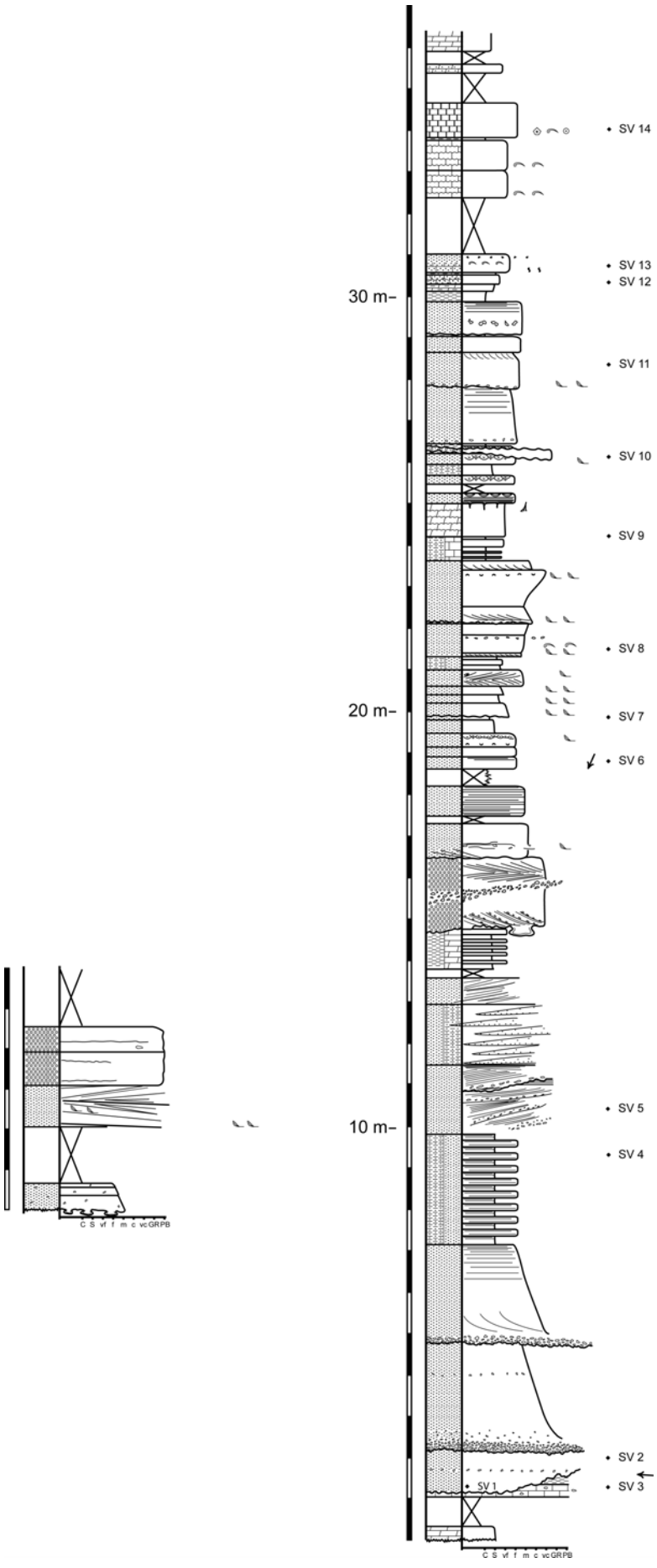

FIGURE 32 – Log of lithozone E, Heiligkreuz Fm., Rifugio San Marco section. Legend as in Fig. 23.

2.3.2 Travenanzes Fm.

The Travenanzes Fm. lies between the Heiligkreuz Fm. and the Dolomia Principale/Hauptdolomit Fm. It overlies the massive dolomite of the Lagazuoi member (Heiligkreuz Fm.) with a sharp, erosional contact of regional extent.

The upper boundary is gradational, corresponding to the fading of the fine siliciclastic levels (Breda et al., 2008).

The Travenanzes Fm. comprises three carbonate-siliciclastic cycles (Breda et al., 2006). The sand-sized deposits are limited to the first interval. In the Dolomite area, this interval is has been studied at the outcrops of Rifugio Dibona, Rifugio S. Marco, and Forcella Falzarego.

Code	Grain size/ lithology	Features	Fossils – bioturbation	Layer thickness	Interpretation
TERMINAL FAN/ALLUVIAL PLAIN					
1	Slt.	Sandy, multicolored, carbonate (caliche) nodules are present	-	m-thick	Flood-basin fine deposits
2	Lms.-Ds.	Nodular, sometimes teepee structures	-	dm-thick	Paleosols, arid setting
3	Cglm.	Massive, fining-upwards, sharp base	-	1m max	River channel, ephemeral
4	Ar.	Massive or faint cross-laminated, sometimes slightly erosive base, scattered caliche pebbles	-	dm	Sheet flood

TABLE 10 – Main siliciclastic facies of the first sedimentary cycle, Travenanzes Fm. Grain size/lithology key as Table 7.

FIGURE 33 – Contact between Heiligkreuz and Travenanzes Fms., Rifugio Dibona section. A) The thick dolomitic lithozone H (Heiligkreuz Fm.) overlain by B) the mixed fine-terrigenous/carbonate Travenanzes Fm.

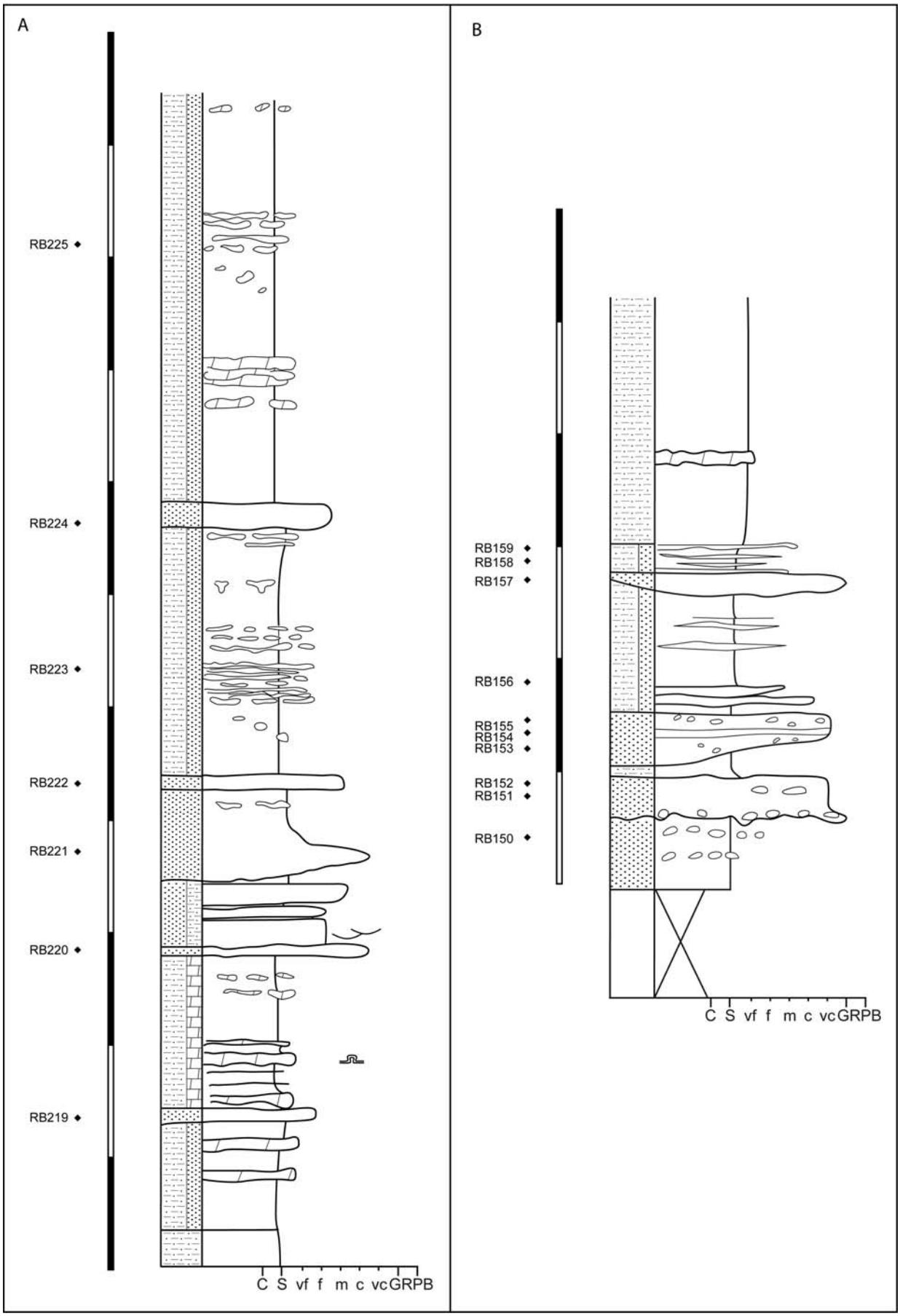

FIGURE 34 – Stratigraphic logs of the coarse siliciclastic deposits (first interval of Travenanzes Fm.). A) Rifugio S. Marco section; B) Forcella Falzarego section. Legend as in Fig. 23.

Rifugio Dibona/Forcella Falzarego/Rifugio S. Marco sections – first interval

Coarse-grained terrigenous material at the Rifugio Dibona/Forcella Falzarego section is organized in dm- to m-thick layers of coarse to medium arenites, massive to faint-laminated, with erosive base and limited lateral continuity; cm-size carbonate nodules can be found. Arenites are alternated to m-thick packages of sandy siltstones with dolomite layers and/or nodules, and to dm-thick dolomite layers of pedogenetic origin.

Interpretation: Arenite layers can be interpreted as channel deposits because of erosive base and lateral wedging. The character of these rivers is of ephemeral streams because of the limited thickness, the frequent lateral avulsion and the carbonate fragments which can be interpreted as derived from arid paleosols (calcisols). The overall environment is continental (flood-basin).

2.3.3 RIO DEL LAGO Fm.

In the Dogna area the very first sand-sized sedimentary input can be found in the Rio del Lago Fm. (lower Carnian) in the Rio Mas and Rio Pontuz sections. These sections/samples have been analyzed for comparison with the overlying deposits.

In both sections, arenites are found in two distinct levels, separated by a few meters of carbonate ramp deposits (see § 1.3.4). The first level is wedge-shaped, dm-thick, with erosional base, rip-up clasts at the base and plane-parallel lamination. The second level is approximately one meter thick, organized in a coarsening-upwards sequence. Grain size ranges from fine to medium, sorting is good, and bivalves and plant remains are observed.

Interpretation: Due to the inner-ramp setting and limited thickness but extended lateral persistence, those deposits are interpreted as terrestrial-derived terrigenous emplaced by longshore currents. This may be testified also by the mixture of marine and continental features (bivalves and plants).

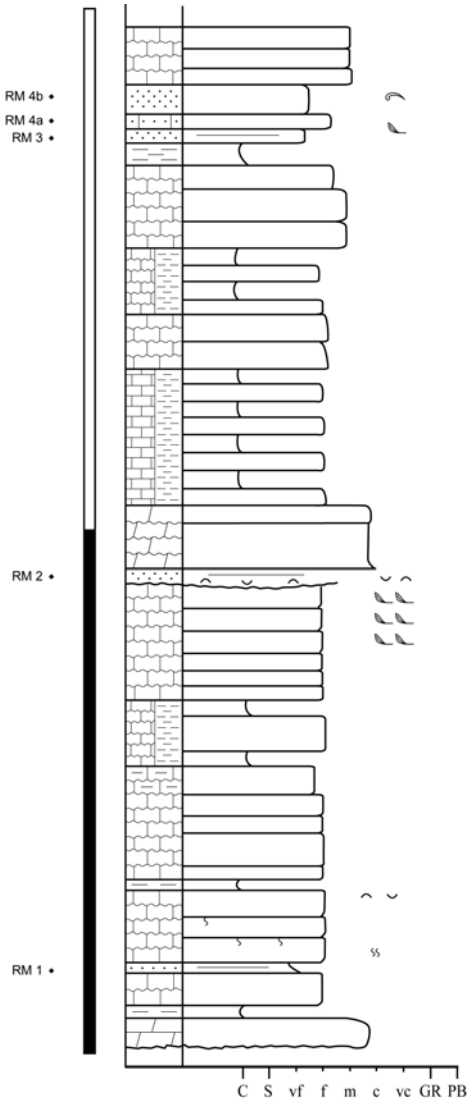

FIGURE 35 – Stratigraphic log of the siliciclastic layers within the Rio del Lago Fm., Rio Mas section. Legend as in Fig. 23.

2.3.4 "DOGNA" fm.

The main coarse siliciclastic input in the Dogna area was observed at the Rio Pontuz, Gran Colle I and II and Rio di Terrarossa III sections. The base of the "Dogna" fm. crops out in the Gran Colle 1 and 2 sections and it is represented by m-thick medium arenites sharply overlaying the carbonate-fine siliciclastic facies of the Rio del Lago Fm. ramp. The boundary is also marked by a horizon with microbially-coated bioclasts (see § 1.4.2).

Overall, the "Dogna" fm. displays two distinct arenite successions separated by a carbonate-dolomite interval ("lower" and "upper" arenites). The different portions of the succession are split between the Gran Colle 1 and 2 (basal "Dogna" fm.) and Rio Pontuz sections (carbonate interval and upper arenites). Rio di Terrarossa succession is more difficult to correlate, but it could tentatively be attributed to the upper arenites.

Correlation has been performed with palynological analyses (see § 2.3.5) and based on fieldwork observations.

Gran Colle 1 and 2 sections – basal "Dogna" fm.

The succession starts off with 2.5m of standard Rio del Lago Fm. deposits, represented by dm-thick layers of wackestone-packstones intercalated to silt-marls, and by m-thick levels of nodular packstones (Fig. 36). The uppermost layers are characterized by microbialite encrustation-erosion (see§ 1.4.2).

These carbonates are sharply overlain by 8m of medium arenites in a dm- to m-thick massive beds, with trough cross-bedding in the thickest layers, bioturbation and bivalves (facies T, B, E, see Table 11). Arenites are intercalated by a 1.5 m-thick level of nodular cherty packstones.

The following 16m are mainly carbonate, with minor arenite intercalations, and are made of dm-thick bioclastic wackestone-packstones.

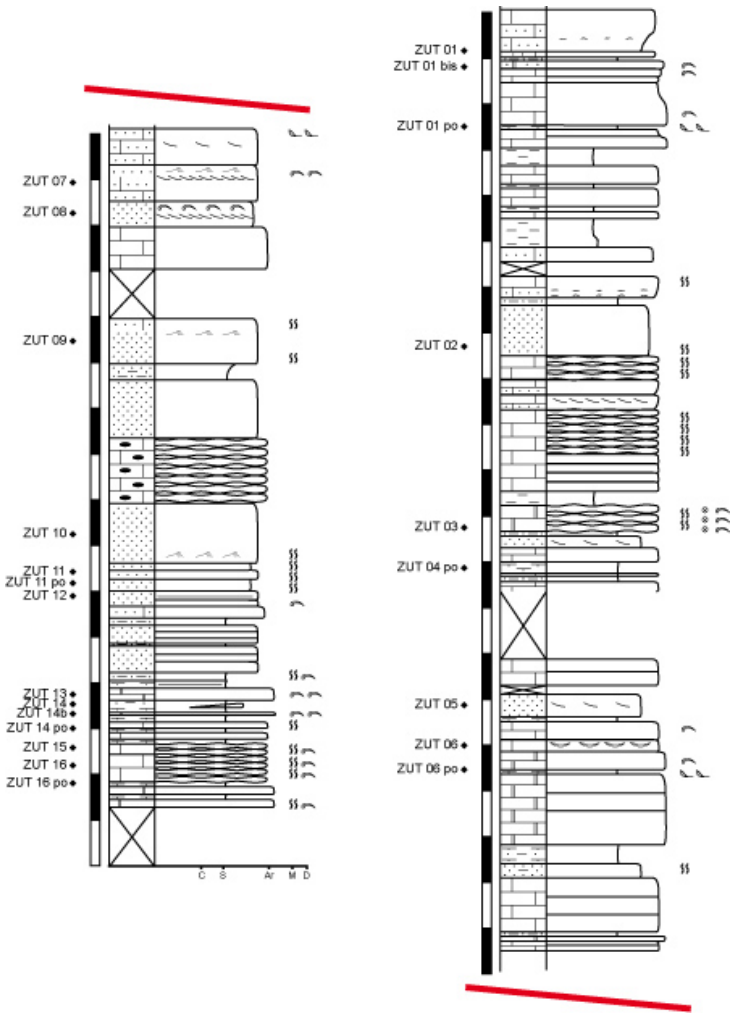

FIGURE 36 – Stratigraphic log of the basal "Dogna" fm., Gran Colle 2 section. Legend as in Fig. 23. Position of samples for palynological analyses is also indicated.

The uppermost 8m are represented by a mixed carbonate-fine siliciclastic succession, with a thick massive arenite layer at the base (facies T). Carbonate deposits are mainly wackestones with bivalves. Plant remains are present, as well as bioturbation.

Interpretation: The overall carbonate facies throughout the succession represent a delta front/inner-ramp environment, in continuity to the uppermost Rio del Lago Fm. deposits. The intercalated arenites are mainly massive, secondarily cross-bedded, with pervasive bioturbation

and bivalve shells. This testifies submarine conditions and leads the interpretation of terrigenous bodies as submerged mouth bars.

Two thicker, massive to cross-bedded layers without marine fossils can be considered as distributary channels.

Distinction between mouth bars and channels has been based mostly on presence of marine fossils. Similarity of facies/geometries between distributary channel and mouth bars has been outlined by Fielding et al. (2005).

Rio di Terrarossa section – lower? arenites

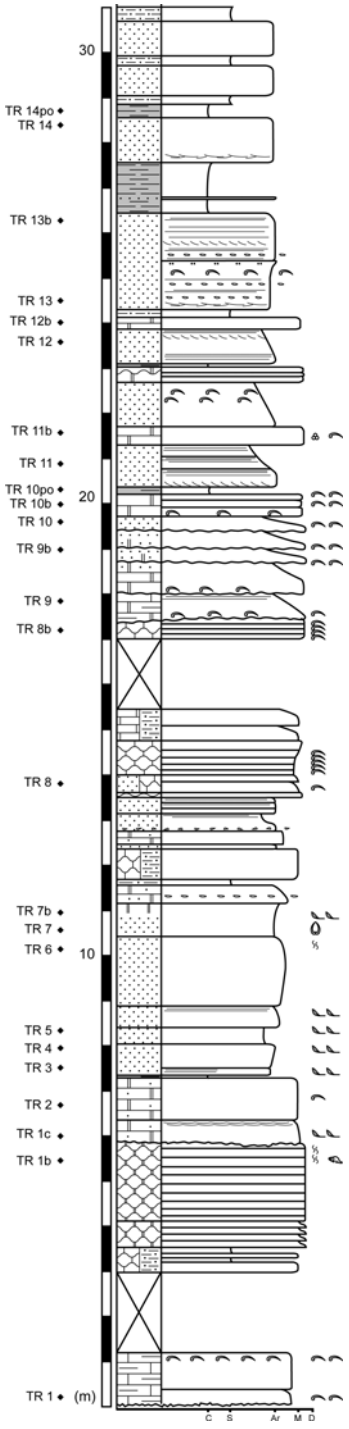

This succession is of not obvious correlation, but it could tentatively be attributed to the Gran Colle 2 section (lower arenites).

The recorded succession starts off with 6m of wackestone/packstones with bivalves and gastropods, slightly nodular to nodular, marly at the base, with thin marl-silt intercalations.

1.5m of brecciated wackestone follow, with slightly erosive base, algal lamination and ostracods.

Arenites overlay the breccia package with sharp base. They are a 4m-thick series of medium to coarse arenites, with vague planar lamination (facies Pl), or massive (facies H), with high plant debris content. The trend is thickening-upwards.

The following 4.5m show dm-thick alternations of packstone and arenite levels. Packstones are slightly nodular to nodular and rich in bivalve shells. Arenites display plane-parallel lamination and sometimes clay chips (facies Fb).

The overlying package shows predominance of arenite layers, which thicken upwards. Lower arenite layers have slightly erosive base, and display plane-parallel lamination and high bivalve content (facies Fb). Following layers show predominant plane-parallel lamination (facies E) and only secondarily cross-bedding, or are massive with bivalve shells (facies T).

FIGURE 37 – Schematic stratigraphic log of the lower "Dogna" fm., Rio di Terrarossa section. Position of samples for palynological analyses is also indicated. Legend as in Fig. 23.

The thickest layer is 2m thick, and show levels of plane-parallel lamination marked by opaque minerals, clay flakes and bivalves (facies E).
Thick (1.5m) dark clays follow (facies Pe) with thin fine arenites intercalations (facies O), capped by a 1m thick massive arenite layer with vague cross-lamination at the base. An alternation of dark clays and massive arenites follows, dm-thick.

Interpretation: The overall sedimentary environment is the same as in the Gran Colle 2 section. The succession displays clastic pulses in the inner ramp carbonate facies with a general transgressive trend. The lover massive or cross-laminated arenites with plant debris and no marine fossils could represent a distributary channel.
The more mixed lithologies could testify the amalgamation of terrestrial input and inner ramp autochtonous sedimentation in the shallow ramp, as confirmed by the abundant bivalves. The following traction-laminated arenites could represent the mouth bar. An emersion is testified by the thick pelitic interval intercalated to fine arenites at the top of the succession, which can be interpreted as a lagoon.
Overall, those features could be found together in a delta front system.

Rio Pontuz section – upper arenites
The upper part of the Rio Pontuz section (above the Rio del Lago Fm., see § 1.3.4) is composed by a first carbonate succession and by subsequent arenites.
The first interval is represented by a 40 m-thick package of mudstones/wackestones, vacuolar dolostones, marly dolostones with clay intercalations occurs. The lower beds contain rare bivalves and plant debris, and are mainly limestones. In the upper part, this interval is more dolomitic, and comprises vacuolar and aphanitic dolostones.
Two arenite layers have been found within the carbonate succession. Both are structureless, made of fine-to medium arenites, and contain no fossils. The first layer is at the very base, m-thick; the second one, dm-thick, lays around 10m above.
The whole interval is interpreted to lay above the lower arenites outcropping in the Gran Colle I/II and in the Rio di Terrarossa III section.

Interpretation: the general succession could be interpreted as a low-energy, extremely proximal carbonate inner ramp. Fossiliferous limestones may indicate subtidal deposits. However, peri-supratidal deposits represented by the vacuolar and aphanitic dolostones are more abundant, and suggest a carbonate coastal mudflat to sabkha in an overall arid setting.

The second part also constitutes the second major siliciclastic input o the "Dogna" fm.. The transition from carbonates to arenites is gradual, represented by an increase in frequency and thickness of arenite layers between the carbonate deposits.

These upper deposits are characterized by rapid alternation of arenites and carbonates, organized in two coarsening/thickening upwards cycles.

The base of the cycle is represented by carbonate intervals, composed by arenaceous dolomites and sometimes clays and nodular mudstone-wackestones (facies D, L).

The following arenites are mainly dm-thick, fine-to medium-grained, bioturbated, massive or with cross-lamination (facies Fa and Fb respectively), sometimes fining-upwards (facies E).

Higher in the succession, arenites mainly display dm-to m-thick massive layers (facies Fc), with less carbonate intercalations, and m-thick layers of medium- to coarse-grain size with plane-parallel and/or cross-lamination (facies H).

At the top of the second cycle, m-thick arenites of facies E predominate, with sometimes erosive base, plane-parallel and cross- lamination and bivalve shells at several layers, intercalated with nodular wackestone-packstone with bivalves (facies L).

Code	Grain size/ lithology	Features	Fossils - bioturbation	Layer thickness	Interpretation
LAGOON					
O	M Ar.	Organic matter flakes.	-	dm	Paralic deposits, vegetated
Pe	Clay-silt	Dark color, plane-parallel lamination	Molluscs	dm to m	Paralic deposits
D	Mds-Wks, Ds.	Brownish, vuggy, marly	Rare bivalves	dm	Coastal mudflat, supratidal, in arid setting
DISTRIBUTARY CHANNEL – LEVEE					
Pl	VF-M Ar.	Plane-parallel lamination.	-	dm	Levee
H	M-C Ar.	(Vague) plane-parallel and cross lamination.	-	dm	Bedload channel deposits
Fc	From M-C Ar. to F. Ar.	Fining-upward sequence, sharp base, massive.	-	m	Non cohesive sheet flow (flashflood events?), channel deposits
C	C Ar.	Erosive base, plane-parallel lamination at the base, low-angle cross-bedding in the middle.	-	> m	Bedload channel deposits
SUBMARINE MOUTH BAR					
Fa	From M-C Ar. to F. Ar.	Normal grading, sharp base, plane-parallel lamination at the base, ripples at the top.	Bivalves, bioturbated	cm- to dm	Submarine mouth bar
Fb	From M-C Ar. to F. Ar.	Normal grading, erosive base, cross-bedding at the base. Rip-up clasts can be present.	Molluscs	m	Submarine mouth bar
T	F-M Ar.	Massive (mottled).	Bivalves, *Thalassinoides*	dm to m	High biotic activity, submarine mouth bar
E	M-F Ar.	Erosive base, fining-up, plane-parallel and/or cross bedding	Bivalves, bioturbation	dm to m	Submarine mouth bar
SUBTIDAL INNER RAMP					
B	F Ar.	Silty, plane-parallel lamination (vague cross-bedding).	Bioturbated, sometimes bivalves	dm	Outer mouth bar/ inner ramp
L	Lms.	Slightly nodular.	Bioturbated	dm	Inner ramp

TABLE 11 – Main facies of siliciclastic units, lower and upper "Dogna" fm. (Rio di Terrarossa/Gran Colle 2 and Rio Pontuz sections, respectively). Grain size/lithology key as Table 7.

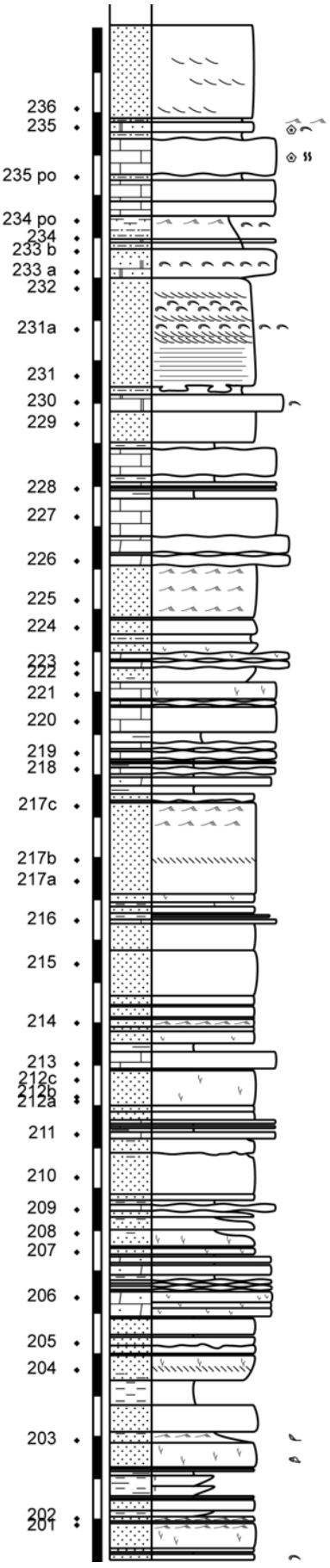

Interpretation: The upper "Dogna" fm. again represents a delta front/inner ramp environment, with the same three main elements (mouth bars, distributary channel and autochtonous carbonate sedimentation) already documented for the lower arenites. The two recognized thickening/coarsening-upward sequences represent a shallowing trend from inner ramp to distributary channel and testify a high lateral facies shift.

The unclear predominance of either wave- or tide-influence points towards a mixed-energy system. Energy increases upwards (thickening).

The two coarse siliciclastic units can be linked to the lithozones A-B and E of the Heiligkreuz Fm. in the Dolomites area (Preto and Hinnov, 2003). The progadational character of the lower arenites of the "Dogna" formation support their correlation to the lithozones A-B.

FIGURE 38 –Schematic stratigraphic log of the upper arenites of the "Dogna" fm., Rio Pontuz section. Legend as in Fig. 23.

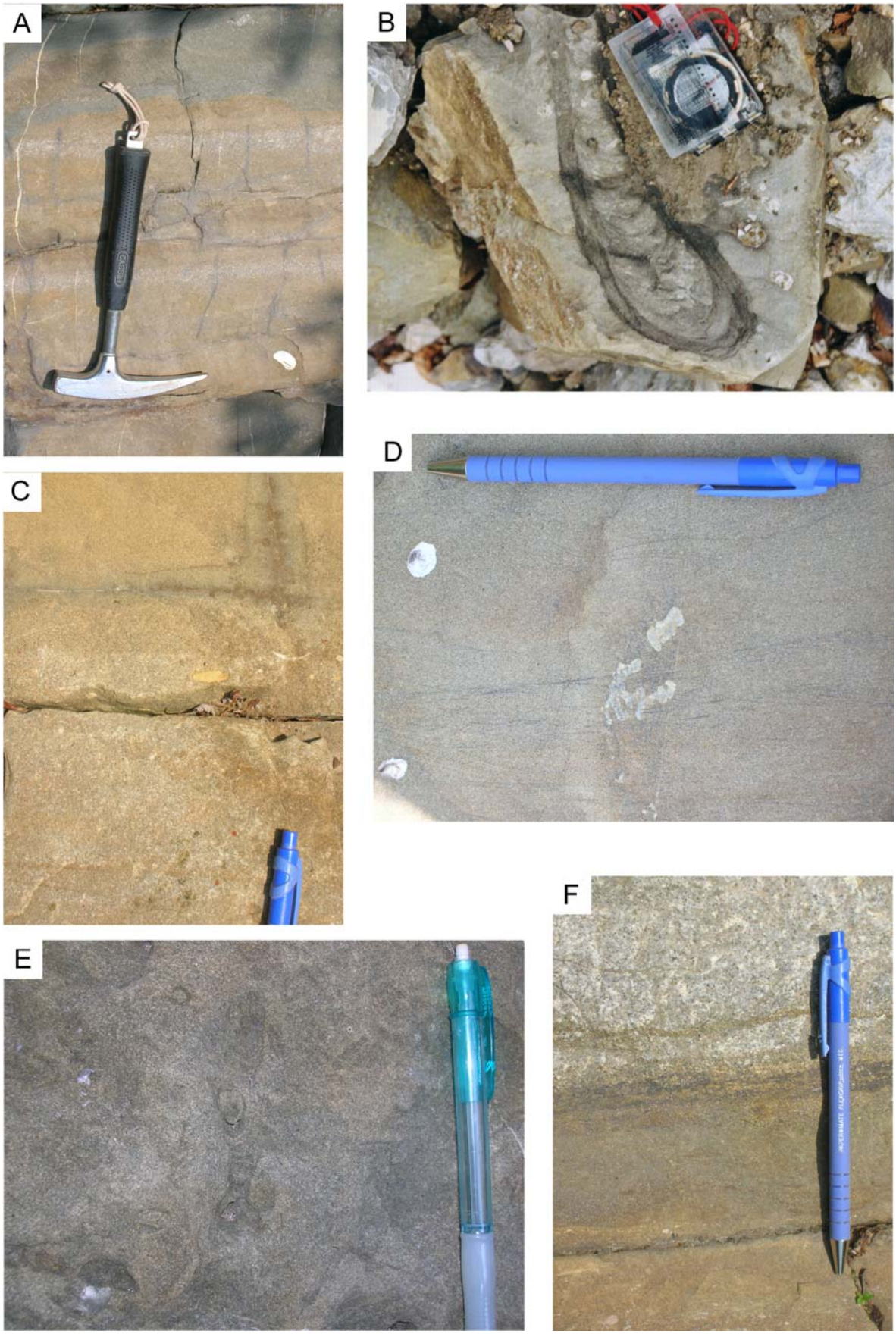

FIGURE 39 – Lithofacies of the "Dogna" fm. A) arenites with bioclasts concentrations, facies T, Rio di Terrarossa section; B) *Diplocraterion* (?) bioturbation, Rio Pontuz section; C) contact between arenites (facies C) and arenites (facies Fb), Rio di Terrarossa section; D) cross-lamination enhanced by opaque minerals, facies H, Rio di Terrarossa section; E) bioturbation in medium-size arenites, facies Fa, Rio di Terrarossa section; F) contact between arenites (facies H) and limestone-wackestone (facies L), Rio di Terrarossa section.

2.3.5 Correlation between the Dogna area and the Dolomites

Physical correlation of layers between the two study areas (Dolomites and Julian Alps) results impossible because of the spatial distance (around 100km). Within the specific Dogna area, moreover, correlation of stratigraphic sections results challenging because of the tectonic dislocations and disturbances. The biostratigraphic approach appeared thus useful for the dating and correlation of the different sections, trough the integration of a qualitative study of palynological samples of three sections in the Julian Alps and ammonoids and conodonts data from literature (Roghi 2004, Preto and Hinnov, 2003 and references therein).

On the whole, 14 samples of the "Dogna" fm. have been analyzed, taken from the Gran Colle II section (8 samples), from the Rio di Terrarossa III section (2 samples) and from the Rio Pontuz section (4 samples).

Pollen analyses were performed by Dr. Guido Roghi, CNR, Padova.

Gran Colle II section (from bottom to top)

ZUT 16

Pyrite, inertinite and wood fragments are absent. Abundant pollens, bright.

Foraminiferal lining

Ovalipollis pseudoalatus	Thiergart, 1949, Schuurman, 1976
Lycopodiacidites keupperi	Klaus, 1960
Duplicisporites granulatus	Leschik, 1956 emend. Scheuring, 1970
Todisporites minor	Couper, 1958
Todisporites major	Couper, 1958

Calamospora sp.

Illinites sp.

Tasmanites sp.

Monosaccite pollen cf. *Heliosaccus sp.*

Luekysporites sp.

Cycadosporites sp.

Sphaeripollenites sp.

Paracirculina/Praecirculina sp.

Converrucosporites sp.

Lunatisporites sp.

Klausipollenites sp.

Concavisporites sp.

Reticulatisporites sp.

ZUT 14

Rich in marine organic matter, pyrite is absent.

Algae spores

Foraminiferal linings

Vallasporites ignacii	Leschik, 1956
Cymatiosphaera sp.	
Todisporites minor	Couper, 1958
Ovalipollis pseudoalatus	Thiergart, 1949, Schuurman, 1976
Pityosporites sp.	
Lunatisporites acutus	Leschik, 1956 emend. Scheuring, 1978
Aratrisporites sp.	
Densosporites sp.	
Triadispora sp.	
Klausipollenites sp.	
Enzonalasporites vigens	Leschik, 1956
Ovalipollis ovalis	Thiergart 1949, Schuurman 1976
Concavisporites sp.	
Lunaporites sp.	

ZUT 11

Pyrite framboids are absent. Intertinite is present.

Deltoidospore sp.	
Vallasporites ignacii	Leschik, 1956
Todisporites sp.	
Duplicisporites granulatus	Leschik, 1956 emend. Scheuring, 1970
Camerosporites secatus	Leschik, 1956 emend. Scheuring, 1978
Trilites tubercoliformis	Cookson, 1947
Todisporites major	Couper, 1958

ZUT 06

Abundant pyrite framboids. Pollens are oxidized. Organic matter of algal origin.

Patinaporites densus	Leschik in Kräusel et Leschik 1956
"Lagenella" sp.	Remarks: 60-62 µm long
Paracirculina sp.	

ZUT 04

Sterile

ZUT 01

Algae spore

Alisporites sp.

Vallasporites sp.

Vallasporites ignacii Leschik, 1956

ZUT 01

Abundant pyrite framboids. Wood fragments and vitrinite are present. Pollen/spores grains are rare.

Patinasporites cf. densus

Vallasporites sp.

Klausipollenites sp. or *Chordasporites sp.*

Rio di Terrarossa III section (from bottom to top)

TR 10

Concavisporites sp.

TR 14

Abundant inertinite, rounded.

Aratrisporites parvispinosus Leschik, 1956

Simplicisporites cf. S. pendens Leschik, 1956

Rio Pontuz section (from bottom to top)

TUZ 189

Inertinite dominates, much diagenesis-affected. Rare vitrinite. Pollen grains are also dark.

Duplicisporites verrucosus Leschik, 1956 emend. Scheuring, 1978

Ellipsovelatisporites rugosus Scheuring, 1970

Calamospore sp.

Uvaesporites gadensis Praehauser-Enzenberg, 1970 Remarks: tetrad configuration

Trilites sp.

Kyrtomisporis sp.

Lunatisporites acutus Leschik, 1956 emend. Scheuring, 1978

Triadispora sp.

Uvaesporites gadensis Praehauser-Enzenberg, 1970

Klausipollenites sp.

Kymatiosphaera sp.

Concavisporites sp.

Vallasporites ignacii Leschik, 1956 Remarks: tetrad configuration

TUZ 190

Less organic matter, both inertinite and vitrinite.

Amber fragment

Uvaesporites sp.

Concavisporites sp.

Gibeosporites hirsutus Leschik, 1956

Duplicisporites verrucosus Leschik, 1956 emend. Scheuring, 1978

Concavisporites sp.

Duplicisporites sp.

Enzonalasporites vigens Leschik, 1956

Lycopodiacidites kuepperi Klaus, 1960

Ovalipollis pseudoalatus Thiergart, 1949, Schuurman, 1976

Trilites tubercoliformis Cookson, 1947

Todisporites minor Couper, 1958

Vallasporites ignacii Leschik, 1956

Triadispora sp.

TUZ 234

More abundant organic matter, less lignitified, made of inertinite, vitrinite, preserved wood fragment (cuticle)

Amber fragments

Todisporites major Couper, 1958

Ovalipollis ovalis

Todisporites minor Couper, 1958

Concavisporites sp.

Sellaspora rugoverrucata Van der Eem, 1983

Accinctisporites sp.

Vallasporites ignacii Leschik, 1956 Remarks: juvenile? Form

Camerosporites secatus Leschik, 1956 emend. Scheuring, 1978

Aratrisporites paraspinosus Klaus, 1960

Ellipsovelatisporites sp.

Aratrisporites scabratus Klaus, 1960

Enzonalasporites vigens Leschik, 1956

Patinasporites cf. Patinasporites densus Leschik in Kräusel et Leschik 1956

Aulisporites astigmosus Leschik, 1956

Marsupipollenites sp.

Lunatisporites sp.

Aratrisporites scabratus

Klausipollenites sp.

Concavisporites sp.

Patinasporites densus Leschik, 1956, emend. Scheuring, 1970

Todisporites major Couper, 1958

Ovalipollis pseudoalatus Thiergart, 1949, Schuurman, 1976

Calamospora sp.

Dulcisporites maljawkinae

Alisporites sp.

Verrucosisporites sp.

Chasmatoporites sp.

Lycopodiacidites kuepperi Klaus, 1960

TUZ 235

More rounded inertinite fragments.

Aratrisporites parvispinosus Leschik, 1956

Vallasporites ignacii Leschik, 1956

Lagenella martinii Leschik, 1956, Klaus, 1960

Enzonalasporites vigens Leschik, 1956

Ovalipollis pseudoalatus Thiergart, 1949, Schuurman, 1976

Lunatisporites acutus Leschik, 1956 emend. Scheuring, 1978

Patinasporites cf. P. densus

Aulisporites astigmosus Leschik, 1956

Infernopollenites sp.

Accinctisporites sp.

Klausipollenites sp.

Aratrisporites paraspinosus Klaus, 1960

Calamospora sp.

Aratrisporites scabratus Klaus, 1960

Paracirculina maljawkinae Klaus, 1960

GENERAL REMARKS:

Gran Colle section

This section contains the boundary between the Rio del Lago Fm. and the "Dogna" fm. (See § 2.3.4).

ZUT 11-14-16: Poor association, but similar to that of the upper Conzen Fm. (Roghi, 2004, Preto et al., 2005). Between these and the uppermost samples an environmental change occurs (pyrite framboids appear). Qualitatively, sample ZUT 11 seems to testify more humid conditions.

ZUT 6: *Lagenella sp.* indicates middle to late Conzen Fm. Pyrite framboids appear in this sample.

Rio di Terrarossa III section

TR 14-10: Pyrite framboids are absent, correlation is questionable.

Rio Pontuz section

TUZ 189-190: The samples can be correlated with the uppermost Conzen Fm. – base of Tor Fm. These samples represent the top of the lower arenites (Fig. 40).

TUZ 234-235: correlate with the middle Tor Fm.

The palynological analyses confirm the relative position of stratigraphic sections of the Dogna area reconstructed from fieldwork, and allows a more detailed correlation with the Dolomites area (Fig. 40, Appendix V). Lower arenites of the "Dogna" fm. (samples ZUT) correlate with the lithozones A/B of the Heiligkreuz Fm., and are characterized by the presence of pyrite framboids. The uppermost lower arenites are represented in the Rio Pontuz section (samples Tuz 189 I and 190 I). Upper arenites (samples Tuz 234 I and 235 I) link to the lithozones E/F. Samples from the Rio di Terrarossa III section cannot be placed definitely, but palynological analyses don't exclude their possible correlation to the lower arenites of the "Dogna" fm., as could be suggested from fieldwork (see § 2.3.4).

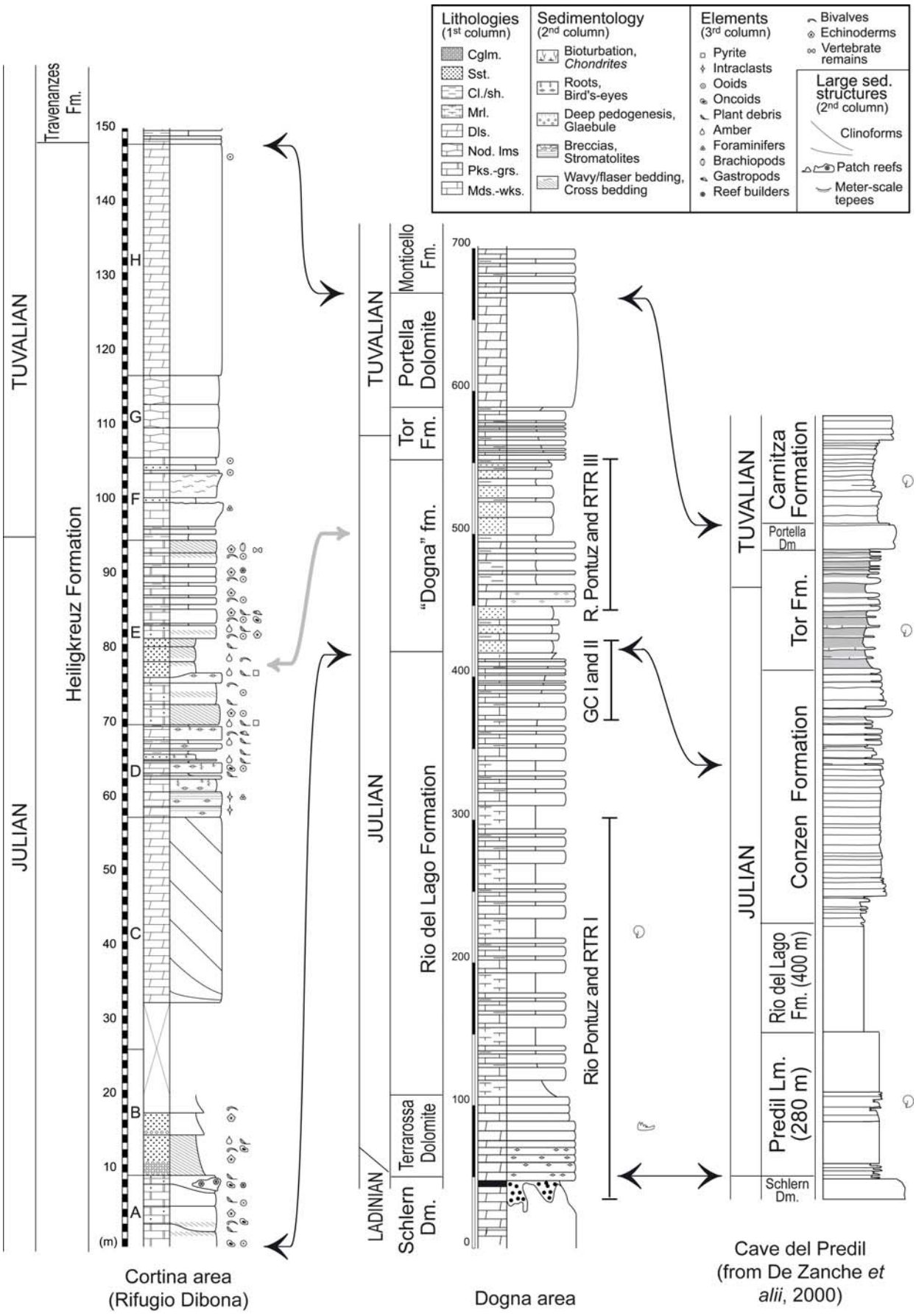

FIGURE 40 – Correlation between the study areas, Dolomites and Julian Alps zones. Mod. from Roghi (2004) and Preto et al. (2005). Dogna area: overall stratigraphic section "merging" the measured logs (indicated to the right). Cortina area: stratigraphic section for a basinal setting, i.e. Rifugio Dibona. Cave del Predil section: reference for palynostratigraphy. Dark arrows: biostratigraphical correlations. Gray arrow: lithological correlation.

2.4 RESULTS

A total of 107 thin sections of arenites have been analyzed, belonging to the Rio del Lago and "Dogna" Fms. of the Julian Alps (5 and 45 samples respectively), and to the Heiligkreuz and Travenanzes Fms. of the Dolomites (30 and 27 samples respectively). Samples were taken from both proximal and distal sections. See Table 12 for sample distribution.

Formation	Member/subdivision	Proximal sections	Distal sections
Rio del Lago Fm.		Rio Pontuz (n = 2) Rio Mas (n = 3)	
"Dogna" fm.		Rio di Terrarossa (n = 11) Rio Pontuz (n = 26)	Gran Colle I (n = 1) Gran Colle II (n = 7)
Heiligkreuz Fm.	Lit. B	Borca di Cadore (n = 4)	Rif. Dibona (n = 5)
	Lit. E	Rif. S. Marco (n = 8)	Rif. Dibona (n = 7)
	Lit. F		Rif. Dibona (n = 2) Lagazuoi (n = 2)
	Lit. H		Passo Falzarego (n = 2)
Travenanzes Fm.	I interval	Rif. S. Marco (n =10)	Rif. Dibona (n = 5) Forcella Falzarego (n = 12)

TABLE 12 – Sampled collected and analyzed with clastic sedimentary petrology techniques.

2.4.1 Components

2.4.1.1 NCE

Quartz broadly represents the 35% of the total rock sample on average for the Heiligkreuz-"Dogna" Fms. and the 48% of the Travenanzes Fm. It is present mostly as monocrystalline grains with straight extinction, with mainly sub-angular outline. Monocrystalline quartz is predominantly volcanic (clear, inclusion-free) (Fig. 42A), and only secondarily plutonic (inclusion-rich, with faint undulose extinction).

Quartz crystals are also present as phenocrysts in volcanic rock fragments, with an average value of 2% of the general composition (Fig. 42C).

Coarse-grained polycrystalline aggregates are rare, mainly found in the "Dogna fm." (2% on average). They present recrystallization features, and are made up by a juxtaposition of crystals (> 63μm) with straight or slightly undulose extinction. Clast outline is sub-angular to sub-rounded (Fig. 41B).

Feldspars are not abundant, as they amount to 5%, with a maximum of 17% on the total rock volume (Travenanzes Fm., Rifugio Dibona section). They are represented by more or less altered, monocrystalline plagioclases with twinning and by rare K-feldspars in single, altered crystals. Shapes are both sub-rounded and sub-angular. Feldspars within rock fragments

(mainly volcanic) make up the 1% of the total rock volume on average (Fig. 42D). Composition gathered from Albite twinning in plagioclase indicates mostly andesine and oligoclase mineralogies (An_{30-50} and An_{10-30} respectively), typical of acidic to intermediate volcanic lithotypes.

Lithic grains are almost exclusively of volcanic origin (47, 44 and 21% of the overall composition on average for the "Dogna", Heiligkreuz and Travenanzes Fms. respectively).

Dominant composition is acidic, with an average value of 43, 35 and 17% on total arenite volume for "Dogna", Heiligkreuz and Travenanzes Fms. respectively.

Recognized textures are mainly porphyric (occasionally fluidal) (Fig. 42C, D, E) and aphanitic (glass). "Acidic" lithologies with porphyric texture and quartz and plagioclase phenocrystals in fine ground mass can be defined as rhyolite (Fig. 42C). When ground mass is richer in opaque minerals and higher birefringence crystals are present (i.e. phyllosilicates), the clast has been classified as "intermediate" volcanic. For the richness in alkali feldspars, those grains could tentatively be interpretable as shoshonite (Fig. 42D).

Between the aphanitic lithologies, a peculiar type of acidic volcanic is represented by juxtaposition of patchy feldspar-quartz crystals. These clasts have been tentatively classified as devitrified volcanics (Fig. 42F). A further kind of glass has been sometimes found, showing as fibrous, concentric, yellowish to brown at parallel polars. At crossed polars interference colors are low. This characteristics belong to spherulites, a structure occurring for quick devitrification. See Fig. 47E ("Dogna" fm.).

For all the volcanic grains, clasts are sub-rounded to sub-angular; sorting and grain size are comparable to the quartz clasts.

Some specimens present silicification and alteration features (Fig. 48C, "Dogna" fm.), and have been listed separately. Those grains maintain shape, roundness and size of non-altered grains, but display juxtaposition of acicular microcrystalline silica (Fig. 48C, E).

Only a few (< 1%) metamorphic clasts can be found in the "Dogna fm." succession. The latter include quartz-rich rocks with evident planar anisotropy enhanced by distribution of mica crystals. Plutonic-gneiss rock fragments (recognizable from juxtaposed large quartz and feldspar crystals) are also rare, with an average amount of 1% of the overall composition.

Sedimentary rock grains (chert, siltstones) are virtually absent in the studied successions.

Carbonate Extrabasinal clasts (CE) result generally a very minor component, with an average value of less than 2% for the "Dogna fm." and are nearly missing in the Heiligkreuz and Travenanzes Fms. They are subdivided on the base of mineralogy (calcite or dolomite) and of crystal dimensions (micritic or sparitic). They are evaluated together with rock fragments for their behavior and provenance meaning.

Micas and Other Minerals are trace minerals, like phyllosilicates (biotite and chlorite), epidotes, opaque minerals and rarely zircon, found in single isolated crystals. Biotite was also sometimes found within volcanic rock fragments.
Average amount of trace minerals in the studied sections is steady, less than 5%, with predominance of opaque minerals.

2.4.1.2 CI

Carbonate intrabasinal clasts are represented by bioclasts, ooids and intraclasts. Bioclasts are rare, found only as entire benthic foraminifera and as fragmented bivalves and echinoderms. Ooids are rare in the studied sections overall, and are recrystallized. Intraclasts (Folk, 1974) are represented by micrite nodules. Round-shaped micritic clasts have been interpreted as carbonate soil fragments/nodules and included in the carbonate intrabasinal group (see Discussion). They occur in the uppermost Heiligkreuz and ”Dogna” formations and are generally widespread in the Travenanzes Fm. Some of them include fine-grained siliciclastic clasts, and have been defined “arenaceous”. Some specimens result soft, slightly squeezed between harder grains.
Carbonate intrabasinal clasts have highly variable values in the studied sections, with a minimum of 0.1% in the lowermost Heiligkreuz Fm. and a steady average value around 30% in the Travenanzes Fm.

2.4.1.3 NCI

This class is made up only by phosphate and green grains. Phosphate grains are pale brown, transparent, isotropic. The latter includes patchy highly birifrangent green particles, probably glauconite. Both categories occur occasionally, generally accounting less than 1% on the overall composition.

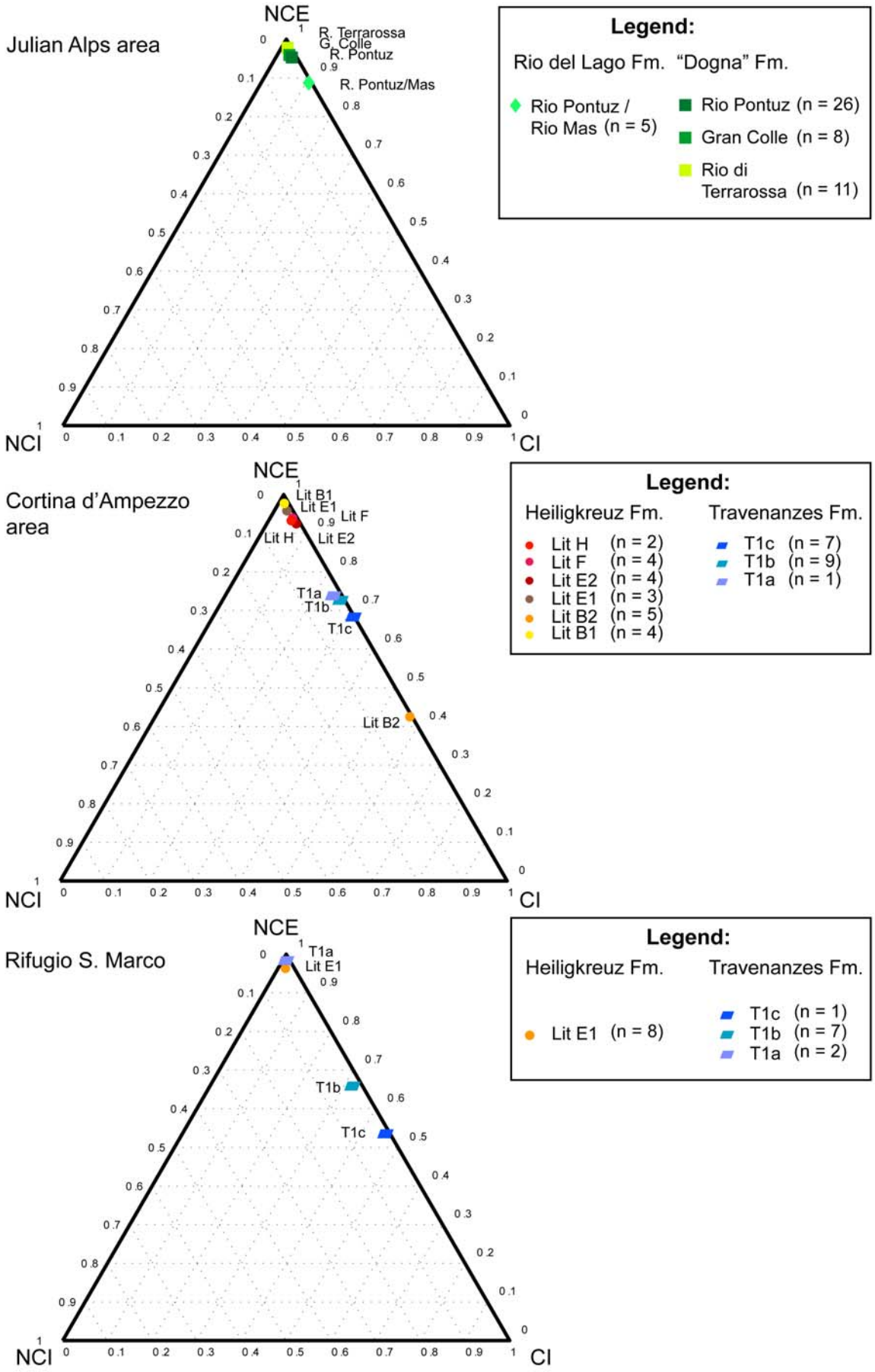

FIGURE 41 – NCE, NCI and CI ternary diagrams for the studied Carnian units, average values. A) Rio del Lago and "Dogna" fms., Julian Alps area; B) Heiligkreuz and Travenanzes Fms., Cortina d'Ampezzo area; C) Heiligkreuz and Travenanzes Fms., Rifugio S. Marco section. The studied samples can be classified as terrigenous arenites; only samples from lithozone B1 (Heiligkreuz Fm., Dolomites) belong to the hybrid arenites category.

2.4.1.4 Interstitial material-considerations on diagenesis

Major diagenetical alterations visible in the studied sections are of chemical origin. Following Harwood (1988), cementation can be defined mainly as disconformable, being represented by calcite and dolomite overgrowth. Quartz cementation is rare, limited to thin rims around quartz clasts (conformable cement). Rarely, dissolution effects have been detected, resulting in oversized pores between clasts (i.e. Heiligkreuz Fm.).

Fine aphanitic calcite cementation has been also found. Carbonate matrix (i.e. micrite) is present in the uppermost Heiligkreuz Fm. and is characteristic of the Travenanzes Fm., possibly as a result of breaking of intrabasinal carbonate soil fragments/nodules.

Clays and kaolinite have been found in interstitial position only rarely. Given the high susceptibility to alteration and dissolution of fine-grained volcanic clasts, the minor contribution of clay cements probably testify an early-stage carbonate cementation.

Mechanical modifications of clasts are limited to squeezing of soft, fine-grained volcanic matrix (pseudomatrix, Dickinson, 1970), typical for Heiligkreuz and "Dogna" formations, or of microcrystalline carbonate grains (more common for Travenanzes Fm.).

Categories for intergranular material are listed in Table 13.

Abbreviation	Feature
Cd	Dolomite cement
Cq	Quartz cement
matr c	Carbonate matrix
matr sil	Siliciclastic matrix
Psm	Pseudomatrix from volcanics
Clays	Clays
Kaolinite	Kaolinite
Pcx	Calcite plague on indeterminate grain
Pqx	Quartz plague on indeterminate grain
Alter	Altered grain
silicif.	Silicified grain
Oth	Other

TABLE 13 – Interstitial material categorization for petrographical analyses of arenites.

Diagenetic modifications result homogeneous throughout the studied sections, both laterally and vertically. Only the basal Heiligkreuz Fm. is distinguished for it's outstanding preservation in the Alpe di Specie area (Russo et al., 1991).

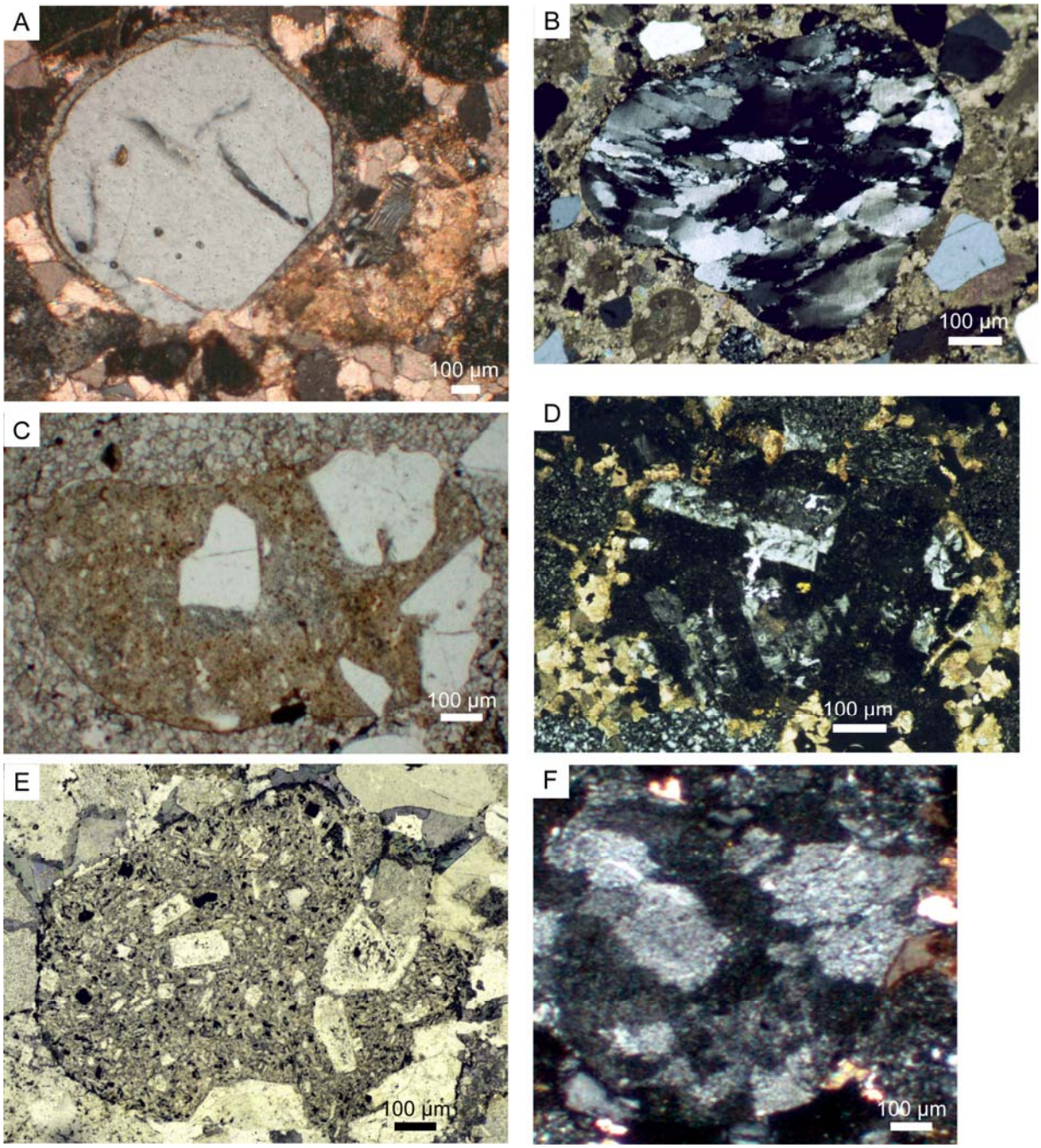

FIGURE 42 – Plate components, Heiligkreuz Fm. A) volcanic quartz and tartan-twinned plagioclase, sample LAGv, 10X, crossed polars, Lagazuoi section; B) polycrystalline quartz grain, sample Lit B, 25X, parallel polars, Rifugio Dibona section; C) volcanic grain with quartz phenocrystals (rhyolite?), sample DB9, 25X, parallel polars, Rifugio Dibona section; D) porphyric volcanic grain, sample Est 2, 25X, parallel polars, Borca di Cadore section. Twinned plagioclase crystals are evident in the ground glass mass. E) Shoshonite (?) clast, sample PG, 25X, parallel polars, Borca di Cadore section; F) Devitrified ground mass, sample Est 3, 25X, crossed polars, Borca di Cadore section.

2.4.2 Framework composition

Major classes Quartz (Q), Feldspars (F) and fine-grained Lithics (together with Carbonate Extrabasinal clasts) have been extracted from the overall counting and recalculated to 100%, provided at least 200 fragments have been evaluated.

Average composition results for the "Dogna" and Heiligkreuz Fms. are $Q_{37}F_6L_{57}$ and $Q_{38}F_5L_{57}$ respectively (litharenites), while Travenanzes Fm. shows $Q_{66}F_7L_{27}$ values (quartzarenites). Sensitive differences within the Heiligkreuz and the Travenanzes Fms. can be detected both vertically and laterally, while the "Dogna" fm. results are quite homogeneous, with a constant increase in lithic content with time (cf. Figg. 44 and 45).

Within the Heiligkreuz Fm., composition of arenites rhythmically alternates between lithic and quartzose in few meters. At a bigger scale, the same shift can be recognized between Heiligkreuz Fm. (mainly lithic) and Travenanzes Fm. (almost exclusively quartzose). Within the Travenanzes Fm. compositional alternation (quartz-lithic) is still present, although attenuated, and the two studied sections show the highest differences in the first interval, where composition is reciprocally inversed, but still with a slight prevalence of quartz for the distal deposits (Rifugio Dibona section).

In the uppermost Heiligkreuz Fm. carbonate intrabasinal clasts appear, and become common in the overlying Travenanzes Fm. The latter results also enriched in opaque minerals.

In general, values differ significantly between lower and upper Carnian units.

Compositional imprint and textural-diagenetic features have been used to defined homogeneous groups of samples with genetical significance, named *petrofacies* (Folk, 1970). Compositional values for the detected petrofacies have been reported in Table 14a, b and c.

FIGURE 43 – (next page) Ternary diagram for average framework composition values (quartz, feldspars, fine-grained lithics plus carbonate extrabasinal clasts). A) Rio del Lago and "Dogna" fms., Julian Alps area; B) Heiligkreuz and Travenanzes Fms., Cortina d'Ampezzo area; C) Heiligkreuz and Travenanzes Fms., Rifugio S. Marco section. An outstanding compositional shift (from litharenites to quartzarenites) from Heiligkreuz to Travenanzes Fms. is noticeable. Differentiation between proximal and distal sections can be appreciated. Compositional alternation is not present in the "Dogna" fm., but a progressive enrichment in lithic grain is observable.

FIGURE 44 – (page 90) Framework composition results (quartz, feldspars, fine-grained lithics plus carbonate extrabasinal clasts) for the studied units in the Dolomites. Within Heiligkreuz and Travenanzes Fms., clear alternation of quartzose and lithic arenites is highlighted, with a progressive quartz enrichment.

FIGURE 45 – (page91) Framework composition results (quartz, feldspars, lithics) for the studied units in the Julian Alps. Shift between Rio del Lago Fm. and "Dogna" fm. is clear. No major alternation in composition can be detected within the "Dogna" fm.

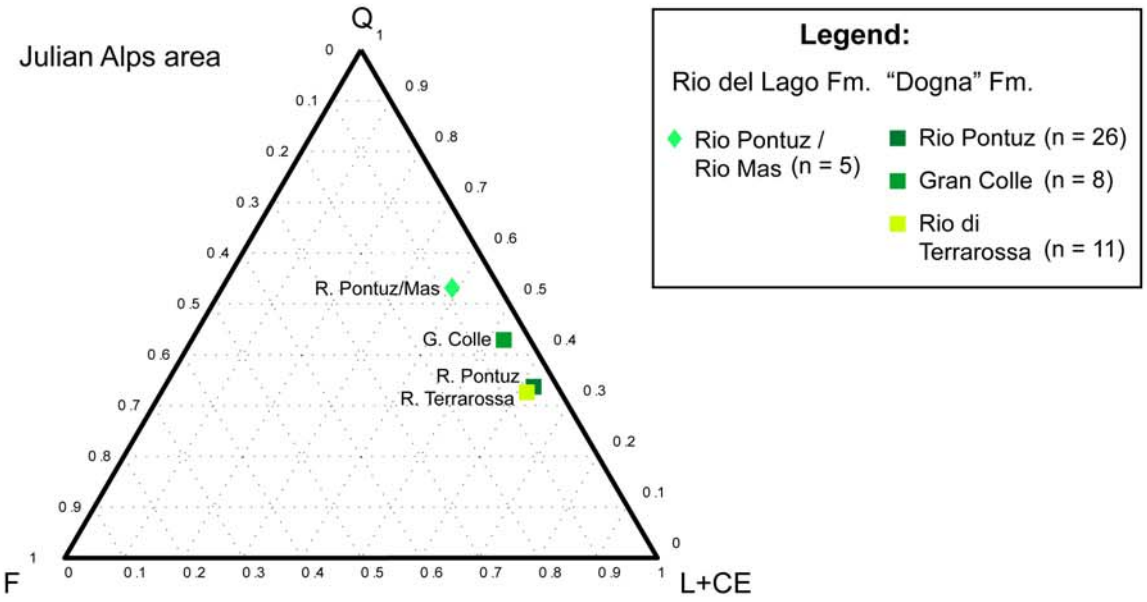
Julian Alps area
Q
F
L+CE
R. Pontuz/Mas
G. Colle
R. Pontuz
R. Terrarossa
Legend:
Rio del Lago Fm.
"Dogna" Fm.
Rio Pontuz / Rio Mas (n = 5)
Rio Pontuz (n = 26)
Gran Colle (n = 8)
Rio di Terrarossa (n = 11)

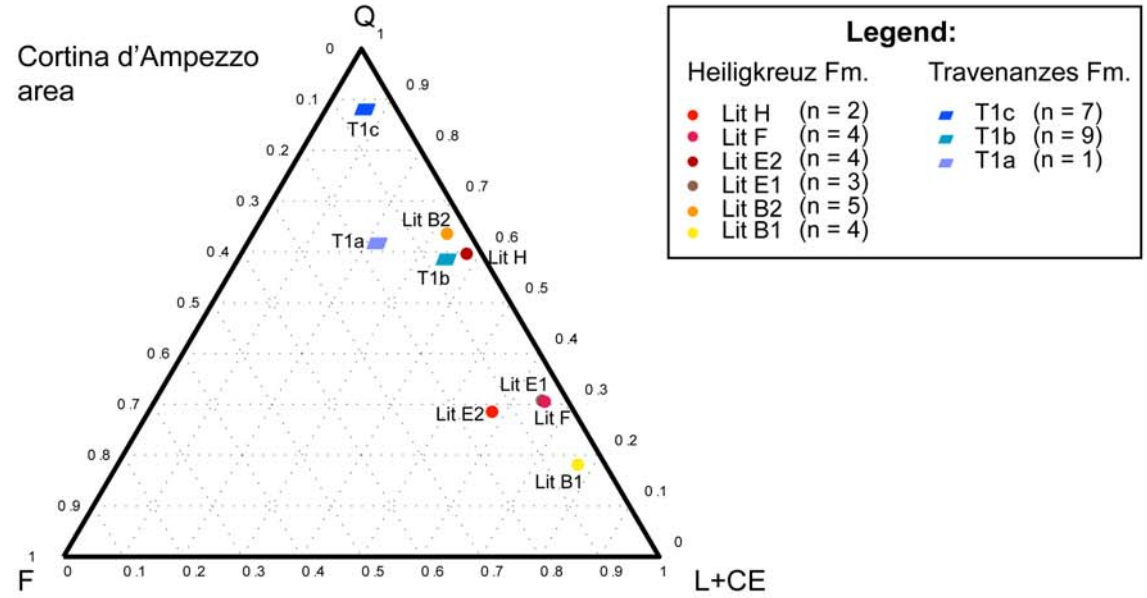
Cortina d'Ampezzo area
Q
F
L+CE
T1c
T1a
T1b
Lit B2
Lit H
Lit E1
Lit E2
Lit F
Lit B1
Legend:
Heiligkreuz Fm.
Travenanzes Fm.
Lit H (n = 2)
Lit F (n = 4)
Lit E2 (n = 4)
Lit E1 (n = 3)
Lit B2 (n = 5)
Lit B1 (n = 4)
T1c (n = 7)
T1b (n = 9)
T1a (n = 1)

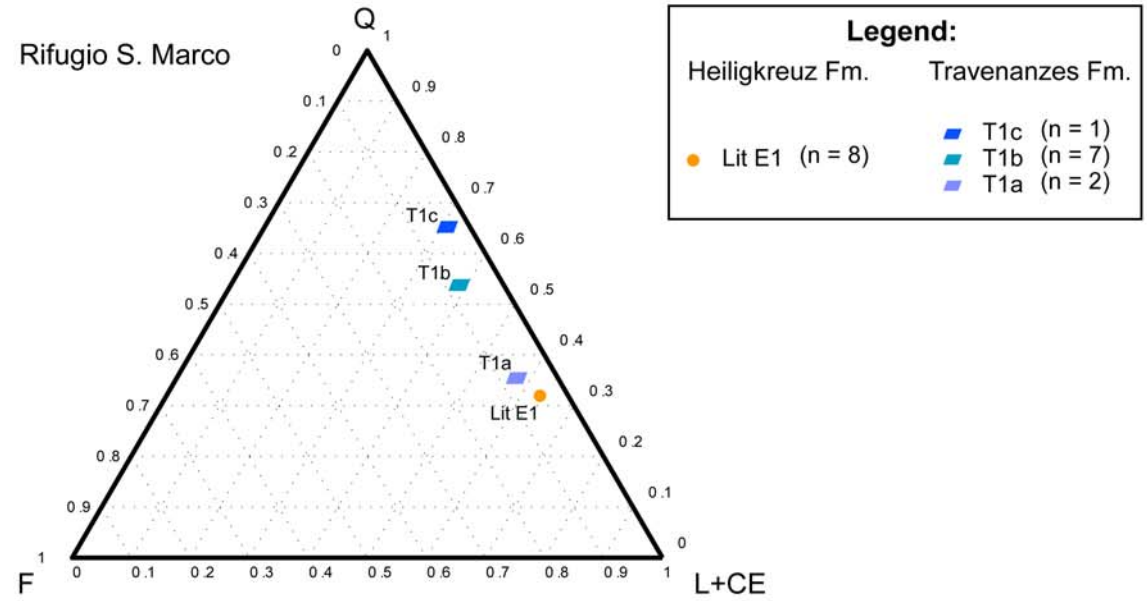
Rifugio S. Marco
Q
F
L+CE
T1c
T1b
T1a
Lit E1
Legend:
Heiligkreuz Fm.
Travenanzes Fm.
Lit E1 (n = 8)
T1c (n = 1)
T1b (n = 7)
T1a (n = 2)

RIFUGIO S. MARCO SECTION

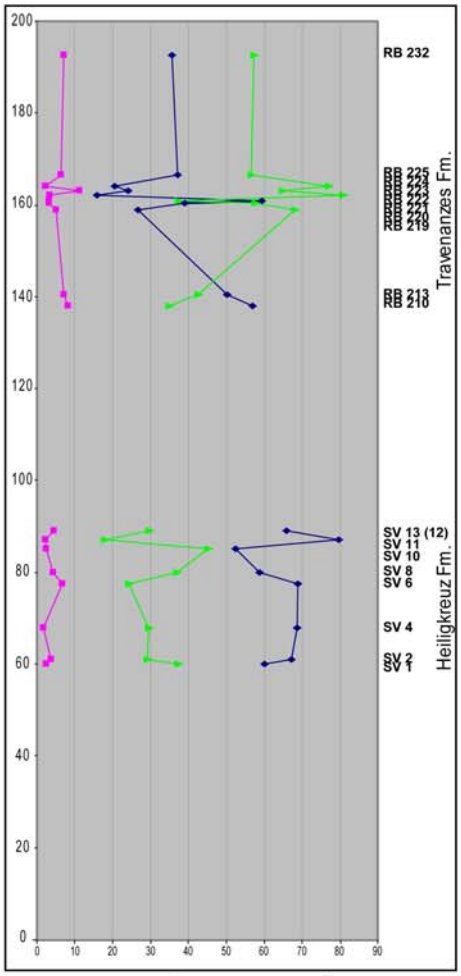

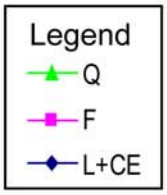

CORTINA AREA

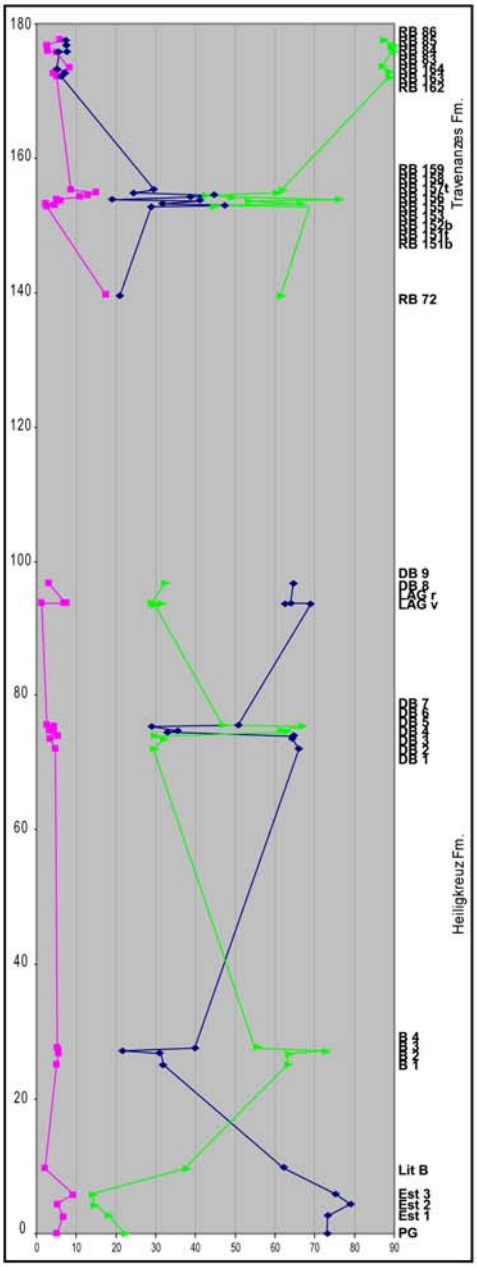

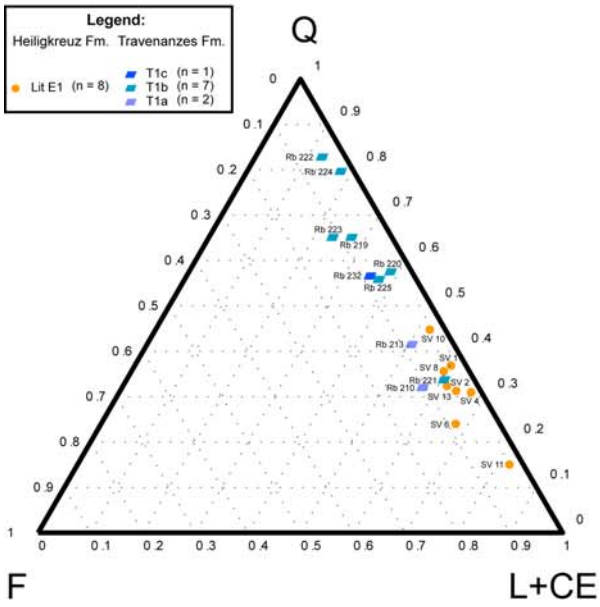

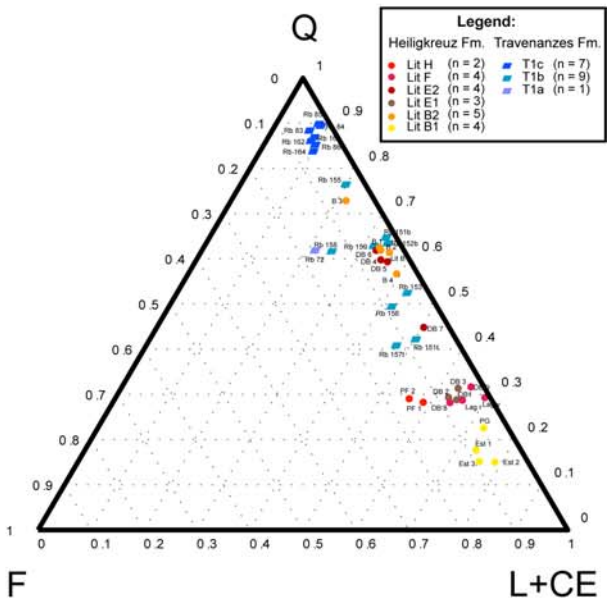

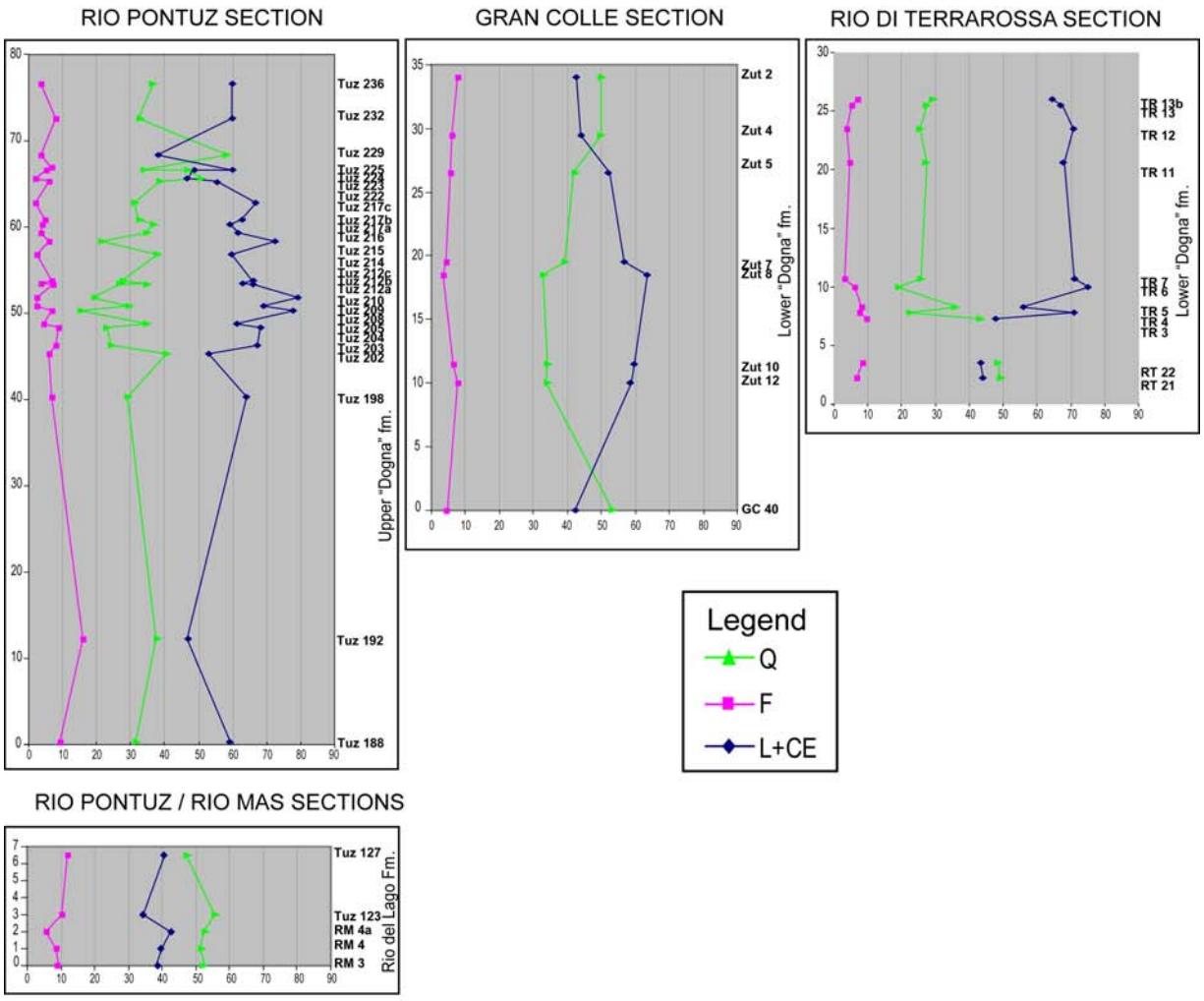
RIO PONTUZ SECTION
GRAN COLLE SECTION
RIO DI TERRAROSSA SECTION
Upper "Dogna" fm.
Lower "Dogna" fm.
Lower "Dogna" fm.
Tuz 236
Tuz 232
Tuz 229
Tuz 225
Tuz 224
Tuz 223
Tuz 222
Tuz 217c
Tuz 217b
Tuz 217a
Tuz 216
Tuz 215
Tuz 214
Tuz 212c
Tuz 212a
Tuz 210
Tuz 209
Tuz 208
Tuz 205
Tuz 204
Tuz 203
Tuz 202
Tuz 198
Tuz 192
Tuz 188
Zut 2
Zut 4
Zut 5
Zut 7
Zut 8
Zut 10
Zut 12
GC 40
TR 13b
TR 13
TR 12
TR 11
TR 7
TR 6
TR 5
TR 4
TR 3
RT 22
RT 21
Legend
Q
F
L+CE

RIO PONTUZ / RIO MAS SECTIONS
Rio del Lago Fm.
Tuz 127
Tuz 123
RM 4a
RM 4
RM 3

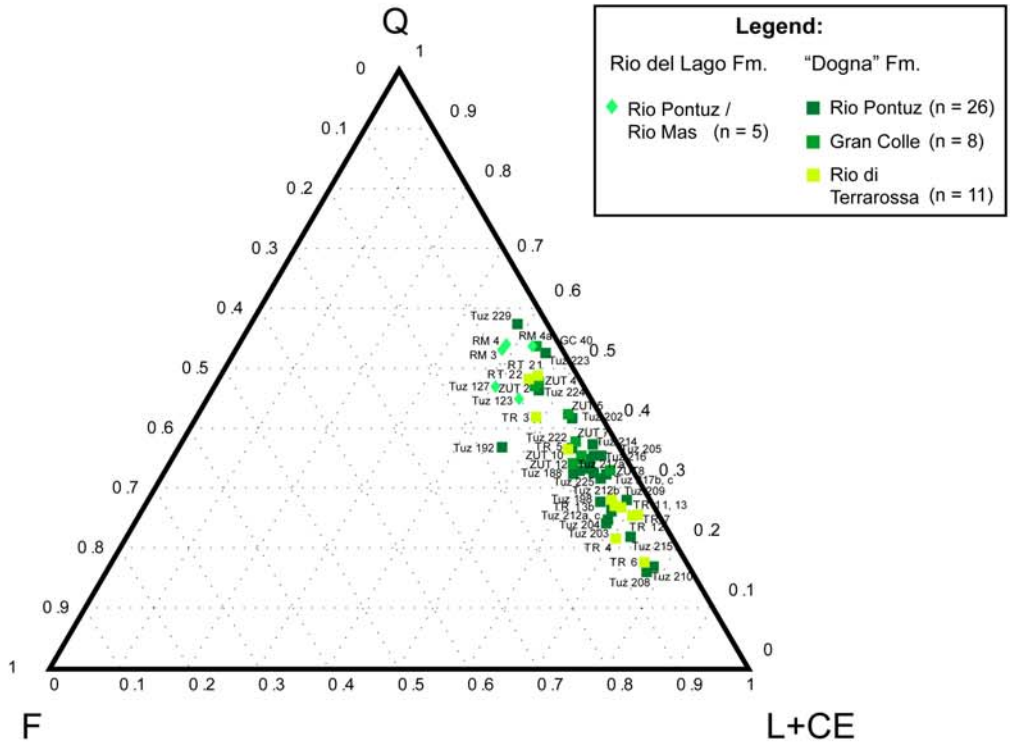
Q
F
L+CE
Legend:
Rio del Lago Fm.
"Dogna" Fm.
Rio Pontuz / Rio Mas (n = 5)
Rio Pontuz (n = 26)
Gran Colle (n = 8)
Rio di Terrarossa (n = 11)

	Heiligkreuz Fm.					Travenanzes Fm.			
	Lit B1	**Lit B2**	**Lit E1**	**Lit E2**	**Lit F**	**Lit H**	**T1a**	**T1b**	**T1c**
Q	17.0	33.3	30.4	59.4	30.3	29.0	61.5	58.1	88.9
F	7.2	18.4	4.5	3.6	4.6	13.5	17.5	7.5	4.1
L+CE	75.8	32.1	65.1	37.0	65.0	57.5	21.1	34.4	7.0

TABLE 14a – Average values for Heiligkreuz and Travenanzes Fms. sub-units, Cortina d'Ampezzo area. Samples from the Rifugio Dibona section cover the stratigraphic succession from lithozone B2 to the whole Travenanzes Fm.; samples from lithozone B1 have been collected in the Borca/S. Vito di Cadore area.

	H. Fm.	Travenanzes Fm.		
	Lit E1	**Lit T1a**	**Lit T1b**	**Lit T1c**
Q	31.3	38.8	63.2	57.3
F	3.5	7.6	4.9	7.1
L+CE	65.2	53.6	31.8	35.7

TABLE 14b – Average values for Heiligkreuz and Travenanzes Fms. sub-units, Rifugio S. Marco section.

	RdL Fm.	**"D" fm.**
Q	31.3	38.8
F	3.5	7.6
L+CE	65.2	53.6

TABLE 14c – Average values for Carnian formations, Julian Alps area. Terrigenous arenites from uppermost Rio del Lago Fm. have been collected in the Gran Colle section, together with basal "Dogna" fm. Bulk samples from "Dogna" fm. have been collected in the Rio Pontuz section, which covers the whole stratigraphic interval.

2.4.3 Petrofacies description

2.4.3.1 Dolomites –Heiligkreuz Fm.

This formation shows the maximum variability degree for both litho-and petrofacies. Within each lower stratigraphical sub-units (Borca and Dibona members) two different petrofacies can be distinguished, based on composition and texture. Upper member (Lagazuoi) is more homogeneous. Differences between localities are much more evident for the Travenanzes Fm., whose deposits are richer in lithic fragments in the S. Marco section (proximal) and in quartz fragment in the Dibona section (distal).

BORCA MEMBER

LITHOZONE B- RIFUGIO DIBONA SECTION

LIT B

Coarse-grained hybrid arenite (Fig. 46A). Sorting is poor, oversized clasts are present. Clast types include mainly quartz and lithics, with bioclasts and rare feldspars. Quartz grains range from sub- rounded to sub-angular. Lithoclasts are almost exclusively volcanic, mainly with aphanitic texture (only secondarily porphyric). Bioclasts are mainly crinoids and bivalves. Cementation is disconformable, followed by dolomitization.

LITHOZONE B - BORCA SECTION

PG

Lithic arenite, coarse-grained/microconglomerate, with quartz and feldspars. Texture results poorly sorted, with presence of *oversized clasts*. Lithoclasts are mainly volcanic, with aphanitic or porphyric texture, with phenocrysts of sanidine and plagioclase (An_{60} on Albite twinning, see picture). Quartz grains are mainly sub-angular.

Cementation is disconformable (calcite); a few areas show opaque minerals cementation (see picture).

EST 1, 2, 3

Medium- to coarse-grained volcanoarenites, poorly sorted. Volcanic lithoclasts mainly have aphanitic texture. Quartz grains result sub-angular. Unaltered biotite and opaque minerals are present. Rare green grains. Some areas show silicification/recrystallization.

Cementation is disconformable (calcite), pervasive (plagues on quartz grains) (Fig. 46D).

DIBONA MEMBER

LITHOZONE E1 - RIFUGIO DIBONA SECTION

DB 1, 2, 3

Fine- to medium-grained lithic arenites, poorly sorted. Volcanic clasts are mainly aphanitic, sometimes silicified. Quartz grains are sub-rounded. Green grains are present.

Interstitial component is fine aphanitic carbonate cement.

LITHOZONE E1 - RIFUGIO S. MARCO SECTION

SAMPLES SV

Medium- to coarse-grained lithic arenites, with conglomerate intercalations (Fig. 46C). Sorting is poor. In the conglomeratic layers clasts are almost exclusively volcanic, sub-angular, sometimes fractured. In the finer beds quartz is also present, and interstitial material is carbonate cement.

LITHOZONE E2- RIFUGIO DIBONA SECTION

DB 4, 5, 6, 7

Medium- to coarse-grained quartz arenites, poorly sorted (presence of oversized clasts) (Fig. 46B). Carbonate intrabasinal grains (micrite intraclasts, bioclasts) increase upwards. Quartz clasts are subangular. Volcanic clasts are mainly aphanitic, sometimes silicified.

Cementation is carbonate, pervasive.

LITHOZONE F- LAGAZUOI SAMPLES

LAGv-LAGr

Coarse-grained lithic arenites, poorly sorted (Fig. 46D). Volcanoclasts are mainly porphyric and well rounded. Some exemplars are silicified (see picture). Quartz grains result sub-angular. Cementation was originally disconformable, then replaced by dolomite.

LITHOZONE F- RIFUGIO DIBONA SECTION

DB 8-9

Medium- to coarse-grained volcanoarenite, poorly sorted. Volcanic clasts are mainly aphanitic, only secondary porphyric, sometimes silicified. Quartz grains are sub-angular. Bioclasts are present. Interstitial material is fine aphanitic carbonate matrix.

LAGAZUOI MEMBER

LITHOZONE H- PASSO FALZAREGO SECTION ("Arenarie di Passo Falzarego", Bosellini et al., 1982)

PF 1, 2

Medium- to coarse- hybrid arenites, quartz-lithic, well sorted. Micrite intraclasts and bioclasts (echinoderms) are common. Volcanoclasts are mainly aphanitic, less frequently porphyric. Quartz ranges from sub-angular to sub-rounded. Feldspars are more abundant if compared to underlying units and result altered or partly dissolved.

Interstitial material is microsparite, recrystallized.

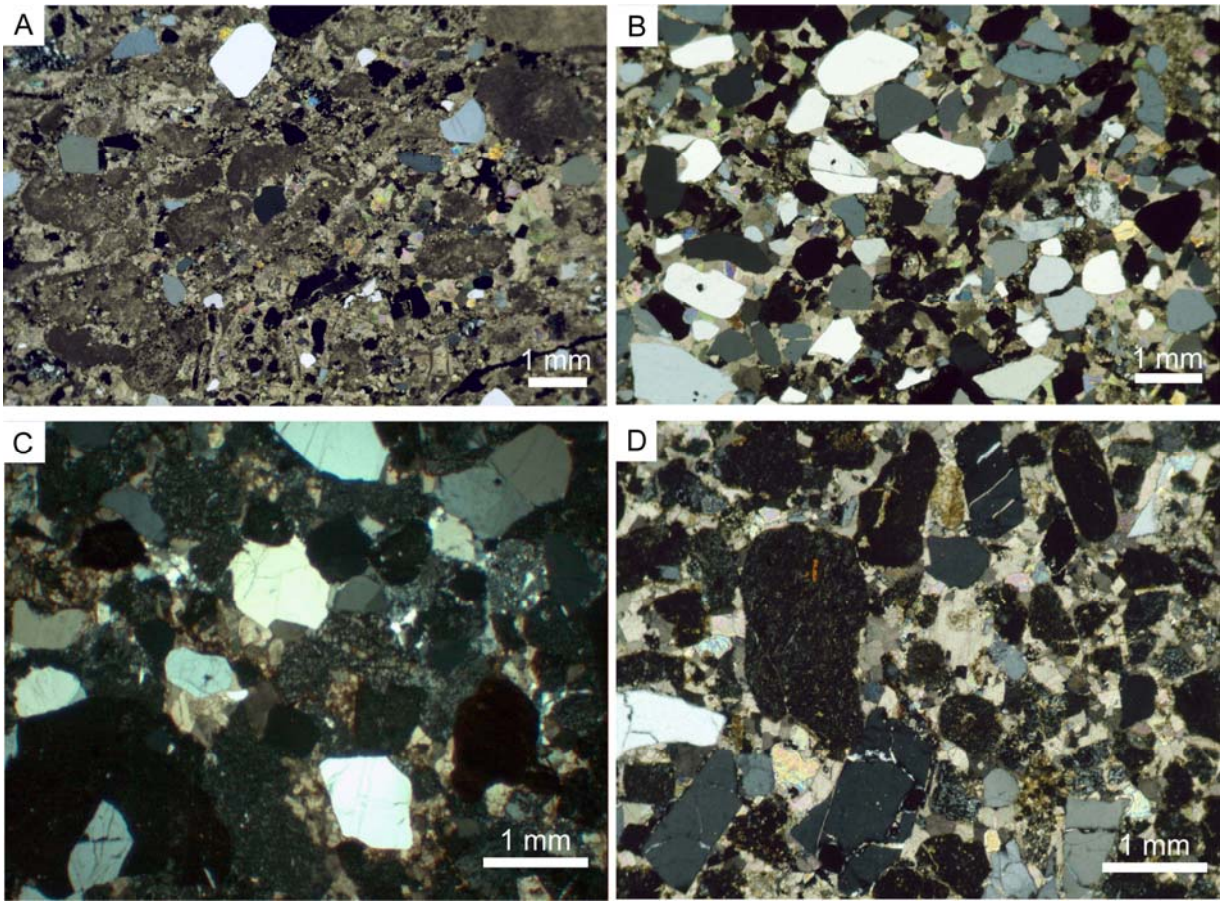

FIGURE 46 – Plate microfacies, Heiligkreuz Fm. A) petrofacies B, sample LIT B, 10X, crossed polars, Rifugio Dibona section; B) petrofacies E2, sample DB6, 10X, crossed polars, Rifugio Dibona section; C) petrofacies E, sample SV4, 10X, crossed polars, Rifugio San Marco section; D) petrofacies F, sample LAGr, 10X, crossed polars, Lagazuoi section.

2.4.3.2 Dolomites – Travenanzes Fm.

Upper Carnian Travenanzes Fm. displays as well high vertical and lateral variability, with a general "step" of quartz values compared to the underlying Heiligkreuz Fm.

The first terrigenous interval of the Travenanzes Fm. contains coarser lithologies suitable for evaluation with petrographical analyses. Within the whole unit, three petrofacies named T1a-T1b and T1c have been distinguished Official nomenclature has not been set yet, therefore denominations are provisional. The two studied sections result still distinguished, with a lower quartz amount for the S. Marco section, as previously observed for the Heiligkreuz Fm. Petrofacies T1a and T1c display the highest degree of differentiation between the studied sections, showing completely reversed compositional values.

Grain sorting and textural maturity are generally higher than in the Heiligkreuz Formation.

INTERVAL T1-RIFUGIO S. MARCO AND RIFUGIO DIBONA SECTIONS

RB 72, 210, 213

Fine- to medium-grained quartz arenites (Fig. 47A). Clasts are sub-angular to sub-rounded. Volcanic grains are mainly aphanitic. This petrofacies is mainly lithic in the Rifugio S. Marco section and mainly quartzose in the Rifugio Dibona section. Micritic intrabasinal clasts become more common.

Interstitial material is mainly microsparite.

INTERVAL T1-RIFUGIO S. MARCO AND RIFUGIO DIBONA SECTIONS

RB 151b to 159 and 219 to 225

Fine- to medium-grained hybrid arenites, lithic-quartzose (Fig. 47D). This petrofacies shows the smallest range between quartz and lithic grains within the entire formation. Grains are generally well sorted, sub-angular to sub-rounded. Volcanic grains are mainly aphanitic, only secondarily porphyric. Intergranular component is represented by fine-aphanitic carbonate cement (micrite).

INTERVAL T1-RIFUGIO S. MARCO AND RIFUGIO DIBONA SECTIONS

RB 83 to 164 and RB 232

Fine- to medium-grained quartz arenites (Fig. 47B,C). Texture results generally well sorted, with lamination produced by finer-grained opaque minerals concentrations. Quartz clasts are dominant, and show sub-angular to sub-rounded shape. Volcanic clasts show mainly aphanitic texture. Soil fragments (carbonate nodules) are common. Interstitial material is mainly microsparite.

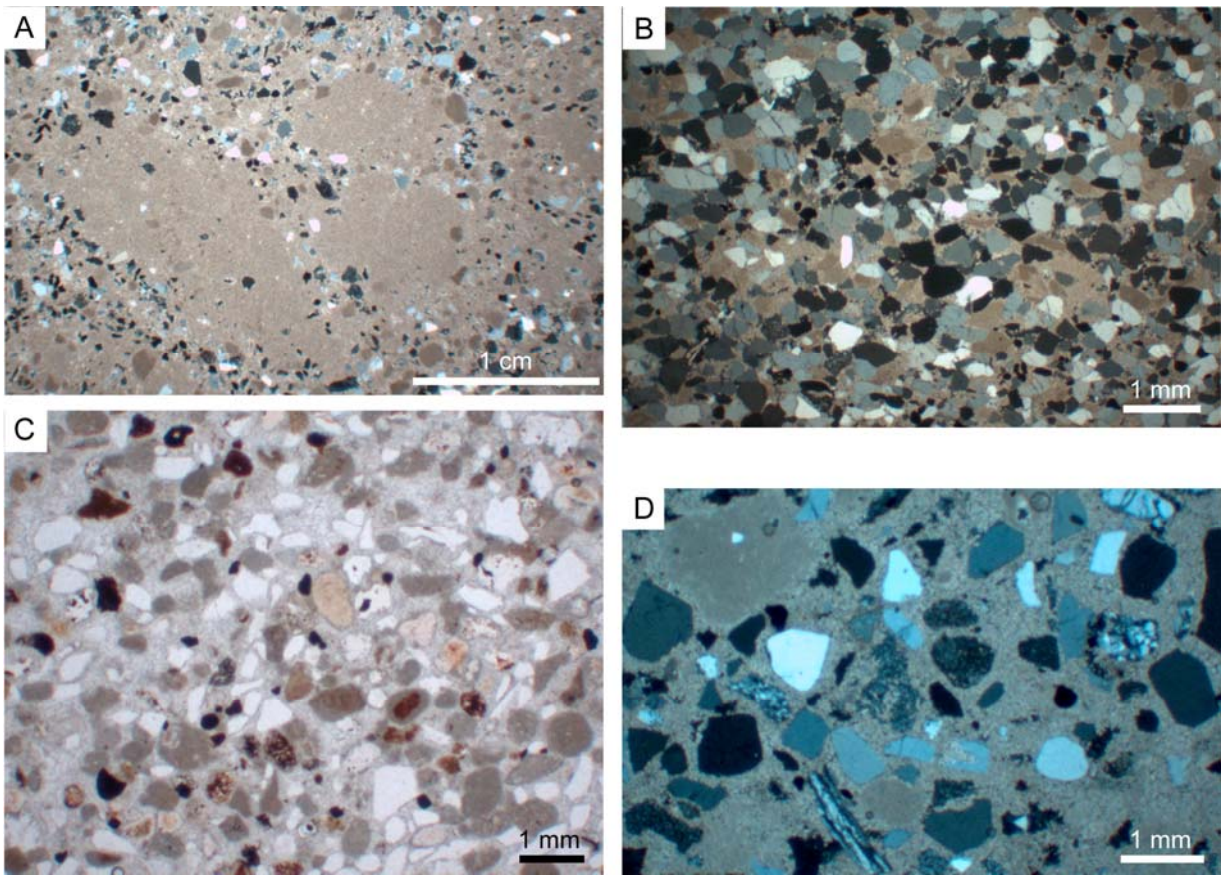

FIGURE 47 – Plate microfacies, Travenanzes Fm. A) sample Rb 72, 2,5X, parallel polars, Rifugio Dibona section. Large micrite objects are interpreted as borrows. B) sample Rb 162, 10X, crossed polars, Rifugio Dibona section. Quartzarenite with sparse lithic and carbonate clasts. C) sample Rb 232, 25X, crossed polars, Rifugio San Marco section. Some micrite-coated grains are present, interpreted as soil fragments. D) sample Rb 224, 10X, crossed polars, Rifugio San Marco section. Aphanitic volcanic clasts and plagioclase are present.

2.4.3.3 Julian Alps – "Dogna" fm.

RIO PONTUZ AND GRAN COLLE SECTIONS

SAMPLES Tuz , GC

Fine- to medium- hybrid arenites, quartz-lithic, generally well sorted (Fig. 48A,B,D). Clasts are mainly sub-angular. Lithic grains are exclusively volcanic, with co-presence of aphanitic and porphyric textures (Fig. 48C,E). Differently from the successions in the Dolomites, "Dogna" fm. samples sometimes contain metamorphic clasts. Diagenetic effects are sometimes intense, with pervasive carbonate cementation and dolomitization.

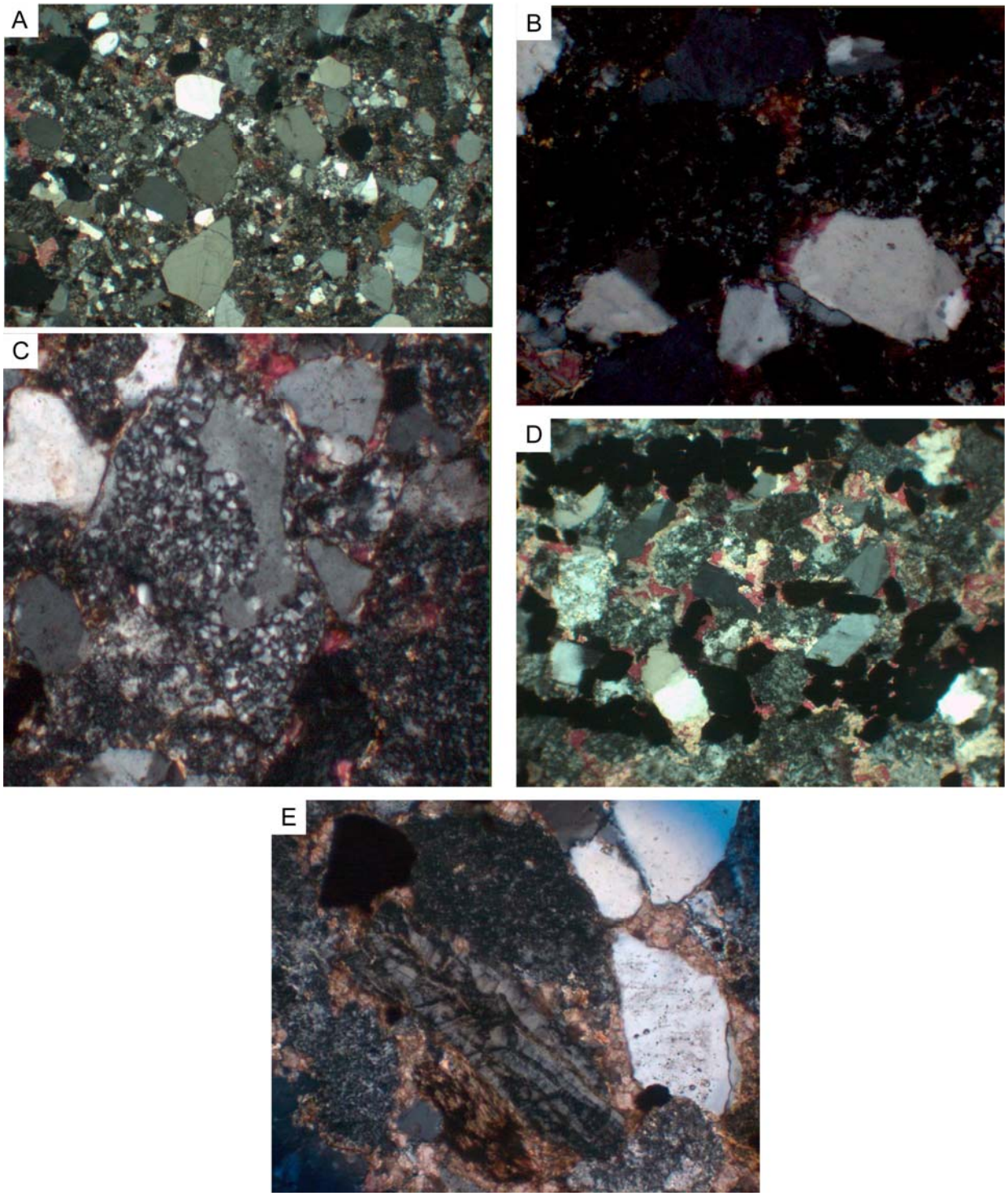

FIGURE 48 – Plate microfacies, "Dogna" fm. A) sample Tuz 205, 25X, crossed polars, Rio Pontuz section; B) sample Tuz 217a, 10X, crossed polars, Rio Pontuz section; C) silicified volcanic grain, sample Tuz 205, 10X, crossed polars, Rio Pontuz section. A quartz phenocrystals can be distinguished from the silicified ground mass. D) sample Tuz 224, 10X, crossed polars, Rio Pontuz section E) biotite and silicified volcanic grain, sample Tuz 217b, 10X, crossed polars, Rio Pontuz section. Elongated chalcedony veins are visible.

2.5 DISCUSSION

2.5.1 Interpretation of volcanic grains

The major constituents of studied arenites are quartz and volcanic grains. The origin of volcanic grains in sedimentary deposits is crucial for a correct interpretation of geological setting and processes. Grains of volcanic origin can in fact represent clasts derived by denudation of ancient volcanic terrains ("paleovolcanic", terrigenous s.s.) or particles derived from contemporary volcanic activity ("neovolcanic"), both inside or outside the sedimentary basin. Origin of volcanic clasts in sedimentary deposits was classified by Zuffa (1987) on the base of texture, depositional features and chemical composition (see Fig. 49).

In the studied arenites, volcanic grains are found mixed with quartz and other clasts ("impure volcanoarenitic beds") and outline, roundness and sorting are similar to those of quartz. Composition is mainly acidic, but basic clasts are also found, and some specimens show alteration.

The observed chemical composition and the predominance of alkali feldspars over plagioclases are also in agreement with the character of Ladinian and earlier volcanic deposits in the Dolomites area (shoshonitic basaltic dykes and hyaloclastites, Predazzo complex; rhyolites, Bolzano area) (Marrocchino et al., 2002; Sloman,1989; Castellarin et al., 1988) (see § 2.5.3). Volcanic clasts can thus be defined as detrital, and classified under V1 ("paleovolcanic extrabasinal").

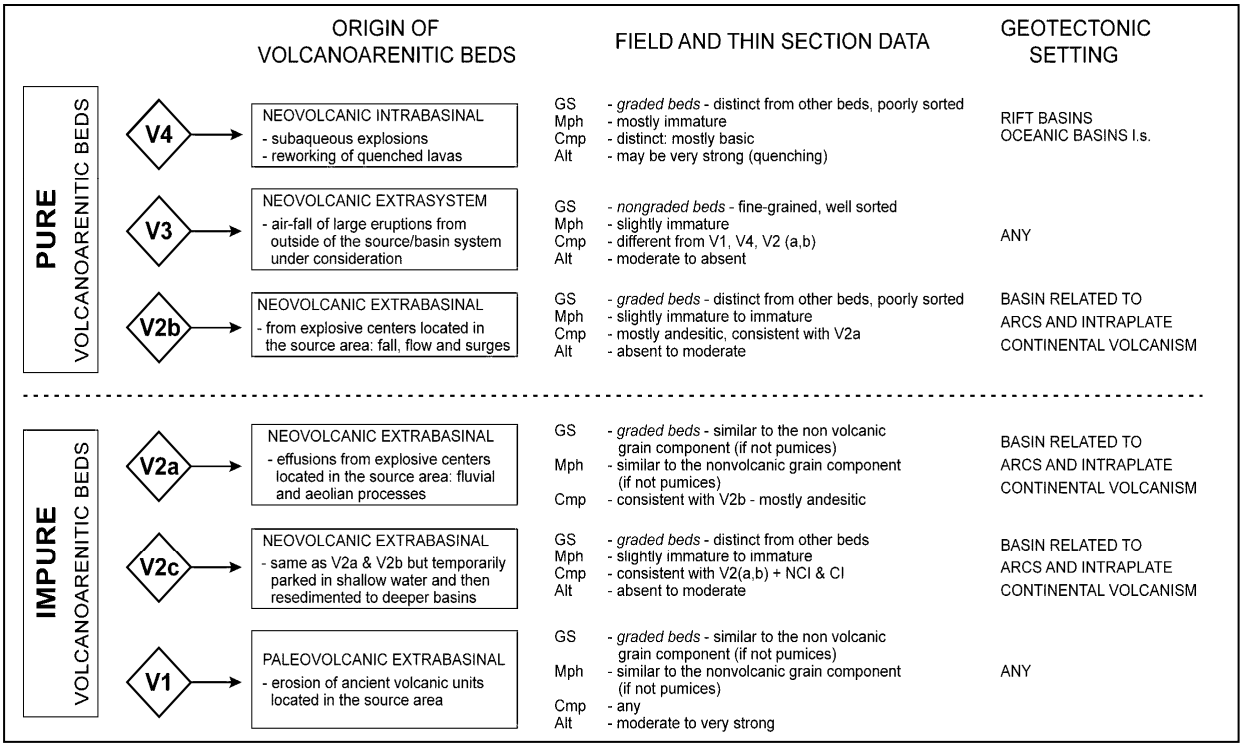

FIGURE 49 – Origin and characteristic of pure and impure volcanoarenite beds. V1, V2 a, b and c, V3 and V4: type of grains; GS: grain size; Mph; morphology; Cmp: composition; Alt: alteration. Modified after Zuffa (1987). Volcanic clasts from the studied samples belong to V1.

2.5.2 Interpretation of carbonate grains

The source of carbonate clasts in arenites requires also a careful evaluation and has major implications about source area and/or basin conditions.

In the studied arenites, carbonate grains are mostly constituted by ooids, bioclasts and micrite clasts. Despite evident recrystallization and alteration, ooids can be considered of intrabasinal origin because of the overall lack of pre-lithified limestone clasts in the studied sections. The same holds for the rare bioclasts found in the Heiligkreuz Fm. They indicate an open marine environment and have been interpreted as coeval because of absence of recrystallization/alteration. The third type of carbonate grains is represented by soft, round micritic clasts, sometimes arenaceous which appear in the uppermost Heiligkreuz Fm. and are abundant in the Travenanzes Fm. They are interpreted as fragments of carbonate soils (caliche) on the base of field observations of soil levels and from comparison with thin section of soil samples. The continental depositional setting in which they are found (Travenanzes Fm.) allows their classification as coeval (see Fig. 50).

CLASSIFICATION OF SAND GRAINS: fluvial basin system			
Criteria			
TEMPORAL	SPATIAL	COMPOSITIONAL	GRAIN TYPES
COEVAL	INTRABASINAL and/or EXTRABASINAL	Carbonate	Pedogenetic Travertine Skeletal
		Non carbonate	Vegetation Pedogenetic Evaporate Skeletal Pelite rip-up clasts Volcanic V2a,b
	EXTRABASINAL	Non carbonate	Volcanic V3
NON COEVAL	INTRABASINAL and/or EXTRABASINAL	Carbonate	Pedogenetic Limestone Dolostone
		Non carbonate	Siliciclast (non volc.) Volcanic V1 Pedogenetic

FIGURE 50 – Classification of grains in arenites from a continental (fluvial) depositional setting. Modified from Zuffa (1987). Carbonate grains in the studied arenites belong to the pedogenetic intrabasinal (coeval) category.

2.5.3 Compositional factors: premises

Observed changes in the composition of the studied arenites are on two different time scales: short-term and long-term. Short-term variations are expressed as repetitive shifts of composition from lithic to quartzose within the Heiligkreuz and Travenanzes Fms., and as less pronounced, repetitive quartz enrichment within the "Dogna" fm. Long-term variations occur between the Heiligkreuz and Travenanzes Formations in the Dolomites, and between Rio del Lago and "Dogna" Formations in the Julian Alps area. This complex variability can be possibly explained by the interplay and feedback between the different factors identified by different Authors as driving arenite composition: diagenesis, depositional processes-setting, recycling, transportation, climate (weathering), and source area relief/configuration (tectonic) (i.e. Zuffa, 1987; Dickinson, 1985; Suttner et al., 1981).

As a working hypothesis, climate is considered as the main driving factor because an important climatic change was recognized in the Tethyan domain in the Carnian, named Carnian Pluvial Event (Simms and Ruffell, 1990). In the Northern Calcareous Alps, this event corresponds also to a major stratigraphic turnover (the "Reingraberen Wende" of Schlager and Schöllnberge, 1974).

Late Triassic climate is generally classified as megamonsoonal (Dubiel et al., 1991; Kutzbach and Gallimore, 1994; Mutti and Weissert, 1995) with predominant arid regime (Price, 1999). The Carnian Pluvial Event is documented as a short-living humid shift of the monsoonal late Triassic climate (Prochnow et al., 2006, Rigo et al. 2006). Its minimum age is constrained to 230.91 My by U-Pb dating on an ash layer in the Lagonegro Basin (Furin et al., 2006).

In the Eastern Southern Alps it is marked by the demise of the underlying carbonate systems and by an abrupt coarse siliciclastic input in the sedimentary environments, near the Julian-Tuvalian boundary (Simms and Ruffell, 1989; Gianolla et al., 1998). This episode is thus recorded by the studied successions and could have determined both the onset of the coarse siliciclastic deposition and its long- and short-term compositional changes. The following paragraphs will deal with the different factors accountable for arenite composition, their importance and their relationships and feedback with the CPE.

The source area for the studied deposits can be individuated in the "Southern Mobile Belt", a structural high indicated as source for deposits from Anisian to Late Triassic (Brusca et al., 1981; Viel, 1981).

The known stratigraphic succession of the eastern Southern Alps includes crystalline basement (phyllites), minor clastic sedimentary rocks (Val Gardena Sandstone Fm.) of Late Permian age and an Early to Middle Triassic succession of evaporates and carbonate units, with minor terrigenous input (e.g., Bosellini et al., 1996).

A major tectono-magmatic event occurred in the Ladinian, with the emplacement of basaltic dikes, pillow lavas and hyaloclastites, and of alkaline intrusions of intermediate to acidic composition at Predazzo and Monzoni (Castellarin et al., 1988).
From detrital modes, the reconstructed source rock assemblage results stable in time and includes dominant volcanic lithologies and only secondarily metamorphic rocks. Sedimentary cover rocks are virtually absent (see § 2.5.1).

2.5.4 Negligible factors (tectonic activity, diagenesis, recycling)

Tectonic activity can affect arenite composition by changes in the configuration of the source area (i.e. denudation, relief) (Basu, 1985) and by volcanic activity (i.e. supply of coeval volcanic grains). (Zuffa, 1987). The late Carnian of Southern Alps seemed to be a period of tectonic quietness (Gianolla et al., 1998a), and no penecontemporary coeval volcanic activity has been recorded (Castellarin et al. 1988). Consequently, no relevant changes in the source area nor increased tectonic denudation can account for the compositional changes. Moreover, in modern monsoonal climates it has been observed that rainfall instead of topography greatly controls sediment yield (Garzanti et al., 2007) (see § 2.7).

Diagenesis can modify the composition of arenites trough dissolution and alteration of susceptible clasts such as feldspars and carbonate grains, possibly resulting in relative quartz increase (Fontana et al., 1989; McBride, 1985).
However, the uniform spatial and vertical distribution of diagenetic processes as observed throughout the studied sections contrasts with the rapid shifts observed in composition and thus cannot be considered as the main factor for compositional change (see § 2.4.1.4).
Moreover, due to coexistence of altered and non-altered grains in the same sample, the above-mentioned devitrification features seem to derive from primary pedogenetic processes and therefore are not relatable to diagenetic alteration.

Recycling seems also not to have affected composition because of the scarcity of sedimentary lithologies in the source-area succession (see § 2.5.3). Furthermore, vertical and lateral uniformity of grain size, roundness and alteration of clasts, the absence of sandstone clasts and of grains derived from other sedimentary rocks, and scarcity of detrital zircon and tourmaline (Zuffa, 1987) point towards a first-cycle detrital arenite and cannot account for the quick compositional variations. However, some of the compositional features observed for the Travenanzes Fm. (heavy minerals concentration, clasts roundness) which are traditionally

linked to recycling, are instead tentatively attributed to sedimentary processes and are therefore discussed in the next paragraph.

2.5.5 Influencing factors

Effects of depositional processes over composition for the studied arenites can be observed both over the short-and long-term variations. Within the Heiligkreuz Fm., differences up to 15% in quartz content can be appreciated between the fluvial deposits of the Rifugio S. Marco section and the corresponding shallow-marine deposits of the Rifugio Dibona section (lithozone E). However, Suttner et al. (1981) concluded that wave reworking alone cannot produce first-cycle quartzose arenites. At a larger scale, different depositional processes are linked to the shift in sedimentary environment and to diverse transportation mechanisms.

Braided river systems of the Heiligkreuz Fm. probably had a long-living but yet seasonal character, while the nature of streams in the terminal fan-sabkha of the Travenanzes Fm. was ephemeral, episodic, short-reaching. The former imply direct delivery of sediments into the basin and a longer transportation distance, and can be represented by the Burdekin river modern analog for a humid highly seasonal climate, which stream occasionally reaches the carbonate shelf bounded by the Great Barrier Reef (Fielding et al., 2002).

The latter involves reworking and incorporation of pedogenic clasts into the channels, testified by the enrichment in carbonate soil grains. A suitable modern analog for this could possibly identified in the Trabancos river in central western Spain, 86km long (Pérez-González, 1982).

Franzinelli and Potter (1983), and Suttner et al. (1981) detected significant modifications in arenite composition only for transportation distance > 75km, and Cavazza et al. (1993) observed that lithic grains decrease takes place in the first 30km. This is in contrast with the petrographical evidence that long-transported deposits of the Heiligkreuz Fm. are richer in lithic grains than the short-transported sediments of the Travenanzes Fm. Transportation alone therefore can’t explain the observed sharp compositional changes but can be considered as an expression of the different climatic regimes between the Heiligkreuz and Travenanzes Fms. time of deposition, and therefore a mechanism for enhancing the compositional changes.

Overall higher quartz content of the shallow-marine deposits of Dogna can be instead explained by longer transportation associated with continuous wave reworking of grains in the shallow marine environment, as testified among others by Zuffa (1987). In this case, the climatic imprint result attenuated/masked by the sedimentary processes, though the main variation trend is still recognizable (Suttner et al., 1981).

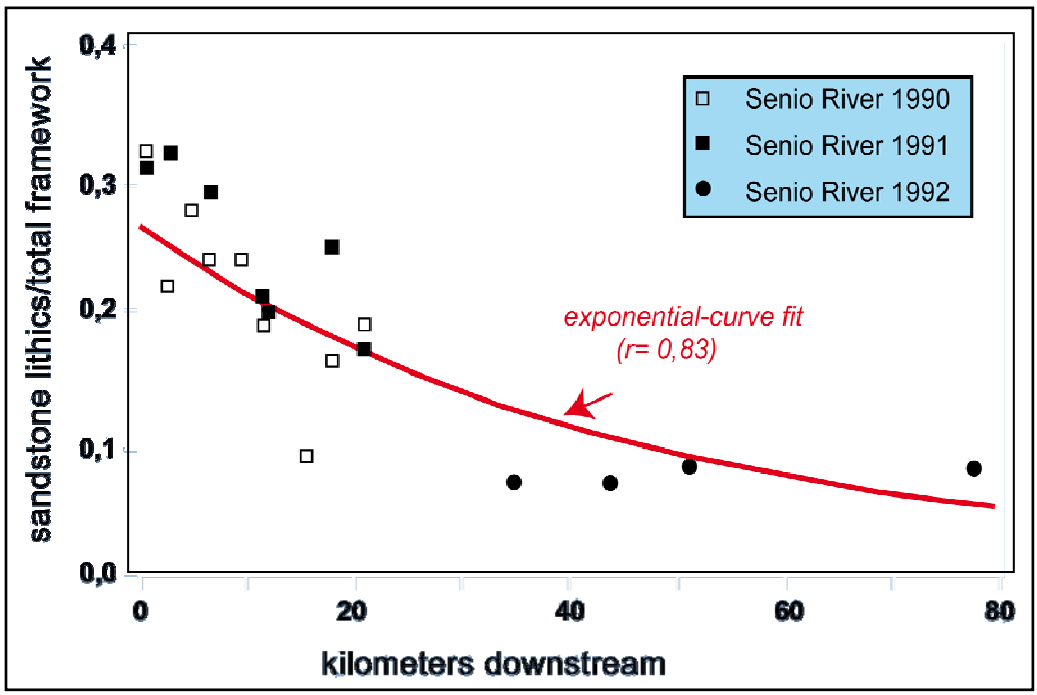

FIGURE 51 – Decrease in lithic grains in sand composition of samples from the Senio river. Relative amount of sand grains remains virtually constant after the first 30km of transport. Modified after Cavazza et al. (1993).

Alteration from subaerial weathering processes is testified from the scattered altered and silicified volcanic clasts (see § 2.4.1.1) present in the analyzed sections and from the paucity of plagioclases. Preservation of this primary alteration of rock volume in the source area in the sedimentary environment was allowed by the early carbonate cementation. Within the Heiligkreuz Fm., the observed almost unaltered immature arenites are thus in accordance with poorly developed pedogenesis (Retallack, 2001). The alternated quartzose arenites are instead the result of a deeper (longer) pedogenesis (see § 2.7).

This mechanism is applicable to the Travenanzes Fm. as well, with an increase of the overall quartz content due to longer and deeper alteration of the source rocks. For the Travenanzes Fm., however, a second-phase pedogenetic alteration can also be observed as a secondary effect of the fluvial regime variation. The ephemeral character of streams allows the alluvial plain to be exposed to a (minor) additional weathering, thus further increasing the quartz content, though maintaining the general trend. Increased quartz content due to a second pedogenetic cycle in the alluvial plain has been described by Suttner et al. (1981). Stream mobility in a flat alluvial plain could cause grain reworking, with further increase of the quartz content.

2.6 CARNIAN PLUVIAL EVENT CORRELATION

2.6.1 Consideration on paleosols

An independent proxy for paleoclimate in the analyzed section can be represented by paleosols. Paleosols levels have been found in both the Heiligkreuz Fm. and Travenanzes Fm. of the Dolomites area, where the sedimentary successions are more proximal than those in the Dogna area.

For the Heiligkreuz Fm. paleosol levels are found in the Rifugio Dibona and the Rifugio S. Marco sections, and are mainly histosols (see Formation nomenclature and description - Introduction) (Breda et al., 2008).

Histosols are typical of tropical wet climate with precipitation ≥ 1500mm (Cecil 1990; Lottes and Ziegler, 1994; Retallack, 2001; cf. Hardie 1977; Enos and Perkins, 1979), and suggest protracted humid conditions for at least some intervals of the Heiligkreuz Fm. (lithozones D and E, Rifugio Dibona section; lithozone E, Rifugio S. Marco section), furthermore confirmed by the findings of amber and plant remains (Gianolla et al., 1998b).

In addition, Prochnow et al. (2006) verify for Late Triassic a humid climatic episode on the base of paleosols, eventually correlated to the Carnian Pluvial Event.

In the Travenanzes Fm., evaporites and caliche soils are found in all the intervals in the Rifugio Dibona and Rifugio S. Marco sections (Breda et al., 2006; 2008).

Calcic horizons and caliches are carbonate soils typical instead of semiarid to arid climates with evaporation > precipitation and precipitation < 760 mm/y (Royer, 1999; Retallack and Royer, 2000; Retallack, 2001). This suggests a mainly arid climate for the uppermost Heiligkreuz Fm (lithozone H, Passo Falzarego section), and Travenanzes Fm.

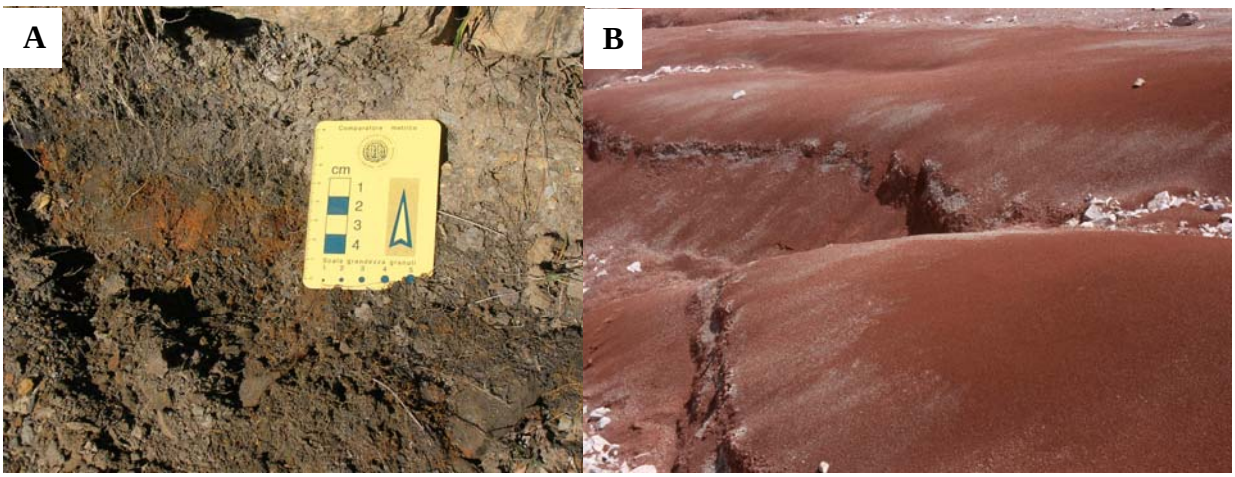

FIGURE 52 – Carnian paleosols. A) Histisol (humid), Heiligkreuz Fm., lit. E, Rifugio Dibona section. B) Calsisol (arid), Travenanzes Fm., Passo Falzarego section.

2.6.2 Anatomy of the Carnian Pluvial Event

The most complete Julian/Tuvalian succession examined is the one at Rio Pontuz section, Dogna area (Carnian Alps), where a remarkable sedimentary event can be observed at the boundary between the Rio del Lago Fm. ramp and the basal arenites of the "Dogna" fm. The general shallow- to marginal-marine setting of the Late Triassic in the Dogna area also allows paleoclimatical considerations with less environmental variables to be accounted.

The boundary between the Rio del Lago Fm. and the "Dogna" fm. is marked by microbial encrustation and bioerosion fabrics (see § 2.3.4) and, slightly later, by the abrupt coarse siliciclastic deposition.

The most likely cause for microbialite encrustation and bioerosion is microbial activity, probably by cyanobacteria. Occurrences of microbialites are rare in the Carnian of Dogna, and were observed in the upper Rio di Terrarossa Dm. (subtidal lagoon), uppermost Rio del Lago Fm. and "Dogna fm." (open-marine inner ramp) (see Chapter I). In the framework of a mesotrophic, terrigenous-affected ramp (see Chapter I), episodes of microbial activity could have been stimulated by a further increase of nutrient availability in the environment (i.e. eutrophication) (Mutti and Hallock, 2003).

Eutrophication of brackish- and near-shore marine-water environments (i.e., estuaries) has been linked to fresh-water influx (Howarth and Marino, 2006). At the Rio del Lago Fm./"Dogna" fm. boundary eutrophication appears particularly intense and is preluding to the first appearance of coarse siliciclastics.

It is tentatively suggested that a sudden, major increase in rainfall (namely, the Carnian Pluvial Event) could have created favorable conditions for eutrophication and at the same time triggered the coarse terrigenous input, and that its onset is recorded at the boundary between the Rio del Lago Fm. and the "Dogna" fm.

In the Dolomites area, the basal Heiligkreuz Fm. differentiates for the higher lithological variability and for the presence of dark shales with and olygotipic fauna (see Formation nomenclature and description). The relationship between the onset of the CPE, eutrophication in the Dogna area and the dark shales in the Dolomites area is proposed, though presently unproved.

2.7 MODEL FOR SHORT-TERM TO LONG-TERM COMPOSITIONAL CHANGES

A model of the complex feedback between weathering, denudation and sedimentary environment is here proposed to explain the observed compositional variations in arenites.

Traditionally, quartzose arenites have been considered the effect of humid climates (Suttner et al. 1981, Basu 1985; Suttner and Dutta, 1986; Nesbitt et al., 1997).

Lithic, mostly unaltered arenites of the humid Heiligkreuz Fm. seem therefore in contrast with this view. The key for explaining this contradiction resides in the extreme seasonality of the Late Triassic monsoonal climate and its effect on the rates of soil development and erosion.

High rock fragments amount has been linked to soil erosion rates exceeding weathering/alteration rate by Nesbitt et al. (1997). On the other hand, enhancement of erosion/denudation processes for wet seasonal climate has been highlighted by Franzinelli and Potter (1983), Cecil (1990), Dosseto et al. (2006) and by Garzanti et al. (2007) who correlated erosion rates with rainfall in the Himalaya. Furthermore, Reed et al. (2005) directly linked a higher lithic content to a more seasonal climate.

From these considerations it appears that the association of high seasonality and high rainfall during the wet season causes the decoupling of weathering intensity and erosion rate, which has an impact on sediment composition. As recognized by Lebedeva et al. (2007) and West et al. (2005), erosion represent a limiting factor for weathering.

The two terrigenous episodes in the Heiligkreuz Fm. can thus tentatively be regarded as two wet phases and the two episodes in the Travenanzes Fm. as two wet phases in a more arid setting.

Similarly, the entire Heiligkreuz Fm. could be tentatively considered as an overall humid interval, while the Travenanzes Fm. could represent an overall dry climate, with internal shorter-term episodes of increased rainfall testifying the waning of the CPE (Breda et al., 2008).

In equilibrium conditions, rainfall in the source area causes both chemical weathering and erosion to take place at the same time.

For a highly seasonal climate, during the periods of increased rainfall volcanic rocks in the source areas could be subject to an increased erosion rate, whereas weathering development was interrupted by the rapid and continuous runoff-denudation. Products of this accelerated erosion were almost unaltered volcanic lithoclasts with quartz grains.

During the span of the wet events, only the unremoved portions of parent rock in the source areas could undergo deeper chemical weathering. In dryer periods, the subsequent erosion of this less mobile rock volumes could have produced mainly quartzose detritus (for argillification/dissolution of ground mass and labile grains, i.e. plagioclase (McBride, 1985).

Compositional response results therefore diachronous to the climatic phase.

This model could be applied both to the long-term scale (formation) and to the lithozone/interval (short-term) scale. At all scales, the observed compositional features (alternation of immature, almost unaltered, and quartzose arenites) are in accordance with calculated time-scale transportation and weathering processes in modern monsoonal climates (100 Ky)(Granet et al., 2007).

At the long-term scale, climatic effects are of regional extent and steer the overall depositional settings, which in turns defined arenite composition with different sedimentary processes.

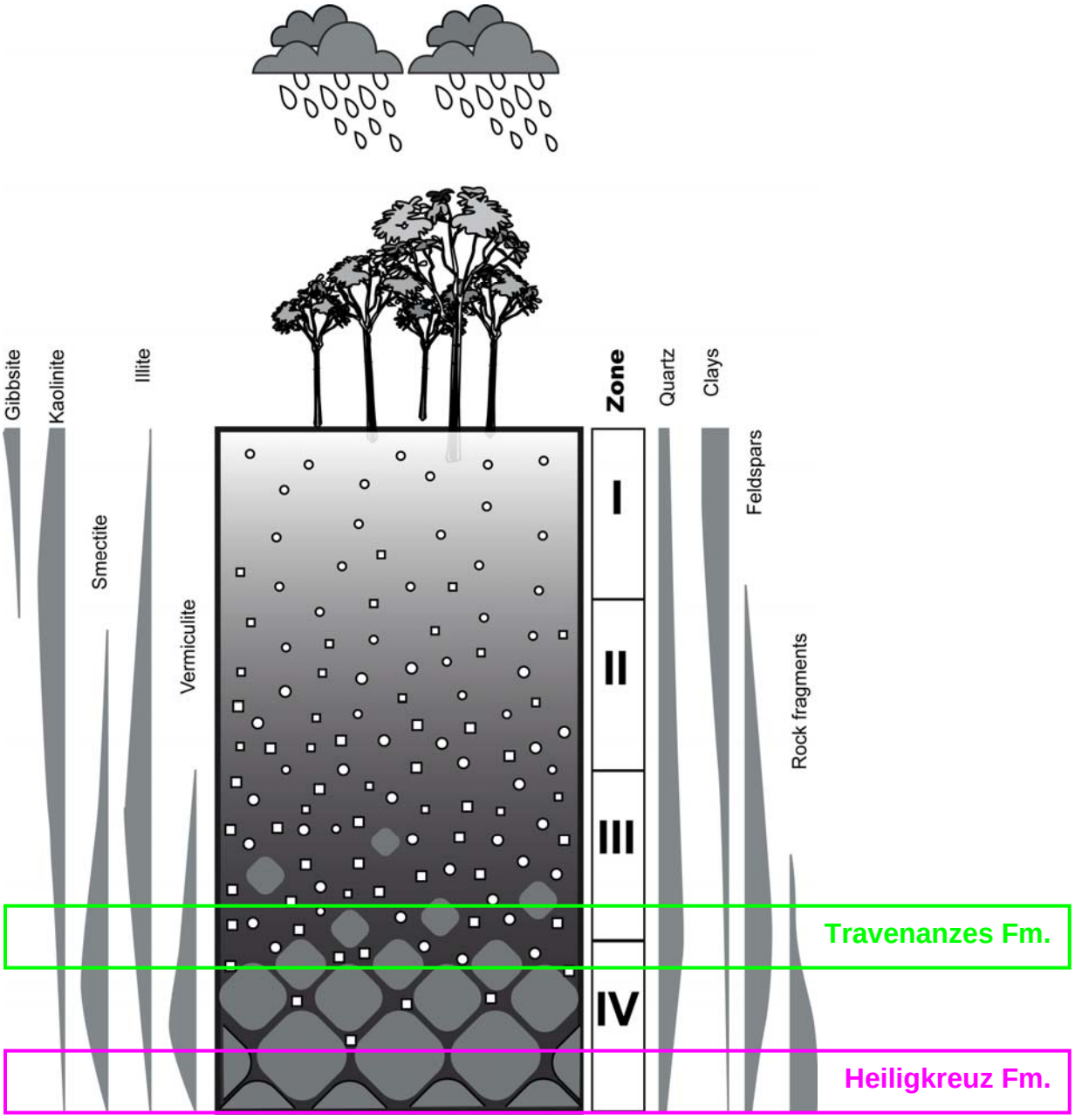

FIGURE 53 – Model for compositional change between Heiligkreuz and Travenanzes Fm., and for rapid changes within the Heiligkreuz Fm. Modified after Nesbitt et al. (1997).

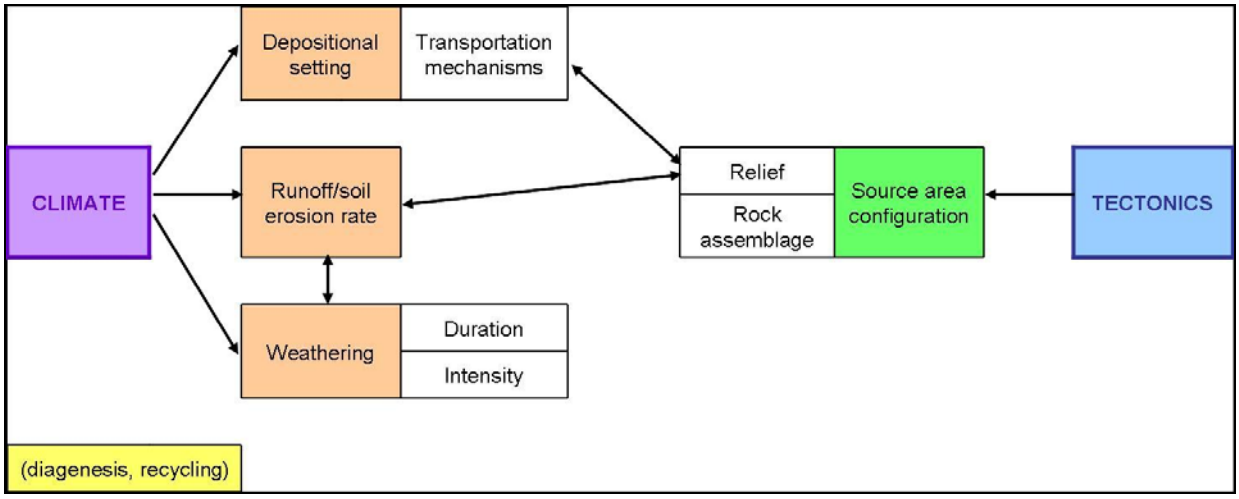

FIGURE 54 – Reconstructed feedback and interaction between factors controlling the composition of the Carnian arenites of the Eastern Southern Alps. The major "superfactors", climate and tectonics, represent the driving force for the main processes (depositional setting, runoff/soil erosion rate, weathering, source area configuration) which control the observed variations in the arenite composition.

2.8 CONCLUSIONS

Traditional arenite petrography analyses have been carried on Carnian deposits of the Southern Alps. 107 samples have been studied, coming from the Dolomites (Rifugio S. Marco and Rifugio Dibona sections) and Julian Alps (Rio Pontuz and Gran Colle sections) areas.

Arenites components are mainly quartz and volcanic clasts (with secondary feldspars and other lithologies). Volcanic grains derived by erosion of pristine magmatic products (paleovolcanic). Clasts remain the same trough time, testifying a stable, volcanic-dominated source area.

Arenites composition shows a marked alternation between the volcanic lithic grains and the quartz clasts for the Heiligkreuz and Travenanzes Fms. (Dolomites), while the oscillation is less pronounced in the "Dogna" fm. (Julian Alps).

On average, compositional results are $Q_{37}F_6L_{57}$ ("Dogna" fm.), $Q_{38}F_5L_{57}$ (Heiligkreuz Fm.) and $Q_{66}F_7L_{27}$ (Travenanzes Fm.), testifying a progressive quartz increase trough time.

The main factor determining the composition of the studied arenites is considered to be climate. Expression of climate influence are twofold: short term (differential weathering) and long-term (depositional setting).

Short term effects are due to decoupling of chemical (weathering) and physical (erosion) processes. Lithic arenites derive from an accelerated erosion rate with respect to weathering rate in a wet phase (removal of unaltered parent rock fragments). Quartz arenites derive from a deeper alteration of the previously altered but unremoved units in the source-area, and testify the wet phases.

Long term effects are of regional extent, and involve the change in the sedimentary setting (from perennial rivers to sporadic streams), with repercussions in the depositional processes and grain alteration.

Compositional response is diachronous to the climatic phase, and reflects both the seasonal and "superseasonal" climatic oscillations (inter- and intra-formational changes, respectively).

Other factors like diagenesis and reworking contribute to composition definition in a minor extent, and are superimposed to the main controlling factor.

From the compositional imprint the CPE develops with a long "superseasonal "periodicity (wet: Heiligkreuz Fm. and "Dogna" fm.; dry Travenanzes Fm.) modulated by a short "seasonal" periodicity (at least two wet/dry phases within the Heiligkreuz Fm. and other two wet/dry phases in the Travenanzes Fm.). Humid pulses are parossistic in the Heiligkreuz Fm. and wane in the Travenanzes Fm.

GENERAL CONCLUSIONS

The present work was focused on the mixed carbonate and siliciclastic deposits of Late Triassic (Carnian) age of the Eastern Southern Alps, Italy, with main focus on the possible influence of a humid climatic event (Carnian Pluvial Event).

A detailed sedimentological and petrographical study of the Julian mixed carbonate-siliciclastic ramp in the Julian Alps (Easternmost Southern Alps) was presented, with special focus on its environmental subdivision.

106 samples from 5 sections were analyzed with sedimentary petrology techniques; data elaboration was carried out with multivariate statistics. 16 samples were then observed with SEM in order to investigate the origin of micrite.

7 facies associations and 13 classes of bioclasts were recognized, representing 5 sedimentary sub-environments: inner, shallow median, median, deeper median and outer ramp.

SEM analyses showed microsparite to have mostly an aragonitic precursor, considered to derive from calcifying green algae: the carbonate ramp of Dogna thus represents a tropical carbonate factory, with a significant contribution of heterotrophic producers in its outer part.

The coexistence of a low-relief carbonate system with the well-known rimmed platforms of the Dolomites in close proximity represents an unexpected finding, with implications for the type of carbonate factory of the Tethys ocean.

A new perspective on Upper Triassic carbonate production is thus provided. The coexistence of tropical- and cool-water features is explained by the terrigenous input, which prevented the growth of autotrophic organisms, as presently occurring in stressed tropical platforms. Besides, it is reported that halimedacean algae appear to be a major carbonate producer already during Late Triassic.

Sedimentology and petrology were applied also to the Late Carnian terrigenous deposits of the Dolomites and Julian Alps, which represented a turnover in the sedimentation pattern. Two main arenite inputs were identified in both the Dolomites (Heiligkreuz Fm.) and "Dogna" fm. (Julian Alps), and a third coarse siliciclastic input is recorded by the Travenanzes Fm. in the Dolomites.

Six localities were analyzed, recording a wide spectrum of sedimentary environments: median ramp (lower arenites, Dolomites), braided river (upper arenites, Dolomites), shallow-marine (upper arenites, Dolomites), delta (lower and upper arenites, Julian Alps) and terminal-fan/sabkha (Travenanzes Fm.)

One hundred and seven samples were analyzed with clastic sedimentary petrology methods, which showed alternation between lithic and quartzose composition within each terrigenous interval. Furthermore, an overall increase in quartz can be recognized.

Climate was recognized as the main driving factor for compositional changes within and between the Heiligkreuz and Travenanzes Formations (Dolomites) and the Rio del Lago and "Dogna" formations in the Julian Alps.

The development of the Carnian Pluvial Event is outlined. It consisted in a parossistic event of extreme seasonality, taking place mainly during the Heiligkreuz Fm./"Dogna" fm. time of deposition (wet), and fading out during the Travenanzes Fm. time of deposition (dry). Within each megaseason, repeated alternation of humid and arid periods occurred, testified by arenites composition and paleosol observations. Lithic arenites are the expression of the humid phases and quartzose arenites of the arid ones, and these compositional variations are linked to differential weathering in the short-term, and to change in overall depositional setting in the long-term, both caused by the climatic variations.

This view strongly contrasts with the current understanding of climate influence on arenite compositions.

REFERENCES

Assereto R. Desio A., Di Cortebaldo D., Passeri L.D., 1968 - Note illustrative della Carta Geologica d'Italia. Foglio 14A Tarvisio. Servizio Geologico Italiano, Roma.

Baccelle L. and Bosellini A., 1965 - Diagrammi per la stima visiva della composizione percentuale nelle rocce sedimentarie. *Annali dell'Università di Ferrara, Sezione IX, Scienze Geologiche e Paleontologiche,* v.1, pp. 59-62.

Bassoullet J.P., Bernier P., Deloffre R., Genot P., Poncet J., Roux A., 1983 - Les Algues Udoteacées du Paleozoique au Cenozoique. *Bulletin du Centre de Recherche d'Exploration et Production Elf-Aquitaine,* v. 7/2, pp. 449-621.

Basu A., 1985 - Influence of climate and relief on compositions of sands released at source areas. In: Zuffa G.G. (Ed.) Provenance of arenites. *NATO-ASI Series. Series C: Mathematical and Physical Sciences*. Reidel Publ. Co., Dordrecht, v. 148; pp. 1-18.

Bechstädt T. and Schweizer T., 1991 - The carbonate-clastic cycles of the East-Alpine Raibl group: result of third-order sea-level fluctuations in the Carnian. *Sedimentary Geology* v. 70, pp. 241-270.

Bosellini A., 1984 - Progradation geometries of carbonate platforms: examples from the Triassic of the Dolomites, Northern Italy. *Sedimentology*, v. 31, pp. 1-24.

Bosellini A., 1996 - Geologia delle Dolomiti. Athesia, Bolzano, 192 pp.

Bosellini A., Masetti D., Neri C., 1982 - La geologia del Passo Falzarego. In: A. Castellarin, G.B. Vai (a cura di): Guida alla Geologia del Sudalpino Centro-Orientale. *Guide geol. reg. S.G.I.*, pp. 273-278.

Brachert T.C., Forst M.H., Pais J.J., Legoinha P., Reijmer J.J.G., 2003 - Lowstand carbonates, highstand sandstones?. *Sedimentary Geology,* v. 155, pp. 1-12.

Breda A., Massari F., Meneguolo R., Preto N., 2006 - An alluvial plain - sabkha - lagoon system in the Upper Triassic of the Dolomites, northern Italy. Poster EGU EGU06-A-08723, EGU General Assembly 2006, 02-07th April 2006, Wien.

Breda A., Preto N., Roghi G., Furin S., Meneguolo R., Ragazzi E., Fedele P., Gianolla P., 2008 - The Carnian Pluvial Event in the Tofane area (Cortina d'Ampezzo, Dolomites, Italy). In: *The Triassic climate Workshop in Triassic palaeoclimatology*, fieldtrip guide. Bolzano (Bozen) (I), 3-7th June 2008.

Brennan, S., Lowenstein, T.K., Horita, J., 2004 - Seawater chemistry and the advent of biocalcification: *Geology*, v. 32, pp. 473-476.

Brusca C., Gaetani M., Jadoul F., Viel G., 1981 – Paleogeografia ladino-carnica e metallogenesi del Sudalpino. *Mem. Soc. Geol. It.,* v. 22, pp. 65-82.

Carannante G., Esteban M., Milliman J.D., Simone L., 1988 - Carbonate lithofacies as paleolatitude indicators: problems and limitations. *Sedimentary Geology,* v. 60, pp. 333-346.

Castellarin, A., Lucchini, F., Rossi, P. L., Selli, L., Simboli, G., 1988 - The Middle Triassic magmatic-tectonic arc development in the Southern Alps. *Tectonophysics,* v. 146/1-4, pp.79-89.

Cavazza W., Zuffa G.G., Camporesi C., Ferretti C., 1993- Sedimentary recycling in a temperate climate drainage basin (Senio River, north-central Italy): composition of source rocks, soil profiles, and fluvial deposits. In: Johnnson M., Basu A. (Eds.) *Processes controlling the composition of Clastic sediments*, Boulder, Colorado, Geol. Soc. Am. Special Publication, v. 284, pp. 247-261.

Cecil C.B., 1990- Paleoclimate controls on stratigraphic repetition of chemical and siliciclastic rocks *Geology*, v.18/6, pp. 533-536.

De Zanche V., Gianolla P., Mietto P., Siorpaes C., Vail P.R., 1993 - Triassic sequence stratigraphy in the Dolomites (Italy). *Memorie di Scienze Geologiche*, v. 45, pp. 1-27.

De Zanche V., Gianolla P., Roghi G., 2000 - Carnian Stratigraphy in the Raibl/Cave del Predil area (Julian Alps, Italy). *Eclogae Geol. Helv.*, v. 93, pp. 331-347.

Dickinson W.R., 1970 – Interpreting provenance relations from detrital modes of sandstones. In: Zuffa G.G. (Ed.) Provenance of arenites. *NATO-ASI Series. Series C: Mathematical and Physical Sciences*. Reidel Publ. Co., Dordrecht, v.148; pp. 361-382.

Dickinson W.R., 1970 - Interpreting detrital models of graywacke and arkose. *Jour. Sed. Petr*., v. 40, pp. 695-707.

Dickinson W.R., Suczek, C.A., 1979 - Plate tectonics and sandstone composition. *AAPG Bull*., v. 63, pp. 2164-2182.

Dickinson W.R., Beard L.S., Brackenridge G.R., Erjavec J.L., Ferguson R.C., Inman K.F., Knepp R.A., Lindberg F.A., Ryberg P.T., 1983 - Provenance of North American Phanerozoic sandstones in relation to tectonic setting. *Geol. Soc. Am. Bull*., v. 94, pp. 222-235.

Dosseto A., Bourdon B., Gaillardet J., Maurice-Bourgoin L., Allègre C.J., 2006 – Weathering and transport of sediments in the Bolivian Andes: Time constraints from uranium-series isotopes. *EPSL*, v. 248, pp. 759-771.

Dragastan O., Richter D., Kube B., Mihai P., Sarbu A., Ciuguleia I., 1997 - A new family of Paleo-Mesozoic calcareous green siphons-algae (order Bryopsidales, Class Bryopsidophyceae, Phylum Siphonophyta). *Revista Espanola de Micropaleontologia*, v. 29 /1, pp.69-135.

Dubiel R. F., Totman Parrish J., Parrish J.M., Good S.C., 1991 – The pangean megamonsoon – evidence from the Upper Triassic Chinle Formation, Colorado plateau. *Palaios*, v. 6, pp. 347-370.

Dunbar G.B., Dickens G.R., 2003 - Massive siliciclastic discharge to slopes of the Great Barrier Reef Platform during sea-level transgression: constraints from sediment cores between 15° S and 16° S latitude and possible explanations. *Sedimentary Geology*, v. 162, pp. 141-158.

Dunham R.J., 1962 - Classification of carbonate rocks according to depositional texture. *AAPG Memoirs*, v. 1, pp. 108-121.

Enos P., Perkins R.D., 1979 Evolution of Florida Bay from island stratigraphy. *GSA Bull.*, v. 90/1, pp. 59-83.

Fielding C.R., Jonathon D.T., Alexander J., 2002 - Sharp-based, flood-dominated mouth bar sands from the Burdekin river delta of Northeastern Australia: extending the spectrum of mouth-bar facies, geometry, and stacking pattern. *Jour. Sed. Res*., v. 75/1, pp. 55-66.

Fontana, D., Zuffa, G.G., Garzanti, E., 1989 - The interaction of eustacy and tectonism from provenance studies of the Eocene Hecho Group Turbidite Complex (south-central Pyrenees, Spain). *Basin Research*, v. 2/4, pp. 223-237.

Folk R.L., 1959 - Practical petrographic classification of limestones. *AAPG Bull.*, v. 43, pp. 1-38

Folk R.L., 1974 - Petrology of sedimentary rocks. Hemphill Publishing Co., Austin, Texas, 182 pp.

Flügel E., 1996 - Microfacies of carbonate rocks: analysis, interpretation and application. Berlin, Springer- Verlag, 976 pp.

Franzinelli E., Potter P.E., 1983 - Petrology, chemistry and texture of modern river sands, Amazon River system. *Jour. Geol.,* v. 91**,** pp. 23-31.

Garzanti E., Vezzoli G., Andò S., Lavé J., Attal M., France-Lanord C., DeCelles P., 2007 – Quantifying sand provenance and erosion (Marsyandi River, Nepal Himalaya). *EPSL,* v. 258, pp. 500-515.

Gazzi P., 1966 Le arenarie del flysch sopracretaceo dell'Appennino modenese: correlazioni con il Flysch di Monghidoro. *Mineralogica Petrografica Acta,* v.12, pp. 69-97.

Gianolla P., Jacquin T., 1998 - Triassic sequence stratigraphic framework of western European basins. In: De Graciansky P.C., Hardenbol J., Jacquin T. and Vail P.R. (Eds.) *Mesozoic and Cenozoic Sequence Stratigraphy of European basins.* SEPM Special Publication v. 60, pp. 643-650.

Gianolla P., De Zanche V., Mietto P., 1998a - Triassic sequence stratigraphy in the Southern Alps (northern Italy): definition of sequences and basin evolution. In: De Graciansky P.C., Hardenbol J., Jacquin T. and Vail P.R. (Eds.) *Mesozoic and Cenozoic Sequence Stratigraphy of European basins.* SEPM Special Publication v. 60, pp. 719-747.

Gianolla P., Ragazzi E., Roghi G., 1998b - Upper Triassic amber from the Dolomites (Northern Italy). A paleoclimatic indicator? *Rivista italiana di Paleontologia e Stratigrafia*, v. 104, pp. 381-390.

Granet M., Chabaux F., Stille P., France-Lanord C., Pelt E., 2007 – Time-scales of sedimentary transfer and weathering processes from U-series nuclides: Clues from the Himalayan rivers. *EPSL*, v. 261, pp. 389-406.

Grantham J.H., Velbel M.A., 1998 - The influence of climate and topography on rock-fragment abundance in modern fluvial sands of the Southern Blue Ridge mountains, North Carolina. *Jour. Sed. Petr.*, v. 58/2, pp. 219-227.

Hardie L.A. 1977 - Distinctive features of a rainy, low-energy, tropical carbonate tidal flat; a summary. In: Hardie L.A. (Ed) S*edimentation on the modern carbonate tidal flats of Northwest Andros Island, Bahamas*, Johns Hopkins University Press, Baltimore, pp. 178-183.

Harwood, G., 1988 - Microscopic techniques:II Principles of sedimentary petrology. In: Tucker M.E. (Ed.) *Techniques in Sedimentology*. Blackwell Science, Oxford.

Hillis-Colinvaux L., 1984 - Systematics of the Siphonales. Systematics of the Green Algae. In: Irvine D.E. and John D.M. (Eds.) *Systematics Association*, Academic Press, Spec. Vol. 27, pp. 271-296.

Hochuli P.A., Frank S.M., 2000 - Palynology (dinoflagellate cysts, spore-pollen) and stratigraphy of the lower Carnian Raibl Group in the Eastern Swiss Alps. *Ecl. Geol. Helv.* v. 93/3, pp. 429-443**.**

Howarth R.W., Marino R., 2006 - Nitrogen as the limiting nutrient for eutrophication in coastal marine ecosystems: Evolving views over three decades. In: Joye S.B., Smith V.H., Howarth R.W., Bachmann R.W., Cloern J.E., Hecky R.E., Schindler D.W. (Eds.) Eutrophication of freshwater and marine ecosystems. *Limnology Oceanography*, v. 51/1, part 2, pp. 364-376.

Jadoul F., Nicora A., Ortenzi A., Pohar C., 2002 - Ladinian stratigraphy and paleogeography of the Southern Val Canale (Pontebbano-Tarvisiano, Southern Alps, Italy). *Memorie della Società Geologica Italiana*, v. 57, pp. 29-43.

Jenkyns H.C., 1980 - Cretaceous anoxic events; from continent to oceans. *Journal of the Geological Society of London*, v. 37, Part 2, pp. 171-188.

Jones B., Manning D.A.C., 1994 - Comparison of geochemical indices used for the interpretation of palaeoredox conditions in ancient mudstones. *Chemical Geology* v. 111/1-4, pp. 111-129.

Keim L., Schlager W., 2001 - Quantitative compositional analyses of a Triassic carbonate platform (Southern Alps, Italy). *Sedimentary Geology*, v. 139, pp. 261-283.

Keim L., Brandner R., Krystyn L., Mette W., 2001 - Termination of carbonate slope progradation; an example from the Carnian of the Dolomites, northern Italy. *Sedimentary Geology*, v. 143/3-4, pp. 303-323.

Kneller, B.J., Branney, M.J., 1995 - Sustained high-density turbidity currents and the deposition of thick massive sands. *Sedimentology*, v. 42, pp. 607- 616.

Koken E., 1913 - Kennitnis der Schichten von Heiligkreuz (Abteital, Südtirol). *Abhandlungen der K.K. Geologischen Reichsandstalt*, v.16/4, pp.1-43.

Krystyn L., 1978 - Aspects of Late triassic palynology; 4 A palynological assemblage from ammonoid-controlled late Carnian (Tuvalian) sediments of Sicily. *Review of Paleobotany and Palynology* v. 26/4, pp. 93-112.

Kutzbach J., Gallimore R., 1994 - Pangaean climates; megamonsoons of the megacontinent. *Journal of Geophysical Research, D, Atmospheres*. v. 94/3, pp. 3341-3357.

Lam D.W. and Zechman F.W., 2006 - Phylogenetic analyses of the Bryopsidales (Ulvophyceae, Chlorophyta) based on RUBISCO large subunit gene sequences. *Journal of Phycology*, v. 42, pp. 669-678.

Lebedeva M.I., Fletcher R.C., Balashov V.N., Brantley S.L., 2007 - A reactive diffusion model describing transformation of bedrock to saprolite. *Chemical Geology*, v. 244, pp. 624-645.

Lottes A., Ziegler A.M., 1994 - World peat occurrence and the seasonality of climate and vegetation. In: Calder J.H., Gibling M.R. (Eds.) The Euroamerican coal province; controls on tropical peat accumulation in the Paleozoic. *Palaeogeography, Palaeoclimatology, Palaeoecology*, v. 106/1-4, pp. 23-37.

Lowe D.R., 1982 - Sediment gravity flows. II. Depositional models with special references to the deposits of high-density turbidity currents. *Jour. Sed. Petr.*, v. 52, pp. 279- 297.

MacIntyre I.G. and Reid R.P., 1992 - Comment on the origin of aragonite needle mud: a picture is worth a thousand words. *Jour. Sed. Petr.*, v. 62, pp. 1095-1097.

MacIntyre I.G. and Reid R.P., 1995 - Crystal alteration in a living calcareous alga (Halimeda): implication for studies in skeletal diagenesis. *Journal of Sedimentary Research A*, vol. 65, pp. 143-153.

Marrocchino E., Coltorti M., Visonà D., Thirwall M. F., 2002 - Petrology of Predazzo Magmatic Complex (Trento, Italy). Goldschmidt Conference Abstracts, *Geoch. Cosmoch. Acta*, v. 65, pp. 486.

Mc Bride E.F., 1985 - Diagenetic processes that affect provenance determination in sandstones. In: Zuffa G.G. (Ed.) Provenance of arenites. *NATO-ASI Series. Series C: Mathematical and Physical Sciences*. Reidel Publ. Co., Dordrecht, v.148; pp. 95-113.

Mellere D., Plink-Bjorklund P., Steel R.J., 2002 - Anatomy of Shelf-Deltas on a prograding Eocene Shelf Margin, Spitsbergen. *Sedimentology*, v. 49/6, pp. 1181-1206.

Milliman J.D., 1993 - Production of calcium carbonate in the ocean: budget of a nonsteady state. *Global Biogeochemical Cycles*, v. 7/4, pp. 927-957.

Morse J.W., Gledhill D.K., Millero F.J., 2003 - CaCO3 precipitation kinetics in waters from the Great Bahama Bank: implications for the relationship between hydrochemistry and whitings. *Geoch. Cosm. Acta*, v. 67, pp. 2819-2826.

Morse J.W., Andersson A.J., Mackenzie F.T., 2006 - Initial responses of carbonate -rich shelf sediments to rising atmospheric *p*CO2 and "ocean acidification": Role of high Mg-calcites. *Geoch. Cosm. Acta*, v. 70, pp. 5814-5830.

Mount, J.F., 1984 - Mixing of siliciclastic and carbonate sediments in shallow-shelf environments. *Geology (Boulder)*, v. 12/7, pp. 432-435.

Mutti M., Hallock P., 2003 - Carbonate systems along nutrient and temperature gradients: some sedimentological and geochemical constraints. *International Journal of Earth Sciences*, v. 92, pp. 465-475.

Mutti M., Weissert H., 1995 - Triassic monsoonal climate and its signature in Ladinian-Carnian carbonate platforms (Southern Alps, Italy). *Jour. Sed. Res., B*, v. 65/3, pp. 357-367.

Muttoni G., Kent D.V., Channell J.E.T., 1996 - Evolution of Pangea: paleomagnetic constrains from the Southern Alps, Italy. *EPSL*, v. 140, pp. 97-112.

Neri C., Gianolla P., Furlanis S., Caputo R., Bosellini A., 2007 - Carta Geologica d'Italia alla scala 1:50.000, foglio 29 Cortina d'Ampezzo, and Note illustrative. APAT, Roma, 200pp.

Neri C., Stefani M., 1998 - Sintesi cronostratigrafica e sequenziale dell'evoluzione permiana superiore e triassica delle Dolomiti. *Mem. Soc. Geol. It*., v. 53, pp. 417-463.

Nesbitt H.W., Young G.M., 1997 – Formation and diagenesis of weathering profiles. *Journal of Geology*, v. 97, pp. 129-147.

Nesbitt H.W., Fedo C.M., Young G.M., 1997 - Quartz and feldspar stability, steady and non-steady-state weathering, and petrogenesis of siliciclastic sands and muds. *Jour. Geol.*, v. 105/2, pp.173-191.

Neumann A.C., Land L.S., 1975 - Lime mud deposition and calcareous algae in the Bight of Abaco, Bahamas: a budget. *Jour. Sed. Petr.*, v. 45, pp. 763-786.

Perez-Gonzales A., 1982 – El Cuaternario de la Région Central de la Cuenca del Duero y sus principales ragsos geomorfològicos. *Temas geològico-mineros IV*, IGME Madrid, pp. 730-735.

Pettijohn F.J., 1957 - Sedimentary rocks (2nd ed.). Harper and Row, New York, 718 pp.

Pia J., 1937 - Stratigraphie und Tektonik der Dolomiten von Prags. Selbstverlag, Wien, 248pp.

Picotti V., Prosser G., 1987 - Studio geologico dell'area compresa tra Lozzo di Cadore ed il gruppo delle Marmarole (Dolomiti, Alpi Meridionali).*Giornale di Geologia*, ser. 3, v. 49/1, pp. 33-50.

Pisa G., Marinelli M., Viel G., 1980 - Infraraibl Group: a proposal (Southern Calcareous Alps, Italy). *Rivista Italiana di Paleontologia e Stratigrafia*, v. 85, pp. 983-1002.

Preto N., Roghi G., Gianolla P., 2005 - Carnian stratigraphy of the Dogna area (Julian Alps, northern Italy): tessera of a complex palaeogeography. In: Eventi del Triassico superiore-Giurassico inferiore nel quadro del break-up di Pangea. *Boll. Soc. Geol. It.*, v. 124/1, pp.269-279.

Preto N., Hinnov L., 2003 - Unravelling the origin of carbonate platform cyclothems in the Upper Triassic Dürrestein Formation (Dolomites, Italy). *Jour. Sed. Res.*, v. 79, pp. 774-789.

Price G.D., 1999 - The evidence and implications of polar ice during the Mesozoic. *Earth-Science Reviews*, v. 48/3, pp. 183-210.

Prochnow S.J., Nordt L.C., Atchley S.C., Hudec M.R., 2006 - Multi-proxy paleosol evidence for Middle and Late Triassic climate trends in eastern Utah. *Pal. Pal. Pal.*, v. 232, pp. 53-72.

Purdy E.G., 1963 - Recent calcium carbonate facies of the Great Bahama Bank. 1. Petrography and reaction groups. *Journal of Geology*, v. 71/3, pp. 334-355.

Read J.F., 1998 - Phanerozoic carbonate ramps from greenhouse, transitional and ice-house worlds: clues from field and modeling studies. *Geological Society Special Publication*, v.149, p.107-135.

Reed J. S., Eriksson K. A., Kowalewski M., 2005 - Climatic, depositional and burial controls on diagenesis of Appalachian Carboniferous sandstones; qualitative and quantitative methods. *Sedimentary Geology, v.* 176/3-4, pp. 225-246.

Rees S.A., Opdyke B.N., Wilson P.A., Henstock T.J., 2007 - Significance of *Halimeda* bioherms to the global carbonate budget based on a geological sediment budget for the Northern Great Barrier Reef, Australia. *Coral Reefs*, v. 26, pp. 177-188.

Retallack G.J., 2001 - Soils of the past: an introduction to paleopedology (2nd edition). Unwin-Hyman Ltd, London, 404 pp.

Retallack G.J., Royer D.L., 2000 - Depth to pedogenic carbonate horizon as a paleoprecipitation indicator?; discussion and reply. *Geology*, v. 28/ 6, pp. 572-573.

Rettori R., Loriga C., Neri C., 1998 - Lower Carnian foraminifers from the type locality of the Calcare del Predil (Raibl Group, Northeastern Italy). *Rivista Italiana di Paleontologia e Stratigrafia*, v. 104/3, pp. 369-380.

Ries J.B., 2005 - Aragonite production in calcite seas: effect of seawater Mg/Ca ratio on the calcification and growth of the calcareous alga *Penicillus capitatus*. *Paleobiology*, v. 31, pp. 445-458.

Ries J.B., 2006 - Aragonite algae in calcite seas: effect of seawater Mg/Ca ratio on algal sediment production. *Jour. Sed. Res.*, v. 76, pp. 515-523.

Roghi G., 2004 – Palynological investigations in the Carnian of the Cave del Predil area (Julian Alps, NE Italy). *Review of Palaeobotany and Palynology*, v. 132/1-2, pp. 1-35.

Roghi G., Ragazzi E., Gianolla P., 2006 – Triassic amber of the Southern Alps (Italy). *Palaios*, v. 21/2, pp. 143-154.

Royer D.L., 1999 - Depth to pedogenic carbonate horizon as a paleoprecipitation indicator? *Geology*, v. 27/12, pp. 1123-1126.

Russo F., Neri C., Mastrandrea A., Laghi G., 1991 - Depositional and diagenetic history of the Alpe di Specie (Seelandalpe) fauna (Carnian, northeastern Dolomites). In: Flugel E. (Ed.) Regional and global controls of carbonate deposition, case studies, platforms, reefs, slopes. *Facies*, v. 25, pp. 187-210.

Russo F., Neri C., Mastandrea A., Baracca A., 1997 - The mud-mound nature of the Cassian platform margins of the Dolomites. A case history: the Cipit boulders from Punta Grohmann (Sasso Piatto Massif, northern Italy). *Facies*, v. 36, pp. 25-36.

Schäfer P., Senowbari-Daryan B., 1981 - Facies development and paleoecologic zonation of four Upper Triassic patch reefs, Northern Calcareous Alps near Salzburg, Austria. In: Toomey D.F., (Ed.) European reef models. *Society of Economic Paleontologists and Mineralogists, Special Publication*, v. 30, pp. 241-259.

Schlager W., 2003 - Benthic carbonate factories of the Phanerozoic. *International Journal of Earth Sciences*, v. 92, pp. 445-464.

Schlager W., 2005 - Carbonate sedimentology and sequence stratigraphy. *SEPM Concepts in Sedimentology and Palaeontology*, v. 8, 200 pp.

Schlager W., Schöllnberge W. 1974 - Das Prinzip stratigraphischer Wenden in der Schichtfolge der Nördlichen Kalkalpen. *Mitt. Geol. Ges.*, v. 66-67, pp. 165-193.

Senowbari-Daryan B. and Zamparelli V., 2005 - Triassic Halimedaceans: new genera and species from the Alps, Sicily and Southern Apennines. *Revista Española de Micropaleontologia*, v. 37/1, pp. 141-169.

Simms M. J., Ruffell A.H., 1989 - Synchroneity of climatic change and extinctions in the Late Triassic. *Geology*, v. 17, pp. 265-268.

Simms M. J., Ruffell A.H., 1990 - Climatic and biotic change in the Late Triassic. *J. Geol. Soc. (London)*, v. 147, pp. 321-327.

Simms M. J., Ruffell A.H., Johnson-Andrew L.A., 1997 - Biotic and climatic changes in the Carnian (Triassic) of Europe and adjacent areas. In: Fraser N. C. e Sues H. D. (Eds.) *In the shadow of the dinosaurs; early Mesozoic tetrapods.*, pp. 352-365.

Sloman L. E., 1989 - Triassic shoshonites from the Dolomites, Northern Italy: alkaline arc rocks in a strike-slip setting. *Journal of Geophysical Research*, v. 94; pp. 4655-4666.

Smosna, R. and Warshauer, S., 1978 - The evolution of a carbonate shelf, Silurian McKenzie Formation, West Virginia: a cluster analytic approach. *Jour. Sed. Petr.*, v. 48/1, pp. 331-336.

Stanley, G.D. jr., 1988 - The history of early Mesozoic reef communities: a three-step process. *Palaios*, v. 3, pp. 170-183.

Stanley G.D. jr., 2001 - Changes among reef ecosystems during the early Mesozoic. *PaleoBios* v. 21/2, Suppl., pp. 119-120.

Stanley, G.D. jr., 2003 - The evolution of modern corals and their early history. *Earth-Science Reviews*, v. 60, p. 195-225.

Stanley S.M., Hardie L.A., 1998 - Secular oscillations in the carbonate mineralogy of reef-building and sediment-producing organisms driven by tectonically forced shifts in seawater chemistry. *Palaeogeography, Palaeoclimatology, Palaeoecology*, v. 144, pp. 3-19.

Stefani M., Brack P., Gianolla P., Keim L., Maurer F., Neri C., Preto N., Riva A., Roghi G., Russo F., 2004 – Triassic carbonate platforms of the Dolomites: carbonate production, relative sea-level fluctuations and the shaping of the depositional architecture. In: Stefani M. (Ed.) *Triassic carbonate platforms of the Dolomites: carbonate production, relative sea-level fluctuations and the shaping of the depositional architecture*, fieldtrip guide. 32nd International Geological Congress, pp.1-44.

Suttner L.J., Basu A., Mack G.H., 1981 - Climate and the origin of quartz arenites. *Jour. Sed. Petr.*, v. 51/4, pp. 1235-1246.

Suttner L.J., Dutta P.K., 1986 - Alluvial sandstones composition and paleoclimate, I. Framework mineralogy. *Jour. Sed. Petr.*, v. 56/3, pp. 329-345.

Vail P.R., Audemard F., Bowman S.A., Eisner P.N., Perez-Cruz C., 1991 - The stratigraphic signatures of tectonics, eustasy and sedimentology-an overview. In: Einsele G., Ricken W., Seilacher, A. (Eds.) *Cycles and Events in Stratigraphy*, Berlin, Springer-Verlag, pp. 617-659.

Van der Plas L., Tobi A.C., 1965 - A chart for judging the reliability of point counting results. *American Journal of Sciences,* v. 263, pp. 87-90.

Van Wagoner J.C., Posamentier H.W., Mitchum R.M., Vail P.R., Sarg J.F., Louitt T.S., Handerbol J., 1988 - An overview of the fundamentals of sequence stratigraphy and key definitions. *Sea Level Changes- An Integrated Approach, SEPM Special Publication* v. 42, pp. 40-45.

Viel G., 1981 – Polarità tettonica e vulcanismo ladino-carnici del Sudalpino. *Mem. Soc. Geol. It.*, v. 21, pp. 19-24.

Weissert H., 1990 – Siliciclastics in the Early Cretaceous Tethys and North Atlantic Oceans: documents of periodic greenhouse climate conditions. *Mem. Soc. Geol. It.*, v. 44, pp. 59-69.

West, A.J., Galy A., Bickle M., 2005 - Tectonic and climatic controls on silicate weathering. *EPSL*, v. 235/1-2 pp. 211-228.

Wilson M.E.J., Vecsei A., 2005 - The apparent paradox of abundant foramol facies in low latitudes: their environmental significance and effect on platform development. *Earth-Science Reviews*, v. 69, pp. 133-168.

Zaninetti L., 1984 - Les Involutinidae (Foraminiferes); proposition pour une subdivision. *Revue de Paleobiologie*, v. 3/2, pp. 205-207.

Zuffa G.G., 1980 - Hybrid arenites: their composition and classification. *Jour. Sed. Petr.*, v. 50, pp. 21-29.

Zuffa G.G., 1985 - Optical analyses of arenites: influence of methodology on compositional results. In: Zuffa G.G. (Ed.) Provenance of arenites. *NATO-ASI Series. Series C: Mathematical and Physical Sciences*. Reidel Publ. Co., Dordrecht, v.148; pp. 383-391.

Zuffa G.G., 1987 - Unravelling hinterland and offshore paleogeography from deep-water arenites. In: Leggett J.K. and Zuffa G.G. (Eds.), *Marine Clastic Sedimentology, models and case studies (a volume in memory of C. Tarquin Teale)*, Graham and Trotman, London, pp. 39-61.

APPENDIXES

	RIO DI TERRAROSSA Dm. (Rio Pontuz section)									
	Tuz 8	**Tuz 9**	**Tuz 10**	**Tuz 11**	**Tuz 51**	**Tuz 54**	**Tuz 56**	**Tuz 58**	**Tuz 60**	**Tuz 64**	**Tuz 98**
Foram. Hyaline	5.4	6.1	0.2	5.4	9.4	8.8	6.9	5.3	7.5	4.2	13.1
Porcel.	14.1	0.6	0.4	14.6	25.3	14.7	16.2	20.4	15.1	7.9	8.5
Agglut.	8.4	0.0	0.4	6.3	12.4	6.1	1.7	2.3	6.8	2.9	6.3
Involut.	19.7	38.3	0.4	29.2	11.0	20.5	19.7	6.3	29.6	6.3	16.9
Biv. calc. Prisms	2.8	12.1	4.1	3.4	9.0	20.5	22.9	46.1	12.4	60.0	23.6
Biv. aragon.mm2	1.6	0.1	-	0.1	2.5	0.7	0.9	0.5	1.1	0.1	0.1
Gastropods	-	1.0	0.4	0.6	1.0	1.1	1.7	0.3	2.3	0.3	1.1
Ostracods (individuals)	2.1	5.2	1.9	1.0	2.0	1.4	1.4	1.8	1.9	6.0	3.7
Echinoderms	18.2	19.4	2.0	24.6	18.4	19.6	25.3	14.7	11.2	7.8	15.3
Calcareous algae	14.3	3.3	1.0	6.1	2.7	3.3	0.8	0.7	7.1	1.3	5.2
Bryozoans	-	-	-	1.7	1.0	2.4	0.5	-	0.4	-	0.4
Sponge spicules	13.4	13.9	89.3	6.9	5.3	0.9	2.1	1.6	4.6	3.3	5.9
Others-unknown	-	-	-	-	-	-	-	-	-	-	-
TOT	**100.0**	**100.0**	**100.0**	**100.0**	**100.0**	**100.0**	**100.0**	**100.0**	**100.0**	**100.0**	**100.0**

	RIO DEL LAGO Fm. (Rio Pontuz section)									
	Tuz 121	**Tuz 122**	**Tuz 130**	**Tuz 132**	**Tuz 133**	**Tuz 135**	**Tuz 138**	**Tuz 189**	**Tuz 190**	**Tuz 191**
Foram. Hyaline	2.2	7.1	4.1	14.1	10.0	9.4	10.6	2.3	2.5	6.4
Porcel.	26.2	10.7	27.5	42.6	35.0	35.7	44.2	24.3	1.3	2.6
Agglut.	10.6	21.8	2.5	4.5	5.9	8.0	2.2	1.0	0.5	2.9
Involut.	0.7	0.2	1.3	0.4	0.3	1.8	1.5	5.7	-	0.5
Biv. calc. Prisms	39.6	12.6	28.4	15.2	24.4	13.9	23.5	56.7	75.8	57.1
Biv. aragon.mm2	0.1	-	5.1	0.3	0.4	0.8	0.1	4.2	1.4	0.2
Gastropods	-	-	0.8	-	0.3	0.6	0.6	-	0.2	-
Ostracods (individuals)	1.7	4.8	4.6	3.4	3.1	10.1	4.9	2.4	11.1	14.5
Echinoderms	17.4	25.1	25.4	18.6	19.4	18.4	12.3	3.4	6.2	15.1
Calcareous algae	1.2	-	-	0.4	0.5	0.8	0.2	-	-	0.3
Bryozoans	0.3	0.2	0.3	0.6	0.5	-	-	-	0.2	-
Sponge spicules	0.1	-	-	-	-	0.2	-	-	0.4	0.4
Others-unknown	-	17.5	-	-	-	0.2	-	-	0.3	0.1
TOT	**100.0**	**100.0**	**100.0**	**100.0**	**100.0**	**100.0**	**100.0**	**100.0**	**100.0**	**100.0**

	RIO DEL LAGO Fm. (Rio di Terrarossa section)																																						
	201	**203**	**204**	**206**	**208**	**209a**	**211a**	**212**	**213**	**214a**	**215**	**215a**	**216**	**218**	**220**	**221**	**223**	**223a**	**223d**	**224bis**	**224d**	**226**	**228a**	**228b**	**230b**	**231**	**232b**	**235**	**239**	**246**	**250**	**252**	**254**	**255**
Foram. Hyaline	1.0	0.7	0.3	6.4	8.5	5.6	11.8	4.8	3.7	4.4	3.8	0.4	15.5	5.2	1.4	1.7	5.4	6.3	6.9	5.2	10.9	13.2	8.1	3.5	2.1	11.3	11.7	25.4	22.5	3.8	7.2	12.6	13.7	5.0
Porcel.	11.3	0.6	10.2	7.5	5.3	18.1	25.6	1.4	4.5	27.5	3.1	25.4	14.0	60.8	2.1	41.8	4.7	37.1	7.7	9.6	7.0	5.9	56.9	10.8	18.0	4.6	53.6	33.8	46.4	8.6	37.3	28.1	3.6	10.8
Agglut.	20.9	5.6	3.0	17.6	14.1	20.8	5.2	4.8	13.2	8.1	2.4	24.1	4.0	8.4	8.2	26.6	9.5	22.3	3.9	9.2	16.1	1.8	8.3	7.3	9.4	3.7	14.8	4.5	12.7	2.2	5.9	13.5	4.9	5.8
Involut.	23.0	22.3	6.5	1.8	14.7	2.8	19.5	5.5	14.4	3.4	0.4	39.1	2.9	0.8	2.9	9.8	1.9	10.8	8.6	8.3	1.6	3.7	1.7	12.9	25.3	3.3	8.5	2.0	4.2	0.7	13.9	10.3	7.2	3.0
Biv. calc. Prisms	25.2	58.8	69.2	5.5	11.7	35.2	15.2	4.9	41.2	10.8	50.3	0.7	10.1	4.5	12.7	1.1	14.2	2.9	-	6.3	8.1	4.6	3.2	16.6	10.4	41.4	0.3	10.5	5.9	40.4	10.3	10.2	1.1	13.0
Biv. aragon.mm2	0.9	3.0	1.7	0.7	0.5	0.2	-	1.0	8.6	0.1	14.8	0.2	0.1	0.2	6.2	7.6	6.3	4.0	0.1	0.5	0.6	1.3	0.2	3.5	3.0	0.5	-	0.3	2.7	0.5	2.8	0.7	0.6	7.5
Gastropods	-	0.8	0.3	0.2	1.5	0.5	0.5	0.5	-	2.8	0.5	1.1	-	0.2	0.3	0.4	1.7	1.7	0.2	-	0.4	-	1.9	0.2	1.5	-	0.6	-	-	-	-	-	-	1.0
Ostracods (individuals)	0.7	0.7	0.2	5.7	4.9	2.6	4.1	7.5	2.3	2.7	5.1	1.2	4.9	2.8	1.6	2.0	3.5	0.6	3.7	3.1	2.6	4.7	5.9	1.4	2.3	1.8	1.7	5.0	1.0	1.2	2.7	4.0	3.9	2.6
Echinoderms	15.2	6.4	7.2	7.7	4.7	7.6	15.7	3.0	8.1	5.8	17.6	1.5	16.3	12.2	16.3	4.3	9.5	7.1	6.9	5.8	11.1	10.3	11.8	18.9	21.4	10.5	1.8	3.9	3.4	12.3	5.9	4.3	9.2	23.3
Calcareous algae	1.8	1.1	1.4	46.5	34.1	6.0	2.3	66.7	4.0	34.0	2.0	5.5	30.6	1.8	8.3	1.7	34.3	7.3	62.1	46.2	40.8	53.6	2.1	24.6	6.4	22.5	6.9	14.1	1.1	29.6	14.1	15.6	29.6	18.7
Bryozoans	-	-	-	0.4	-	0.6	-	-	-	0.4	-	0.8	1.5	3.2	0.3	-	0.7	-	-	0.2	0.2	-	-	0.2	0.2	0.3	-	0.2	-	0.7	-	0.2	3.6	1.4
Sponge spicules	-	-	-	-	-	-	-	-	-	-	-	-	-	-	39.7	3.2	8.4	-	-	5.6	0.6	0.9	-	-	-	0.2	-	0.2	-	-	-	0.4	22.6	8.0
Others-unknown	-	-	-	-	-	-	-	-	-	-	-	-	-	-	-	-	-	-	-	-	-	-	-	-	0.2	-	-	-	-	-	-	-	-	-
TOT	**100.0**	**100.0**	**100.0**	**100.0**	**100.0**	**100.0**	**100.0**	**100.0**	**100.0**	**100.0**	**100.0**	**100.0**	**100.0**	**100.0**	**100.0**	**100.0**	**100.0**	**100.0**	**100.0**	**100.0**	**100.0**	**100.0**	**100.0**	**100.0**	**100.0**	**100.0**	**100.0**	**100.0**	**100.0**	**100.0**	**100.0**	**100.0**	**100.0**	**100.0**

	RIO DEL LAGO Fm. (Gran Colle section)																																						
	GC 1	**GC 2**	**GC 4**	**GC 5**	**GC 6**	**GC 7**	**GC 8**	**GC 9**	**GC 10**	**GC 11**	**GC 12**	**GC 13**	**GC 14II**	**GC 15**	**GC 16**	**GC 17**	**GC 18**	**GC 19**	**GC 20**	**GC 22**	**GC 23**	**GC 24**	**GC 25**	**GC 26**	**GC 27**	**GC 29**	**GC 30**	**GC 31**	**GC 32**	**GC 33**	**GC 34**	**GC 35**	**GC 36**	**GC 37**	**GC 38**	**GC 39**	**GC 41**	**GC 42**	**GC 43**	**GC 44**	**GC 45**	**GC 46**	**GC 47**	**GC 48**
Foram. Hyaline	6.6	3.4	7.8	13.0	13.9	1.0	12.4	5.6	4.0	10.5	2.7	3.5	4.4	10.5	4.3	8.2	3.7	2.8	2.8	5.5	7.6	10.0	1.0	7.6	3.2	17.5	9.6	18.1	12.2	22.7	18.3	12.8	2.0	3.3	28.3	16.8	5.8	8.2	11.7	4.2	5.0	8.7	1.4	1.6
Porcel.	34.4	18.9	30.0	32.0	40.5	21.7	20.1	9.0	37.6	16.0	32.8	52.9	23.4	36.3	25.8	4.5	40.2	11.3	45.3	10.7	29.5	26.4	23.2	22.9	5.3	19.9	24.8	24.2	24.1	38.1	34.6	29.5	43.2	18.0	13.9	14.4	24.7	3.6	11.3	46.4	3.7	67.6	23.1	18.4
Agglut.	8.1	3.0	5.5	5.6	6.0	25.9	4.6	1.7	22.0	3.6	3.7	19.7	6.4	3.6	3.4	2.8	0.5	4.9	13.6	4.4	11.1	9.7	4.2	15.1	2.0	3.2	5.6	4.4	8.2	11.5	19.4	6.7	0.6	6.8	-	6.3	1.5	2.0	1.6	0.3	0.5	0.4	5.0	6.4
Involut.	7.1	3.6	6.8	5.4	4.5	5.4	16.4	9.3	24.1	10.1	1.6	1.3	29.9	3.8	22.9	9.3	4.8	7.0	6.8	1.4	17.7	11.7	17.2	33.3	8.5	6.9	5.6	4.2	8.7	12.9	10.7	10.3	0.5	24.1	22.0	7.6	18.0	25.4	36.4	6.5	3.2	7.5	0.7	1.7
Biv. calc. Prisms	1.7	1.8	4.7	3.8	3.4	16.3	1.8	0.6	3.1	1.1	41.7	12.8	22.6	2.8	20.7	3.9	23.1	33.6	1.1	46.3	25.5	21.9	46.0	3.4	6.7	1.0	3.4	4.7	0.4	4.8	0.8	19.6	49.2	32.1	20.5	14.1	34.4	30.8	6.6	33.8	61.0	5.4	59.8	62.3
Biv. aragon.mm2	0.1	0.4	0.1	0.6	0.1	4.7	0.6	0.2	-	0.2	-	0.2	0.3	0.1	3.8	0.1	1.1	0.1	4.3	-	-	0.1	2.3	-	0.4	0.5	-	0.1	0.1	0.8	-	0.1	0.2	0.8	0.1	0.1	0.2	0.5	2.4	3.2	1.3	0.4	1.1	-
Gastropods	0.6	0.6	1.2	0.8	0.2	2.2	0.4	1.5	-	1.3	0.5	1.1	1.4	1.7	5.6	0.2	2.1	0.7	1.3	0.3	0.8	0.7	-	0.6	0.8	0.6	0.2	0.4	0.2	0.6	0.6	0.2	-	1.3	-	0.9	0.4	1.4	1.0	-	0.3	-	0.1	-
Ostracods (individuals)	1.8	1.0	1.7	4.0	3.3	1.6	2.4	1.7	3.1	2.4	0.7	2.9	0.6	3.3	3.4	2.6	3.6	1.5	4.5	0.7	0.7	3.5	1.8	2.4	3.1	3.9	7.1	2.3	3.1	1.9	6.1	7.4	3.4	1.6	7.7	6.1	1.6	4.1	2.2	0.7	3.9	2.0	1.6	2.6
Echinoderms	4.1	4.4	6.2	10.7	8.6	13.8	5.5	3.9	5.5	10.5	4.1	3.9	9.0	5.9	6.9	17.0	16.7	15.0	19.8	6.0	6.1	11.6	3.2	11.6	7.3	2.6	12.8	8.0	3.2	5.0	4.7	10.3	0.9	5.1	4.5	18.3	7.0	15.2	11.1	3.6	16.0	3.7	6.3	6.4
Calcareous algae	35.0	62.4	35.9	24.0	19.3	7.6	35.4	65.3	0.6	41.3	11.5	1.7	1.7	31.3	2.5	42.0	4.2	21.8	0.2	24.6	0.6	4.1	0.2	2.7	45.3	36.2	30.8	30.3	39.5	1.7	0.8	3.1	-	5.3	2.9	15.5	6.0	5.4	10.2	0.4	2.7	4.3	-	-
Bryozoans	-	-	-	-	0.2	-	0.2	-	-	-	0.4	-	-	-	0.4	-	-	0.3	0.2	-	0.3	-	0.2	0.4	0.2	-	-	-	0.4	-	0.2	-	-	0.2	-	-	0.3	1.1	-	-	-	0.8	0.2
Sponge spicules	0.4	0.4	-	-	-	-	-	1.3	-	3.0	-	-	0.3	0.8	0.4	9.5	-	0.9	-	-	-	0.3	0.7	-	17.1	7.6	-	3.4	-	-	3.7	-	-	-	-	-	-	1.8	5.5	0.9	1.6	-	-	0.3
Others-unknown	-	-	-	-	-	-	-	-	-	-	0.4	-	-	-	-	-	-	-	0.2	-	-	-	-	-	-	-	-	-	-	-	-	-	-	1.3	-	-	-	0.7	-	-	0.8	-	-	-
TOT	**100.0**	**100.0**	**100.0**	**100.0**	**100.0**	**100.0**	**100.0**	**100.0**	**100.0**	**100.0**	**100.0**	**100.0**	**100.0**	**100.0**	**100.0**	**100.0**	**100.0**	**100.0**	**100.0**	**100.0**	**100.0**	**100.0**	**100.0**	**100.0**	**100.0**	**100.0**	**100.0**	**100.0**	**100.0**	**100.0**	**100.0**	**100.0**	**100.0**	**100.0**	**100.0**	**100.0**	**100.0**	**100.0**	**100.0**	**100.0**	**100.0**	**100.0**	**100.0**	**100.0**

	TOR Fm. (Rio di Terrarossa section)						
	TUB 1	**TUB 3**	**TUB 6**	**TUB 19**	**TUB 22**	**TUB 23**	**TUB 27**
Foram. Hyaline	2.8	1.0	8.1	5.6	3.4	1.2	3.5
Porcel.	20.6	20.3	15.1	2.5	3.6	1.2	2.7
Agglut.	17.2	28.0	5.2	1.1	1.2	1.1	0.5
Involut.	1.2	0.3	1.2	0.5	0.4	0.9	0.7
Biv. calc. Prisms	4.0	40.6	0.2	29.4	15.9	56.2	25.7
Biv. aragon.mm2	0.1	1.7	0.3	0.2	-	0.1	1.0
Gastropods	0.4	-	-	0.3	0.4	0.2	0.5
Ostracods (individuals)	1.0	0.8	8.5	4.9	7.9	3.4	0.8
Echinoderms	7.5	7.1	28.9	12.8	15.4	10.2	18.8
Calcareous algae	17.2	-	0.2	2.5	6.0	0.3	25.3
Bryozoans	10.1	-	-	0.2	-	6.1	1.3
Sponge spicules	9.5	0.3	32.3	40.0	45.7	19.0	19.2
Others-unknown	8.3	-	-	-	-	-	-
TOT	**100.0**	**100.0**	**100.0**	**100.0**	**100.0**	**100.0**	**100.0**

PETROGRAPHICAL RESULTS, SUBTIDAL RAMP OF DOGNA

	HEILIGKREUZ Fm.																													
	CORTINA																					S. MARCO								
	PG	**Est 1**	**Est 2**	**Est 3**	**B1**	**B2**	**B3**	**B4**	**Lit B**	**DB1**	**DB2**	**DB3**	**DB4**	**DB5**	**DB6**	**DB7**	**LAG v**	**LAG r**	**DB8**	**DB9**	**PF1**	**PF2**	**SV 1**	**SV 2**	**SV 4**	**SV 6**	**SV 8**	**SV 10**	**SV 11**	**SV 13(12)**
QmP	1.6	0.6	0.4	0.8	-	-	-	-	0.6	-	0.8	0.6	1.4	4.6	12.8	-	-	0.8	0.4	-	0.4	7.4	-	-	-	-	-	-	-	-
QmV	8.4	6.2	0.8	3.6	16.6	19.3	26.7	12.6	29.7	12.8	16.4	16.0	37.0	37.7	28.2	20.1	17.0	16.7	18.0	19.8	10.1	8.2	25.7	15.1	14.9	15.9	17.5	39.0	12.1	17.6
QmU	0.6	0.3	-	0.8	-	0.2	0.5	0.2	0.4	0.6	0.4	0.4	1.4	0.4	2.3	0.4	0.4	0.7	1.4	-	0.4	0.9	0.3	0.2	0.6	1.0	0.6	-	0.4	0.6
Qpxc	1.2	1.3	-	1.6	-	-	0.3	0.2	0.4	-	0.2	0.2	2.4	0.8	0.3	0.2	1.0	0.5	1.2	-	0.8	2.3	0.8	0.2	0.2	0.8	0.4	0.2	0.4	0.2
Qva	1.8	1.2	0.8	3.0	-	-	-	0.2	0.6	2.4	0.4	0.6	1.2	0.6	0.6	0.4	1.4	0.6	-	2.0	2.2	1.0	0.5	1.4	4.7	2.8	0.8	0.5	2.0	1.6
Qpl/gn	-	-	-	-	-	-	-	-	-	-	-	-	-	-	-	-	-	-	-	-	0.2	0.2	-	-	-	-	-	-	0.2	-
Qmet	-	-	-	-	-	-	-	-	-	-	-	-	-	-	-	-	-	-	-	-	-	-	-	-	-	-	-	-	-	-
Cqm	0.6	2.1	6.2	0.6	-	-	0.2	0.2	2.6	5.8	3.8	2.4	3.2	1.0	4.0	5.5	0.2	3.2	2.0	2.6	4.3	0.8	0.3	2.4	1.2	-	4.0	-	-	2.6
Cqva	0.2	0.4	1.2	0.2	-	-	-	0.4	-	1.0	0.4	-	1.0	-	0.2	0.6	0.2	0.2	-	0.2	1.0	0.2	1.6	1.8	2.2	-	0.8	-	-	0.4
Cqpl/gn	-	-	-	-	-	-	-	-	-	-	-	-	-	-	-	-	-	-	0.4	-	0.2	0.2	-	-	-	-	-	-	-	-
Cqpx	-	0.4	-	0.2	-	-	-	-	-	0.2	-	0.2	0.2	0.2	0.2	-	0.2	1.2	0.4	-	0.2	1.0	-	-	-	-	-	-	-	-
Calced.	2.8	2.3	1.8	2.2	-	-	-	0.4	0.6	0.8	2.0	0.8	-	0.2	-	2.0	1.0	2.0	0.4	0.6	2.2	1.2	1.8	2.4	2.2	1.0	1.7	0.3	2.0	2.4
Pl	0.8	1.0	-	0.8	-	-	0.2	0.4	0.4	0.6	0.8	1.2	0.8	1.6	1.4	0.8	-	0.8	2.2	0.8	2.2	3.9	0.3	0.2	0.2	1.0	0.4	0.5	-	0.2
Pl alter	-	1.4	0.4	0.8	-	-	-	-	-	0.2	-	0.2	0.4	-	0.2	0.2	-	0.2	0.6	0.4	1.4	2.9	-	-	-	1.2	0.2	0.2	-	0.2
Ppl/gn	-	0.2	-	-	-	-	-	-	-	-	-	-	-	-	-	-	-	-	0.8	-	0.4	1.0	-	-	-	-	-	-	-	-
Plv	0.6	1.0	1.4	2.2	-	-	0.2	-	-	0.2	-	0.2	0.4	-	-	-	0.2	0.2	0.2	-	0.4	0.4	-	0.2	0.4	0.4	-	0.2	0.2	-
Cpl	0.2	1.0	1.0	0.6	-	-	-	-	0.6	0.6	0.6	0.4	0.2	-	0.4	-	0.4	2.8	1.4	0.2	1.0	0.2	-	-	-	-	-	0.2	-	0.4
Kfs	1.2	0.6	0.4	1.6	1.3	1.7	1.7	1.0	0.2	0.8	0.6	0.8	1.4	0.8	0.8	0.6	0.2	1.0	0.6	0.6	2.2	2.7	1.8	1.0	0.8	3.3	1.7	0.9	1.6	1.4
Kfs alter	-	0.8	0.2	0.2	-	-	-	-	-	-	0.2	0.6	-	-	-	-	-	-	-	0.4	0.6	0.4	-	0.4	0.4	0.4	0.2	0.3	-	0.4
Kpl/gn	-	-	-	-	-	-	-	-	-	-	-	-	-	-	-	-	-	-	-	-	0.4	-	-	-	-	-	-	-	0.2	-
Kv	1.6	0.4	1.0	2.4	-	-	-	-	-	0.6	0.4	-	0.2	-	0.2	-	0.2	-	0.2	-	0.2	0.2	-	0.8	1.4	1.0	0.2	-	0.2	0.4
Ckfs	-	0.2	0.2	0.2	-	-	-	-	-	0.8	-	0.4	-	-	0.2	-	-	0.8	-	-	0.4	0.2	-	0.4	-	-	0.6	-	-	0.8
Va	5.0	11.8	14.0	18.6	5.2	6.4	3.8	2.3	-	15.0	4.0	13.0	5.6	3.6	2.2	6.3	4.5	3.2	9.2	12.2	10.1	11.2	22.9	28.1	20.5	28.1	17.3	19.8	37.0	25.9
Vi	20.2	7.9	13.2	10.5	-	-	0.2	-	4.6	8.4	18.8	6.2	9.0	5.2	7.8	2.0	17.2	11.6	5.6	4.4	3.2	2.5	0.3	0.8	0.6	3.0	-	0.2	2.4	1.2
Va silicif	6.0	5.8	8.4	4.2	2.7	2.8	2.6	4.5	3.4	6.2	3.2	4.2	1.0	3.0	2.0	3.1	4.3	4.0	4.4	4.4	7.7	8.8	6.8	5.9	9.0	14.8	5.3	4.6	9.5	5.3
Vi alter	3.0	7.7	8.4	5.1	0.4	-	0.2	1.0	1.2	2.0	7.0	3.2	1.6	1.2	1.4	0.8	8.8	9.2	1.2	3.2	2.0	0.6	0.8	-	1.0	2.6	1.7	0.2	2.0	0.6
Glass	12.2	9.9	15.4	11.5	-	-	0.2	1.8	5.4	13.8	6.0	7.6	3.4	5.8	4.4	11.0	11.5	9.4	8.8	17.4	11.1	7.6	13.5	14.1	14.3	4.1	8.8	15.7	14.4	12.7
Dvtr	11.0	13.7	1.4	11.1	0.2	0.4	1.4	0.8	4.2	7.8	9.4	11.4	4.4	7.2	3.4	8.3	2.7	14.3	20.0	8.6	10.9	10.8	5.2	5.1	9.8	11.2	7.8	6.0	10.5	10.5
Pl/gn	0.2	1.2	-	0.4	-	-	-	-	0.2	-	0.4	0.6	-	-	-	-	-	-	2.0	-	0.4	1.4	-	-	-	-	-	-	-	-
Mmic	-	-	-	0.6	-	-	-	-	-	-	-	-	-	-	-	-	-	-	-	-	-	-	-	-	-	-	-	-	-	-
Mq	0.4	1.5	-	1.4	-	-	-	-	-	-	-	-	-	0.2	-	-	0.4	0.2	1.6	-	0.4	1.2	-	-	-	-	-	-	-	-
Ch	0.2	-	-	-	-	-	-	-	-	-	-	-	-	-	-	-	-	-	-	-	-	-	-	-	-	-	-	-	-	-
Silt	0.2	-	-	-	-	-	-	-	-	-	-	-	-	-	-	-	-	-	-	-	-	-	-	-	-	-	-	-	-	-
Bt	-	1.4	0.4	0.4	-	-	-	-	-	-	0.2	0.2	-	-	-	0.4	-	-	-	0.4	-	-	-	0.4	-	0.2	-	-	-	0.2
Chl	-	0.2	-	-	-	-	-	-	-	-	-	0.2	-	-	-	-	-	-	-	-	-	-	0.3	-	-	0.6	-	-	0.4	-
Ep	-	-	-	-	-	-	-	-	-	-	-	-	-	-	-	-	-	-	-	-	-	-	-	-	-	-	-	-	-	0.2
Op	0.4	0.8	1.0	0.4	2.5	4.4	1.0	1.6	2.2	2.2	1.8	7.8	2.0	0.8	0.4	2.8	1.8	0.6	3.4	4.4	0.4	-	0.3	0.4	3.5	2.2	8.6	0.2	1.0	2.0
Zr	0.4	0.6	-	0.2	-	-	-	-	-	-	-	-	0.2	-	-	0.2	0.4	0.2	0.2	-	0.2	-	-	-	-	0.2	-	-	-	-
Btv	0.4	0.2	1.2	0.6	-	-	-	-	-	-	-	-	0.2	-	-	-	0.6	0.6	-	-	-	-	0.3	-	-	-	-	-	-	-
Bio	-	-	-	-	10.9	10.6	9.9	17.7	9.2	-	0.6	0.2	-	-	0.4	4.1	0.4	0.4	0.6	7.4	0.4	0.6	-	-	-	-	5.7	1.2	-	-
Carb. intr.	0.2	-	-	-	56.5	46.6	42.9	34.6	16.7	1.6	1.6	4.0	1.2	2.2	1.8	10.8	0.4	0.6	0.4	8.0	5.1	2.2	-	-	-	-	1.9	2.2	-	0.2
Cl aren.	-	-	-	-	-	-	-	-	-	-	-	-	-	-	-	-	-	-	-	-	-	-	-	-	-	-	-	-	-	-
Nod.	-	-	-	-	-	-	-	-	-	-	-	-	-	-	-	-	-	-	-	-	-	-	-	-	-	-	-	-	-	-
Gr fosfatici	-	0.4	0.2	1.4	-	-	-	-	-	-	0.2	-	-	-	0.2	-	-	-	-	0.2	-	0.2	-	-	-	-	-	-	-	-
Gr verdi	-	-	-	0.2	-	-	-	-	-	1.2	0.2	0.6	-	0.2	0.2	-	-	-	-	0.2	-	-	-	-	-	0.2	0.2	-	0.4	3.2
Cmc	-	-	-	-	-	-	-	-	-	-	-	-	-	-	-	-	-	-	-	0.2	-	-	-	-	-	-	-	-	-	-
Cms	-	-	-	-	-	-	-	-	-	-	-	-	-	-	-	-	-	-	-	-	-	-	-	-	-	-	-	-	-	-
Dsp	-	-	-	-	-	-	-	-	0.4	-	-	-	-	-	-	-	-	-	-	-	-	-	-	-	-	-	-	-	-	-
Dpx	-	-	-	-	-	-	-	-	0.6	-	-	-	-	-	-	-	-	-	-	-	-	-	-	-	-	-	-	-	-	-
cc	-	-	-	-	-	-	-	-	-	-	-	5.2	-	-	0.2	-	-	-	-	-	7.7	-	-	-	-	2.6	-	-	-	-
cd	13.2	12.0	17.8	7.3	-	7.6	7.9	16.5	6.8	13.0	16.8	-	15.8	20.6	19.2	14.0	19.7	10.8	9.4	-	-	5.3	16.9	18.9	11.0	-	11.6	8.0	2.8	8.5
cq	-	-	0.2	0.2	-	-	-	-	-	-	-	-	0.2	-	0.2	0.2	-	-	-	-	-	0.2	-	-	0.4	0.6	-	-	-	-
matr c	0.2	-	-	-	3.8	-	-	3.7	4.4	-	-	1.0	0.4	0.8	0.4	1.6	-	-	0.4	-	5.7	7.6	-	-	-	-	1.7	-	-	-
matr sil	-	-	-	-	-	-	-	-	-	-	-	-	0.2	-	1.0	-	-	-	0.8	-	-	-	-	-	-	-	-	-	-	-
psm	-	-	-	0.2	-	-	-	-	-	-	-	-	-	-	0.2	-	-	-	-	-	-	-	-	-	0.6	-	-	-	0.6	-
clays	0.6	-	0.6	-	-	-	-	-	-	0.4	-	-	0.6	-	0.6	-	2.3	0.2	0.2	0.2	0.8	0.6	-	-	0.4	1.0	0.4	-	-	0.4
kaolinite	0.2	0.2	0.2	0.4	-	-	-	-	-	0.2	0.4	0.2	-	-	0.2	0.4	0.2	-	-	-	0.8	-	-	-	-	-	-	-	-	-
pcx	0.4	-	-	0.2	-	-	-	-	2.8	-	-	8.4	0.4	-	-	1.4	-	0.8	0.2	1.0	-	0.6	-	-	-	-	-	-	-	-
pqx	0.2	0.4	0.6	0.2	-	-	-	-	-	-	-	-	2.0	-	1.0	-	-	-	0.2	-	-	-	-	-	-	-	-	-	-	-
alter	-	-	-	-	-	-	-	-	-	-	-	-	-	-	0.8	-	-	-	-	-	-	3.5	-	-	-	-	-	-	-	-
silicif.	2.4	3.3	0.8	2.4	-	-	-	-	1.8	0.8	2.2	0.8	0.4	1.4	-	2.0	2.5	2.2	1.4	0.2	2.2	-	-	-	-	-	-	-	-	-
oth	1.4	-	0.6	1.0	-	-	-	-	0.2	-	0.2	0.2	0.2	-	0.2	-	0.2	0.2	-	-	-	-	-	-	-	-	-	-	-	-
TOT	**100.0**	**100.0**	**100.0**	**100.0**	**100.0**	**100.0**	**100.0**	**100.0**	**100.0**	**100.0**	**100.0**	**100.0**	**100.0**	**100.0**	**100.0**	**100.0**	**100.0**	**100.0**	**100.0**	**100.0**	**100.0**	**100.0**	**100.0**	**100.0**	**100.0**	**100.0**	**100.0**	**100.0**	**100.0**	**100.0**

PETROGRAPHICAL RESULTS, HEILIGKREUZ FM.

	RIO DEL LAGO Fm.					DOGNA Fm.										
	RIO PONTUZ		RIO MAS			RIO DI TERRAROSSA										
	Tuz 123	Tuz 127	RM 3	RM 4	RM 4a	RT 21	RT 22	TR 3	TR 4	TR 5	TR 6	TR 7	TR 11	TR 12	TR 13	TR 13b
QmP	-	-	-	-	-	-	-	-	-	-	-	-	-	-	-	-
QmV	20.8	21.0	35.5	40.4	25.1	34.3	37.4	29.7	13.7	21.3	10.7	14.8	18.1	16.9	17.4	19.3
QmU	0.4	0.4	0.8	1.4	1.0	0.6	0.8	1.6	0.6	1.3	0.0	0.6	1.4	0.2	0.8	1.0
Qpxc	-	-	0.6	0.2	0.2	0.2	1.5	2.0	1.0	2.1	0.8	0.6	0.8	1.3	0.6	0.2
Qva	1.6	2.4	1.0	0.4	0.4	1.4	0.8	1.4	1.4	2.1	1.8	1.8	1.6	1.7	0.4	2.4
Qpl/gn	-	-	-	-	-	-	-	-	-	-	-	-	-	-	-	-
Qmet	-	-	-	-	-	-	-	-	-	-	-	-	-	-	-	-
Cqm	8.6	6.6	7.4	3.3	1.9	5.0	2.5	2.9	1.6	4.4	3.0	2.6	1.0	1.5	2.6	3.0
Cqva	1.8	1.2	1.0	0.2	0.8	1.2	0.2	1.0	1.2	1.9	1.4	1.0	0.8	1.5	0.4	0.6
Cqpl/gn	-	-	-	-	-	-	-	-	-	-	-	-	-	-	-	-
Cqpx	-	-	-	-	-	-	-	-	0.2	-	-	-	0.2	-	-	-
Calced.	-	0.2	0.4	0.2	0.2	0.2	1.0	0.2	0.6	0.8	0.2	0.2	0.6	0.4	0.4	0.0
Pl	2.2	2.2	2.3	2.9	0.8	2.2	2.7	2.9	1.8	0.4	0.6	0.4	1.4	0.9	1.6	1.4
Pl alter	0.8	1.6	-	0.2	-	-	-	-	0.2	0.2	-	-	-	0.2	-	-
Ppl/gn	-	-	-	-	-	-	-	-	-	-	-	-	-	-	-	-
Plv	-	0.2	-	-	-	-	-	-	0.4	0.2	-	-	-	-	-	0.2
Cpl	0.6	0.8	1.0	-	-	0.6	0.2	0.4	-	0.2	0.2	0.2	0.2	0.4	0.2	0.2
Kfs	1.6	3.0	4.3	4.1	2.3	3.2	4.6	5.1	3.8	5.0	4.0	1.4	2.2	1.9	1.4	3.6
Kfs alter	0.2	0.2	-	-	-	-	-	-	0.2	1.5	-	0.2	-	-	-	-
Kpl/gn	-	-	-	-	-	-	-	-	-	-	-	-	-	-	-	-
Kv	-	-	-	-	-	-	-	0.2	0.2	0.2	-	0.2	0.2	0.2	-	0.4
Ckfs	0.6	-	0.4	0.4	-	-	0.2	-	0.4	-	1.0	0.4	0.2	-	1.2	0.6
Va	1.4	3.4	14.7	18.2	10.8	25.2	13.0	19.8	21.4	13.7	21.7	20.9	21.5	20.1	19.5	20.7
Vi	-	0.6	0.2	-	-	1.0	0.4	1.4	0.6	0.6	1.0	-	-	0.9	0.6	0.4
Va silicif	13.0	15.6	7.6	8.2	6.4	7.7	7.9	4.3	5.4	6.2	8.1	6.7	3.8	5.1	3.2	8.2
Vi alter	1.8	1.8	-	-	-	-	0.2	0.4	0.4	1.3	-	1.2	0.8	0.8	0.6	-
Glass	0.8	2.0	5.0	6.1	4.8	2.8	12.1	9.0	19.6	12.9	20.4	16.4	16.5	19.2	18.1	14.5
Dvtr	3.6	4.0	5.6	2.9	1.7	2.0	5.7	7.9	17.9	17.1	20.4	14.0	18.1	19.0	12.8	15.1
Pl/gn	-	-	-	-	-	-	-	-	-	-	-	-	-	-	-	0.2
Mmic	-	-	-	-	-	-	-	-	-	-	-	-	-	-	-	-
Mq	-	-	-	-	-	-	-	-	-	0.4	0.6	-	0.2	0.4	0.6	0.2
Ch	-	-	-	-	-	-	-	-	-	-	-	-	-	-	-	-
Silt	-	-	-	-	-	-	-	0.4	-	-	-	-	-	-	-	-
Bt	1.8	1.0	0.6	0.6	0.6	-	-	-	0.4	0.6	-	0.4	0.4	0.2	-	0.6
Chl	1.2	0.8	0.2	0.4	-	0.2	-	-	-	0.2	-	0.2	-	-	-	-
Ep	-	-	-	-	-	-	-	-	-	-	-	-	-	-	-	-
Op	4.0	1.6	2.3	1.0	1.5	2.4	2.3	1.6	1.2	2.3	0.2	2.8	3.2	1.1	4.1	2.0
Zr	0.2	0.0	0.4	-	-	-	0.4	-	-	-	-	-	-	-	0.4	0.2
Btv	-	-	-	-	-	-	-	-	-	-	-	-	-	-	-	-
Cmc	-	-	-	-	-	-	-	-	-	-	-	-	-	-	-	-
Cms	-	-	-	-	-	-	-	-	-	-	-	-	-	-	-	-
Dsp	-	-	-	-	-	-	-	-	-	-	-	-	-	-	-	-
Dpx	-	-	-	-	-	-	-	-	-	-	-	-	-	-	-	-
Bio	0.6	0.2	-	-	7.7	-	-	1.2	0.4	-	0.4	0.6	-	0.8	0.6	-
Carb. intr.	6.0	4.8	0.2	0.6	27.0	-	-	0.2	-	0.2	0.2	5.1	-	0.4	6.1	-
Cl aren.	-	-	-	-	-	-	-	-	-	-	-	-	-	-	-	-
Nod.	-	-	-	-	-	-	-	-	-	-	-	-	-	-	-	-
Gr fosfatici	-	-	-	-	-	-	-	-	-	-	-	0.2	-	-	-	-
Gr verdi	-	-	-	0.2	-	-	-	-	0.2	-	-	0.2	-	-	0.4	-
cc	8.8	9.8	1.2	-	-	-	-	3.9	1.0	0.4	-	-	-	-	-	3.6
cd	-	-	6.0	7.8	6.6	6.7	6.3	-	3.4	2.1	3.4	6.9	5.4	3.4	6.1	0.2
cq	-	0.4	-	-	-	-	-	-	-	0.2	-	-	-	-	-	-
matr c	9.0	6.4	0.6	-	0.2	1.6	-	2.4	-	-	0.2	-	-	1.5	-	-
matr sil	-	-	-	-	-	-	-	-	-	-	-	-	-	-	-	-
psm	-	-	-	-	-	-	-	0.2	-	-	-	-	-	-	-	-
clays	5.0	5.2	0.6	0.4	-	0.6	-	-	-	-	-	-	0.2	-	-	0.8
kaolinite	2.2	2.2	0.4	-	-	-	-	-	-	-	-	-	0.2	-	-	-
pcx	0.8	0.2	-	-	-	1.0	-	-	1.0	0.2	-	-	1.0	-	-	0.6
pqx	-	-	-	-	-	-	-	-	-	-	-	-	-	-	-	-
alter	-	-	-	-	-	-	-	-	-	-	-	-	-	-	-	-
silicif.	-	-	-	-	-	-	-	-	-	-	-	-	-	-	-	-
oth	0.6	0.2	-	-	-	-	-	-	-	-	-	-	-	-	-	-
TOT	**100.0**	**100.0**	**100.0**	**100.0**	**100.0**	**100.0**	**100.0**	**100.0**	**100.0**	**100.0**	**100.0**	**100.0**	**100.0**	**100.0**	**100.0**	**100.0**

	DOGNA Fm.													
	RIO PONTUZ													
	Tuz 188	Tuz 192	Tuz 198	Tuz 202	Tuz 203	Tuz 204	Tuz 205	Tuz 208	Tuz 209	Tuz 210	Tuz 212a	Tuz 212b	Tuz 212c	Tuz 214
QmP	-	-	-	-	-	-	19.4	-	0.2	-	-	-	-	-
QmV	15.6	22.4	13.9	22.0	16.1	13.2	1.8	6.7	19.2	12.5	16.9	20.7	13.4	26.3
QmU	0.2	1.2	1.5	1.6	0.2	0.6	0.6	0.6	2.6	0.2	1.2	1.7	0.6	-
Qpxc	-	-	-	0.2	-	-	4.2	1.2	0.6	0.4	1.0	0.8	0.8	0.2
Qva	1.0	2.0	3.1	2.6	3.0	2.4	0.6	1.4	2.4	2.0	3.0	4.3	3.8	2.2
Qpl/gn	0.2	0.6	0.2	-	-	0.4	-	-	-	-	-	0.2	-	-
Qmet	-	-	-	-	0.2	-	1.2	-	-	-	-	-	-	-
Cqm	2.0	1.8	2.4	6.4	0.8	0.6	1.6	-	0.8	1.0	0.2	0.6	2.5	0.7
Cqva	0.6	1.2	3.1	0.6	1.0	1.4	-	-	-	-	0.2	0.4	0.6	-
Cqpl/gn	-	-	-	-	-	-	-	-	-	-	-	-	-	-
Cqpx	-	-	-	-	-	-	-	-	-	-	-	-	-	-
Calced.	1.2	1.0	0.6	1.0	0.2	2.0	0.6	3.1	-	0.4	1.6	1.7	1.3	0.6
Pl	0.6	3.0	0.6	0.2	-	1.2	1.4	2.3	1.2	0.4	2.0	0.4	2.1	0.6
Pl alter	1.2	0.6	0.4	0.2	0.6	0.8	0.2	0.8	0.2	0.6	-	0.6	0.2	0.2
Ppl/gn	0.2	-	-	-	-	0.2	-	-	-	-	0.2	0.2	-	0.2
Plv	0.4	0.4	-	-	0.8	0.2	0.4	-	0.2	0.2	1.0	0.4	0.4	0.2
Cpl	-	1.2	0.2	0.4	-	0.2	0.2	-	-	-	0.2	-	0.4	0.6
Kfs	2.0	3.8	0.7	1.2	3.6	3.6	1.0	2.2	0.4	0.6	2.2	1.2	1.7	0.2
Kfs alter	1.4	0.8	1.3	1.6	0.8	0.4	0.4	0.4	-	-	-	0.4	0.4	0.2
Kpl/gn	0.2	-	-	-	0.2	0.2	-	-	-	-	0.4	-	0.2	-
Kv	-	0.6	0.2	0.2	1.0	0.4	0.4	0.2	-	0.2	0.6	0.2	0.2	-
Ckfs	-	2.4	2.4	1.4	0.2	0.6	0.4	-	-	-	-	-	-	0.2
Va	5.0	10.0	18.3	16.4	25.8	22.7	17.2	25.6	20.2	22.4	15.9	13.4	17.1	8.6
Vi	-	-	0.6	-	-	0.6	0.4	3.1	2.0	1.6	0.8	0.2	0.8	1.3
Va silicif	11.0	8.4	6.9	8.6	12.9	10.1	11.6	10.0	17.4	14.3	8.5	8.7	6.0	8.2
Vi alter	1.8	1.4	1.1	1.6	1.0	1.0	1.4	1.0	1.6	-	0.2	1.2	0.4	1.5
Glass	4.6	5.2	7.6	5.6	4.6	6.1	8.4	12.9	9.8	14.3	13.9	18.0	13.8	14.2
Dvtr	12.6	9.4	18.7	11.0	14.7	19.4	13.2	13.9	9.4	18.3	20.0	14.3	16.7	14.0
Pl/gn	0.6	0.6	-	-	-	0.2	-	-	-	-	-	-	-	-
Mmic	-	-	-	-	-	-	-	-	-	-	-	-	-	-
Mq	-	-	-	-	-	0.4	0.2	0.2	0.2	0.2	0.4	0.4	-	0.2
Ch	-	-	-	-	-	-	-	-	-	0.2	-	-	-	-
Silt	-	-	-	-	-	-	0.4	-	0.2	-	-	-	0.2	-
Bt	-	-	-	0.2	0.2	0.6	0.6	0.2	1.4	-	0.2	0.4	-	0.4
Chl	-	-	0.2	-	0.2	0.4	-	-	1.0	-	-	0.4	0.2	-
Ep	-	-	-	-	-	-	0.2	-	-	-	-	-	-	-
Op	0.2	2.2	0.7	2.4	4.2	2.2	2.8	0.6	2.2	2.8	2.0	2.9	2.3	7.8
Zr	-	0.4	0.2	-	0.4	-	0.4	-	0.2	0.2	-	-	0.2	0.2
Btv	-	-	-	-	-	-	-	-	-	-	-	-	-	0.2
Cmc	2.0	2.6	-	-	-	-	-	-	0.4	-	-	-	0.2	-
Cms	1.8	-	-	-	-	-	0.2	-	-	-	-	-	-	0.4
Dsp	-	-	0.2	0.2	-	-	-	-	-	-	-	0.2	-	0.2
Dpx	-	-	0.4	1.4	-	-	-	-	-	-	-	-	-	-
Bio	1.8	-	-	-	-	-	-	-	-	-	-	-	-	0.6
Carb. intr.	9.6	-	-	-	-	-	-	3.9	0.2	0.8	0.8	1.2	4.4	1.9
Cl aren.	-	-	-	-	-	-	-	-	-	-	-	-	-	-
Nod.	-	-	-	-	-	-	-	-	-	-	-	-	-	-
Gr fosfatici	-	-	-	0.2	-	-	-	0.2	-	-	-	-	-	-
Gr verdi	-	-	0.2	-	-	0.6	-	-	0.6	0.2	-	-	0.2	-
cc	11.2	8.2	4.3	2.8	2.6	0.2	-	8.0	0.2	3.6	-	1.9	6.5	8.4
cd	-	-	-	-	0.6	2.2	4.2	-	0.2	-	-	-	-	-
cq	-	-	-	-	0.2	-	1.2	-	0.2	-	0.6	-	-	-
matr c	7.2	7.2	6.3	6.6	0.2	0.4	-	-	0.8	1.4	3.8	1.6	2.1	-
matr sil	-	-	-	-	0.2	-	-	1.0	0.4	-	0.2	-	-	-
psm	-	-	0.2	-	-	-	-	-	1.2	-	-	-	-	-
clays	2.8	0.2	1.9	0.6	2.6	2.6	2.0	0.4	1.6	1.0	1.6	1.6	0.4	-
kaolinite	0.2	1.2	-	1.6	0.8	1.6	0.6	-	0.4	0.4	0.2	-	-	-
pcx	0.8	0.2	1.5	1.2	-	0.4	0.2	0.2	0.2	-	-	-	-	-
pqx	-	-	-	-	-	-	0.2	-	-	-	-	-	-	-
alter	-	-	-	-	-	-	-	-	-	-	-	-	-	-
silicif.	-	-	0.2	-	0.2	-	0.2	-	0.2	-	0.4	-	-	-
oth	-	-	0.2	-	-	0.2	0.2	-	0.2	-	-	-	-	-
TOT	**100.0**	**100.0**	**100.0**	**100.0**	**100.0**	**100.0**	**100.0**	**100.0**	**100.0**	**100.0**	**100.0**	**100.0**	**100.0**	**100.0**

	DOGNA Fm.																			
	RIO PONTUZ												GRAN COLLE I and II							
	Tuz 215	Tuz 216	Tuz 217a	Tuz 217b	Tuz 217c	Tuz 222	Tuz 223	Tuz 224	Tuz 225	Tuz 229	Tuz 232	Tuz 236	GC 40	ZUT 12	ZUT 10	ZUT8	ZUT 7	ZUT 5	ZUT 4	ZUT 2
QmP	-	-	-	-	-	-	-	-	-	-	-	-	-	-	-	-	-	-	-	-
QmV	9.5	15.6	21.8	20.7	17.1	23.2	23.2	25.8	20.4	31.9	23.4	22.0	30.3	26.9	18.0	19.3	23.2	32.3	34.6	35.8
QmU	-	0.6	1.2	0.4	0.2	1.6	0.4	0.2	0.6	3.2	1.2	1.2	1.2	0.8	1.5	1.4	1.4	0.8	0.4	3.2
Qpxc	0.2	0.4	1.4	0.8	-	0.4	-	1.0	1.0	-	3.0	2.6	1.0	0.8	2.7	1.0	1.2	0.6	2.2	1.8
Qva	5.3	1.2	5.7	3.1	2.8	5.0	0.8	7.4	4.7	8.2	2.0	1.0	0.2	1.4	3.2	3.1	3.3	0.6	1.0	1.0
Qpl/gn	-	-	-	-	-	-	-	-	-	-	-	-	-	-	-	-	-	-	-	-
Qmet	-	-	-	-	-	-	-	-	-	-	-	-	-	0.2	-	-	-	-	-	-
Cqm	0.8	1.8	1.6	2.0	1.2	3.6	0.4	4.6	1.4	7.2	0.8	4.8	4.4	0.6	3.4	3.3	3.9	1.8	0.6	1.8
Cqva	0.4	0.4	0.8	1.0	0.6	1.2	-	2.4	0.2	1.6	-	0.2	0.2	0.4	1.1	1.5	2.4	-	0.2	0.4
Cqpl/gn	-	-	-	-	-	-	-	-	-	-	-	-	-	-	-	-	-	-	-	-
Cqpx	-	-	0.2	-	-	-	-	-	-	-	0.2	-	-	0.2	0.4	-	0.2	-	0.2	0.2
Calced.	3.2	0.6	2.0	1.8	4.4	1.0	-	0.6	1.2	0.2	0.4	0.4	1.0	0.4	0.9	0.4	1.2	1.0	1.4	1.4
Pl	1.2	0.8	0.2	0.4	0.2	2.0	-	1.8	1.6	0.8	0.6	0.4	0.4	2.8	0.9	0.4	1.2	1.6	1.4	1.0
Pl alter	0.4	0.2	1.2	1.6	0.4	1.0	-	0.8	0.6	0.2	-	-	-	1.0	0.4	-	-	0.4	-	0.2
Ppl/gn	-	-	-	-	-	-	-	-	0.2	-	-	-	-	-	-	-	-	-	-	-
Plv	0.8	-	0.6	0.4	-	0.8	0.4	0.6	0.8	1.2	0.2	-	-	0.4	-	-	-	-	0.2	0.2
Cpl	0.2	0.2	0.2	0.4	0.2	0.4	-	0.4	-	-	0.2	-	-	0.2	0.6	-	-	-	-	-
Kfs	2.2	0.4	1.0	1.6	0.6	1.2	0.6	0.6	1.8	0.6	6.2	2.4	2.7	2.6	2.8	2.1	2.6	2.8	3.3	5.5
Kfs alter	-	-	0.4	-	0.4	-	-	-	0.4	-	-	0.2	-	0.2	0.2	-	-	0.2	-	-
Kpl/gn	-	-	0.2	-	-	-	-	-	-	-	-	-	-	-	-	-	-	-	-	-
Kv	0.8	0.2	0.2	0.2	-	0.4	-	-	0.6	0.4	0.4	-	-	-	0.6	0.6	0.2	-	-	-
Ckfs	-	0.4	-	-	-	-	-	0.2	-	-	-	0.2	0.2	-	0.2	0.2	-	-	-	-
Va	21.7	15.2	10.7	10.6	8.0	9.1	4.4	7.2	14.9	8.8	16.3	17.3	6.6	18.9	17.6	17.8	15.4	14.3	22.4	12.3
Vi	0.8	-	0.8	2.6	0.6	-	-	0.6	0.8	1.4	0.4	0.2	-	1.8	1.7	0.6	0.6	-	0.2	0.4
Va silicif	7.5	5.1	5.9	11.6	11.0	9.1	4.0	4.8	8.0	6.0	10.3	5.8	4.2	6.0	8.2	10.6	7.7	6.2	5.9	4.0
Vi alter	1.0	1.6	2.2	1.0	1.6	1.0	0.6	1.0	1.2	0.6	-	1.2	1.0	0.2	-	-	-	-	-	-
Glass	15.0	7.1	21.0	15.7	18.1	15.7	9.0	14.6	13.5	9.8	12.9	13.1	9.7	16.7	15.0	14.9	16.1	15.5	6.7	13.2
Dvtr	18.7	5.3	15.2	15.6	16.3	16.7	3.8	13.4	13.1	6.8	17.7	13.9	8.3	11.6	9.9	14.3	13.6	9.8	0.4	8.7
Pl/gn	-	-	-	-	0.2	-	-	-	-	-	-	-	-	-	0.2	-	-	-	-	-
Mmic	0.4	-	-	-	-	-	-	-	-	-	-	-	-	0.2	-	0.2	-	-	-	-
Mq	-	-	0.2	-	0.6	-	-	-	0.2	-	-	1.4	0.4	-	1.7	-	-	0.4	0.2	0.4
Ch	0.2	-	-	0.2	-	-	-	-	-	-	-	-	-	-	-	-	-	-	-	-
Silt	-	-	-	-	-	-	-	-	1.6	-	-	-	-	-	0.2	-	-	-	-	-
Bt	0.2	-	-	-	0.2	0.2	0.4	0.2	0.2	0.4	-	-	0.4	1.2	0.6	-	-	-	-	0.4
Chl	-	-	0.4	0.2	-	0.4	-	0.4	0.2	-	-	0.2	0.2	0.4	-	-	-	-	-	0.2
Ep	-	-	-	-	-	-	-	-	0.2	-	-	-	-	-	-	-	-	-	-	-
Op	2.2	1.4	0.4	2.6	0.2	0.8	2.8	4.8	2.7	2.8	0.4	2.0	2.5	1.6	0.6	1.7	1.4	2.4	1.8	1.2
Zr	-	-	-	0.2	-	-	0.2	0.2	0.2	-	0.4	-	0.2	0.2	0.2	0.2	0.2	0.2	0.2	-
Btv	-	-	-	-	-	-	-	-	-	-	-	-	-	-	-	-	-	-	-	-
Cmc	-	-	-	-	0.4	0.2	-	-	-	-	-	-	-	-	-	-	-	-	-	-
Cms	-	-	-	-	-	-	1.0	-	-	0.4	-	-	-	-	-	-	-	-	-	-
Dsp	-	-	0.2	-	-	-	-	0.2	-	0.2	-	-	-	-	-	-	-	-	-	-
Dpx	-	0.4	-	0.2	-	-	-	-	-	-	-	-	-	-	-	-	-	-	-	-
Bio	-	3.6	0.2	-	2.8	-	3.4	-	-	-	-	-	8.9	-	-	-	-	-	-	-
Carb. intr.	1.2	19.0	-	-	4.2	1.2	29.0	-	0.2	-	-	0.2	8.3	-	-	-	-	2.2	7.1	1.2
Cl aren.	-	-	-	-	-	-	-	-	-	-	-	-	-	-	-	-	-	-	-	-
Nod.	-	-	-	-	-	-	-	-	-	-	-	-	-	-	-	-	-	-	-	-
Gr fosfatici	-	-	-	-	-	-	0.6	-	-	-	-	-	0.2	-	-	-	-	-	-	-
Gr verdi	-	0.2	-	-	-	-	-	0.2	-	-	-	0.4	0.6	0.2	0.2	-	-	-	0.2	-
cc	5.1	10.3	2.4	3.9	4.0	2.8	15.0	3.6	-	4.4	-	-	-	-	-	-	-	-	-	-
cd	-	-	-	-	-	-	-	-	6.7	-	3.2	7.7	7.1	1.2	6.5	5.0	3.0	1.4	-	0.2
cq	-	-	-	-	-	-	-	-	-	0.8	-	-	-	-	-	-	-	-	-	-
matr c	0.4	6.7	-	-	2.8	0.2	-	-	-	0.2	-	-	-	-	-	-	-	5.6	9.6	5.3
matr sil	0.2	-	-	-	-	-	-	-	-	-	-	-	-	0.2	-	-	-	-	-	-
psm	0.2	-	-	0.2	-	-	-	-	-	-	-	0.4	-	-	-	-	-	-	-	-
clays	0.2	0.6	1.8	1.2	0.2	1.0	-	1.6	0.8	1.6	-	1.0	-	0.6	0.2	0.2	-	-	-	0.2
kaolinite	-	0.2	-	-	0.8	-	-	0.4	-	0.2	-	-	-	-	-	-	-	-	-	-
pcx	-	0.4	-	-	-	-	-	0.4	-	0.2	-	-	-	0.2	-	1.4	1.4	-	-	-
pqx	-	-	-	-	-	-	-	-	-	-	-	-	-	-	-	-	-	-	-	-
alter	-	-	-	-	-	-	-	-	-	-	-	-	-	-	0.4	-	-	-	-	-
silicif.	0.2	-	-	-	-	-	-	-	0.2	-	-	-	-	-	-	-	-	-	-	-
oth	-	-	-	-	-	-	-	-	-	-	-	-	-	-	-	-	-	-	-	-
TOT	**100.0**	**100.0**	**100.0**	**100.0**	**100.0**	**100.0**	**100.0**	**100.0**	**100.0**	**100.0**	**100.0**	**100.0**	**100.0**	**100.0**	**100.0**	**100.0**	**100.0**	**100.0**	**100.0**	**100.0**

PETROGRAPHICAL RESULTS, RIO DEL LAGO AND "DOGNA" FMS.

	TRAVENANZES Fm.																									
	CORTINA																S. MARCO									
	RB 72	**RB 151b**	**RB 151t**	**RB 152b**	**RB 153**	**RB 155**	**RB 156**	**RB 157t**	**RB 158**	**RB 159**	**RB 162**	**RB 163**	**RB 164**	**RB 83**	**RB 84**	**RB 85**	**RB 86**	**RB 210**	**RB 213**	**RB 219**	**RB 220**	**RB 221**	**RB 222**	**RB 223**	**RB 224**	**RB 225**	**RB 232**
QmP	-	-	-	-	-	-	-	-	-	-	-	-	-	-	-	-	-	-	-	-	-	-	-	-	-	-	-
QmV	23.8	40.5	12.6	43.6	29.4	41.5	37.2	27.5	44.8	30.2	59.0	33.4	44.3	44.3	38.6	62.3	57.7	29.1	35.4	40.2	24.6	19.6	43.4	33.4	48.4	16.9	25.9
QmU	2.4	-	-	-	0.4	-	0.2	0.6	-	1.2	0.8	0.2	0.2	0.2	-	0.2	0.4	0.6	0.8	0.4	-	-	0.2	0.6	-	0.2	-
Qpxc	-	-	-	-	-	-	-	-	-	-	-	-	-	-	-	-	-	-	0.4	-	-	0.2	0.2	0.2	-	-	-
Qva	0.6	-	0.4	0.4	0.4	-	3.9	0.2	-	0.4	0.6	0.2	0.2	-	-	-	-	3.5	3.5	0.4	-	0.4	-	0.4	-	-	0.6
Qpl/gn	-	-	-	-	-	-	-	-	-	-	-	-	-	-	-	-	-	-	-	-	-	-	-	-	-	-	-
Qmet	-	-	-	-	-	-	-	-	-	-	-	-	-	-	-	-	-	-	-	-	-	-	-	-	-	-	-
Cqm	5.3	0.2	0.6	-	1.2	0.2	1.2	2.9	1.5	1.4	0.8	0.6	2.7	-	-	-	1.9	-	-	0.2	-	-	-	0.2	-	2.0	0.2
Cqva	0.4	-	-	-	0.2	-	1.0	1.3	0.5	0.2	0.8	-	-	-	-	-	-	-	0.2	-	-	0.2	-	0.2	-	0.6	-
Cqpl/gn	-	-	-	-	-	-	-	-	-	-	-	-	-	-	-	-	-	-	-	-	-	-	-	-	-	-	-
Cqpx	-	-	-	-	-	-	-	-	-	-	-	-	-	-	-	-	-	-	-	-	-	-	-	-	-	-	-
Calced.	0.8	-	-	-	0.2	0.2	0.4	-	-	-	0.4	0.4	-	-	-	-	-	0.2	-	0.2	0.4	0.2	-	-	0.2	-	0.4
Pl	5.7	-	-	-	1.6	-	1.2	0.6	1.8	2.7	2.2	-	1.7	0.6	0.2	0.6	1.7	1.8	1.6	0.8	0.4	0.4	0.9	2.5	0.7	0.4	-
Pl alter	-	-	-	0.2	0.4	-	0.4	1.5	0.7	-	0.2	0.2	0.2	0.2	-	-	0.4	0.4	0.4	0.2	0.4	0.2	-	0.2	-	-	-
Ppl/gn	-	-	-	-	-	-	-	-	-	-	-	-	-	-	-	-	-	-	0.2	-	-	-	-	-	-	-	-
Plv	-	-	-	-	-	-	0.2	0.2	-	0.2	-	-	-	-	-	-	-	0.6	0.2	-	-	-	-	-	-	-	-
Cpl	0.6	-	-	-	-	-	0.2	0.4	-	0.6	-	-	0.2	0.2	-	-	-	-	-	-	-	-	-	-	-	-	-
Kfs	2.4	0.9	1.0	0.9	0.2	2.2	3.5	4.2	8.6	1.9	1.2	1.0	1.9	1.7	0.8	0.9	1.2	4.1	3.3	2.1	0.6	1.0	0.9	3.3	0.7	1.2	3.1
Kfs alter	0.2	0.2	0.4	0.2	0.8	-	1.2	0.6	0.2	-	-	0.4	0.2	-	-	0.4	0.6	-	-	-	-	-	-	-	-	-	0.2
Kpl/gn	-	-	-	-	0.2	-	-	-	-	-	-	-	-	-	-	-	-	-	-	-	-	-	-	-	-	-	-
Kv	0.2	-	-	-	-	-	2.6	0.4	-	-	-	-	-	-	-	-	-	1.0	1.0	-	-	0.2	-	-	-	-	-
Ckfs	0.6	0.4	0.2	0.2	0.4	0.5	0.4	1.9	0.4	-	-	-	0.4	-	-	-	0.2	-	-	-	-	-	-	-	-	0.6	-
Va	5.3	2.1	2.2	1.3	2.4	1.6	2.4	0.8	1.1	4.1	0.2	-	2.3	-	0.6	-	0.4	16.7	19.0	7.4	8.1	9.9	2.9	6.6	3.1	0.8	4.9
Vi	0.2	-	-	15.5	-	-	-	0.4	-	-	-	-	-	-	-	-	-	0.2	0.4	0.4	-	-	-	-	-	1.0	-
Va silicif	2.4	11.6	8.4	2.4	9.9	6.9	25.2	19.5	12.0	4.7	3.8	1.8	0.4	2.1	1.4	5.0	3.3	10.0	9.2	3.7	3.1	12.1	2.0	4.5	5.7	5.6	8.4
Vi alter	1.2	1.7	3.8	-	7.5	1.4	1.8	4.2	1.3	2.9	0.2	0.8	-	-	-	-	0.2	0.6	0.6	0.4	0.8	1.2	-	-	-	-	1.8
Glass	2.0	-	-	0.6	0.6	0.9	-	2.7	1.3	2.1	-	-	-	-	0.2	-	0.6	10.8	8.6	2.1	3.1	3.4	2.7	0.2	-	-	0.4
Dvtr	0.6	1.7	1.2	0.9	3.0	-	5.3	6.3	3.5	1.2	0.2	0.2	0.2	0.4	-	0.2	0.8	16.1	9.8	2.3	1.8	6.1	0.9	1.7	2.6	3.2	1.4
Pl/gn	-	-	-	-	-	-	-	-	-	0.8	-	-	-	-	-	-	-	-	-	-	-	-	-	-	-	-	-
Mmic	-	-	-	-	-	-	-	-	-	0.4	-	-	-	-	-	-	-	-	-	-	-	-	-	-	-	-	-
Mq	-	-	-	-	-	-	-	-	-	-	-	-	-	-	-	-	-	-	-	-	-	-	-	-	-	-	-
Ch	-	-	-	-	-	-	-	-	-	-	-	-	-	-	-	-	-	-	-	-	-	-	-	-	-	-	-
Silt	0.4	-	-	-	1.6	-	0.2	-	-	1.0	-	0.4	0.2	-	-	-	-	-	-	-	-	-	-	-	-	-	-
Bt	-	-	-	-	-	-	-	-	-	-	-	0.2	-	-	-	-	-	0.4	0.2	-	0.2	0.2	-	-	-	-	0.2
Chl	0.2	-	-	-	-	-	0.4	-	-	-	-	-	0.2	-	-	-	-	0.2	-	-	-	0.2	-	-	-	-	-
Ep	-	-	-	-	-	-	-	-	-	-	-	-	-	-	-	1.5	-	0.2	-	-	-	-	-	-	-	-	-
Op	6.7	4.3	2.8	2.8	4.7	3.6	3.7	1.3	7.3	3.1	3.6	2.1	4.1	0.2	0.6	-	7.9	1.0	2.9	5.8	12.8	6.7	6.4	4.5	6.6	4.4	2.5
Zr	-	0.2	-	-	-	-	0.2	-	0.4	-	0.2	0.2	0.6	-	-	-	0.4	0.2	-	-	0.2	-	-	0.4	-	0.2	-
Btv	-	-	-	-	-	-	-	-	-	-	-	-	-	-	-	-	-	-	-	-	-	-	-	-	-	-	-
Bio	-	-	-	-	-	-	-	-	-	-	-	-	-	-	-	-	-	-	-	-	-	-	-	0.4	-	-	1.4
Carb. intr.	19.8	32.8	35.3	26.0	17.9	25.8	4.5	12.2	8.4	26.3	12.7	40.8	18.6	32.2	34.5	22.8	12.7	-	-	20.5	27.8	20.4	29.9	35.7	17.9	44.3	37.3
Cl aren.	-	1.9	1.4	1.3	0.8	0.9	-	-	-	-	-	1.2	0.2	1.6	1.4	3.9	-	-	-	0.2	-	-	0.5	-	0.4	-	-
Nod.	-	0.2	13.0	3.6	2.2	13.0	-	-	-	-	-	0.2	-	-	0.6	0.4	-	-	-	-	-	1.4	-	-	-	-	3.3
Gr fosfatici	1.2	0.2	0.2	0.2	-	-	-	-	-	0.8	-	-	0.2	-	-	-	-	-	-	-	-	0.2	-	0.2	-	-	-
Gr verdi	-	-	-	-	-	-	-	-	-	-	-	-	-	-	-	-	-	0.2	-	-	-	-	-	-	-	-	-
Cmc	-	-	-	-	-	-	-	-	-	-	-	-	-	-	0.6	-	-	-	-	-	-	-	-	-	-	-	-
Cms	-	-	-	-	-	-	-	-	-	-	-	-	-	-	-	-	-	-	-	-	-	-	-	-	-	-	-
Dsp	-	-	-	-	-	-	-	-	-	-	-	-	-	-	-	-	-	-	-	-	-	-	-	-	-	-	-
Dpx	-	-	-	-	-	-	-	-	-	-	-	-	-	-	-	-	-	-	-	-	-	-	-	-	-	-	-
cc	0.6	-	-	-	0.8	-	-	-	-	1.0	-	-	-	-	-	-	-	-	-	-	-	-	-	-	-	-	-
cd	-	-	0.6	-	-	-	-	2.3	3.3	-	9.3	1.6	-	0.2	-	1.9	1.9	0.2	1.8	1.0	-	-	-	-	12.1	1.8	5.1
cq	-	-	-	-	-	-	0.6	-	1.5	-	3.8	-	-	-	-	-	0.4	-	0.4	-	-	-	-	-	-	-	-
matr c	16.0	1.1	15.8	-	13.2	1.4	1.8	7.8	1.5	12.8	-	13.3	20.9	16.1	20.5	-	7.5	-	-	11.4	15.7	15.4	8.9	4.9	-	14.3	2.9
matr sil	-	-	0.2	-	-	-	-	-	-	-	-	0.6	-	-	-	-	-	-	-	0.2	-	0.4	-	-	-	0.2	-
psm	-	-	-	-	-	-	-	-	-	-	-	-	-	-	-	-	-	-	-	-	-	-	-	-	-	-	-
clays	0.2	-	-	-	-	-	-	0.4	-	-	-	0.4	0.2	-	-	-	-	1.8	0.2	0.2	-	-	-	-	-	-	-
kaolinite	-	-	-	-	-	-	0.4	-	-	0.2	-	-	-	-	-	-	-	-	-	-	-	-	-	-	-	-	-
pcx	0.2	-	-	-	0.2	-	-	-	-	-	-	-	-	-	-	-	-	-	-	-	-	-	-	-	-	-	-
pqx	-	-	-	-	-	-	-	-	-	-	-	-	-	-	-	-	-	-	-	-	-	-	-	-	-	-	-
alter	-	-	-	-	-	-	-	-	-	-	-	-	-	-	-	-	-	-	-	-	-	-	-	-	-	-	-
silicif.	-	-	-	-	-	-	-	-	-	-	-	-	-	-	-	-	-	-	-	-	-	-	-	-	-	-	-
oth	-	-	-	-	-	-	-	-	0.2	-	-	-	-	-	-	-	-	-	-	-	-	-	-	-	-	-	-
TOT	**100.0**	**100.0**	**100.0**	**100.0**	**100.0**	**100.0**	**100.0**	**100.0**	**100.0**	**100.0**	**100.0**	**100.0**	**100.0**	**100.0**	**100.0**	**100.0**	**100.0**	**100.0**	**100.0**	**100.0**	**100.0**	**100.0**	**100.0**	**100.0**	**100.0**	**100.0**	**100.0**

PETROGRAPHICAL RESULTS, TRAVENANZES FM.

RIFUGIO S. MARCO SECTION

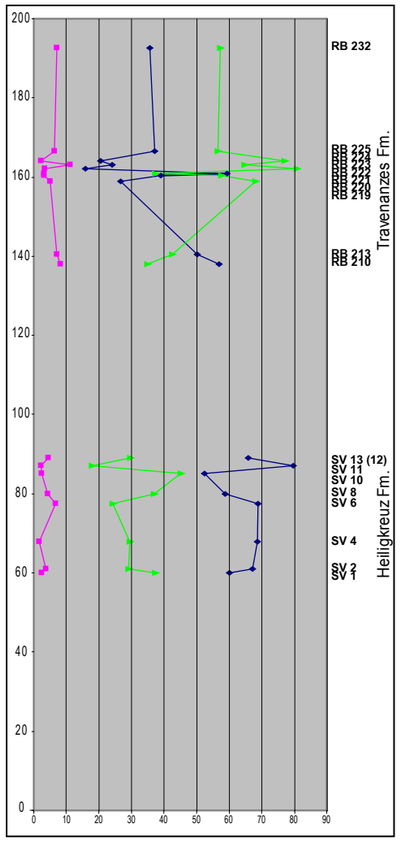

CORTINA AREA

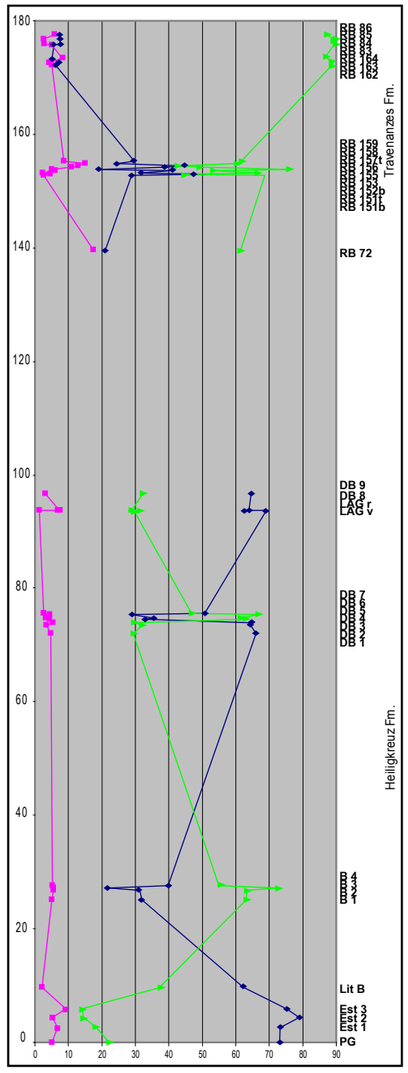

RIO PONTUZ SECTION

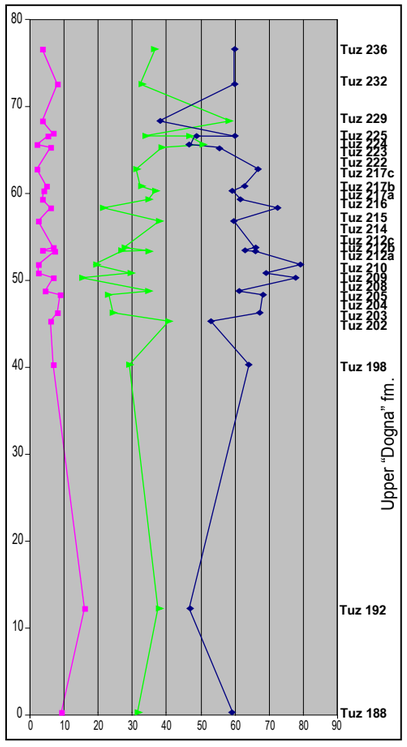

Legend
Q
F
L+CE

GRAN COLLE SECTION

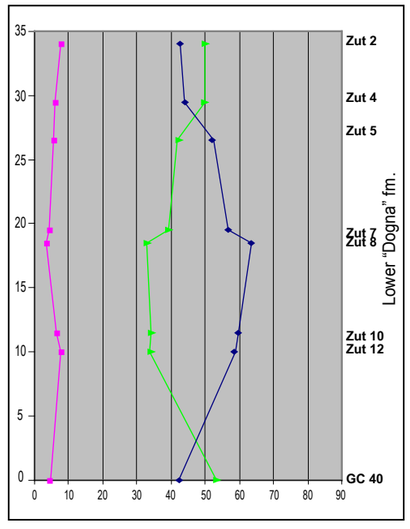

RIO DI TERRAROSSA SECTION

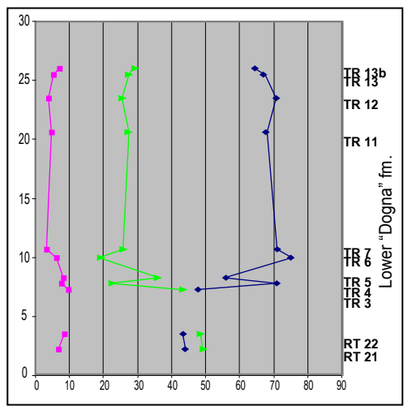

R. PONTUZ / R. MAS SECTIONS

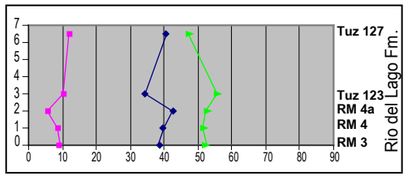

CORRELATION PANEL OF PETROGRAPHIC RESULTS